frontiers | Research Topics

Strategies in overcoming the chemoresistance in colorectal cancer

Edited by
Veronika Vymetalkova, Tomas Buchler
and Sona Vodenkova

Published in
Frontiers in Oncology
Frontiers in Pharmacology

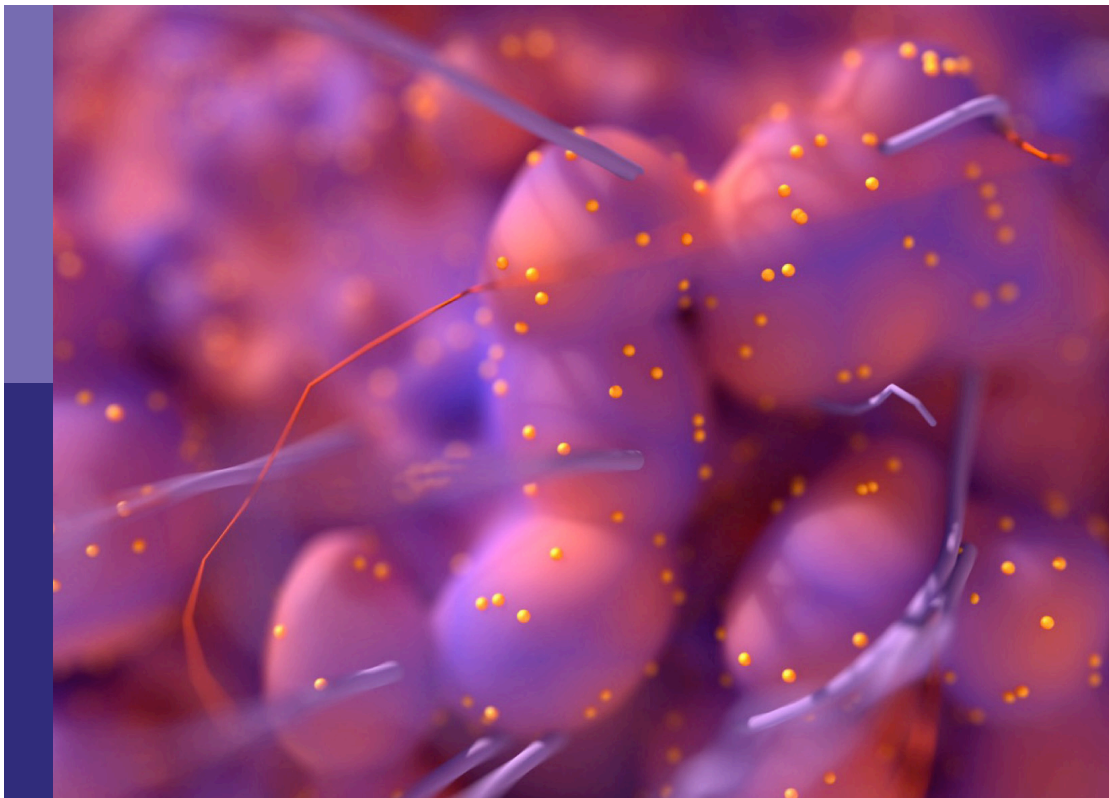

ISSN 1664-8714
ISBN 978-2-8325-3725-1
DOI 10.3389/978-2-8325-3725-1

About Frontiers

Frontiers is more than just an open access publisher of scholarly articles: it is a pioneering approach to the world of academia, radically improving the way scholarly research is managed. The grand vision of Frontiers is a world where all people have an equal opportunity to seek, share and generate knowledge. Frontiers provides immediate and permanent online open access to all its publications, but this alone is not enough to realize our grand goals.

Frontiers journal series

The Frontiers journal series is a multi-tier and interdisciplinary set of open-access, online journals, promising a paradigm shift from the current review, selection and dissemination processes in academic publishing. All Frontiers journals are driven by researchers for researchers; therefore, they constitute a service to the scholarly community. At the same time, the *Frontiers journal series* operates on a revolutionary invention, the tiered publishing system, initially addressing specific communities of scholars, and gradually climbing up to broader public understanding, thus serving the interests of the lay society, too.

Dedication to quality

Each Frontiers article is a landmark of the highest quality, thanks to genuinely collaborative interactions between authors and review editors, who include some of the world's best academicians. Research must be certified by peers before entering a stream of knowledge that may eventually reach the public - and shape society; therefore, Frontiers only applies the most rigorous and unbiased reviews. Frontiers revolutionizes research publishing by freely delivering the most outstanding research, evaluated with no bias from both the academic and social point of view. By applying the most advanced information technologies, Frontiers is catapulting scholarly publishing into a new generation.

What are Frontiers Research Topics?

Frontiers Research Topics are very popular trademarks of the *Frontiers journals series*: they are collections of at least ten articles, all centered on a particular subject. With their unique mix of varied contributions from Original Research to Review Articles, Frontiers Research Topics unify the most influential researchers, the latest key findings and historical advances in a hot research area.

Find out more on how to host your own Frontiers Research Topic or contribute to one as an author by contacting the Frontiers editorial office: frontiersin.org/about/contact

Strategies in overcoming the chemoresistance in colorectal cancer

Topic editors

Veronika Vymetalkova — Academy of Sciences of the Czech Republic (ASCR), Czechia

Tomas Buchler — Charles University, Czechia

Sona Vodenkova — Institute of Experimental Medicine (ASCR), Czechia

Citation

Vymetalkova, V., Buchler, T., Vodenkova, S., eds. (2023). *Strategies in overcoming the chemoresistance in colorectal cancer*. Lausanne: Frontiers Media SA.

doi: 10.3389/978-2-8325-3725-1

Table of contents

frontiers | Frontiers in Oncology

TYPE Editorial
PUBLISHED 02 October 2023
DOI 10.3389/fonc.2023.1295204

OPEN ACCESS

EDITED AND REVIEWED BY
Yun Dai,
Peking University, China

*CORRESPONDENCE
Veronika Vymetalkova
veronika.vymetalkova@iem.cas.cz

RECEIVED 15 September 2023
ACCEPTED 18 September 2023
PUBLISHED 02 October 2023

CITATION
Vodenkova S, Buchler T and Vymetalkova V (2023) Editorial: Strategies in overcoming the chemoresistance in colorectal cancer. *Front. Oncol.* 13:1295204. doi: 10.3389/fonc.2023.1295204

Editorial: Strategies in overcoming the chemoresistance in colorectal cancer

Sona Vodenkova[1,2], Tomas Buchler[3] and Veronika Vymetalkova[1,2,4]*

[1]Department of Molecular Biology of Cancer, Institute of Experimental Medicine of the Czech Academy of Sciences, Prague, Czechia, [2]Biomedical Centre, Faculty of Medicine in Pilsen, Charles University, Pilsen, Czechia, [3]Department of Oncology, Second Faculty of Medicine, Charles University and Motol University Hospital, Prague, Czechia, [4]Institute of Biology and Medical Genetics, First Faculty of Medicine, Charles University, Prague, Czechia

KEYWORDS

chemoresistance, colorectal cancer, platinum derivates, traditional Chinese medicine, fruquintinib, radiotherapy, adjuvant chemotherapy

Editorial on the Research Topic
Strategies in overcoming the chemoresistance in colorectal cancer

Colorectal cancer (CRC) may display innate or acquired chemoresistance, and each is important in determining initial and subsequent lines of systemic treatment. Innate resistance is noted during early therapy phases, while acquired resistance develops during systemic antineoplastic treatment (1).

To prevent ineffective treatment and to select optimal regimens, there is an urgent need to identify biomarkers associated with therapy response. Therefore, the identification and validation of biomarkers for prediction and monitoring of the response of CRC patients to a specific regimen might shift the therapy towards precision medicine.

In this Research Topic, entitled "*Strategies in Overcoming the Chemoresistance in Colorectal Cancer*", in a collection of ten papers the authors focused on the different aspects that play significant roles in the therapy efficacy. These studies provided insights into the potential of new therapeutic strategies (Zhang et al., Zheng et al., Hu et al., Jiang et al., Lin et al.), presented new predictive markers (Li et al.) or different prospectives and possibilities of applying adjuvant therapy in rectal cancer patients (Kuo et al.) as well as molecular mechanisms involved in the treatment response of CRC patients (Horak et al., Moretton et al., Liu et al.).

New therapeutic strategies

Many natural compounds that have been used in Eastern medicine for centuries are currently being reevaluated in the context of current treatment approaches. Many of them are well tolerated by the patients and do not display toxic effects even at high doses (2). Their interactions with conventional chemotherapeutics represent a new direction in

cancer therapy research. Lin et al. explored the potential of traditional Chinese medicine (TCM) as a sensitizer of anti-CRC drugs, and they believe TCM has a promising future as a natural, less toxic, alternative, and complementary therapy for clinical CRC treatment in developing new sensitizers to other anticancer drugs.

Jiang et al. focused on signalling targets controlled by protein tyrosine kinases to emphasize the potential of kinase inhibitors as treatment agents for metastatic CRC (mCRC). Over 50 tyrosine kinase inhibitors (TKIs) have been approved by the U.S. Food and Drug Administration (3). However, around 42 TKIs demonstrating preclinical antitumour activity, and despite numerous clinical trials, only regorafenib has been approved for clinical use in mCRC.

Zhang et al. studied fruquintinib, a small-molecule TKI that targets the vascular endothelial growth factor receptor. The authors focused on a combination of fruquintinib with PD-1 inhibitors in patients with microsatellite stable (MSS) or mismatch repair-proficient (pMMR) advanced CRC. They discovered that this combination evinced antitumor activity and manageable safety in MSS/pMMR advanced CRC patients.

Similarly, Hu et al. analysed the effect of Sorafenib, an oral multi-kinase inhibitor with a tumour-suppressing effect targeting the RAF-MEK-ERK pathway. However, its clinical application is limited due to complex drug resistance and many side effects. GW5074, one of the C-RAF inhibitors, has the potential to enhance chemotherapy efficiency. The authors demonstrated that GW5074 served as a Sorafenib sensitizer through mitochondria dysfunction and thus might reduce the risk of chemoresistance in CRC.

In a study by Zheng et al., a potentially targetable surface molecule in cancer cells, protocadherin 7 (PCDH7) was studied. One of the described and identified properties of PCDH7 was found to facilitate the development of chemoresistance in CRC cells by positively modulating Mcl-1 expression.

Radiotherapy resistance in rectal cancer patients and treatment planning

Li et al. focused on the complication of lipoprotein receptor-related protein-1 (LRP-1) and survivin-associated radiotherapy resistance. They demonstrated that radiomics analysis of dynamic contrast-enhanced magnetic resonance imagining promotes preoperative assessment of LRP-1 and survivin expression in locally advanced rectal cancer and that their model displays significant potential to diagnose patients with radiotherapy resistance.

Different prospectives and possibilities of applying adjuvant therapy in rectal cancer patients

Kuo et al. studied whether to administer adjuvant therapy for patients with rectal cancer with good response (ypT0-2N0) after neoadjuvant chemoradiotherapy and surgery. Based on the outcomes from 720 patients, the authors stated that in these circumstances adjuvant chemotherapy can be omitted.

Functional studies

DNA damaging agents are frequently used in different therapy regimens and DNA damage response pathways are involved in the mechanism of chemoresistance (Horak et al.). Platinum derivatives, inducing highly cytotoxic DNA crosslinks, are one of the keystone chemotherapeutics in CRC. Since cisplatin treatment is often associated with high toxicity and, eventually, resistance, scientists are trying to develop more active and less toxic derivatives. Moretton et al. synthesized a series of clickable cisplatin derivates as a molecular tool that can be used for the identification, visualization, localization, and isolation of DNA-cisplatin crosslinks, and thus understanding the chemoresistance mechanisms.

Oxaliplatin is used to treat mCRC (1). The innate or acquired resistance to oxaliplatin-based combinations is still the leading cause of treatment failure. Horak et al. identified that microRNA miR-140 led to MRE11 downregulation and improved oxaliplatin therapy response in CRC.

With the outset of targeted therapy, the survival of CRC patients has substantially improved. Over the last two decades, targeted therapy for CRC has made considerable progress and is used in a majority of patients with mCRC throughout their treatment. However, resistance to targeted therapy also occurs and represents a significant clinical problem. Thus, investigating the resistance mechanism and finding strategies to overcome the resistance to targeted therapy is a constant challenge in the treatment of mCRC patients and is also a Research Topic of study of Liu et al.. The authors studied platycodon-D, a bioactive compound isolated from the Chinese herb platycodon grandiflorum, to inhibit PI3K/Akt pathway during the treatment of cetuximab in *KRAS*-mutated CRC cells. In this functional study, the increased sensitivity of *KRAS*-mutated CRC cells to cetuximab after platycodon-D treatment was recorded.

In summary, this Research Topic illustrates the several aspects of overcoming or preventing the failure of cancer therapy. We are

aware we did not manage to cover all aspects of the issue of chemoresistance, however, we believe this Research Topic has shed light on many elements and will be helpful for further research on the issue of chemoresistance in CRC patients.

Author contributions

SV: Conceptualization, Funding acquisition, Writing – original draft, Writing – review & editing. TB: Supervision, Writing – review & editing. VV: Conceptualization, Funding acquisition, Supervision, Writing – original draft, Writing – review & editing.

Funding

SV was supported by the Czech Health Research Council of the Ministry of Health of the Czech Republic (grant no. NU22J-03-00033). VV was supported by the Grant Agency of the Czech Republic (grant no. 22-05942S).

Conflict of interest

The authors declare that the research was conducted in the absence of any commercial or financial relationships that could be construed as a potential conflict of interest.

Publisher's note

References

1. Vodenkova S, Buchler T, Cervena K, Veskrnova V, Vodicka P, Vymetalkova V. 5-fluorouracil and other fluoropyrimidines in colorectal cancer: Past, present and future. *Pharmacol Ther* (2020) 206:107447. doi: 10.1016/j.pharmthera.2019.107447

2. Rejhová A, Opattová A, Čumová A, Slíva D, Vodička P. Natural compounds and combination therapy in colorectal cancer treatment. *Eur J Med Chem* (2018) 144:582–94. doi: 10.1016/j.ejmech.2017.12.039

3. Iyer KK, van Erp NP, Tauriello DVF, Verheul HMW, Poel D. Lost in translation: Revisiting the use of tyrosine kinase inhibitors in colorectal cancer. *Cancer Treat Rev* (2022) 110:102466. doi: 10.1016/j.ctrv.2022.102466

frontiers | Frontiers in Oncology

ORIGINAL RESEARCH
published: 02 June 2022
doi: 10.3389/fonc.2022.874201

Clickable Cisplatin Derivatives as Versatile Tools to Probe the DNA Damage Response to Chemotherapy

Amandine Moretton[1,2], *Jana Slyskova*[1,2], *Marwan E. Simaan*[2,3,4], *Emili A. Arasa-Verge*[1], *Mathilde Meyenberg*[1,2], *D. Alonso Cerrón-Infantes*[2,3,4,5], *Miriam M. Unterlass*[2,3,4,5] *and Joanna I. Loizou*[1,2*]

[1] Center for Cancer Research, Comprehensive Cancer Center, Medical University of Vienna, Vienna, Austria, [2] CeMM Research Center for Molecular Medicine of the Austrian Academy of Sciences, Vienna, Austria, [3] Institute of Materials Chemistry, Technische Universität Wien, Vienna, Austria, [4] Institute of Applied Synthetic Chemistry, Technische Universität Wien, Vienna, Austria, [5] Department of Chemistry, Solid State Chemistry, Universität Konstanz, Konstanz, Germany

OPEN ACCESS

Edited by:
Sona Vodenkova,
Institute of Experimental Medicine (ASCR), Czechia

Reviewed by:
Wayne Crismani,
University of Melbourne, Australia
Anton Gartner,
Ulsan National Institute of Science and Technology, South Korea

***Correspondence:**
Joanna I. Loizou
joanna.loizou@meduniwien.ac.at

Specialty section:
This article was submitted to Gastrointestinal Cancers: Colorectal Cancer, a section of the journal Frontiers in Oncology

Received: 11 February 2022
Accepted: 29 April 2022
Published: 02 June 2022

Citation:
Moretton A, Slyskova J, Simaan ME, Arasa-Verge EA, Meyenberg M, Cerrón-Infantes DA, Unterlass MM and Loizou JI (2022) Clickable Cisplatin Derivatives as Versatile Tools to Probe the DNA Damage Response to Chemotherapy. Front. Oncol. 12:874201. doi: 10.3389/fonc.2022.874201

Cisplatin induces DNA crosslinks that are highly cytotoxic. Hence, platinum complexes are frequently used in the treatment of a broad range of cancers. Efficiency of cisplatin treatment is limited by the tumor-specific DNA damage response to the generated lesions. We reasoned that better tools to investigate the repair of DNA crosslinks induced by cisplatin would therefore be highly useful in addressing drug limitations. Here, we synthesized a series of cisplatin derivatives that are compatible with click chemistry, thus allowing visualization and isolation of DNA-platinum crosslinks from cells to study cellular responses. We prioritized one alkyne and one azide Pt(II) derivative, Pt-alkyne-53 and Pt-azide-64, for further biological characterization. We demonstrate that both compounds bind DNA and generate DNA lesions and that the viability of treated cells depends on the active DNA repair machinery. We also show that the compounds are clickable with both a fluorescent probe as well as biotin, thus they can be visualized in cells, and their ability to induce crosslinks in genomic DNA can be quantified. Finally, we show that Pt-alkyne-53 can be used to identify DNA repair proteins that bind within its proximity to facilitate its removal from DNA. The compounds we report here can be used as valuable experimental tools to investigate the DNA damage response to platinum complexes and hence might shed light on mechanisms of chemoresistance.

Keywords: cisplatin, chemotherapy, chemoresistance, DNA Damage, DNA crosslinks, DNA repair, click chemistry

INTRODUCTION

DNA crosslinks and adducts are highly cytotoxic lesions that are utilized in cancer treatment due to their strong transcription and replication inhibitory potential. Clinically, the most relevant source of DNA crosslinks is represented by platinum-based {Pt(II)} compounds (1, 2). Of those, cisplatin displays remarkable versatility and efficiency in a broad range of different malignancies. Cisplatin and other Pt(II) drugs induce cellular toxicity by binding to DNA and generating inter- and intrastrand crosslinks that are subsequently recognized by the DNA damage response machinery (3, 4). Due to the complexity of DNA crosslinks and their potent cytotoxicity, eukaryotic cells have

evolved highly efficient DNA repair pathways that deal with their removal. Nucleotide excision repair (NER) pathways, and the Fanconi anemia (FA) repair pathway, are well documented to function on such lesions thus maintaining genome stability (5, 6). NER can remove intrastrand crosslinks in a transcription dependent, or independent manner (7–9), while the FA pathway is involved in the replication-dependent repair of interstrand crosslinks (10).

A caveat of using Pt(II) derivatives as chemotherapeutics is the emergence of resistance that occurs as an outcome of re-wiring of metabolism as well as DNA repair processes and apoptotic signaling (11, 12). In addition, while some progress has been made, it remains unclear why cells of different genetic backgrounds and origins display differential responses to cisplatin and develop chemoresistance (13, 14). This hinders patient stratification since it is undefined which patients would most benefit from administration of cisplatin as a chemotherapeutic. To better understand resistance mechanisms and gene- and cell-type-specific responses to platinum coordination compounds, better tools are required that allow for cellular investigations into the removal and repair of DNA crosslinks induced by cisplatin and other platinum-based compounds.

Here, we synthesized a series of Pt(II) derivatives by adding various azide or alkyne linkers to cisplatin that are amenable to a bio-orthogonal 'click reaction', i.e., the Cu(I)-catalyzed azide–alkyne cycloaddition (CuAAC), which is a Huisgen 1,3-dipolar cycloaddition. This reaction typically fulfills the criteria of 'click chemistry', meaning it is high in yield, wide in scope, stereospecific, and facile to perform at room temperature and in aqueous solvents (15–17). Following a stringent prioritization pipeline, we present two Pt(II) derivatives, an alkyne (Pt-alkyne-53, **Figure 1C**) and an azide (Pt-azide-64, **Figure 1C**), with biological properties in human cellular models. By exposing either wildtype, NER- or FA-defective isogenic cell lines to the compounds, we demonstrate them to be cytotoxic, due to induction of DNA damage. DNA lesions generated by the compounds can be visualized and quantified in cells by clicking the compounds with a fluorescent probe or biotin, respectively. Finally, by using azide-functionalized biotin to pull-down Pt-alkyne-53, we were able to identify DNA repair proteins that directly bind to DNA crosslinks to facilitate their removal from DNA. Taken together, we present versatile clickable Pt(II) compounds that can be utilized in a variety of approaches to investigate DNA repair pathways that remove platinum complexes.

RESULTS

Cisplatin binds covalently to DNA at the N^7 position of purines, resulting in intrastrand adducts (90-95% of lesions), as well as interstrand crosslinks (~2% of lesions) and mono-adducts (~5%; **Figure 1A**) (18). To circumvent the lack of available tools to investigate the presence of cisplatin on DNA, we synthesized four azide-based clickable cisplatin derivatives (Pt-30, Pt-51, Pt-52 and Pt-64). Pt-30 is a known complex and its clickable nature has been previously demonstrated (19). Thus, alongside the synthesis

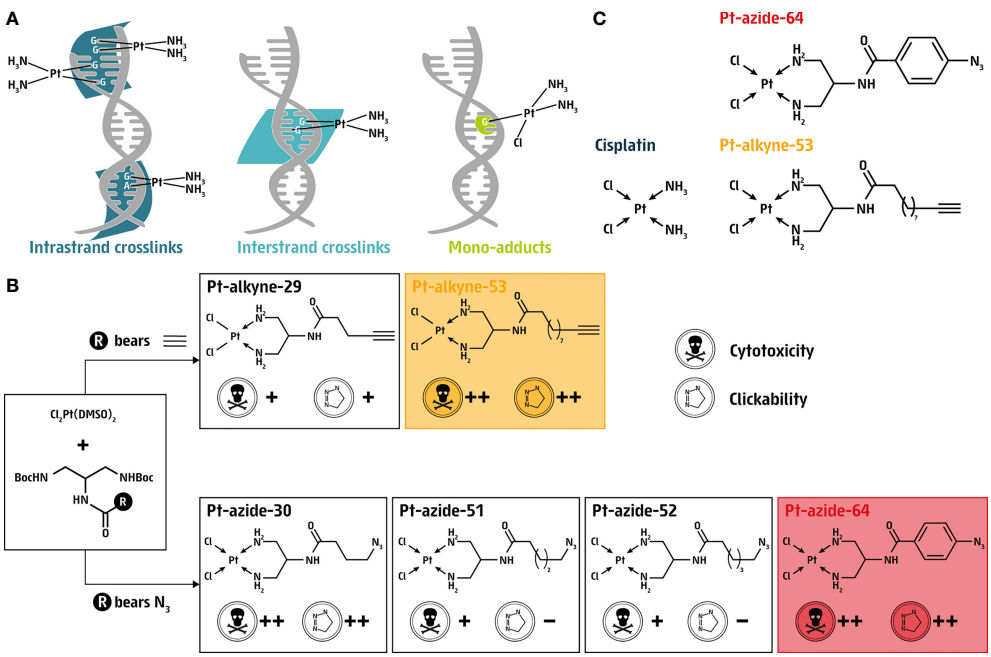

FIGURE 1 | Synthesis of clickable cisplatin derivatives. **(A)** Schematic representation of intrastrand and interstrand crosslinks as well as mono-adducts induced by cisplatin. **(B)** Selection criteria for the generation of clickable cisplatin derivatives generated in this study; Pt-alkyne or Pt-azide compounds. **(C)** Chemical structures of cisplatin along with the two prioritized clickable cisplatin derivatives Pt-alkyne-53 and Pt-azide-64.

of Pt-30, we also generated complexes Pt-51, Pt-52 and Pt-64 as novel compounds designed to vary in their azide side chain length (Pt-51 and Pt-52 bear different lengths of aliphatic azides) and electronic nature (Pt-64 bears an aromatic azide). In addition to the azide-based clickable platinum complexes, we also generated alkyne-based complexes, therefore two additional platinum coordination compounds were designed, Pt-29 bearing a five-carbon terminal-alkyne side chain, which has been previously demonstrated as a potential tool for the detection and isolation of Pt-bound biomolecules (19), and the novel complex Pt-53 bearing a ten-carbon terminal-alkyne side chain (**Figure 1B**; **Supporting Information**).

The compounds were tested for cytotoxicity and clickability, revealing two azide compounds (Pt-30 and Pt-64) and one alkyne compound (Pt-53) that fulfilled both criteria (**Figure 1B**). While the synthesis and isolation of most of the platinum complexes was feasible, the preparation of Pt-30 was less successful which led to its isolation in a low overall yield. Despite numerous attempts, we were unable to isolate the final product with yields surpassing 5%. While the reason behind the low yield remains unknown, we hypothesize that it could be due to failure in the precipitation techniques of the final platinum complex. Therefore, and because Pt-30 is structurally similar to Pt-53 featuring an *n*-alkyl amide linker between Pt^{2+} and the clickable function, we next prioritized the alkyne compound Pt-53 and the azide compound Pt-64 for further investigations, from here on referred to as Pt-alkyne-53 and Pt-azide-64 (**Figure 1C**). Thus, utilizing Pt-alkyne-53 and Pt-azide-64 allowed us to further investigate the amenability of alkylamide- and arylamide-linked cisplatin derivatives as tools for investigating aspects of DNA damage response.

Since DNA is the major target of cisplatin, it is an effective chemotherapeutic drug that is cytotoxic across a range of cancers and cell lines. To address if the two prioritized compounds Pt-alkyne-53 and Pt-azide-64 would depict chemotherapeutic activity, we tested their cytotoxicity on two human cancer-derived cell lines: U2OS from osteosarcoma and HAP1 from a cell line of chronic myeloid leukemia origin. The compounds were found to be cytotoxic on both cell lines tested, albeit at a higher concentration compared to cisplatin (**Figures 2A, B)**. In U2OS cells the lethal dose 50 (LD_{50}) of cisplatin was 8.2 μM, for Pt-alkyne-53 this was 26 μM and for Pt-azide-64 this was 24.3 μM (**Figure S1A**). In HAP1 cells the LD_{50} was 0.9 μM for cisplatin, 3.2 μM for Pt-alkyne-53 and 3.5 μM for Pt-azide-64 (**Figure S1B**). Thus, Pt-alkyne-53 and Pt-azide-64 are cytotoxic to human cancer-derived cell lines.

In response to cisplatin, cells activate DNA repair pathways to detect and remove cisplatin-induced DNA crosslinks. A major pathway responsible for removal of interstrand crosslinks from DNA during replication is FA and cells deficient in FA proteins are hypersensitive to DNA crosslinking agents (20). To determine if Pt-alkyne-53 and Pt-azide-64 induce hypersensitivity of FA deficient cells, we exposed HAP1 cells that had been engineered by CRISPR-Cas9 to lack the FA protein FANCD2 (ΔFANCD2; **Figure S1C**) to the compounds and measured cellular sensitivity to the compounds. As compared to their wildtype (WT) counterpart, ΔFANCD2 HAP1 cells displayed hypersensitivity to both Pt-alkyne-53 (**Figure 2C**) and Pt-azide-64 (**Figure 2D**), as well as cisplatin (**Figure S1D**). These observations were also confirmed by a clonogenic assay (**Figures 2E–G** and **Figure S1E**). This data indicates that Pt-alkyne-53 and Pt-azide-64 generate DNA lesions that are cleared by the FA pathway.

To confirm that clickable Pt(II) derivatives generate DNA damage, we measured the number of γH2AX foci (a well-established marker of DNA damage) in the nuclei of cells treated for 3 hours with different concentrations of cisplatin, Pt-alkyne-53, and Pt-azide-64, respectively, after which the cells were cultured for up to 48 hours in compound-free media and analyzed for γH2AX foci at different time points. We observed a dose- and time-dependent increase in γH2AX foci following treatment with all three compounds, with the number of nuclear foci peeking at 4-8 hours post-treatment in WT U2OS cells (**Figure S2A**). At 24 and 48 hours of recovery, the number of γH2AX foci decreased in WT cells, indicating clearance of DNA damage (**Figure S2A**). Hence, Pt-alkyne-53 and Pt-azide-64 induce DNA damage that is cleared in a time resolved manner, with comparable kinetics to cisplatin.

A key enzyme in the repair of cisplatin-induced DNA damage is the endonuclease XPF, as it functions in both the NER and the FA pathways to excise the damaged DNA strand, thus removing the DNA lesion. To investigate whether XPF is involved in the clearance of DNA damage induced by the platinum derivatives, we exposed WT and CRISPR-Cas9 engineered XPF-deficient (XPFΔ/Δ, **Figure S2B**) U2OS cells for 3 hours to cisplatin, Pt-alkyne-53, and Pt-azide-64, respectively, and measured γH2AX foci overtime. While γH2AX foci in WT cells were cleared after 48 hours post-treatment, in XPFΔ/Δ cells the γH2AX foci accumulated over time, reaching approximately five-fold higher levels after 48 hours in compound-free medium, as compared to untreated cells (**Figures 3A–C**). This indicates a lack of clearance of cisplatin-, Pt-alkyne-53-, and Pt-azide-64-induced DNA lesions in XPFΔ/Δ cells. Taken together, our data show that Pt-alkyne-53 and Pt-azide-64 are cytotoxic due to the generation of DNA damage that is cleared in a DNA repair-dependent manner through the NER and the FA pathway.

Next, we directly measured the cellular distribution and DNA-binding capacity of Pt-alkyne-53 and Pt-azide-64, by means of immunofluorescence and dot-blot after CuAAC click reactions with a fluorescent dye or biotin, respectively (**Figure 4A**). To investigate cellular distribution by immunofluorescence, U2OS cells were treated with either Pt-alkyne-53 or Pt-azide-64 for 3 hours, fixed and permeabilized, before the CuAAC click reaction was performed with the alkyne- (for Pt-azide-64) or azide- (for Pt-alkyne-53) functionalized dye Alexa Fluor 488 (AF488). This allowed for visualization and cellular localization of the compounds. Both Pt-alkyne-53 and Pt-azide-64 showed enrichment in the nucleus and nucleoli, while Pt-alkyne-53 was also detectable in the cytoplasm (**Figure 4B; Figure S3**). To investigate DNA binding capacity by dot blot, we exposed U2OS cells for 5 hours to the

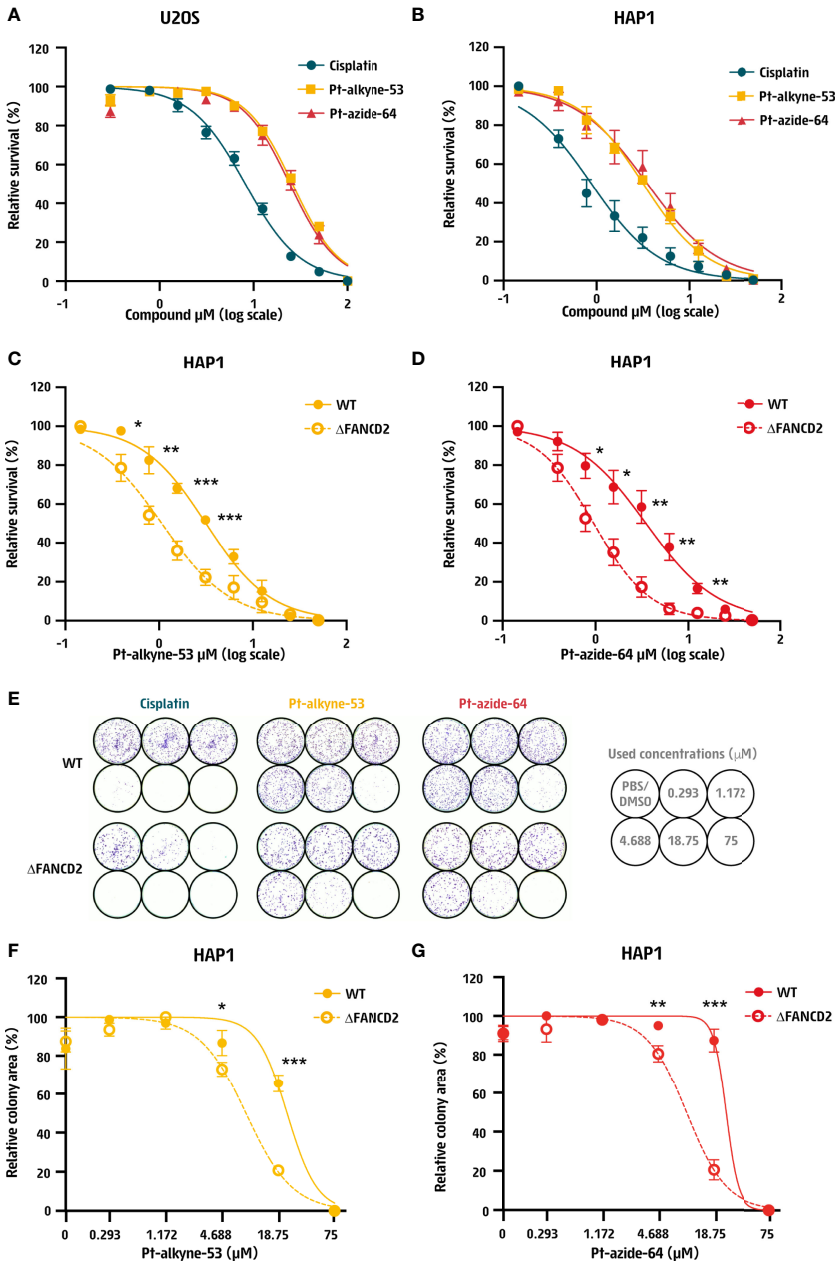

FIGURE 2 | Cisplatin derivatives confer DNA repair-dependent cytotoxicity. **(A, B)** Dose response curve of human **(A)** U2OS cells and **(B)** HAP1 cells treated for 3 days with cisplatin, Pt-alkyne-53 or Pt-azide-64 prepared as 2-fold serial dilutions starting at 100 µM in U2OS cells or 50 µM in HAP1 cells. Cellular survival was measured after 3 days using Cell Titer Glo®. **(C, D)** Dose response curve of wildtype (WT) and FANCD2 deficient (ΔFANCD2) HAP1 cells treated with the indicated doses of **(C)** Pt-alkyne-53 and **(D)** Pt-azide-64 for 3 days. Cellular survival was measured using Cell Titer Glo®. Data represent mean and SEM of 3 independent experiments performed in technical duplicates. **(E–G)** Clonogenic assay of wildtype (WT) and FANCD2 deficient (ΔFANCD2) HAP1 cells treated with the indicated doses of cisplatin, Pt-alkyne-53 and Pt-azide-64 for 7-8 days. **(E)** Representative images from 3 independent experiments and quantification of the surface area occupied by cells. **(F, G)** Quantification of the surface occupied by cells after treatment with **(F)** Pt-alkyne-53 and **(G)** Pt-azide-64. Data represent mean and SD of 3 independent experiments. P-values were calculated using multiple unpaired t-test. *<0.05, **<0.01, ***<0.001.

compounds, then performed the CuAAC click reaction on Pt-alkyne-53 and Pt-azide-64 with alkyne- or azide-linked biotin. After DNA extraction, we measured the intercalation of the compounds within genomic DNA using a horseradish peroxidase conjugated anti-streptavidin antibody (**Figure 4C**). Using this approach, we were able to quantify Pt-alkyne-53 or Pt-azide-64 bound to genomic DNA.

DNA crosslinks are rapidly recognized and bound by DNA repair proteins to facilitate their removal from DNA. To identify DNA repair proteins bound to Pt-alkyne-53, U2OS cells were

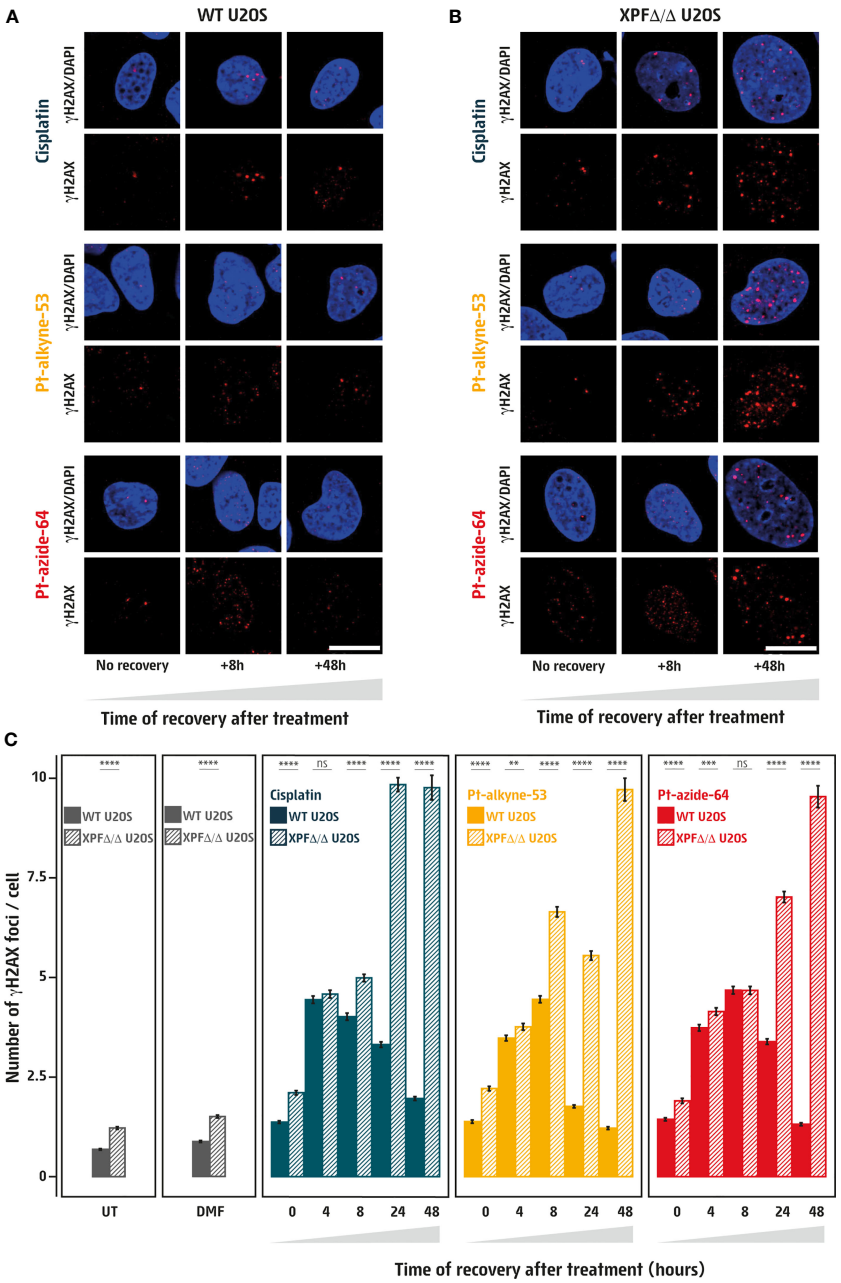

FIGURE 3 | Pt-alkyne-53 and Pt-azide-64 induce DNA damage that is cleared through DNA repair. **(A, B)** Visualization of the DNA damage marker γH2AX (in red) within DAPI stained nuclei (in blue) in wildtype [WT, **(A)**] or XPF deficient [XPFΔ/Δ, **(B)**] human U2OS cells. Cells were untreated (UT), or treated for 3 hours with vehicle (DMF), 1μM cisplatin, 5μM Pt-alkyne-53 or Pt-azide-64, followed by culturing the cells in compound-free media for up to 48 hours. Images were acquired on an Olympus spinning disk confocal microscope, scale bar represents 20μm. **(C)** Quantification of images corresponding to conditions in **(A, B)** represented as mean number of γH2AX foci per nucleus. A minimum of 1,700 cells were quantified for each condition, using CellProfiler, from images acquired with an Opera high-throughput microscope. Error bars represent standard error of the mean. P-values were calculated using t-test. **<0.01, ***<0.001, ****<0.0001, ns, not significant.

treated for 12 hours, and by performing the CuAAC click reaction with biotin-azide, DNA repair proteins were pulled down using streptavidin beads and identified by immunoblotting (**Figure 4D**). This approach revealed an enrichment of the FA protein FANCD2, and the DNA synthesis-specific protein PCNA bound to Pt-alkyne-53 (**Figure 4E**). The specificity of the FANCD2 antibody was confirmed by transfection of U2OS cells with siRNA targeting FANCD2 (**Figure S3B**). Histone H3 was also found to bind Pt-alkyne-53, since it is localized near DNA (**Figure 4E**). This data indicates that Pt-alkyne-53 can be used as a tool to identify DNA repair proteins that bind to the compound and facilitate its removal from DNA.

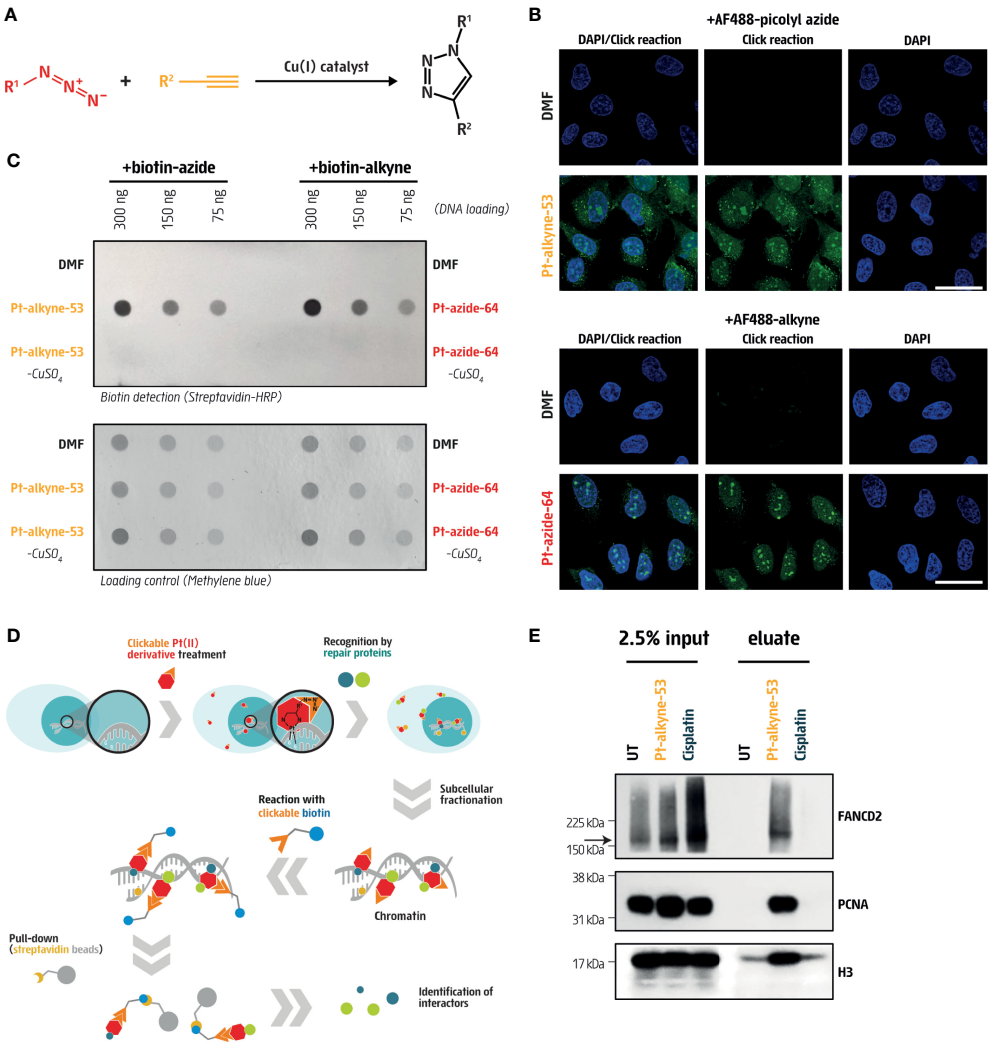

FIGURE 4 | Cisplatin derivatives are clickable and bind DNA repair proteins. **(A)** Schematic representation of the copper-catalyzed click reaction (CuAAC) in which an azide (purple) and an alkyne (orange) compound were covalently bound to form a triazole conjugate. **(B)** Visualization of clickable Pt-alkyne-53 with AF488-picolyl azide and Pt-azide-64 with AF488-alkyne in U2OS cells treated for 3 hours with the indicated compounds at 5 µM or 25 µM, respectively (green). DAPI (blue) was used to counterstain nuclei. Vehicle treated cells (DMF) were used as a negative control. Scale bar represents 20 µm. **(C)** Dot blot of DNA from U2OS cells, immobilized on a nitrocellulose membrane and stained with streptavidin-HRP to detect DNA-bound biotin. Cells were pre-incubated for 5 hours with 100µM Pt-alkyne-53 or Pt-azide-64, followed by fixation and subjected to a CuAAC click reaction with biotin-azide or biotin-alkyne. Vehicle treated cells (DMF), as well as cells exposed to the CuAAC click reaction without the copper catalyst (-$CuSO_4$), were used as negative controls. Methylene blue staining of the nitrocellulose membrane was used to control for loading. **(D)** Scheme of the experimental approach to pull-down DNA repair proteins that interact with the cisplatin derivatives. **(E)** Pull-down of Pt-alkyne-53 from U2OS cells treated with 10µM cisplatin or 100µM Pt-alkyne-53 for 12 hours. The CuAAC click reaction was performed with biotin-azide on chromatin fractions and streptavidin beads were used to pull down the Pt-alkyne-53 along with the proteins bound to it. Proteins enriched in chromatin fractions (input) as well as proteins pulled down with the streptavidin beads (eluate) were probed with the indicated antibodies. The arrow indicates the expected size of the FANCD2 protein.

DISCUSSION

Research geared at understanding how cells respond to platinum-induced crosslinks is hampered due to the lack of available tools that can be used to visualize and quantify these sources of DNA damage. To circumvent this, we reasoned that clickable cisplatin derivatives would be highly valuable research tools for the DNA damage and repair field and hence we synthesized a series of both alkyne and azide cisplatin derivatives. Following a set of selection criteria, based on ease of synthesis, clickability, and cytoxicity, we prioritized one alkyne and one azide cisplatin derivative, Pt-alkyne-53 and Pt-azide-64, respectively. By testing both compounds on isogenic cell lines engineered to lack the DNA repair pathway FA, we reveal that they induce DNA damage-dependent cytotoxicity. We found that the platinum compounds are approximately 3-4-fold less

cytotoxic than cisplatin with regards to LD_{50}, potentially due to their decreased uptake or altered metabolism within cells.

Since both Pt-alkyne-53 and Pt-azide-64 are clickable with either fluorescent labels or biotin, we propose that they can be used to follow the kinetics of DNA repair, using fluorescent microscopy on cells, or by performing dot blots on genomic DNA. By microscopy, we show that the cisplatin derivatives are distributed within the nucleus, and enriched within nucleoli, an observation which is in line with previous reports (21, 22). Platinum compounds are known to also bind RNA and proteins, which are highly abundant in the nucleoli, where transcription of ribosomal RNA occurs (23, 24). While it would be of interest to assess if DNA damage also accumulates in nucleoli, since nucleoli have a very low content of DNA and γH2AX foci are not easily detectable in this cellular compartment, an alternative approach would be needed to directly quantify DNA crosslinks (25). Additionally, we hypothesize that the discrete foci we observe in the cytoplasm, especially for Pt-alkyne-53, indicate the formation of aggregates, in agreement with previous observations using isotope-labelled platinum drugs. In this report, it was suggested that the cytoplasmic localization indicated endocytosis of compound aggregates (22). Moreover, mitochondrial DNA is a known target of cisplatin in addition to nuclear DNA (26, 27), therefore co-staining with mitochondrial markers could provide additional information on the nature of these cytoplasmic foci. Microscopy-based experiments assessing co-localisation with DNA repair proteins could additionally provide valuable information on the cellular mechanisms dealing with cisplatin-induced DNA damage. Thus, we suggest that they can be valuable tools that will allow conclusions to be drawn on the functionality of DNA repair pathways that resolve DNA crosslinks, in Pt(II) resistant cancers and in different genetic backgrounds (**Figure 5**). Moreover, these compounds could be used to address longstanding questions about differential cellular responses to Pt(II) compounds in cell types of different origins.

We additionally show that by clicking Pt-alkyne-53 to biotin, we can identify DNA repair proteins which specifically bind to it, within the cells. Based on this data, we propose that these compounds can be used to further investigate the proteins that bind DNA crosslinks and facilitate their resolution, in a time-resolved manner thus shedding light on proteins involved in different steps of repair from damage signaling to the excision. By clicking these compounds to biotin, mass spectrometry could then be used to identify interacting proteins thus allowing for an unbiased approach aimed at identifying the order of events by which DNA repair proteins function to remove crosslinks.

Additionally, spatial information of where DNA lesions are generated and how they are repaired across the genome is highly important. We propose that these platinum tools can also be

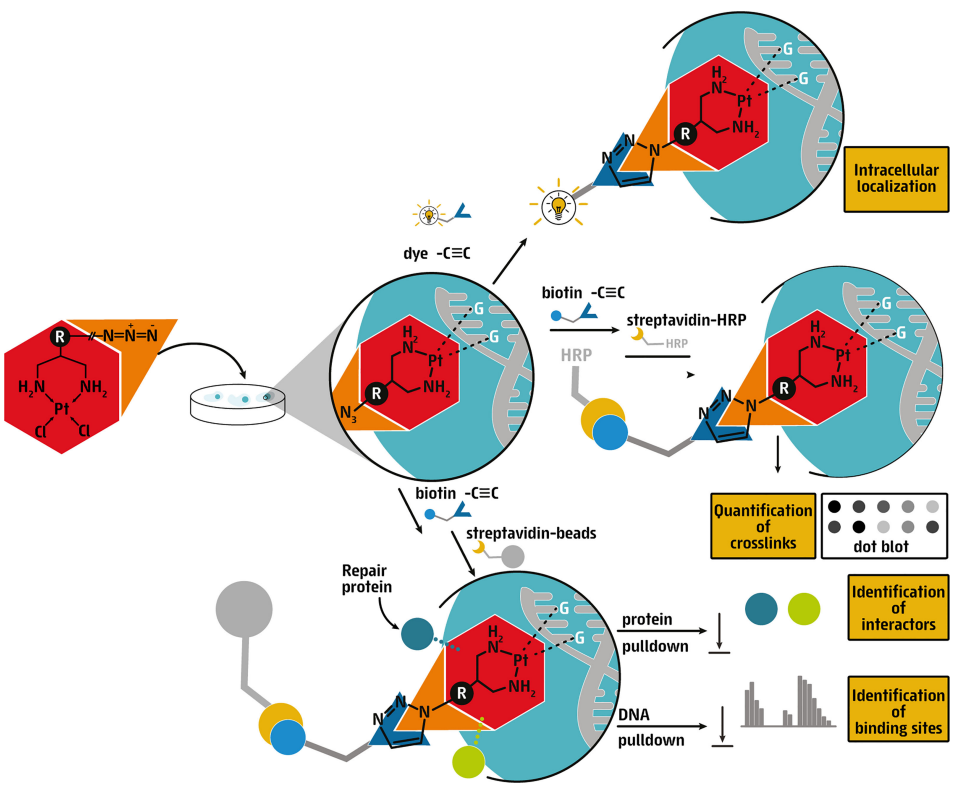

FIGURE 5 | Graphical depiction of the use of clickable cisplatin derivatives to study the DNA damage response. Cisplatin can be modified with azide or alkyne moieties that are clickable to allow for downstream visualization within nuclei of cells, quantification of abundance in DNA and interactions with proteins.

used to identify regions within the genome that are specifically vulnerable to DNA crosslinks. By clicking the compounds to biotin, followed by chromatin pull-down with streptavidin beads, and genome sequencing, this could identify where DNA crosslinks occur in the genome and how they are repaired. This approach has already been successfully used to identify origins of replication, by labeling nascent DNA with 5-ethynyl-2′-deoxyuridine (EdU), an analogue of thymidine, and clicking EdU with biotin-azide (28).

Several other tools have been generated to investigate the localization and clearance of platinum compounds. Amongst these, an antibody has been raised against cisplatin-DNA adducts (ICR4, also called CP9/19) (29), and has been very useful in understanding the DNA damage response following cisplatin treatment (30, 31). This monoclonal antibody recognizes with high sensitivity specifically the intrastrand crosslinks formed by cisplatin between adjacent guanines (32). While these types of lesions are the most common (60-65%), the other types of intrastrand crosslinks (20-25%) as well as the interstrand crosslinks (~2%), remain undetected by the antibody yet are important with regards to Pt(II) compound toxicity (18, 33). In comparison, the clickable platinum compounds we report here do not have such limitations as they detect all types of DNA lesions. Moreover, it is known that cisplatin can crosslink proteins and generate DNA-protein crosslinks (34, 35). The clickable compounds described in this study, could be used to investigate this additional layer of cellular damage induced by platinum compounds.

In addition to the compounds reported here, other clickable platinum compounds have been synthesized (36) that have been mainly tested *in vitro* and in *S. cerevisiae*, and their subcellular localization has been investigated by microscopy (19, 21, 23, 37). *In vitro* studies have limitations, as cellular uptake and drug metabolism can restrict the range of applications of the synthesized compounds *in cellulo*. Treatment of *S. cerevisiae* with azide functionalized Pt(II) compounds allowed the identification of Pt-RNA modifications, showing that tRNA and rRNA are platinum drug substrates, thus suggesting a ribotoxic mechanism for cisplatin cytotoxicity (23). This study also identified 152 platinated proteins, including proteins involved in the ER-stress response (37). Here, we investigate the biological activity of these compounds, by assessing the response of human wildtype cells, compared to their DNA repair-deficient counterparts, to the clickable Pt(II) derivatives alongside cisplatin. We verified that the derivatives behave similarly to cisplatin, generating DNA damage that is cleared with similar kinetics, and accumulates in relevant DNA repair-deficient genetic backgrounds, leading to higher toxicity. Moreover, we were able to identify known DNA repair proteins interacting transiently with the derivatives bound to DNA. We hypothesize that labelling of the clickable derivatives using a Cu-free click reaction, that is not toxic for cells, will broaden the range of applications we report here, for example by allowing real-time tracking of the compounds in live cells. Thus, we envisage that Pt-alkyne-53 and Pt-azide-64 could be used to complement the existing Pt(II) tools currently available, to investigate the repair of DNA crosslinks using a wide range of approaches, leading to a better understanding of the cellular pathways that function in response to cisplatin treatment. This is crucial to explain acquired chemoresistance, stratify patients and design more efficient strategies of chemotherapy.

MATERIALS AND METHODS

Synthesis of Cisplatin Derivatives

All platinum complexes were prepared *via* the following multistep synthesis (**Figure 6** and **Supporting Information**). Compound 1 was obtained by reacting 1,3-diamino-propan-2-ol with di-tert-butyl dicarbonate. Mesytilation of 1 generated compound 2 which was directly converted to 3 *via* nucleophilic substitution with sodium azide at elevated temperatures. Hydrogenation of azide 3 yielded amine 4 which was coupled with the relevant carboxylic acid to give amide 5. Deprotection of 5 using anhydrous HCl gave ammonium salt 6. Finally, platination of 5 with $[Pt(DMSO)_2Cl_2]$ yielded the final Pt-complexes 7 in varying low to moderate yields

Pt-alkyne-53 (MW 519.37 g/mol) and Pt-azide-64 (MW 485.23 g/mol) were dissolved at a concentration of 25 mM in dimethylformamide (DMF) at room temperature, with sonication. Compounds were aliquoted and stored at -20°C. Cisplatin (THP Medical) was dissolved in phosphate buffer saline (PBS) at a 10 mM concentration.

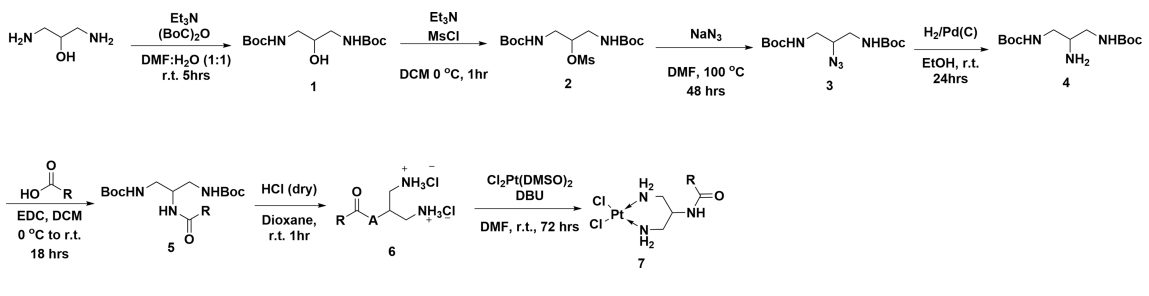

FIGURE 6 | Synthesis of clickable platinum compounds.

Human Cell Culture and CRISPR-Cas9-Mediated Knockout Cell Lines

All cells were grown at 37°C at 5% CO_2 and 3% O_2 and regularly analyzed for mycoplasma contamination. The human near-haploid chronic myeloid leukemia-derived HAP1 cell line was obtained from Horizon Discovery and grown in Iscove's Modified Dulbecco's Medium (IMDM, Gibco), containing L-glutamine and 25 nM N-(2-Hydroxyethyl)piperazine-N′-(2-ethanesulfonic acid) (HEPES) and supplemented with 10% Fetal Bovine Serum (FBS, Gibco) and 1% Penicillin/Streptomycin (P/S, Sigma-Aldrich). Human bone osteosarcoma epithelial U2OS cells were purchased from the ATCC cell repository and cultured in Dulbecco's Modified Eagle Medium (DMEM, Gibco), supplemented with 10% FBS and 1% P/S.

Clonal HAP1 cells deficient for FANCD2 were a kind gift from Ketan J. Patel (MRC Laboratory of Molecular Biology, Cambridge, UK). Ablation of protein expression was confirmed by immunoblotting for FANCD2. To generate clonal U2OS cells lacking XPF, cells were transiently transfected with plentiCRISPRv2 expressing a sgRNA targeting XPF (5'-TGGAACTGCTCGACACTGAC-3'). Transfected cells were selected with puromycin and clonally expanded. Ablation of protein expression was confirmed by immunoblotting for XPF, and hypersensitivity to ultraviolet and cisplatin of the knockout cells compared to wildtype was additionally validated. U2OS cells depleted for FANCD2 were generated by transfection using Lipofectamin RNAiMAX reagent and an siRNA targeting FANCD2 (5'-GCACCGUAUUCAAGUACAAUU-3').

Cell Viability Assay

Cells were seeded at a density of 3,000 cells per well in 96-well plates in appropriate media supplemented with the indicated compounds. A two-fold serial dilution starting from an initial concentration of 100 μM or 50 μM was used for U2OS or HAP1 cells, respectively. DMF alone was used as the background control for the cisplatin derivatives. After 3 days of treatment, residual cell viability was measured by addition of CellTiter-Glo 2.0 solution (Promega) following the manufacturer's recommendations. Luminescence was evaluated using the plate reader Infinite 200 PRO (Tecan Life Sciences). Relative cell viabilities normalized to the DMF-treated control of each cell line were calculated using the Prism software version 9.2.0 (GraphPad).

Colony Formation Assay

Cells were seeded at a density of 800 cells per well in 6-well plates in medium containing respective concentrations of cisplatin, or its derivatives. Different compound concentrations were prepared by four-fold serial dilutions starting from an initial concentration of 75 μM. DMF alone was used as the negative control for the cisplatin derivatives. After 7-8 days of treatment, cells were gently washed with PBS, fixed with 3.7% formaldehyde and stained with 0.1% crystal violet in 10% ethanol in water for 30 minutes. Stained cells were then washed with water and let dried. Colony area was quantified using the ColonyArea plugin in ImageJ (38) and normalized to the highest value. The experiment was performed in three biological replicates.

Pull-Down of Clickable Platinum Derivatives

Pull-down of Pt-alkyne-53 was performed according to the published aniPOND method (39). Briefly, after treatment of U2OS cells with Pt-alkyne-53 or cisplatin for 12 hours, chromatin fractions were extracted in native conditions. The CuAAC click reaction was then performed with biotin-dPEG7-azide (QBD10825, Sigma-Aldrich) and after washes, the clicked chromatin fractions were solubilized by sonication in lysis buffer. After protein quantification using the Protein Assay Dye Reagent (Biorad), equal amounts of inputs were incubated with streptavidin agarose beads overnight. The following day, after extensive washes, bound proteins were eluted in NuPAGE LDS Buffer (Invitrogen). Input samples were also mixed with NuPAGE LDS Buffer and boiled for 5 minutes before immunoblotting.

Immunoblotting

Cells were lysed in RIPA lysis buffer (New England Biolabs), sonicated and protein concentrations were measured using the Protein Assay Dye Reagent (Biorad). Samples were mixed with NuPAGE LDS Sample Buffer (Invitrogen), boiled for 5 minutes at 98°C and proteins were separated on SDS-PAGE gels and transferred onto Amersham™ Protran nitrocellulose membranes (0.45μm, Cytiva) for confirmation of the knockout status of cell lines, or onto Amersham™ Hybond PVDF membrane (0.2 μm, Cytiva) for the identification of Pt-alkyne-53 interactors. After 1 hour of blocking in 5% milk in TBS-T (0.1% Tween 20 in 1x Tris-buffered saline), membranes were incubated with primary antibodies at 4°C overnight. Primary antibodies used were against FANCD2 (diluted 1:1,000, EPR2302 Abcam), XPF (diluted 1:500, 3F2/3 Santa Cruz), PCNA (diluted 1:500, PC10 Santa Cruz) and H3 (diluted 1:15000, ab1791 Abcam), and as a loading control, against Tubulin (diluted 1:10,000, DM1A Cell Signaling). Anti-mouse and anti-rabbit HRP-conjugated goat secondary antibodies (Jackson Immunochemicals) were used at a final dilution of 1:5,000. Immunoblots were imaged using a Curix 60 (AGFA) table-top processor.

Immunofluorescence and Microscopy

For microscopy-based experiments, cells were either seeded in 384-well plates (CellCarrier-Ultra, Perkin Elmer) for γH2AX immunofluorescence, or 18-well Ibidi chambers for detection of the cisplatin derivatives by CuAAC click reaction with a fluorescent dye. After treatment with cisplatin derivatives, DMF, or cisplatin, U2OS cells were fixed with 2% paraformaldehyde in PBS for 20 minutes at room temperature, washed twice with PBS, permeabilized with 0.5% Triton-X in PBS for 10 minutes at room temperature, washed twice with PBS and blocked for 1 hour with 5% BSA in 0.1% Tween20 in PBS (PBS-T).

For γH2AX immunofluorescence, staining with γH2AX antibody (diluted 1:800, JBW301 Merck Millipore) was performed overnight at 4°C in 5% BSA in PBS-T. After three washes with 3% BSA in PBS, staining with mouse-AF568

secondary antibody (diluted 1:2,000, A11004 Molecular Probes) was performed for 1 hour at room temperature. After three washes with 3% BSA in PBS and one wash with PBS, followed by DAPI staining and washes with PBS, cells were imaged. Imaging was performed either with an Opera high-throughput microscope (Perkin Elmer), using the x40 magnification in confocal mode for quantification, or Olympus IXplore SpinSR spinning disk confocal microscope, using the x63 magnification for display of representative images.

For microscopy following the CuAAC click reaction of the cisplatin derivatives, cells were washed with PBS after blocking, and CuAAC click reaction mix was applied to the cells within 10 minutes of preparation, for 1 hour in the dark. The CuAAC click reaction mix composition was: 1 μM AF488-picolyl-azide (from kit C10641, Invitrogen) or 5 μM AF488-alkyne (CLK-1277-1, Jena Bioscience), pre-mixed $CuSO_4$:THPTA (2 mM $CuSO_4$ (Jena Bioscience), 4 mM THPTA (762342, Sigma-Aldrich), final concentrations), 10 mM sodium ascorbate (PHR1279, Sigma-Aldrich) diluted in PBS. After extensive washes (3% BSA in PBS for 5 minutes, 0.5% Triton-X in PBS for 2x10 minutes, PBS for 2x10 minutes), followed by DAPI staining and washes with PBS, cells were imaged, using Zeiss LSM700 confocal microscope and x63 magnification.

Quantification of the number of foci per cell was done using CellProfiler software version 4.1.3 and visualization with ImageJ Fiji.

Dot Blot of Clickable Platinum Compounds

After treatment with cisplatin derivatives, DMF or cisplatin, U2OS cells were fixed with 1% formaldehyde in PBS for 10 minutes at room temperature. Formaldehyde was quenched with glycine, and after washing with 0.05% Tween20 in PBS, cells were scrapped off, and pellets were frozen in liquid nitrogen. After thawing and washing with PBS, cells were permeabilized with 0.25% Triton-X in PBS for 45 minutes at room temperature. After washes using 0.5% BSA in PBS followed by PBS, CuAAC click reaction on whole cell extracts was performed for 1 hour at room temperature in the dark. The CuAAC click reaction mix composition was: 100 μM biotin-dPEG7-azide (QBD10825, Sigma-Aldrich) or 100 μM biotin-PEG4-alkyne (764213, Sigma-Aldrich), pre-mixed CuSO4:THPTA (2 mM CuSO4 (Jena Bioscience), 4 mM THPTA (762342, Sigma-Aldrich), final concentrations), 10 mM sodium ascorbate (PHR1279, Sigma-Aldrich) diluted in PBS. Cells were washed with 0.5% BSA in PBS and PBS, lysed in 50 mM TrisHCl pH 8.0 with 0.5% SDS and sonicated. Following 45 minute RNaseA treatment at 37°C and overnight crosslink-reversal with proteinase K and SDS at 65°C, DNA was extracted using phenol:chloroform: isoamylalcohol (25:24:1, ThermoFisher) and ethanol precipitated.

After Qubit quantification, equal quantities of DNA were denatured by addition of NaOH and EDTA (final concentrations: 0.4 M NaOH, 10mM EDTA) and heating at 100 oC for 10 minutes, followed by neutralization with an equal volume of cold 2 M ammonium acetate, pH 7.0. Blotting was done on a nitrocellulose membrane using a Bio-Dot apparatus (Biorad). After baking of the membrane for 2 hours at 80°C under vacuum, the membrane was washed once with TBS-T and blocked with 5% BSA in TBS-T for 1 hour at room temperature. The membrane was incubated with streptavidin-HRP (diluted 1:5,000 in 3% BSA in TBS-T, Cell signaling) for 45 minutes at room temperature, then washed once with 0.5% BSA in TBS-T for 10 minutes, twice with 10mM TrisHCl pH 8.0 with 10mM NaCl and 2mM MgCl2 for 5 minutes, and once with TBS-T for 5 minutes. Biotin-streptavidin-HRP complex was detected with ECL. Quantification of DNA loading was performed using methylene blue (0.1% in 0.5 M sodium acetate, pH 5.2).

DATA AVAILABILITY STATEMENT

The original contributions presented in the study are included in the article/**Supplementary Material**. Further inquiries can be directed to the corresponding author.

AUTHOR CONTRIBUTIONS

AM, JS, MMU and JIL conceptualized the study. JS, MMU and JIL obtained funding. MES carried out all chemical synthesis and chemical characterization of the compounds. AM, JS, MM and EAA-V carried out all cell-based investigations. AM, JS and DAC-I performed analysis and visualization. MMU and JIL supervised the study. JIL wrote the original draft and all authors reviewed and edited the final manuscript.

FUNDING

AM was funded by the Austrian Science Fund (grant number P 33024 awarded to JIL). JS was supported by a Marie Sklodowska-Curie Individual Fellowship of the European Commission (843630 REAP). The Loizou lab is funded by an ERC Synergy Grant (DDREAMM Grant agreement ID: 855741). The Unterlass lab's contributions to this study were funded by the Austrian Science Fund FWF START grant HYDROCOF (number Y1037-N38) and the Vienna Science and Technology Fund (WWTF) under grant number LS17-051. This work was funded, in part, by a donation from Benjamin Landesmann. The funder was not involved in the study design, collection, analysis, interpretation of data, the writing of this article or the decision to submit it for publication. CeMM is funded by the Austrian Academy of Sciences.

ACKNOWLEDGMENTS

We are thankful to Prof KJ Patel (Weatherall Institute of Molecular Medicine, Oxford, UK) for providing the FANCD2 deficient HAP1 cell line. We thank Gerald Timelthaler (Institute of Cancer Research, Imaging Facility) for assistance with the microscopy. We are grateful to all other members of the Loizou lab, as well as Fabián Amaya-García and all members of the Unterlass lab, for helpful discussions and feedback.

SUPPLEMENTARY MATERIAL

The Supplementary Material for this article can be found online at: https://www.frontiersin.org/articles/10.3389/fonc.2022.874201/full#supplementary-material

REFERENCES

1. Chen X, Wu Y, Dong H, Zhang CY, Zhang Y. Platinum-Based Agents for Individualized Cancer Treatment. *Curr Mol Med* (2013) 13(10):1603–12. doi: 10.2174/15665240133666131111125515
2. Rottenberg S, Disler C, Perego P. The Rediscovery of Platinum-Based Cancer Therapy. *Nat Rev Cancer* (2021) 21(1):37–50. doi: 10.1038/s41568-020-00308-y
3. Chirnomas D, Taniguchi T, de la Vega M, Vaidya AP, Vasserman M, Hartman AR, et al. Chemosensitization to Cisplatin by Inhibitors of the Fanconi Anemia/Brca Pathway. *Mol Cancer Ther* (2006) 5(4):952–61. doi: 10.1158/1535-7163.MCT-05-0493
4. Hu J, Lieb JD, Sancar A, Adar S. Cisplatin DNA Damage and Repair Maps of the Human Genome at Single-Nucleotide Resolution. *Proc Natl Acad Sci USA* (2016) 113(41):11507–12. doi: 10.1073/pnas.1614430113
5. Lopez-Martinez D, Liang CC, Cohn MA. Cellular Response to DNA Interstrand Crosslinks: The Fanconi Anemia Pathway. *Cell Mol Life Sci* (2016) 73(16):3097–114. doi: 10.1007/s00018-016-2218-x
6. Noll DM, Mason TM, Miller PS. Formation and Repair of Interstrand Cross-Links in DNA. *Chem Rev* (2006) 106(2):277–301. doi: 10.1021/cr040478b
7. Fousteri M, Mullenders LH. Transcription-Coupled Nucleotide Excision Repair in Mammalian Cells: Molecular Mechanisms and Biological Effects. *Cell Res* (2008) 18(1):73–84. doi: 10.1038/cr.2008.6
8. Marteijn JA, Lans H, Vermeulen W, Hoeijmakers JH. Understanding Nucleotide Excision Repair and Its Roles in Cancer and Ageing. *Nat Rev Mol Cell Biol* (2014) 15(7):465–81. doi: 10.1038/nrm3822
9. Vermeulen W, Fousteri M. Mammalian Transcription-Coupled Excision Repair. *Cold Spring Harb Perspect Biol* (2013) 5(8):a012625. doi: 10.1101/cshperspect.a012625
10. Niedernhofer LJ, Lalai AS, Hoeijmakers JH. Fanconi Anemia (Cross)Linked to DNA Repair. *Cell* (2005) 123(7):1191–8. doi: 10.1016/j.cell.2005.12.009
11. Chen SH, Chang JY. New Insights Into Mechanisms of Cisplatin Resistance: From Tumor Cell to Microenvironment. *Int J Mol Sci* (2019) 20(17):4136. doi: 10.3390/ijms20174136
12. Siddik ZH. Cisplatin: Mode of Cytotoxic Action and Molecular Basis of Resistance. *Oncogene* (2003) 22(47):7265–79. doi: 10.1038/sj.onc.1206933
13. Hill DP, Harper A, Malcolm J, McAndrews MS, Mockus SM, Patterson SE, et al. Cisplatin-Resistant Triple-Negative Breast Cancer Subtypes: Multiple Mechanisms of Resistance. *BMC Cancer* (2019) 19(1):1039. doi: 10.1186/s12885-019-6278-9
14. Patel TH, Norman L, Chang S, Abedi S, Liu C, Chwa M, et al. European Mtdna Variants Are Associated With Differential Responses to Cisplatin, an Anticancer Drug: Implications for Drug Resistance and Side Effects. *Front Oncol* (2019) 9:640. doi: 10.3389/fonc.2019.00640
15. Kolb HC, Finn MG, Sharpless KB. Click Chemistry: Diverse Chemical Function From a Few Good Reactions. *Angewandte Chemie Int Edition* (2001) 40(11):2004–21. doi: 10.1002/1521-3773(20010601)40:11<2004::Aid-anie2004>3.0.Co;2-5
16. Rostovtsev VV, Green LG, Fokin VV, Sharpless KB. A Stepwise Huisgen Cycloaddition Process: Copper(I)-Catalyzed Regioselective "Ligation" of Azides and Terminal Alkynes. *Angewandte Chemie Int Edition* (2002) 41(14):2596–9. doi: 10.1002/1521-3773(20020715)41:14<2596::Aid-anie2596>3.0.Co;2-4
17. Tornoe CW, Christensen C, Meldal M. Peptidotriazoles on Solid Phase: [1,2,3]-Triazoles by Regiospecific Copper(I)-Catalyzed 1,3-Dipolar Cycloadditions of Terminal Alkynes to Azides. *J Org Chem* (2002) 67 (9):3057–64. doi: 10.1021/jo011148j
18. Kelland L. The Resurgence of Platinum-Based Cancer Chemotherapy. *Nat Rev Cancer* (2007) 7(8):573–84. doi: 10.1038/nrc2167
19. Wirth R, White JD, Moghaddam AD, Ginzburg AL, Zakharov LN, Haley MM, et al. Azide Vs Alkyne Functionalization in Pt(Ii) Complexes for Post-Treatment Click Modification: Solid-State Structure, Fluorescent Labeling, and Cellular Fate. *J Am Chem Soc* (2015) 137(48):15169–75. doi: 10.1021/jacs.5b09108
20. van der Heijden MS, Brody JR, Dezentje DA, Gallmeier E, Cunningham SC, Swartz MJ, et al. *In Vivo* Therapeutic Responses Contingent on Fanconi Anemia/Brca2 Status of the Tumor. *Clin Cancer Res* (2005) 11(20):7508–15. doi: 10.1158/1078-0432.CCR-05-1048
21. Ding S, Qiao X, Suryadi J, Marrs GS, Kucera GL, Bierbach U. Using Fluorescent Post-Labeling to Probe the Subcellular Localization of DNA-Targeted Platinum Anticancer Agents. *Angew Chem Int Ed Engl* (2013) 52 (12):3350–4. doi: 10.1002/anie.201210079
22. Legin AA, Schintlmeister A, Sommerfeld NS, Eckhard M, Theiner S, Reipert S, et al. Nano-Scale Imaging of Dual Stable Isotope Labeled Oxaliplatin in Human Colon Cancer Cells Reveals the Nucleolus as a Putative Node for Therapeutic Effect. *Nanoscale Adv* (2021) 3(1):249–62. doi: 10.1039/d0na00685h
23. Osborn MF, White JD, Haley MM, DeRose VJ. Platinum-Rna Modifications Following Drug Treatment in sCerevisiae Identified by Click Chemistry and Enzymatic Mapping. *ACS Chem Biol* (2014) 9(10):2404–11. doi: 10.1021/cb500395z
24. Karasawa T, Sibrian-Vazquez M, Strongin RM, Steyger PS. Identification of Cisplatin-Binding Proteins Using Agarose Conjugates of Platinum Compounds. *PloS One* (2013) 8(6):e66220. doi: 10.1371/journal.pone.0066220
25. Cowell IG, Sunter NJ, Singh PB, Austin CA, Durkacz BW, Tilby MJ. Gammah2ax Foci Form Preferentially in Euchromatin After Ionising-Radiation. *PloS One* (2007) 2(10):e1057. doi: 10.1371/journal.pone.0001057
26. Podratz JL, Knight AM, Ta LE, Staff NP, Gass JM, Genelin K, et al. Cisplatin Induced Mitochondrial DNA Damage in Dorsal Root Ganglion Neurons. *Neurobiol Dis* (2011) 41(3):661–8. doi: 10.1016/j.nbd.2010.11.017
27. Yang Z, Schumaker LM, Egorin MJ, Zuhowski EG, Guo Z, Cullen KJ. Cisplatin Preferentially Binds Mitochondrial DNA and Voltage-Dependent Anion Channel Protein in the Mitochondrial Membrane of Head and Neck Squamous Cell Carcinoma: Possible Role in Apoptosis. *Clin Cancer Res* (2006) 12(19):5817–25. doi: 10.1158/1078-0432.CCR-06-1037
28. Macheret M, Halazonetis TD. Monitoring Early S-Phase Origin Firing and Replication Fork Movement by Sequencing Nascent DNA From Synchronized Cells. *Nat Protoc* (2019) 14(1):51–67. doi: 10.1038/s41596-018-0081-y
29. Tilby MJ, Johnson C, Knox RJ, Cordell J, Roberts JJ, Dean CJ. Sensitive Detection of DNA Modifications Induced by Cisplatin and Carboplatin *In Vitro* and *In Vivo* Using a Monoclonal Antibody. *Cancer Res* (1991) 51(1):123–9.
30. Yang Y, Adebali O, Wu G, Selby CP, Chiou YY, Rashid N, et al. Cisplatin-DNA Adduct Repair of Transcribed Genes Is Controlled by Two Circadian Programs in Mouse Tissues. *Proc Natl Acad Sci U.S.A.* (2018) 115(21):E4777–E85. doi: 10.1073/pnas.1804493115
31. Yimit A, Adebali O, Sancar A, Jiang Y. Differential Damage and Repair of DNA-Adducts Induced by Anti-Cancer Drug Cisplatin Across Mouse Organs. *Nat Commun* (2019) 10(1):309. doi: 10.1038/s41467-019-08290-2
32. Meczes EL, Azim-Araghi A, Ottley CJ, Pearson DG, Tilby MJ. Specific Adducts Recognised by a Monoclonal Antibody Against Cisplatin-Modified DNA. *Biochem Pharmacol* (2005) 70(12):1717–25. doi: 10.1016/j.bcp.2005.09.025
33. Deans AJ, West SC. DNA Interstrand Crosslink Repair and Cancer. *Nat Rev Cancer* (2011) 11(7):467–80. doi: 10.1038/nrc3088
34. Casini A, Reedijk J. Interactions of Anticancer Pt Compounds With Proteins: An Overlooked Topic in Medicinal Inorganic Chemistry? *Chem Sci* (2012) 3 (11):3135–44. doi: 10.1039/c2sc20627g
35. Chvalova K, Brabec V, Kasparkova J. Mechanism of the Formation of DNA-Protein Cross-Links by Antitumor Cisplatin. *Nucleic Acids Res* (2007) 35 (6):1812–21. doi: 10.1093/nar/gkm032
36. Farrer NJ, Griffith DM. Exploiting Azide-Alkyne Click Chemistry in the Synthesis, Tracking and Targeting of Platinum Anticancer Complexes. *Curr Opin Chem Biol* (2020) 55:59–68. doi: 10.1016/j.cbpa.2019.12.001
37. Cunningham RM, DeRose VJ. Platinum Binds Proteins in the Endoplasmic Reticulum of S. Cerevisiae and Induces Endoplasmic Reticulum Stress. *ACS Chem Biol* (2017) 12(11):2737–45. doi: 10.1021/acschembio.7b00553
38. Guzman C, Bagga M, Kaur A, Westermarck J, Abankwa D. Colonyarea: An Imagej Plugin to Automatically Quantify Colony Formation in Clonogenic Assays. *PloS One* (2014) 9(3):e92444. doi: 10.1371/journal.pone.0092444
39. Leung KH, Abou El Hassan M, Bremner R. A Rapid and Efficient Method to Purify Proteins at Replication Forks Under Native Conditions. *Biotechniques* (2013) 55(4):204–6. doi: 10.2144/000114089

Conflict of Interest: The authors declare that the research was conducted in the absence of any commercial or financial relationships that could be construed as a potential conflict of interest.

this article, or claim that may be made by its manufacturer, is not guaranteed or endorsed by the publisher.

frontiers | Frontiers in Oncology

ORIGINAL RESEARCH
published: 07 June 2022
doi: 10.3389/fonc.2022.925653

The Synergistic Cytotoxic Effects of GW5074 and Sorafenib by Impacting Mitochondrial Functions in Human Colorectal Cancer Cell Lines

Je-Ming Hu[1,2], *Yung-Lung Chang*[1,3], *Cheng-Chih Hsieh*[4,5] *and Shih-Ming Huang*[1,3*]

[1] *Institute of Medical Sciences, National Defense Medical Center, Taipei, Taiwan,* [2] *Department of Surgery, Division of Colorectal Surgery, Tri-Service General Hospital, National Defense Medical Center, Taipei, Taiwan,* [3] *Department of Biochemistry, National Defense Medical Center, Taipei, Taiwan,* [4] *School of Pharmacy and Institute of Pharmacy, National Defense Medical Center, Taipei, Taiwan,* [5] *Department of Pharmacy, Kaohsiung Veterans General Hospital, Kaohsiung, Taiwan*

OPEN ACCESS

Edited by:
Veronika Vymetalkova, Academy of Sciences of the Czech Republic (ASCR), Czechia

Reviewed by:
Monika Sramkova, Biomedical Research Center SAS, Slovakia
Alessio Naccarati, Italian Institute for Genomic Medicine (IIGM), Italy

***Correspondence:**
Shih-Ming Huang
shihming@ndmctsgh.edu.tw

Specialty section:
This article was submitted to Gastrointestinal Cancers: Colorectal Cancer, a section of the journal Frontiers in Oncology

Received: *21 April 2022*
Accepted: *18 May 2022*
Published: *07 June 2022*

Citation:
Hu J-M, Chang Y-L, Hsieh C-C and Huang S-M (2022) The Synergistic Cytotoxic Effects of GW5074 and Sorafenib by Impacting Mitochondrial Functions in Human Colorectal Cancer Cell Lines. Front. Oncol. 12:925653. doi: 10.3389/fonc.2022.925653

Colorectal cancer (CRC) ranks third in the United States for incidence or mortality. Surgical resection is the primary treatment for patients at an early stage, while patients with advanced and metastatic CRC receive combined treatment with chemotherapy, radiotherapy, or targeted therapy. C-RAF plays a key role in maintaining clonogenic and tumorigenic capacity in CRC cells and it might be a potential therapeutic target for CRC. Sorafenib is a popular oral multi-kinase inhibitor, including a B-RAF inhibitor that targets the RAF-MEK-ERK pathway. Sorafenib, as a single agent, has tumor-suppressing efficacy, but its clinical application is limited due to many complex drug resistance mechanisms and side effects. GW5074 is one of the C-RAF inhibitors and has the potential to enhance the efficacy of existing cancer chemotherapies. In this study, we investigated whether the combination of sorafenib with GW5074 could reduce the dosage of sorafenib and enhance its tumor-suppressive effect in two CRC cell lines, HCT116 and LoVo cells. Our findings demonstrate that GW5074 can potentiate the cytotoxicity of sorafenib and dramatically reduce the half-maximal inhibitory concentration (IC50) dose of sorafenib from 17 and 31 μM to 0.14 and 0.01 μM in HCT116 and LoVo cells, respectively. GW5074, similar to sorafenib, suppressed the cellular proliferation and induced cellular apoptosis and cytosolic ROS, but had no further enhancement on the above-mentioned effects when combined with sorafenib. The synergistic effects of GW5074 and sorafenib were mainly found in mitochondrial functions, including ROS generation, membrane potential disruption, and fission–fusion dynamics, which were examined by using the flow cytometry analysis. In summary, the C-RAF inhibitor GW5074 might potentiate the cytotoxicity of the B-RAF inhibitor sorafenib mediated through mitochondrial dysfunctions, suggesting that GW5074 potentially serves as a sensitizer for sorafenib application to reduce the risk of drug resistance of CRC treatment. Our findings also provide novel

insights on using C-RAF inhibitors combined with sorafenib, the current CRC therapeutic drug choice, in CRC treatment.

Keywords: colorectal cancer, C-RAF inhibitor, multi-kinase inhibitor, mitochondrial dysfunction, the combination index

INTRODUCTION

In the 2022 annual cancer statistics report of the American Cancer Society, colorectal cancer (CRC) ranks third in the United States for incidence or mortality, regardless of gender (1). Genetic and environmental factors contribute significantly to the etiology of CRC, including family history, smoking, alcohol intake, obesity, diabetes, inflammatory bowel disease, etc. (2). Surgical resection is the primary treatment for patients at an early stage, while patients with advanced and metastatic CRC (mCRC) are treated with chemotherapy such as 5-fluorouracil, oxaliplatin, etc., combined with radiotherapy and targeted therapy (3). However, in 25% of patients with advanced mCRC, the surgical effect is very limited. The efficacy of chemotherapy may also be reduced by the development of drug resistance and cancer recurrence. Therefore, a new drug or combinatory therapy for CRC treatment, especially mCRC, is urgently needed to improve its overall survival rate.

Since CRC is a disease that accumulates multiple genetic mutations in the epithelial tissue of the colon and rectum, molecular biomarkers play an important role in the individualized treatment of CRC patients (4). Using these biomarkers such as RAS, B-RAF, and microsatellite instability status, the prognosis for CRC patients can be stratified, and more precise adjuvant treatment plans can be provided (5). Activation of mitogen-activated protein kinase (MAPK) pathways that regulate multiple cellular activities including proliferation, differentiation, and apoptosis have been identified as the critical oncogenic mechanisms in CRC (6). RAF kinases (A-RAF, B-RAF, and C-RAF), which play an integral role in this pathway, are regulated through a network of protein–protein interactions and phosphorylation–dephosphorylation events (7). B-RAF is the family member most easily activated by RAS because both A-RAF and C-RAF need additional steps to reach maximal activation. In addition, B-RAF (V600E) mutation is a driver mutation—it constitutively activates the MAPK/extracellular signal-regulated kinase (ERK) kinase (MEK)-ERK signaling pathway downstream of KRAS (8), which is present in 5–15% of CRC (9).

The contribution of RAF to the hallmarks and phenotypes of cancer is reported. Three types of RAF enforce the dimerization of endogenous RAFs, such as B-RAF with C-RAF or A-RAF. RAF kinases are prime targets for the design and application of molecule-target therapies for cancers, including melanoma, renal cancer cells, and hepatocellular carcinoma. Cancer cells develop chemo-resistance by several different molecular mechanisms involving the activation of other MEK kinases, but also the upregulation of receptor tyrosine kinases and other pathways downstream from RAS (10). The underlying mechanism is an allosteric effect of the RAF inhibitors, the paradoxical increase in the proliferation and activation of the MEK–ERK pathway in cells. Until now, RAF is still a fascinating topic for basic and clinical researchers.

Sorafenib is an oral multi-kinase inhibitor that targets the RAF-MEK-ERK pathway, which can promote apoptosis and reduce angiogenesis and inhibit tumor cell proliferation (11–13). Furthermore, it modulates the RAF-MEK-ERK pathway by inhibiting C- and B-RAF, thereby affecting tumor cell proliferation, even in KRAS-mutated cancers (14). Sorafenib has recently been used as a targeted treatment for mCRC patients, where its therapeutic value has been recognized (15, 16). However, while sorafenib has tumor-suppressing efficacy as a single agent, its clinical application is limited by many complex drug resistance mechanisms and side effects. C-RAF plays a key role in maintaining clonogenic and tumorigenic capacity in CRC cells (containing KRAS mutations), and it might be a potential therapeutic target for CRC (17). GW5074 is one of the C-RAF inhibitors which are broad-spectrum antitumor agents and have the potential to enhance the efficacy of existing cancer chemotherapies (18, 19). Despite their potency, C-RAF inhibitors lack relative therapeutic efficacy due to poor bioavailability.

A recent study demonstrated the effectiveness of the combination of sorafenib and GW5074 for renal cancer cells, targeting C-RAF for the regulation of its mitochondrial localization and function involved in cell death cascades (20). Here, we investigated whether the combination of sorafenib with GW5074 could reduce the dosage of sorafenib and enhance its tumor-suppressive effect in two CRC cell lines, HCT116 and LoVo cells. Our findings also provide novel insights on using C-RAF inhibitors in CRC treatment.

MATERIALS AND METHODS

Cell Culture and Chemical

HCT116 and LoVo cells were cultured in Dulbecco's modified Eagle's medium (DMEM) containing 10% fetal bovine serum (FBS) and 1% penicillin streptomycin (Invitrogen, CA, USA) at 37°C and 5% CO_2. GW5074 (3-(3,5-Dibromo-4-hydroxy-benzylidene)-5-iodo-1,3-dihydro-indol-2-one), sorafenib, and 2',7-dichlorofluorescein diacetate (DCFH-DA) were obtained from Sigma-Aldrich (MO, USA).

Metabolic Activity Analysis and the Combination Index

MTS (3-(4,5-dimethylthiazol-2-yl)-5-(3-carboxymethoxyphenyl)-2-(4-sulfophenyl)- 2H-tetrazolium) assay was performed using the CellTiter 96 Aqueous One Solution Cell Proliferation Assay kit (Promega, WI, USA). Briefly, HCT116 and LoVo cells were seeded

onto 96-well plates and cultured in the presence of the indicated drugs for 24 h. The cells were then incubated with MTS solution (20 μl/well) for 2 h at 37°C, and the absorbances at 490 nm were measured using an ELISA plate reader (Multiskan EX, Thermo, MA, USA). The relative metabolic activity was calculated based on the absorbance ratio between cells cultured with the indicated drugs and the vehicle control, which were assigned a value of 100.

The combination index (CI) was calculated utilizing CalcuSyn (Biosoft, Cambridge, UK) to generate the isobolograms for the determination of synergistic, additive, and antagonistic combinatory effect. Typically, a CI value <1 denotes a synergistic combination effect, and a CI value >1 denotes an antagonistic combination effect (21).

Fluorescence-Activated Cell Sorting, Cell Cycle Profiling, and Cellular Proliferation Analyses

For cell cycle profile and cellular proliferation, we performed BrdU/7-AAD analysis with the FITC BrdU Flow Kit (BD Biosciences, CA, USA) according to the manufacturer's instructions. Cell cycle profiles were measured according to cellular DNA content using FACS. Cells were fixed in 70% ice-cold ethanol, stored at −30°C overnight, washed two times with ice-cold PBS supplemented with 1% FBS, and then stained with 7-AAD (7-Aminoactinomycin D). The percentage of positive HCT116 and LoVo cells was determined using flow cytometry. All samples were analyzed using a FACSCalibur flow cytometer (BD Biosciences). Data were analyzed using Cell Quest Pro software (BD Biosciences). Procedural details were described previously (22, 23).

Apoptosis and ROS Assays

To evaluate the incidence of apoptosis, we used the PE Annexin V Apoptosis Detection Kit according to the manufacturer's instructions (BD Biosciences). Apoptotic cells were then analyzed using flow cytometry. To detect the production of ROS, we plated cells in 6-well plates and treated GW5074 and sorafenib. After 24 h of drug treatment, living cells were stained with 20 μM DCFH-DA (Sigma-Aldrich) and incubated at 37°C for 1 h. Stained cells were determined using flow cytometry.

Mitochondrial ROS Assay

The fluorescent marker MitoSOX^{TM}Red (Invitrogen) was used to determine mitochondrial ROS levels. Cells were incubated for the indicated times with different combinations of GW5074 and sorafenib. Living cells were then stained with 5 μM MitoSOX^{TM}Red and harvested for 10 min at 37°C. After washing the cells once with PBS, they were determined using flow cytometry.

Mitochondrial Fission–Fusion Transient Analysis

HCT116 and LoVo cells were seeded onto 6-well plates. After treating the cells for the indicated times with selected combinations of GW5074 and sorafenib, the cells were washed, incubated with 100 nM MitoView^{TM}Green (Biotium, CA, USA) at 37°C for 15 min, and washed again three times with PBS. They were determined using flow cytometry.

Mitochondrial Membrane Potential Analysis

Mitochondrial depolarization was measured as a function of a decrease in the red/green fluorescence intensity ratio. All dead and viable cells were harvested, washed with PBS, and incubated with 1× binding buffer containing the MMP-sensitive fluorescent dye JC-1 for 30 min at 37°C in the dark. After washing the cells once with PBS, JC-1 fluorescence was analyzed on channels FL-1 and FL-2 of the FACSCalibur flow cytometer using Cell Quest Pro software (BD Biosciences) to detect monomer (green fluorescence) and aggregate (red fluorescence) forms of the dye, respectively. The cell volume gating strategy involved forward scatter height (FSC-H) and side scatter height (SSC-H), and the median fluorescence intensity of the vehicle was used as the starting point for M2 gating.

Western Blotting

HCT116 and LoVo cells were lysed in radioimmunoprecipitation assay buffer (100 mM Tris-HCl (pH 8.0), 150 mM NaCl, 0.1% SDS, and 1% Triton X-100) at 4°C. Proteins in the resultant lysates were separated by sodium dodecyl sulfate-polyacrylamide gel electrophoresis and analyzed by immunoblotting with antibodies against ACTN (sc-17829, mouse), ATF1 (sc-243, mouse), ATF3 (sc-81189, mouse), ATF4 (sc-390063, mouse), ATF5 (sc-377168, mouse), catalase (sc-271803, mouse), DRP-1 (sc-101270, mouse), Mfn1 (sc-166644, mouse), Nrf2 (sc-365949, mouse), p62 (sc-28359, mouse), Parkin (sc-133167, mouse), PGC-1α (sc-518052, mouse), SOD1 (sc-101523, mouse), SOD2 (sc-133134, mouse), SOD3 (sc-377168, mouse), mtTFA (sc-376672, mouse), TFEB (sc-166736, mouse), Tom20 (sc-17764, mouse) (Santa Cruz Biotechnology, CA, USA), HO-1 (ADI-SPA-895-F, rabbit, Enzo life sciences, NY, USA), γ.H2AX (ab81299, rabbit, Abcam, Cambridge, UK), GAPDH (60004-1-1g, mouse), α-Tubulin (13730-1-AP, mouse) (Proteintech, IL, USA), XBP1 (NBP1-77253, rabbit), ATF6 (NBP1-40256, mouse) (Novus, CO, USA), AMPK (2535, rabbit), p-AMPK (5831, rabbit), Caspase 3 (9662, rabbit), CHOP (2895, mouse), p70S6K (2708, rabbit), p-p70S6K (9205, rabbit). p-DRP-1 (3455, rabbit), eIF2α (9722, rabbit), p-eIF2α (9721, rabbit), LC3B (2775, rabbit), and PARP (9542, rabbit) (Cell Signaling Technology, MA, USA). Thereafter, the blots were incubated with horseradish peroxidase-conjugated secondary antibody (Santa Cruz Biotechnology). The immunoreactive proteins were detected using ECL^{TM} Western Blotting Detection Reagent and Amersham Hyperfilm^{TM} ECL (GE Healthcare, IL, USA).

RNA Extraction and Reverse Transcription PCR

HCT116 and LoVo cells were lysed by TRIzol reagent (Invitrogen) to isolate total RNAs. Reverse transcription for first-strand cDNA synthesis was conducted using MMLV reverse transcriptase (Epicenter Biotechnologies, WI, USA) with 1 μg of total RNA for 60 min at 37°C. PCR reactions

were operated on a Veriti Thermal Cycler (Applied Biosystems, MA, USA). Primers and the number of PCR reaction cycles used were listed in **Table 1**.

Immunofluorescent Staining

Cells were incubated for 24 h on glass coverslips and then fixed for 5 min in 10% formaldehyde in PBS, permeabilized with 0.1% Triton X-100 in PBS, blocked with 1% BSA (Sigma, Burlington, MA, USA) in PBS, and incubated with mouse anti-human PGC-1a (Santa Cruz Biotechnology) or mouse anti-human Tom20 (Santa Cruz Biotechnology) in 1% BSA overnight at 4°C. Thereafter, the cells were washed three times with PBS and incubated with Alexa 488-goat anti-mouse IgG secondary antibody (1:400; ThermoFisher Scientific, Waltham, MA, USA) in 1% BSA for1 h at room temperature. After three more washes with PBS for 5 min each, the nuclei were stained with DAPI (Sigma, Burlington, MA, USA) for 5 min at room temperature. Finally, the coverslips were mounted on glass slides with a mounting medium (ThermoFisher Scientific, Waltham, MA, USA) and examined under a Leica Thunder microscope.

Statistical Analysis

Values were expressed as the mean ± SD of at least three independent experiments. All comparisons between groups (vehicle and drug) were conducted using Student's *t*-test. Statistical significance was set at $p < 0.05$.

RESULTS

The Cytotoxicity of Sorafenib and GW5074 and Their Combinatory Effect on HCT116 and LoVo Cell Lines

To explore the effects of two RAF inhibitors, B-RAF inhibitor sorafenib, and C-RAF inhibitor GW5074, on the human CRC cell lines, HCT116 and LoVo cells, the changes in cell viability were first determined using the MTT analysis. The results indicated that a significant decrease in metabolic activity was observed in HCT116 and LoVo cells with sorafenib treatment (**Figure 1**). Moreover, despite the higher dose of GW5074, the cell viability of HCT116 was still approximately 60% (**Figure 1A**), while LoVo cells did not respond at all (**Figure 1C**). Both HCT116 and LoVo cells responded well at a higher dosage of Sorafenib (**Figures 1B, D**). We further examined whether GW5074 had a synergistic effect on cell viability with sorafenib on HCT116 and LoVo cells using the combination index analysis. When the combination index score is less than 1, it means there is a synergistic effect, and when the score is greater than 1, it means there is an antagonistic effect. The results showed that combined treatment had a synergistic effect in HCT116 and LoVo cells, both of which could dramatically reduce the IC50 dose of sorafenib from 17 and 31 μM to 0.14 and 0.01 μM at the dosage of GW5074 0.034 and 0.003 μM, respectively (**Figure 2**).

The Functional Interactions Between Sorafenib and GW5074 in the Cell Cycle, Cellular Apoptosis, and Cellular Proliferation

Figure 1 showed that GW5074 consistently potentiates the cytotoxicity of sorafenib in CRC cells, similar to our previous finding in renal carcinoma cells (20). Next, we explored the effects of combined treatment on different cellular mechanisms of CRC cells, including the cell cycle profile, cellular apoptosis, cellular proliferation, and ROS generation. To determine the functional roles of sorafenib, GW5074, and both combined in the cell cycle profile, we treated HCT116 and LoVo cells with indicated amounts of sorafenib (0, 1, 3, 5, 7, and 10 μM), GW5074 (0, 20, and 40 μM), and both combined (0, 20, and 40 μM GW5074 combined with 10 μM sorafenib). Sorafenib increased the populations of subG1, G1, and G2/M phases and decreased the population of the S phase in a dose-dependent manner (**Figures 3A, C**). GW5074 increased the population of the subG1 phase and decreased the population of the S phase in a dose-dependent manner (**Figures 3B, D**). The combined results indicate that GW5074 failed to potentiate the effects of sorafenib

TABLE 1 | Primers were used in this study.

Gene name	Primer sequence (Forward)	Primer sequence (Reverse)	Cycle #
ATF1	5'-GCTCAACAGGTATCATCTTTATCAG-3'	5'-accacagtttgtggcagaga-3'	30
ATF3	5'-GAGGATTTTGCTAACCTGAC-3'	5'-TAGCTCTGCAATGTTCCTTC-3'	28
ATF4	5'-TTCCAGCAAAGCACCGCAAC-3'	5'-AGGGCATCCAAGTCGAACTCCT-3'	30
ATF5	5'-AAGTCGGCGGCTCTGAGGTA-3'	5'-GGACTCTGCCCGTTCCTTCA-3'	30
ATF6	5'-ATGAAGTTGTGTCAGAGAAC-3'	5'-GGGTGCTATTGTAATGACTCA-3'	30
CHOP	5'-CATTGCCTTTCTCCTTCGGG-3'	5'-GCCGTTCATTCTCTTCAGCT-3'	30
eIF2a	5'-ACCTCAGAATGCCGGGTCTA-3'	5'-GTGGGGTCAAGCGCCTATTA-3'	28
XBP1	5'-CCTTGTAGTTGAGAACCAGG-3'	5'-GGGGCTTGGTATATATGTGG-3'	30
TOM20	5'-GTGTATGCGGGGCCCTTTTC-3'	5'-ACATCATCTTCAGCCAAGCTCT-3'	28
mtTFA	5'-GCGTTTCTCCGAAGCATGTG-3'	5'-TTGTGCGACGTAGAAGATCC-3'	30
PGC-1α	5'-GTGTCACCACCCAAATCCTTA-3'	5'-ATTCTTCCCTCTTCAGCCTCT-3'	35
Parkin	5'-AAGGAGGTGGTTGCTAAGCGAC-3'	5'-CTGGGTCAAGGTGAGCGTTGC-3'	35
TFEB	5'-GGTGTTGAAGGTGCAGTCC-3'	5'-GGGTAGCGTGTTGGGCATCTG-3'	30
AMPK	5'-CGGCAAAGTGAAGGTTGGC-3'	5'-TCCTTCGTGGAGCCTGTTTT-3'	30
p70S6K	5'-GGAGCCTGGGAGCCCTGATGTA-3'	5'-GAAGCCCTCTTTGATGCTGTCC-3'	30
18S	5'-CAGCCACCCGAGATTGAGCA-3'	5'-TAGTAGCGACGGGCGGTGTG-3'	32

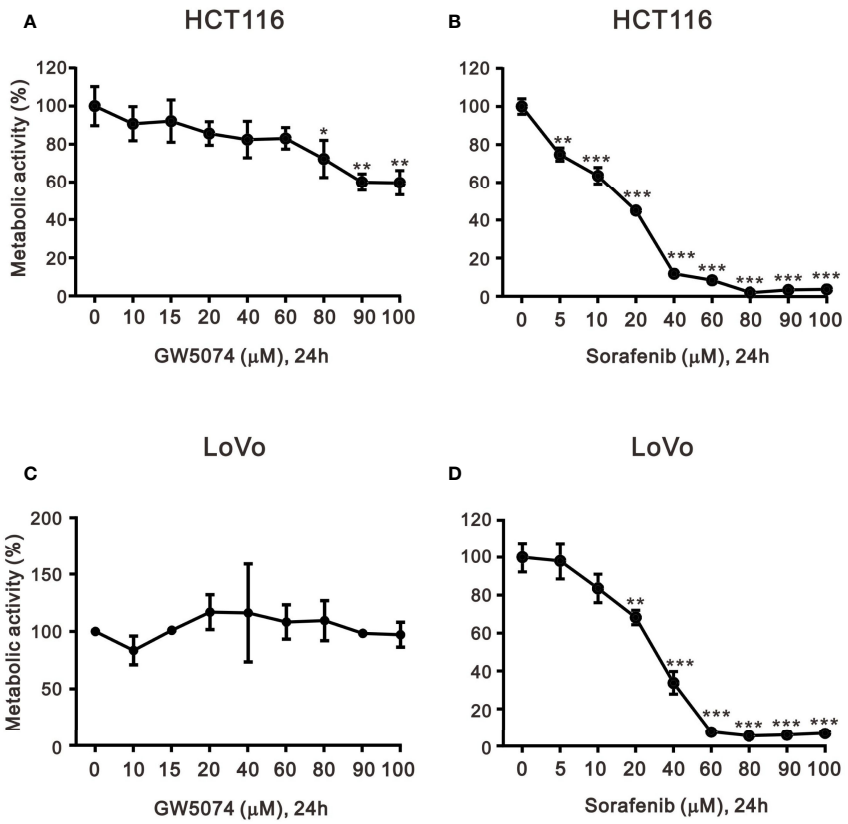

FIGURE 1 | The effects of GW5074 and sorafenib on the cytotoxicity of HCT116 and LoVo cells. HCT116 and LoVo cells **(A, C)** were treated with 0, 10, 15, 20, 40, 60, 80, and 100 μM GW5074 for 24 h; **(B, D)** were treated with 0, 5, 10, 20, 40, 60, 80, 90, and 100 μM sorafenib for 24 h. Metabolic activity was measured using MTS assays. The results are representative of three independent experiments. $^{*}p < 0.05$, $^{**}p < 0.01$, and $^{***}p < 0.001$.

on the cell cycle profile, except for the population of the subG1 phase in the highest dose combination (**Figures 3B, D**). The cleavage forms of PARP and caspase 3 are biomarkers for cellular apoptosis (24). Hence, we further examined the cleaved trends of PARP and caspase 3 to confirm the increase in the population of subG1 in HCT116 and LoVo cells. We observed increasing amounts of cleaved PARP and caspase 3 by sorafenib combined with increasing amounts of GW5074

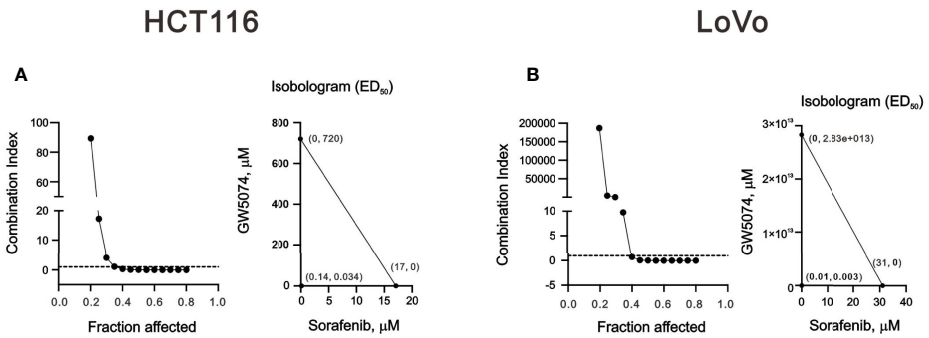

FIGURE 2 | The combination index of GW5074 and sorafenib in HCT116 and LoVo cells. HCT116 **(A)** and LoVo **(B)** cells were treated with 0, 0.313, 0.625, 1.25, 2.5, 5, 10, and 20 μM sorafenib for 24 h and 0, 0.625, 1.25, 2.5, 5, 10, 20, and 40 μM GW5074 for 24 h. Metabolic activity was measured using MTS assays. The combination index of sorafenib plus GW5074 in HCT116 **(A)** and LoVo **(B)** cells. Isobolograms (ED_{50}) of sorafenib or GW5074 were calculated using CalcuSyn software.

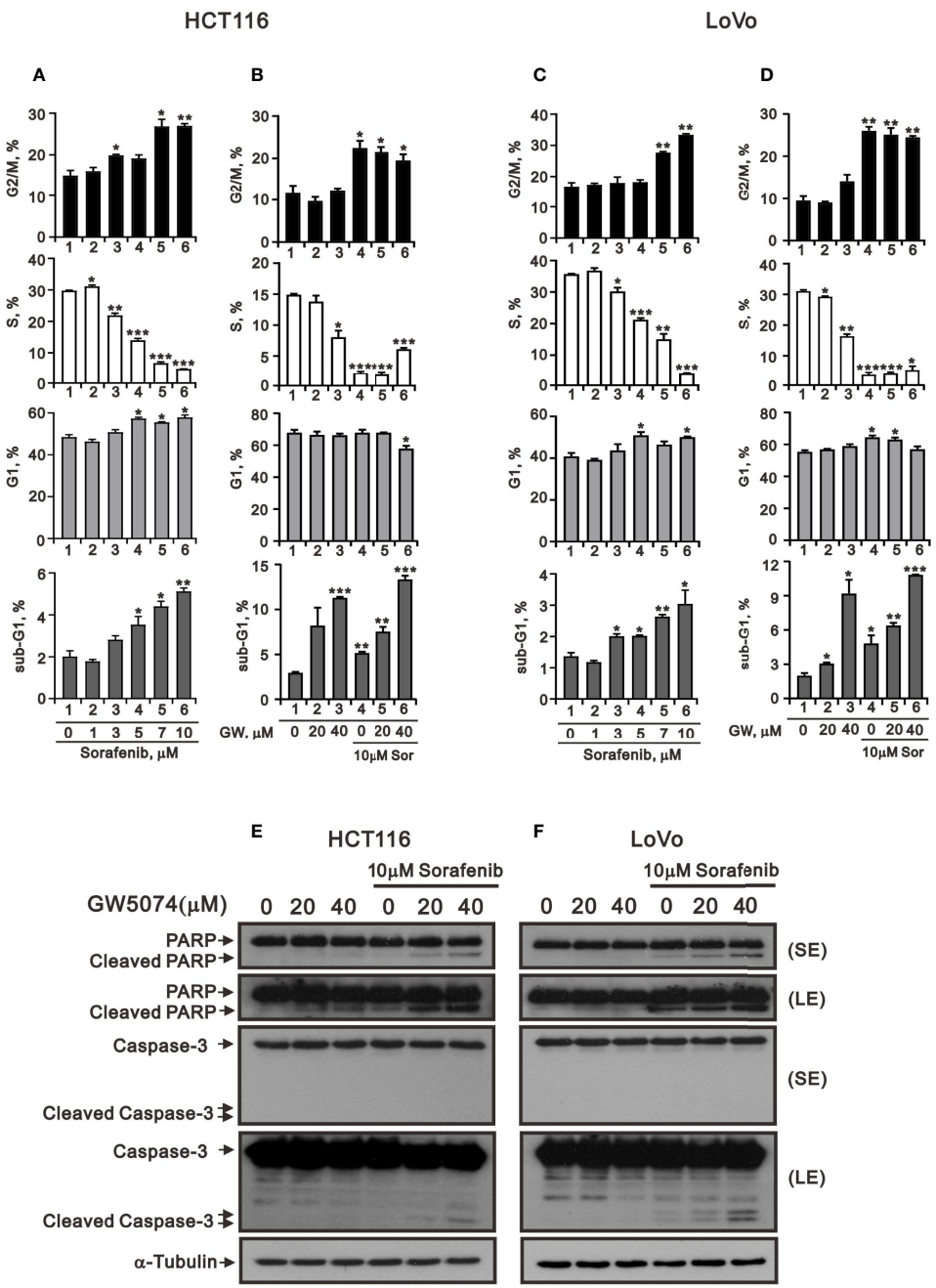

FIGURE 3 | The effects of GW5074 and sorafenib on the cell cycle profile of HCT116 and LoVo cells. HCT116 **(A)** and LoVo **(C)** cells were treated with 0, 1, 3, 5, 7, and 10 μM sorafenib for 24 h. HCT116 **(B)** and LoVo **(D)** cells were treated for 24 h with 0, 20, and 40 μM GW5074 in the absence or presence of 10 μM sorafenib. **(E, F)** Western blot analysis was applied for the cleavage off PARP and Caspase 3 proteins. α-tubulin is a loading control protein. SE: shorter exposure; LE: longer exposure. The results (A–D) are representative of three independent experiments. *$p < 0.05$, **$p < 0.01$, and ***$p < 0.001$.

(**Figures 3E, F**). In the Annexin V-PE/7-AAD double fluorescence staining apoptosis analysis, our results demonstrated that sorafenib, GW5074, and a combination of both did not affect the early apoptosis stage in HCT116 and LoVo cells (**Figure 4**). We detected the apparent effects on the late apoptosis stages treated with sorafenib and GW5074. However, both combinations revealed that GW5074 failed to enhance the effect of sorafenib because of the dramatic induction by GW5074 itself.

We applied the BrdU analysis for cellular proliferation to confirm the suppressive effect of sorafenib on the population of the S phase in HCT116 and LoVo cells (**Figures 3A–D**).

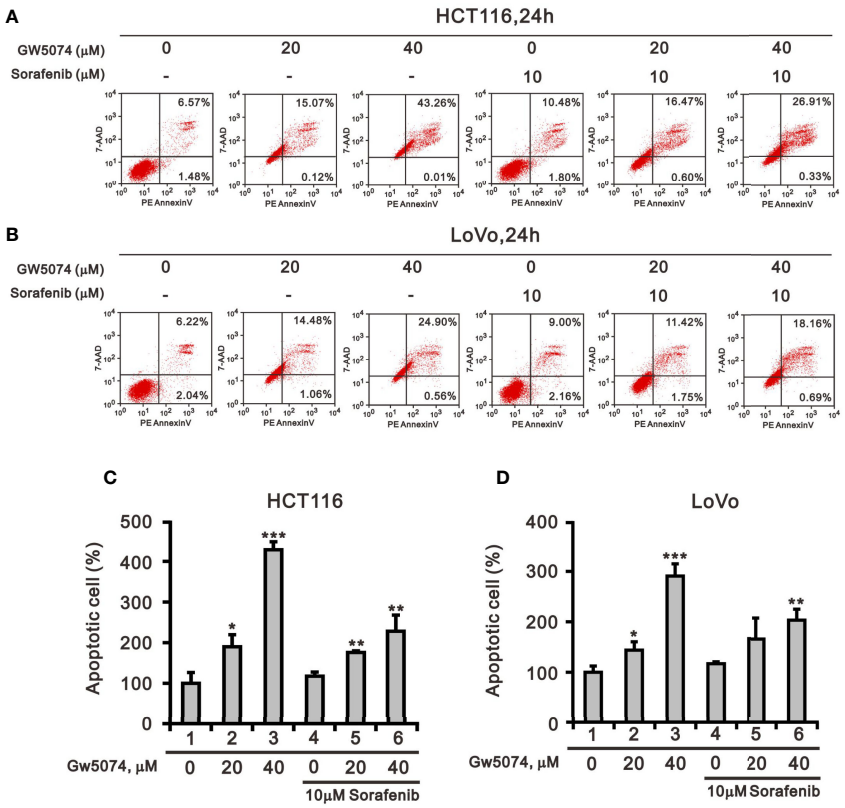

FIGURE 4 | The effects of GW5074 and sorafenib on cellular apoptosis of HCT116 and LoVo cells. HCT116 **(A)** and LoVo **(B)** cells were treated with 0, 20, and 40 μM GW5074 in the absence or presence of 10 μM sorafenib for 24 h. They were then subjected to Annexin V apoptosis analysis. Early apoptotic cells are PE Annexin V-positive and 7-AAD-negative, while late apoptotic cells are both PE Annexin V- and 7-AAD-positive. HCT116 **(C)** and LoVo **(D)** cells were measured the percentage (early apoptosis plus late apoptosis) compared with vehicle alone (100%). The results are representative of three independent experiments. $^{*}p < 0.05$, $^{**}p < 0.01$, and $^{***}p < 0.001$.

Sorafenib suppressed cellular proliferation in a dose-dependent manner and its more suppressive effects than GW5074 in HCT116 and LoVo cells (**Figure 5**). GW5074 failed to further suppress the sorafenib-suppressed cellular proliferation in HCT116 and LoVo cells. However, in the combined treatment, GW5074 failed to potentiate the suppressive effect of 10 μM sorafenib on the cellular proliferation capacity in both cell lines (**Figures 5B, D**).

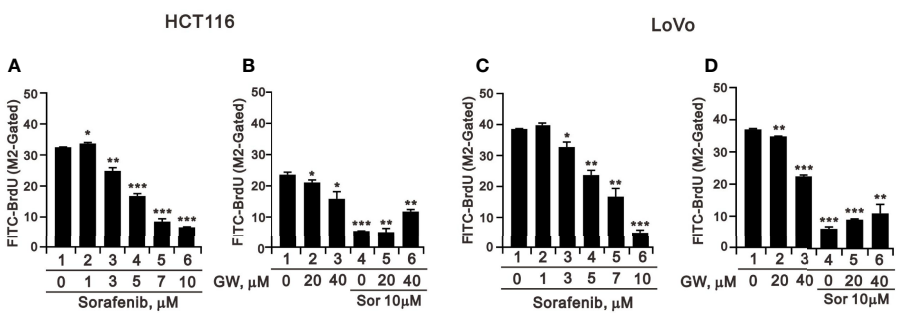

FIGURE 5 | The effects of GW5074 and sorafenib on cellular proliferation of HCT116 and LoVo cells. HCT116 **(A)** and LoVo **(C)** cells were treated with 0, 1, 3, 5, 7, and 10 μM sorafenib for 24 h. HCT116 **(B)** and LoVo **(D)** cells were treated for 24 h with 0, 20, and 40 μM GW5074 in the absence or presence of 10 μM sorafenib. They were subjected to BrdU proliferation analysis. The results are representative of three independent experiments. $^{*}p < 0.05$, $^{**}p < 0.01$, and $^{***}p < 0.001$.

The Cytotoxic Effects of Combined Sorafenib and GW5074 on the Endoplasmic Reticulum Stress and the ROS Status in HCT116 and LoVo Cells

Tyrosine kinase inhibitors can result in cytotoxicity mediated through the pathways of endoplasmic reticulum (ER) stress, autophagy, and oxidative stress (25, 26). To deal with the ER stress response, cells activate a series of signaling pathways, including PKR-like ER kinase (PERK), inositol-requiring transmembrane kinase/endoribonuclease 1α (IRE1α), and activating transcription factor 6 (ATF6) pathways, termed the unfolded protein response (UPR), which can either be protective (usually in the short term) or detrimental (usually in the long term). Here, we examined ER stress-related proteins and the consistent increasing trends of ATF3, ATF4, and CHOP in HCTA116 and LoVo cells treated with sorafenib, GW5074, and both combined using the western blotting analysis (**Figures 6A, B**). ATF5 and ATF6 had consistent increasing trends in HCTA116 and LoVo cells treated with individual sorafenib and GW5074 but had decreasing trends with both combined (**Figures 6A, B**). The decreased trend by both combined was observed in the ratio of p-eIF2/eIF2 and XBP-1, even sorafenib elevated the p-eIF2/eIF2 ratio in HCT116 cells. We further examined these above effects on related mRNAs using the RT-PCR analysis (**Figures 6C, D**). ATF3 and CHOP mRNAs were consistently increasing trend with their proteins in HCTA116 and LoVo cells. ATF4 mRNA was inconsistent with its protein-increasing trend. Other mRNAs were hard to make clear relation between protein and mRNA expression.

A previous study pointed out that C-RAF maintains cell survival by controlling ROS production and Ca^{2+} homeostasis of mitochondria (27). Next, we used the ROS-sensitive dye DCF-DA and the specific mitochondrial superoxide indicator MitoSOX™Red with flow cytometry for monitoring the generation of ROS in cytoplasm and mitochondria of HCT116 and LoVo cells treated with sorafenib, GW5074, and both combined (**Figures 7**, **8**). The generation of cytosolic ROS was significantly enhanced by sorafenib and GW5074, but GW5074 failed to potentiate the capacity of sorafenib at 10 and 40 μM in HCT116 and 40 μM in LoVo cells (**Figures 7A, B**). The generation of mitochondrial ROS was significantly enhanced by sorafenib and GW5074 (**Figures 8A, B**). The combined therapy had a significant additive effect on increasing ROS in mitochondria of HCT116 and LoVo cells. The oxidative capacity is determined by oxidative stress, which highlights the crucial role of antioxidant defenses in the redox homeostasis of the organism. Hence, we analyzed proteins related to oxidative stress, such as NRF2 and HO-1, and antioxidant defense mechanisms, such as catalase, superoxide dismutase 1 (SOD1), SOD2, and SOD3, in HCT116 and LoVo cells. Our Western blotting data showed that sorafenib and GW5074 elevated the level of NRF2 in HCT116 cells, and both combined decreased the levels of SOD1 and SOD2 in HCT116 and LoVo cells (**Figures 7C, D**). A well-known DNA damage biomarker, γH2A.x, was suppressed in the presence of sorafenib-treated HCT116 cells and increased by both combined in LoVo cells.

The effects of Sorafenib, GW5074, and Both Combined on Mitochondrial Functions in HCT116 and LoVo Cells

Mitochondria are dynamic organelles that respond to cell stress by continuously undergoing biogenesis, fission, fusion, mitophagy, and motility (28). Mitochondrial fission is necessary for the selective elimination of mitochondria damaged by mitophagy, and mitochondrial fusion enables surviving fragmented mitochondria to return to the mitochondrial network (29). To test whether sorafenib, GW5074, and both combined treatments affected mitochondrial mass *via* the fission-fusion transient, we stained mitochondria with MitoView™Green, a membrane potential independent dye, and analyzed by flow cytometry. The results indicated that GW5074 and both combined treatments significantly reduced mitochondrial mass in HCT116 and LoVo cells (**Figures 9A, B**). Two outer mitochondrial membrane proteins, dynamin-related protein 1 (DRP1) and mitofusin 1 (Mfn1), are involved in the dynamic processes of mitochondrial fission and fusion, respectively (30, 31). The ratio of p-DRP1/DRP1, the biomarker for mitochondrial fission, was reduced by sorafenib, GW5074, and both combined treatments in HCT116 cells (**Figure 9C**), whereas the ratio of p-DRP1/DRP1 was increased by sorafenib and both combined treatments in LoVo cells (**Figure 9D**).

According to a previous report, each member of the RAF family presents a specific distribution at the level of cellular membranes, and C-RAF is the only isoform that directly targets mitochondria—it plays an important role in mitochondria, regulating the shape and the cellular distribution of mitochondria and making it a target of the combination of sorafenib and GW5074 in some cancers (32). Mitochondrial dysfunction is involved in the induction of apoptosis and is even considered to be the core of the apoptosis pathway (33). Therefore, we used JC-1 dye to examine the disruption of mitochondrial membrane potential after the combination of sorafenib and GW5074 in HCT116 and LoVo cells, which is considered a hallmark of apoptosis. In non-apoptotic cells, stained red JC-1 exists in the form of dimers and accumulates in the form of aggregates in mitochondria. In apoptotic cells, JC-1 exists in the cytoplasm as a monomer and is stained green. The results showed that when HCT116 and LoVo cells were treated alone with GW5074, mitochondrial membrane potential loss levels increased with dose (**Figure 10**). Combination treatment with sorafenib 10 μM dramatically increased the loss of mitochondrial membrane potential. This finding suggests that the combined treatment of sorafenib and GW5074 led to more severe mitochondrial damage in HCT116 and LoVo cells.

Changes in overall mitochondrial mass represent changes in the balance of mitochondrial biogenesis and mitophagy levels (34). Mitochondrial transcription factor A (mtTFA) and peroxisome-proliferator-activated receptor γ co-activator-1α (PGC-1α) are two key mitochondrial biogenic and respiratory factors for mitochondrial respiratory function (35, 36). Therefore, we subsequently examined the protein levels of mitochondrial biogenesis, respiration, and mitophagy such as

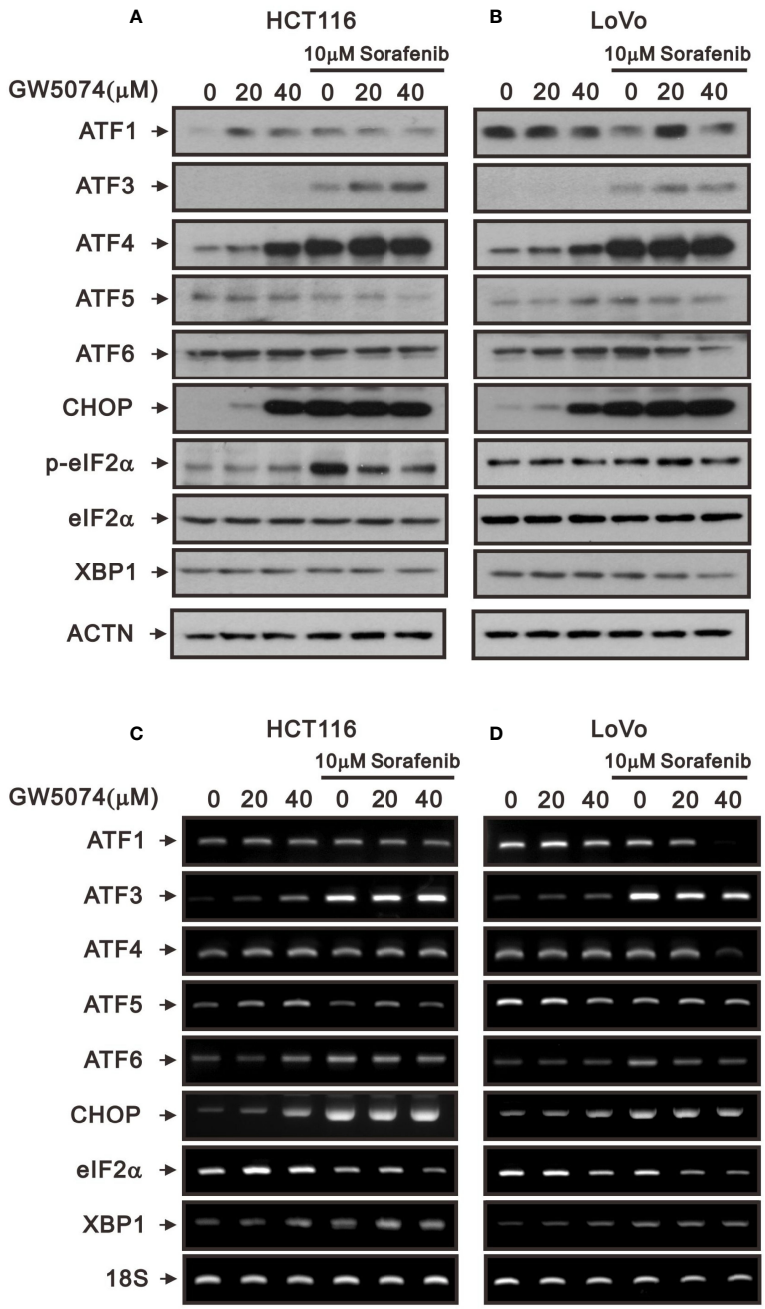

FIGURE 6 | The effects of GW5074 and sorafenib on ER stress of HCT116 and LoVo cells. HCT116 and LoVo cells were treated with 0, 20, and 4 μM GW5074 in the absence or presence of 10 μM sorafenib for 24 h. **(A, B)** Cell lysates were subjected to Western blotting analysis. ACTN is a loading control protein. **(C, D)** Total RNA were subjected to RT-PCR analysis. 18S is a loading control.

PGC-1α, mtTFA, Tom20, parkin, and autophagy using Western blotting analysis. The protein levels of Tom20, mtTFA, and PGC-1α were affected variably by sorafenib and GW5074 in HCT116 and LoVo cells; however, GW5074 had the suppressive effect of sorafenib on these proteins in both cells (**Figures 11A, B**). The mRNA levels of mtTFA and PGC-1α were suppressed by sorafenib which was enhanced by GW5074 (**Figures 11C, D**). Autophagy plays a dynamic tumor-suppressive or tumor-promoting role in different contexts and stages of cancer development. We further examined the biomarker of autophagy, LC3B; the II/I ratios were increased in HCTA116 and LoVo cells treated with sorafenib, GW5074, and both combined (**Figures 11A, B**). An autophagic cargo p62 did not follow the trend in both cell lines. Mitophagy, selective autophagy in

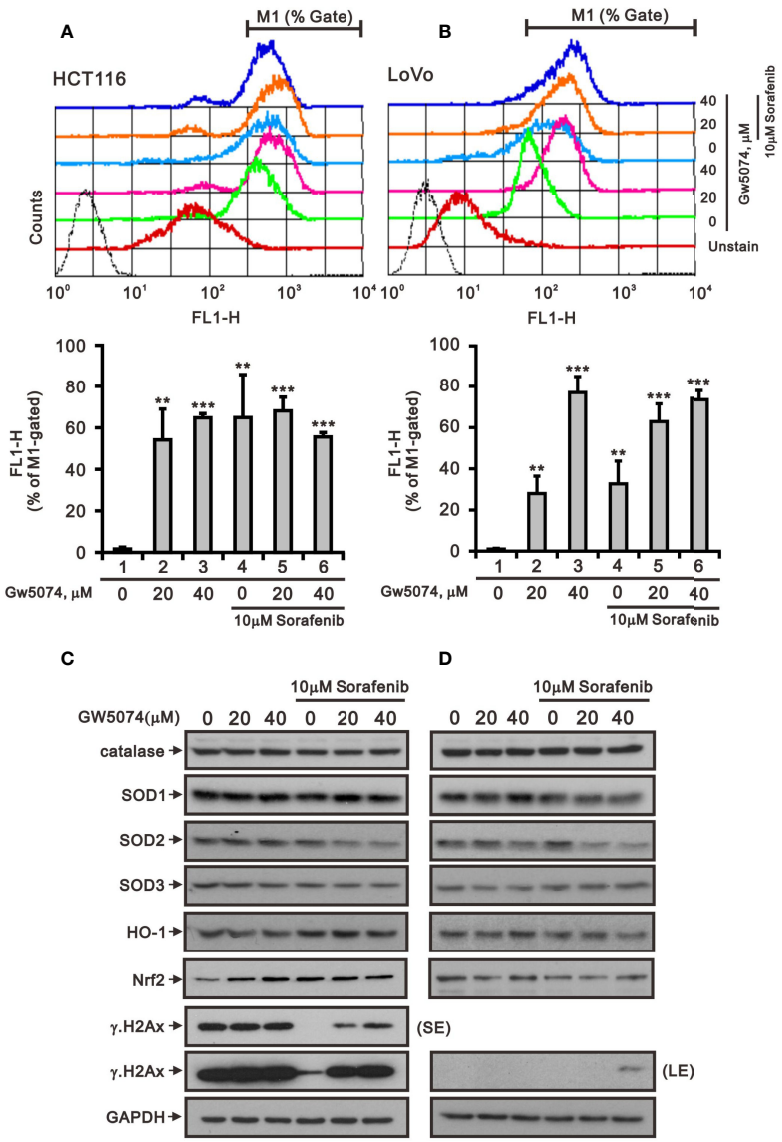

FIGURE 7 | The effects of GW5074 and sorafenib on the cytosolic ROS generation of HCT116 and LoVo cells. HCT116 **(A)** and LoVo **(B)** cells were treated with 0, 20, and 40 μM GW5074 in the absence or presence of 10 μM sorafenib for 24 h, after which the live cells were stained with 20 μM DCFH-DA for 10 min at 37°C and assayed using a flow cytometer. **(C, D)** Cell lysates were subjected to Western blotting analysis with antibodies against SOD 1-3, Nrf2, HO-1, and γH2A.x. GAPDH is a loading control protein. SE, shorter exposure; LE, longer exposure. The results **(A, B)** are representative of three independent experiments. **$p < 0.01$ and ***$p < 0.001$.

mitochondria, is regulated by PINK1 and parkin proteins. The parkin proteins were suppressed with the combination of sorafenib and GW5074 (**Figures 11A, B**), but the mRNAs were enhanced in HCT116 and LoVo cells (**Figures 11C, D**). TFEB (transcription factor E3) is one of the master transcriptional regulators of autophagy and the AMPK-p70S6K pathway is a positive pathway for autophagy. The protein and mRNA levels of TFEB did not show a clear trend. The ratio of p-AMPK/AMPK was elevated by sorafenib, which could be slightly suppressed by GW5074 in both cells; the ratio of p-p70S6K/p70S6K was strongly suppressed by GW5074 in LoVo cells, and the mRNA levels of p70S6K were decreased by sorafenib combined with GW5074 in LoVo cells.

We observed mitochondrial morphology by immunofluorescence staining for PGC-1α and TOM20 with sorafenib, GW5074, and the combined treatment in HCT116 and LoVo cells (**Figures 12**, **13**). The amounts of PGC-1α were elevated by sorafenib and the subcellular distributions were changed by GW5074 and sorafenib (**Figure 12**). More nuclear PGC-1α proteins were observed with the combination of sorafenib and GW5074 in HCT116 and LoVo cells. The subcellular distributions of TOM20 were changed from fragmented to tubular forms by GW5074 and sorafenib (**Figure 13**).

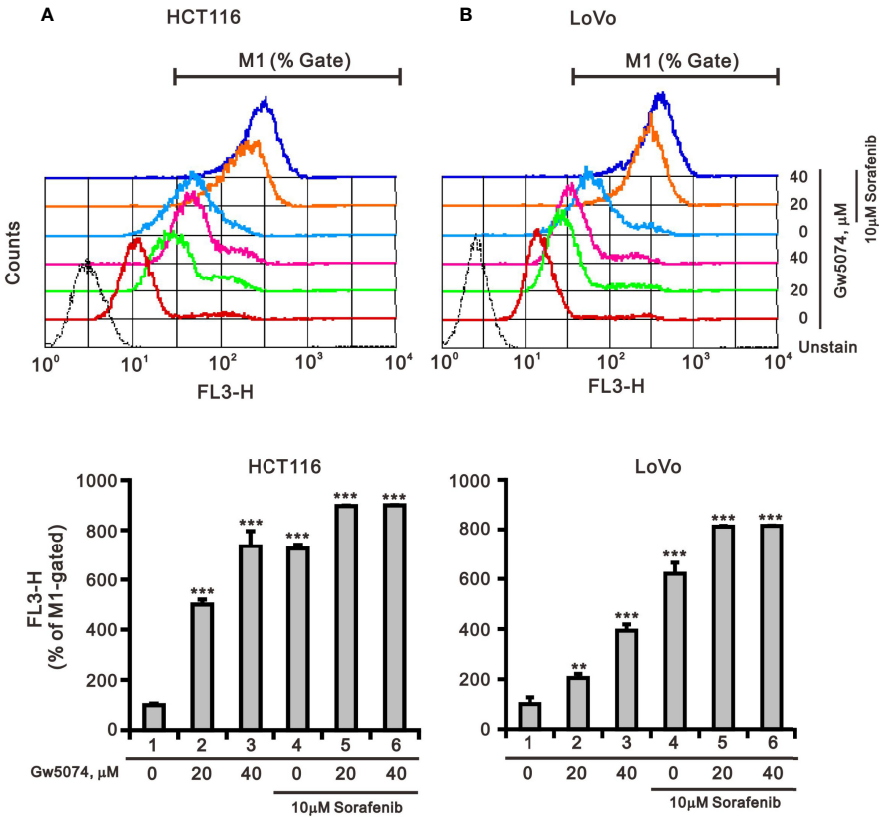

FIGURE 8 | The effects of GW5074 and sorafenib on the mitochondrial ROS generation of HCT116 and LoVo cells. HCT116 **(A)** and LoVo **(B)** cells were treated with 0, 20, and 40 μM GW5074 in the absence or presence of 10 μM sorafenib for 24 h, after which the live cells were stained with 5 mM MitoSOX™Red for 10 min at 37°C and assayed using a flow cytometer. The results are representative of three independent experiments. $^{**}p < 0.01$ and $^{***}p < 0.001$.

DISCUSSION

The efficacy of sorafenib target therapy may also be altered by the development of drug resistance and cancer recurrence in CRC. In this study, we combined sorafenib with GW5074 to reduce the dose of sorafenib and enhance its cytotoxicity in two CRC cell lines, HCT116 and LoVo cells. Our findings demonstrate that GW5074 can potentiate the cytotoxicity of sorafenib and dramatically reduce the IC50 dose of sorafenib from 17 and 31 μM to 0.14 and 0.01 μM in HCT116 and LoVo cells, respectively. GW5074, similar to sorafenib, suppressed the cellular proliferation and induced cellular apoptosis and cytosolic ROS, but had no further enhancement on the above-mentioned effects when combined with sorafenib. The synergistic effects of GW5074 and sorafenib were mainly exerted in impacting mitochondrial functions, including ROS generation, membrane potential disruption, and fission–fusion dynamics, which were examined by using the flow cytometry analysis. In summary, the C-RAF inhibitor GW5074 might potentiate the cytotoxicity of the B-RAF inhibitor sorafenib mediated through mitochondrial dysfunctions, suggesting that GW5074 potentially serves as a sensitizer for sorafenib application to reduce the risk of drug resistance of CRC treatment.

pC-RAF^{S338} interacted with pDAPK^{S308} and directed it to become colocalized in the mitochondria (37). A study by Cha showed that sorafenib and GW5074 bound to mitochondrial C-RAF and induced a conformational change to compromise its mitochondrial targeting capability (20). GW5074 and sorafenib combination therapy resulted in the translocation of pC-RAF^{S338} from the mitochondria to the cytoplasm, concomitant with a decrease in mitochondrial membrane potential and an increase in ROS generation in RCC. In CRC, we observed similar effects of GW5074 and sorafenib combination therapy on the disruption of mitochondrial membrane potential and the induction of ROS generation with decreasing amounts of pDAPK^{S308} (data not shown). The cytotoxicity of GW5074 alone was hard to detect in LoVo cells, whereas it could induce mitochondrial ROS generation and the disruption of mitochondrial membrane potential and fission–fusion dynamics. The detailed mechanisms involved in the regulation of mitochondrial function by pDAPK^{S308} and pC-RAF^{S338} and the effectiveness of various mitochondrial functions are worthy of further investigation in CRC.

Sorafenib is a multi-kinase inhibitor with activity against B/C-RAF, B-RAF^{V600E}, Flt3, Kit, RET, VEGFR1/2/3, and PDGFRβ (11, 12, 38). Sorafenib is the only first-line therapeutic targeted drug for advanced hepatocellular carcinoma (HCC) (39, 40).

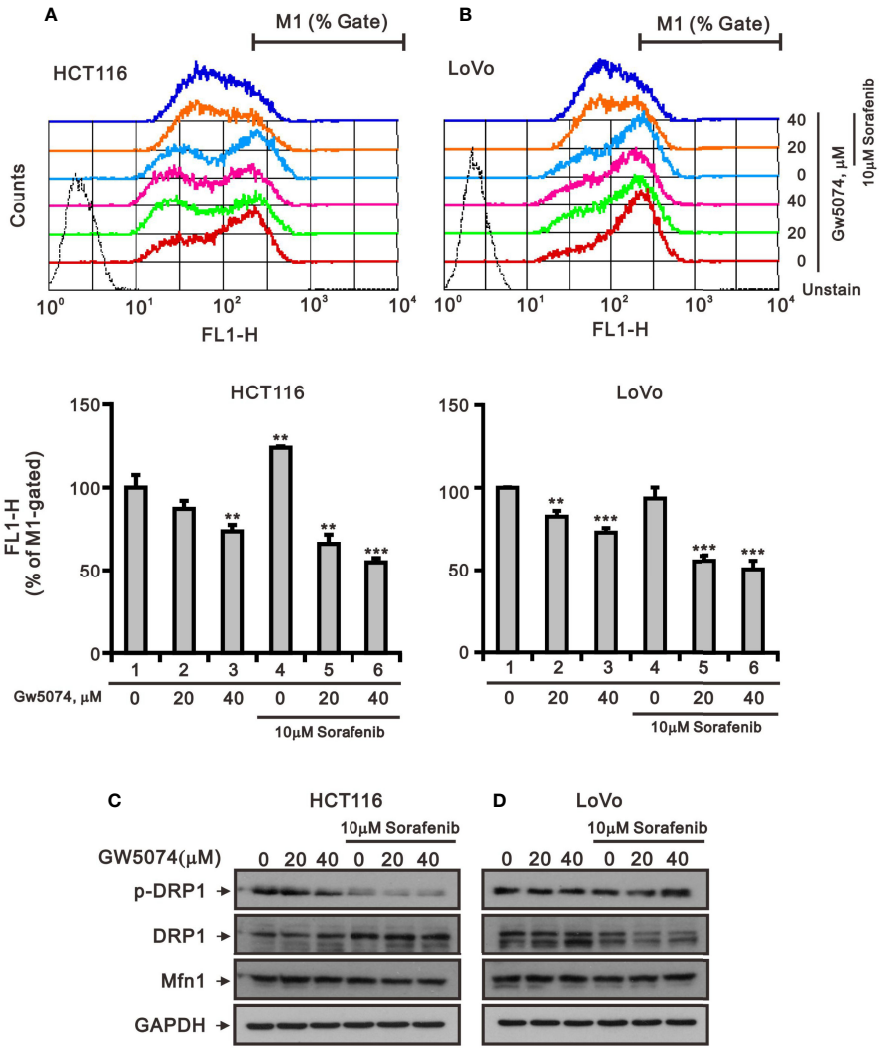

FIGURE 9 | The effects of GW5074 and sorafenib on the mitochondrial fission–fusion transient of HCT116 and LoVo cells. HCT116 **(A)** and LoVo **(B)** cells were treated with 0, 20, and 40 μM GW5074 in the absence or presence of 10 μM sorafenib for 24 h, after which the live cells were stained with 100 nM MitoView™Green for 15 min at 37°C and assayed using a flow cytometer. **(C, D)** Cell lysates were subjected to Western blotting analysis with antibodies against DRP, p-DRP, and Mfn1. GAPDH is a loading control protein. The results **(A, B)** are representative of three independent experiments. **p < 0.01 and ***p < 0.001.

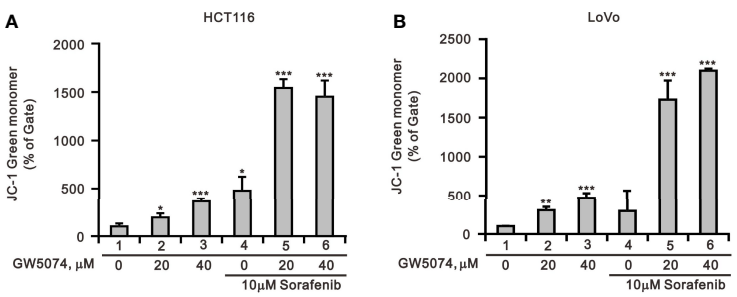

FIGURE 10 | The effects of GW5074 and sorafenib on the mitochondrial membrane potential of HCT116 and LoVo cells. HCT116 **(A)** and LoVo **(B)** cells were treated with 0, 20, and 40 μM GW5074 in the absence or presence of 10 μM sorafenib for 24 h and assayed with JC-1 dye using a flow cytometer. The results are representative of three independent experiments. *$p < 0.05$, **$p < 0.01$, and ***$p < 0.001$.

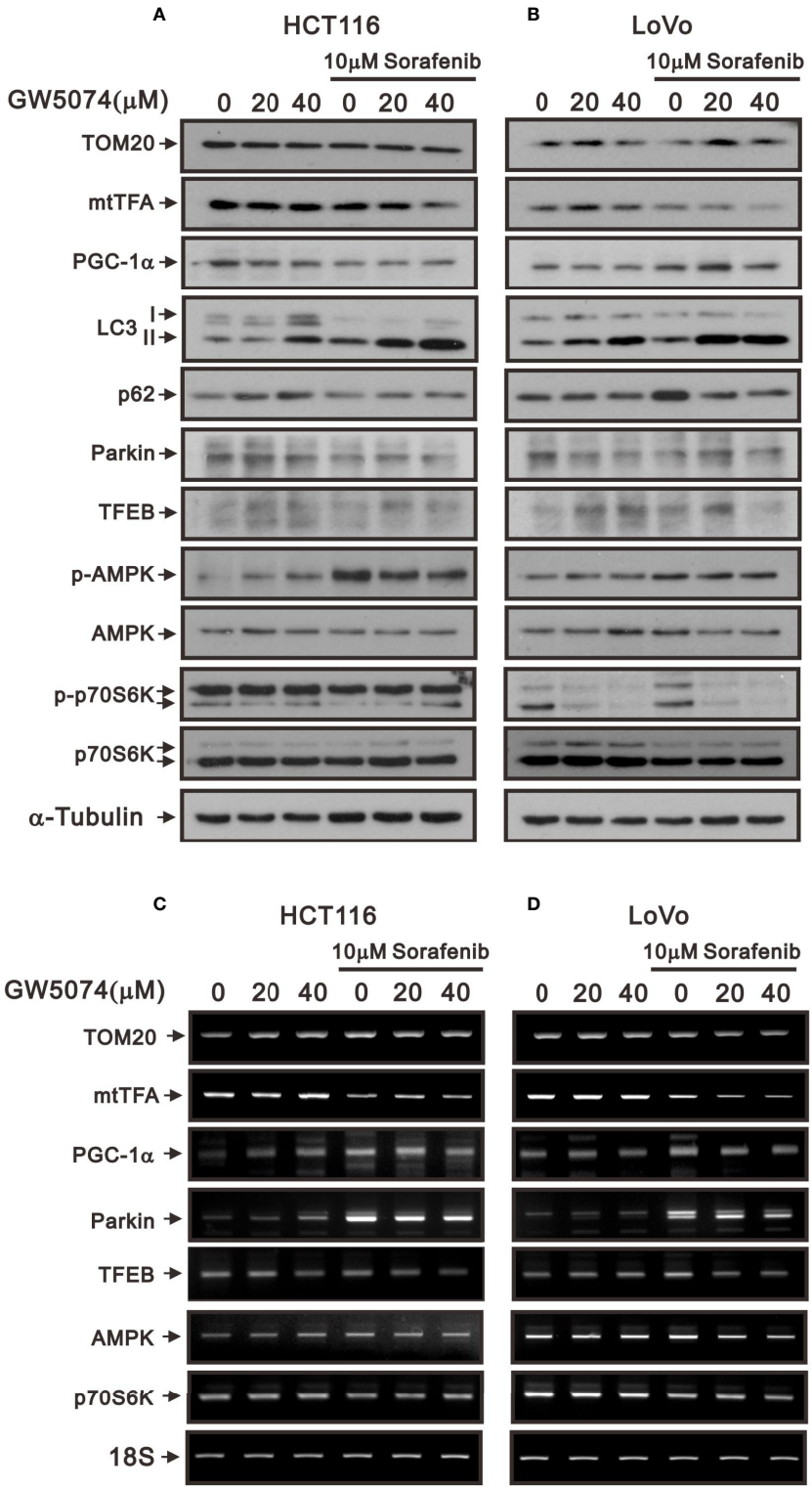

FIGURE 11 | The effects of GW5074 and sorafenib on the mitochondrial autophagy and biogenesis of HCT116 and LoVo cells. HCT116 and LoVo cells were treated with 0, 20, and 40 μM GW5074 in the absence or presence of 10 μM sorafenib for 24 h. **(A, B)** Cell lysates were subjected to Western blotting analysis. α-Tubulin is a loading control protein. **(C, D)** Total RNA were subjected to RT-PCR analysis. 18S is a loading control.

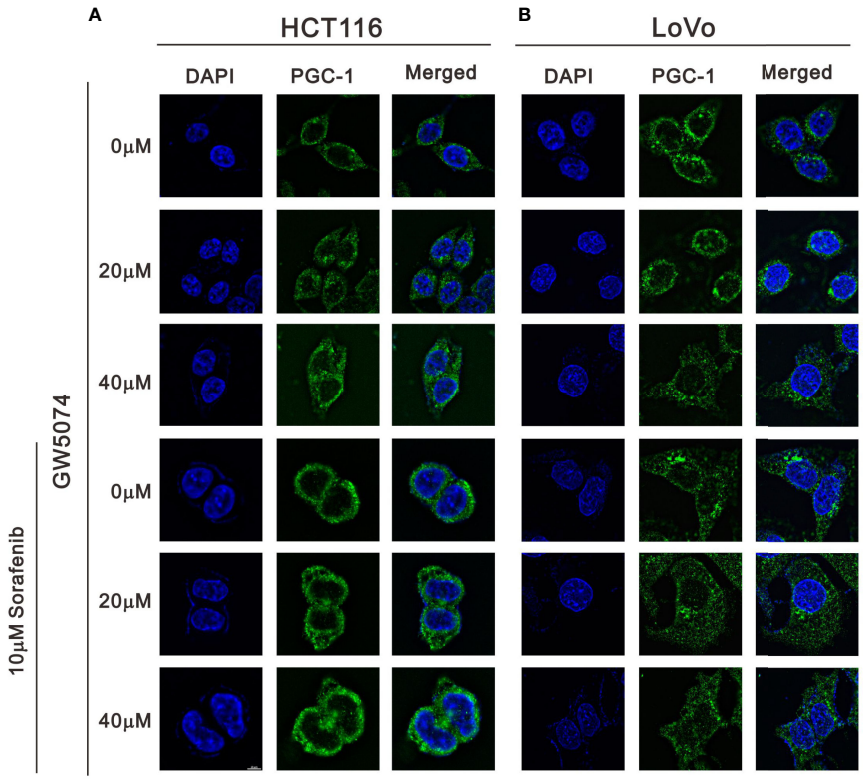

FIGURE 12 | The effects of GW5074 and sorafenib on the expression of PGC-1α in HCT116 and LoVo cells. HCT116 **(A)** and LoVo **(B)** cells were treated with 0, 20, and 40 μM GW5074 in the absence or presence of 10 μM sorafenib for 24 h and were immune-stained with anti-PGC-1α (green) and DAPI (blue). Images were examined under a Leica Thunder microscope with a 100x objective. Scale Bar=10 μm.

Sorafenib resistance is mainly focused on the activation of sorafenib targets and downstream signaling, the regulation of cell proliferative and apoptotic signals, and the epithelial–mesenchymal transition and stemness. Studies have demonstrated that sorafenib induces autophagy, correlated with the reduction in sorafenib sensitivity (25). Research literature has demonstrated that activated ER stress can induce autophagy (41). A recent study demonstrated that melatonin regulates ER stress-induced autophagy to overcome apoptosis resistance and increase the sensitivity to sorafenib in HCC cells (42). Here, compared with sorafenib alone, the combination of GW5074 with sorafenib induced ATF4-CHOP and reduced ATF6 and the ratio of p-eIF2/eIF2 in HCT116 and LoVo cells. In addition, mTOR pathway activation is responsible for the acquisition of resistance to sorafenib in HCC therapy (43). In our study, GW5074 combined with sorafenib reduced the ratio of pAMPK/AMPK in HCT116 and the amount of p62 in LoVo cells. Hence, the combination of GW5074 with sorafenib might mediate through the induction of ER stress and suppression of mTOR activation to decrease the chance of sorafenib resistance in our current study. However, the detailed mechanism should be checked in sorafenib-resistant CRC cell lines.

ROS plays a central role in cell signaling mediated by mitochondria (26). A two-hit working model of sorafenib combined with GW5074 was proposed, where cytosolic translocation of C-RAF/pDAPK^{S308} induces mitochondrial dysfunction to produce ROS (first hit) and triggers PP2A-mediated de-phosphorylation and activation of DAPK (second hit) in RCC (20). Our data on cytosolic and mitochondrial ROS generation suggest that GW5074 synergistically enhances the ability of ROS generation in mitochondria, not in the cytosol, which might be mediated through the disruption of mitochondrial membrane potential. Mitochondria also have an important role in triggering and regulating apoptosis; this synergy effect was not found in our apoptotic Annexin V analysis. The generation of ROS in cells exists in equilibrium with a variety of antioxidant defenses, including SODs (44). We observed the downregulation of SOD1 and SOD2 with the combination of GW5074 and sorafenib in HCT116 and LoVo cells. It is important to elucidate how mitochondrial or cytosolic ROS are involved in the induction of apoptosis using mitochondrial or cytosolic ROS scavengers.

The synergistic effect between sorafenib and GW5074 on the cytotoxicity and mitochondrial functions might be the primary contribution of our current work which also is encouraged by these ongoing clinical trials. However, the limitation of the current study is a lack of a sorafenib-resistant HCT116 or LoVo cell line to verify the synergistic effect of GW5074 on

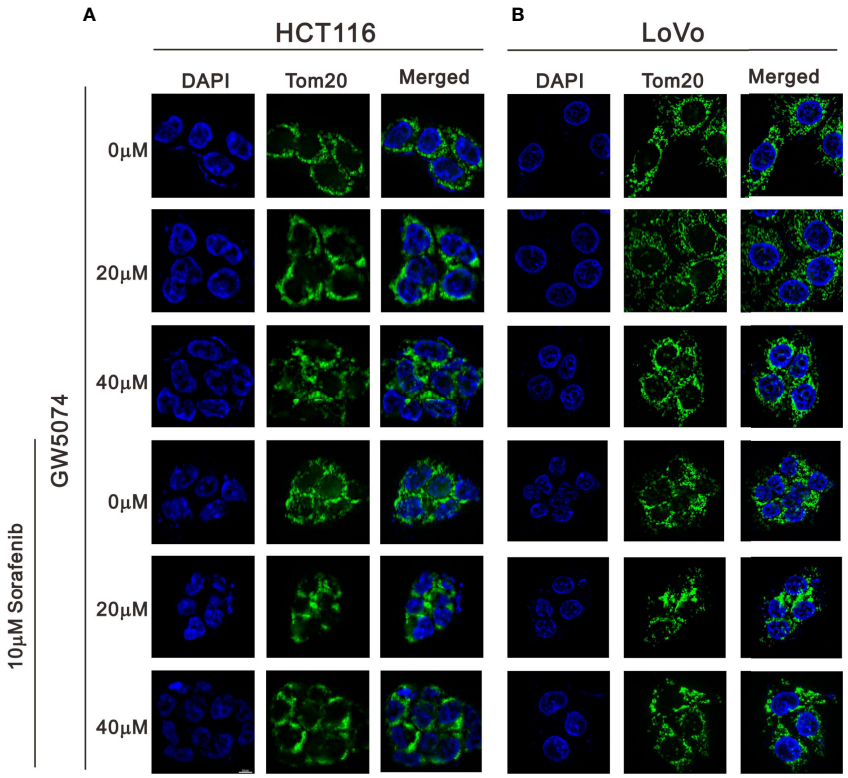

FIGURE 13 | The effects of GW5074 and sorafenib on the expression of Tom20 in HCT116 and LoVo cells. HCT116 **(A)** and LoVo **(B)** cells were treated with 0, 20, and 40 μM GW5074 in the absence or presence of 10 μM sorafenib for 24 h and were immune-stained with anti-Tom20 (green) and DAPI (blue). Images were examined under a Leica Thunder microscope with a 100x objective. Scale Bar=10 μm.

these resistant CRC cells. In addition to DAPK, more phosphorylation status of B-RAF and C-RAF targets by GW5074 and/or sorafenib should be examined to support our findings *via* the inhibitors for B-RAF and C-RAF.

DATA AVAILABILITY STATEMENT

The original contributions presented in the study are included in the article/supplementary material. Further inquiries can be directed to the corresponding author.

AUTHOR CONTRIBUTIONS

Conceptualization, J-MH and S-MH. Methodology, Y-LC. Validation, J-MH and Y-LC. Formal analysis, J-MH. Investigation, J-MH. Resources, C-CH. Data curation, J-MH. Writing—original draft preparation, J-MH. Writing—review and editing, S-MH. Supervision, S-MH. Project administration, C-CH. All authors have read and agreed to the published version of the manuscript. All authors contributed to the article and approved the submitted version.

FUNDING

This work was supported by a grant from the Tri-Service General Hospital [TSGH-E-111194 to J-M Hu], Taiwan, Republic of China.

ACKNOWLEDGMENTS

We thank Zih-Syuan Wu and Jhao-Ying Chen for their technical support.

REFERENCES

1. Siegel RL, Miller KD, Fuchs HE, Jemal A. Cancer Statistics 2022. *CA: A Cancer J Clin* (2022) 72(1):7–33. doi: 10.3322/caac.21708
2. Dekker E, Tanis PJ, Vleugels JLA, Kasi PM, Wallace MB. Colorectal Cancer. *Lancet* (2019) 394(10207):1467–80. doi: 10.1016/s0140-6736(19)32319-0
3. Biller LH, Schrag D. Diagnosis and Treatment of Metastatic Colorectal Cancer: A Review. *Jama* (2021) 325(7):669–85. doi: 10.1001/jama.2021.0106
4. Alzahrani SM, Al Doghaither HA, Al–Ghafari AB. General Insight Into Cancer: An Overview of Colorectal Cancer (Review). *Mol Clin Oncol* (2021) 15(6):271. doi: 10.3892/mco.2021.2433

5. Taieb J, Jung A, Sartore-Bianchi A, Peeters M, Seligmann J, Zaanan A, et al. The Evolving Biomarker Landscape for Treatment Selection in Metastatic Colorectal Cancer. *Drugs* (2019) 79(13):1375–94. doi: 10.1007/s40265-019-01165-2
6. Slattery ML, Mullany LE, Sakoda LC, Wolff RK, Samowitz WS, Herrick JS. The MAPK-Signaling Pathway in Colorectal Cancer: Dysregulated Genes and Their Association With MicroRNAs. *Cancer Inform* (2018) 17:1176935118766522. doi: 10.1177/1176935118766522
7. Wang X, Wu F, Wang H, Duan X, Huang R, Tuersuntuoheti A, et al. PDCD6 Cooperates With C-Raf to Facilitate Colorectal Cancer Progression *via* Raf/MEK/ERK Activation. *J Exp Clin Cancer Res* (2020) 39(1):147. doi: 10.1186/s13046-020-01632-9
8. Kochi M, Hinoi T, Niitsu H, Miguchi M, Saito Y, Sada H, et al. Oncogenic Mutation in RAS-RAF Axis Leads to Increased Expression of GREB1, Resulting in Tumor Proliferation in Colorectal Cancer. *Cancer Sci* (2020) 111(10):3540–9. doi: 10.1111/cas.14558
9. Ducreux M, Chamseddine A, Laurent-Puig P, Smolenschi C, Hollebecque A, Dartigues P, et al. Molecular Targeted Therapy of BRAF-Mutant Colorectal Cancer. *Ther Adv Med Oncol* (2019) 11:1758835919856494. doi: 10.1177/1758835919856494
10. Maurer G, Tarkowski B, Baccarini M. Raf Kinases in Cancer-Roles and Therapeutic Opportunities. *Oncogene* (2011) 30(32):3477–88. doi: 10.1038/onc.2011.160
11. Adnane L, Trail PA, Taylor I, Wilhelm SM. Sorafenib (BAY 43-9006, Nexavar), a Dual-Action Inhibitor That Targets RAF/MEK/ERK Pathway in Tumor Cells and Tyrosine Kinases VEGFR/PDGFR in Tumor Vasculature. *Methods Enzymol* (2006) 407:597–612. doi: 10.1016/S0076-6879(05)07047-3
12. Marisi G, Cucchetti A, Ulivi P, Canale M, Cabibbo G, Solaini L, et al. Ten Years of Sorafenib in Hepatocellular Carcinoma: Are There Any Predictive and/or Prognostic Markers? *World J Gastroenterol* (2018) 24(36):4152–63. doi: 10.3748/wjg.v24.i36.4152
13. Tang W, Chen Z, Zhang W, Cheng Y, Zhang B, Wu F, et al. The Mechanisms of Sorafenib Resistance in Hepatocellular Carcinoma: Theoretical Basis and Therapeutic Aspects. *Signal Transduct Target Ther* (2020) 5(1):87. doi: 10.1038/s41392-020-0187-x
14. Beeram M, Patnaik A, Rowinsky EK. Raf: A Strategic Target for Therapeutic Development Against Cancer. *J Clin Oncol* (2005) 23(27):6771–90. doi: 10.1200/JCO.2005.08.036
15. Moreira RB, de Sousa Cruz MR. Clinical Response to Sorafenib in a Patient With Metastatic Colorectal Cancer and FLT3 Amplification. *Case Rep Oncol* (2015) 8(1):83–7. doi: 10.1159/000375483
16. Xie H, Lafky JM, Morlan BW, Stella PJ, Dakhil SR, Gross GG, et al. Dual VEGF Inhibition With Sorafenib and Bevacizumab as Salvage Therapy in Metastatic Colorectal Cancer: Results of the Phase II North Central Cancer Treatment Group Study N054C (Alliance). *Ther Adv Med Oncol* (2020) 12:1758835920910913. doi: 10.1177/1758835920910913
17. Borovski T, Vellinga TT, Laoukili J, Santo EE, Fatrai S, van Schelven S, et al. Inhibition of RAF1 Kinase Activity Restores Apicobasal Polarity and Impairs Tumour Growth in Human Colorectal Cancer. *Gut* (2017) 66(6):1106–15. doi: 10.1136/gutjnl-2016-311547
18. Lackey K, Cory M, Davis R, Frye SV, Harris PA, Hunter RN, et al. The Discovery of Potent Craf1 Kinase Inhibitors. *Bioorg Med Chem Lett* (2000) 10(3):223–6. doi: 10.1016/s0960-894x(99)00668-x
19. Chin PC, Liu L, Morrison BE, Siddiq A, Ratan RR, Bottiglieri T, et al. The C-Raf Inhibitor GW5074 Provides Neuroprotection *In Vitro* and in an Animal Model of Neurodegeneration Through a MEK-ERK and Akt-Independent Mechanism. *J Neurochem* (2004) 90(3):595–608. doi: 10.1111/j.1471-4159.2004.02530.x
20. Tsai YT, Chuang MJ, Tang SH, Wu ST, Chen YC, Sun GH, et al. Novel Cancer Therapeutics With Allosteric Modulation of the Mitochondrial C-Raf-DAPK Complex by Raf Inhibitor Combination Therapy. *Cancer Res* (2015) 75(17):3568–82. doi: 10.1158/0008-5472.CAN-14-3264
21. Chou TC. Theoretical Basis, Experimental Design, and Computerized Simulation of Synergism and Antagonism in Drug Combination Studies. *Pharmacol Rev* (2006) 58(3):621–81. doi: 10.1124/pr.58.3.10
22. Chang YL, Hsu YJ, Chen Y, Wang YW, Huang SM. Theophylline Exhibits Anti-Cancer Activity *via* Suppressing SRSF3 in Cervical and Breast Cancer Cell Lines. *Oncotarget* (2017) 8(60):101461–74. doi: 10.18632/oncotarget.21464
23. Kuo CL, Hsieh Li SM, Liang SY, Liu ST, Huang LC, Wang WM, et al. The Antitumor Properties of Metformin and Phenformin Reflect Their Ability to Inhibit the Actions of Differentiated Embryo Chondrocyte 1. *Cancer Manag Res* (2019) 11:6567–79. doi: 10.2147/CMAR.S210637
24. Simpson KL, Cawthorne C, Zhou C, Hodgkinson CL, Walker MJ, Trapani F, et al. A Caspase-3 'Death-Switch' in Colorectal Cancer Cells for Induced and Synchronous Tumor Apoptosis *In Vitro* and *In Vivo* Facilitates the Development of Minimally Invasive Cell Death Biomarkers. *Cell Death Dis* (2013) 4:e613. doi: 10.1038/cddis.2013.137
25. Heqing Y, Bin L, Xuemei Y, Linfa L. The Role and Mechanism of Autophagy in Sorafenib Targeted Cancer Therapy. *Crit Rev Oncol Hematol* (2016) 100:137–40. doi: 10.1016/j.critrevonc.2016.02.006
26. Redza-Dutordoir M, Averill-Bates DA. Activation of Apoptosis Signalling Pathways by Reactive Oxygen Species. *Biochim Biophys Acta* (2016) 1863(12):2977–92. doi: 10.1016/j.bbamcr.2016.09.012
27. Kuznetsov AV, Smigelskaite J, Doblander C, Janakiraman M, Hermann M, Wurm M, et al. Survival Signaling by C-RAF: Mitochondrial Reactive Oxygen Species and Ca2+ Are Critical Targets. *Mol Cell Biol* (2008) 28(7):2304–13. doi: 10.1128/mcb.00683-07
28. Nunnari J, Suomalainen A. Mitochondria: In Sickness and in Health. *Cell* (2012) 148(6):1145–59. doi: 10.1016/j.cell.2012.02.035
29. Hernandez-Resendiz S, Prunier F, Girao H, Dorn G, Hausenloy DJ. Targeting Mitochondrial Fusion and Fission Proteins for Cardioprotection. *J Cell Mol Med* (2020) 24(12):6571–85. doi: 10.1111/jcmm.15384
30. Grandemange S, Herzig S, Martinou JC. Mitochondrial Dynamics and Cancer. *Semin Cancer Biol* (2009) 19(1):50–6. doi: 10.1016/j.semcancer.2008.12.001
31. Youle RJ, van der Bliek AM. Mitochondrial Fission, Fusion, and Stress. *Science* (2012) 337(6098):1062–5. doi: 10.1126/science.1219855
32. Galmiche A, Fueller J, Santel A, Krohne G, Wittig I, Doye A, et al. Isoform-Specific Interaction of C-RAF With Mitochondria. *J Biol Chem* (2008) 283(21):14857–66. doi: 10.1074/jbc.M709098200
33. Ly JD, Grubb DR, Lawen A. The Mitochondrial Membrane Potential (Deltapsi(M)) in Apoptosis; An Update. *Apoptosis* (2003) 8(2):115–28. doi: 10.1023/a:1022945107762
34. Twig G, Hyde B, Shirihai OS. Mitochondrial Fusion, Fission and Autophagy as a Quality Control Axis: The Bioenergetic View. *Biochim Biophys Acta (BBA) - Bioenergetics* (2008) 1777(9):1092–7. doi: 10.1016/j.bbabio.2008.05.001
35. Jornayvaz FR, Shulman GI. Regulation of Mitochondrial Biogenesis. *Essays Biochem* (2010) 47:69–84. doi: 10.1042/bse0470069
36. Scarpulla RC. Metabolic Control of Mitochondrial Biogenesis Through the PGC-1 Family Regulatory Network. *Biochim Biophys Acta* (2011) 1813(7):1269–78. doi: 10.1016/j.bbamcr.2010.09.019
37. Widau RC, Jin Y, Dixon SA, Wadzinski BE, Gallagher PJ. Protein Phosphatase 2A (PP2A) Holoenzymes Regulate Death-Associated Protein Kinase (DAPK) in Ceramide-Induced Anoikis. *J Biol Chem* (2010) 285(18):13827–38. doi: 10.1074/jbc.M109.085076
38. Roskoski RJr. Targeting Oncogenic Raf Protein-Serine/Threonine Kinases in Human Cancers. *Pharmacol Res* (2018) 135:239–58. doi: 10.1016/j.phrs.2018.08.013
39. Cheng Z, Wei-Qi J, Jin D. New Insights on Sorafenib Resistance in Liver Cancer With Correlation of Individualized Therapy. *Biochim Biophys Acta Rev Cancer* (2020) 1874(1):188382. doi: 10.1016/j.bbcan.2020.188382
40. Lin H, Zhang R, Wu W, Lei L. Comprehensive Network Analysis of the Molecular Mechanisms Associated With Sorafenib Resistance in Hepatocellular Carcinoma. *Cancer Genet* (2020) 245:27–34. doi: 10.1016/j.cancergen.2020.04.076
41. Rashid HO, Yadav RK, Kim HR, Chae HJ. ER Stress: Autophagy Induction, Inhibition and Selection. *Autophagy* (2015) 11(11):1956–77. doi: 10.1080/15548627.2015.1091141
42. Zhou B, Lu Q, Liu J, Fan L, Wang Y, Wei W, et al. Melatonin Increases the Sensitivity of Hepatocellular Carcinoma to Sorafenib Through the PERK-ATF4-Beclin1 Pathway. *Int J Biol Sci* (2019) 15(9):1905–20. doi: 10.7150/ijbs.32550

43. Masuda M, Chen WY, Miyanaga A, Nakamura Y, Kawasaki K, Sakuma T, et al. Alternative Mammalian Target of Rapamycin (mTOR) Signal Activation in Sorafenib-Resistant Hepatocellular Carcinoma Cells Revealed by Array-Based Pathway Profiling. *Mol Cell Proteomics* (2014) 13(6):1429–38. doi: 10.1074/mcp.M113.033845
44. Birben E, Sahiner UM, Sackesen C, Erzurum S, Kalayci O. Oxidative Stress and Antioxidant Defense. *World Allergy Organ J* (2012) 5(1):9–19. doi: 10.1097/WOX.0b013e3182439613

Conflict of Interest: The authors declare that the research was conducted in the absence of any commercial or financial relationships that could be construed as a potential conflict of interest.

Publisher's Note: All claims expressed in this article are solely those of the authors and do not necessarily represent those of their affiliated organizations, or those of the publisher, the editors and the reviewers. Any product that may be evaluated in this article, or claim that may be made by its manufacturer, is not guaranteed or endorsed by the publisher.

frontiers | Frontiers in Oncology

TYPE Original Research
PUBLISHED 29 August 2022
DOI 10.3389/fonc.2022.881341

OPEN ACCESS

EDITED BY
Tomas Buchler,
Charles University, Czechia

REVIEWED BY
Junsu Park,
Chungnam National University Sejong Hospital, South Korea
Hong Zhu,
Xiangya Hospital, Central South University, China

*CORRESPONDENCE
Zengxin Lu
luzx777@163.com

SPECIALTY SECTION
This article was submitted to Gastrointestinal Cancers: Colorectal Cancer, a section of the journal Frontiers in Oncology

RECEIVED 22 February 2022
ACCEPTED 01 August 2022
PUBLISHED 29 August 2022

CITATION
Li Z, Huang H, Wang C, Zhao Z, Ma W, Wang D, Mao H, Liu F, Yang Y, Pan W and Lu Z (2022) DCE-MRI radiomics models predicting the expression of radioresistant-related factors of LRP-1 and survivin in locally advanced rectal cancer.
Front. Oncol. 12:881341.
doi: 10.3389/fonc.2022.881341

DCE-MRI radiomics models predicting the expression of radioresistant-related factors of LRP-1 and survivin in locally advanced rectal cancer

Zhiheng Li[1], Huizhen Huang[2], Chuchu Wang[2], Zhenhua Zhao[1], Weili Ma[1], Dandan Wang[1], Haijia Mao[1], Fang Liu[3], Ye Yang[3], Weihuo Pan[4] and Zengxin Lu[1]*

[1]Department of Radiology, Shaoxing People's Hospital, Shaoxing Hospital, Zhejiang University School of Medicine, Shaoxing, China, [2]Shaoxing University School of Medicine, Shaoxing, China, [3]Department of Pathology, Shaoxing People's Hospital, Shaoxing Hospital, Zhejiang University School of Medicine, Shaoxing, China, [4]Department of Colon and Rectal Surgery, Shaoxing People's Hospital, Shaoxing Hospital, Zhejiang University School of Medicine, Shaoxing, China

Objective: Low-density lipoprotein receptor-related protein-1 (LRP-1) and survivin are associated with radiotherapy resistance in patients with locally advanced rectal cancer (LARC). This study aimed to evaluate the value of a radiomics model based on dynamic contrast-enhanced magnetic resonance imaging (DCE-MRI) for the preoperative assessment of LRP-1 and survivin expressions in these patients.

Methods: One hundred patients with pathologically confirmed LARC who underwent DCE-MRI before surgery between February 2017 and September 2021 were included in this retrospective study. DCE-MRI perfusion histogram parameters were calculated for the entire lesion using post-processing software (Omni Kinetics, G.E. Healthcare, China), with three quantitative parameter maps. LRP-1 and survivin expressions were assessed by immunohistochemical methods and patients were classified into low- and high-expression groups.

Results: Four radiomics features were selected to construct the LRP-1 discrimination model. The LRP-1 predictive model achieved excellent diagnostic performance, with areas under the receiver operating curve (AUCs) of 0.853 and 0.747 in the training and validation cohorts, respectively. The other four radiomics characteristics were screened to construct the survivin predictive model, with AUCs of 0.780 and 0.800 in the training and validation cohorts, respectively. Decision curve analysis confirmed the clinical usefulness of the radiomics models.

Conclusion: DCE-MRI radiomics models are particularly useful for evaluating LRP-1 and survivin expressions in patients with LARC. Our model has significant

potential for the preoperative identification of patients with radiotherapy resistance and can serve as an essential reference for treatment planning.

KEYWORDS

dynamic contrast-enhanced magnetic resonance imaging (DCE-MRI), locally advanced rectal cancer, radiomics models, LRP-1, survivin

Introduction

Rectal cancer is the third most common malignant tumor worldwide, and approximately 70% of patients have locally advanced rectal cancer (LARC) at the initial diagnosis (1). At present, radiotherapy before surgical resection is the recommended treatment for patients with LACR (2). Preoperative radiotherapy can reduce the risk of local recurrence and ultimately improve the quality of life of patients by downstaging tumors and increasing the preservation rate of the sphincter (3). However, this effect is not ideal because the response of different individuals to preoperative radiotherapy is highly variable (4). In addition, radiotherapy is associated with long-term treatment-related toxicity, such as chronic pain, urinary incontinence, sexual dysfunction, and secondary malignant tumors (5). The identification of radioresistant LARC is a significant hurdle for patient-specific treatment.

Although the mechanism underlying radioresistance has not been fully clarified, the therapeutic effect of radiotherapy is known to depend on the cell cycle of cancer cells (6). Among all cell division phases, cells in the S, G0/G1, and G2/M phases are resistant, relatively sensitive, and sensitive to radiotherapy, respectively (7). Hence, several proteins that function in the cell cycle have been considered as potential biomarkers of radiotherapy resistance in rectal cancer. Low-density lipoprotein receptor-related protein-1 (LRP-1) is widely expressed in a wide variety of tissues; it exhibits functionalities in supporting tumor cell proliferation by promoting the entry of the cell cycle into the S phase and decreasing apoptosis (8, 9). A previous study has shown that patients with high LRP-1 expression who were subjected to radiotherapy had a poor prognosis, implying that LRP-1 could be an important marker for discriminating radioresistant rectal cancer (10). Additionally, studies have reported that survivin can also affect the radioresistance of LARC by regulating the cell cycle. Survivin is an inhibitor of apoptotic proteins that regulate both cell cycle progression and cell survival (11). According to the literature, targeted inhibition of survivin can reduce radiation-induced G2/M arrest, which means that survivin can cause more irradiation-damaged cells to enter mitosis, thus playing a vital role in radiotherapy (12). Identifying LRP-1 and survivin expressions preoperatively is helpful in making individualized treatment plans. However, the detection of LRP-1 and survivin expressions mainly depends on tissue sampling, which is limited by the invasiveness of the operation and may not reflect the entire tumor. Thus, identifying a noninvasive method for detecting LRP-1 and survivin will be beneficial and provide a reference for treatment decisions.

Radiomics analysis is an emerging field of image analysis that reflects the biological characteristics of tumors by transforming gray information into high-dimensional image features (13). Accumulating evidence indicates that radiomics can be used to quantitatively analyze tumor heterogeneity and is closely related to pathology (14). Deng et al. (15) found that radiomics predictive models have the potential to noninvasively differentiate lymph node metastasis and vascular endothelial growth factor expressions in cervical cancer. In previous studies, radiomics features have always been extracted from computed tomography angiography, T1-weighted imaging (T1WI), T2-weighted imaging (T2WI), diffusion-weighted imaging (DWI), and apparent diffusion coefficient (ADC) maps. Unlike the abovementioned imaging techniques, dynamic contrast-enhanced magnetic resonance imaging (DCE-MRI) is a relatively novel imaging modality that combines tumor morphology and changes in hemodynamics (16). DCE-MRI parameters can also reflect tumor angiogenesis and, therefore, provide essential information about the prognosis and effect of treatment for LARC (17). Moreover, in various oncology fields, several researchers have recommended using DCE-MRI to assess response to radiotherapy (18, 19). Li et al. (20) showed that radiomics features based on breast DCE-MRI could identify the status of some pathological markers (HER2 and Ki-67). Thus, radiomics analysis based on DCE-MRI might be a noninvasive method for predicting LRP-1 and survivin expressions in LARC.

This study aimed to construct and validate a noninvasive model using DCE-MRI to predict LRP-1 and survivin expressions in LARC, thus guiding clinical treatment options and improving the level of medical care.

Materials and methods

This retrospective study was carried out in accordance with the Declaration of Helsinki and was approved by the

Institutional Review Board of Shaoxing People's Hospital. The requirement for written informed consent to review the medical records or images of the patients was waived because of the study's retrospective nature.

Study participants

The data of patients with pathologically confirmed LARC by biopsy or surgery from February 2017 to August 2021 at Shaoxing People's Hospital were consecutively assessed in this study. The detailed inclusion criteria were as follows (1): histologically confirmed primary rectal adenocarcinoma (2), DCE-MRI within 2 weeks before biopsy or surgery (3), LARC determined by pretreatment MRI (≥T3 and/or N+), and (4) absence of antitumor treatment, such as neoadjuvant chemoradiotherapy, before MRI. The exclusion criteria were as follows (1): poor image quality (with severe artifacts) or failure to obtain measurements (2), severe systemic disease and absolute contraindications (3), lack of pre-surgical carcinoembryonic antigen (CEA) and carbohydrate antigen (CA)199 data (4), metastatic disease, and (5) a maximum tumor diameter of <1 cm. The standard of care for patients with LARC at our hospital was neoadjuvant chemoradiotherapy followed by total mesorectal excision (TME). However, some patients underwent TME plus adjuvant chemotherapy because of their age, risk of toxic effects, possibility of tumor progression, or painfully long treatment period. Additionally, some elderly patients chose other treatment options for the above reasons. Finally, 100 patients were enrolled in this study; among these, 64 were treated with TME plus adjuvant chemotherapy, 21 were treated with neoadjuvant chemotherapy plus TME, 12 received neoadjuvant chemoradiotherapy followed by TME, and 3 received neoadjuvant radiotherapy plus TME.

Dynamic contrast-enhanced magnetic resonance imaging protocol

All imaging data of patients with LARC were obtained using a 3.0-T MRI scanner (Verio, Siemens, Germany) with a 12-channel phased-array body coil. Patients were required to fast for at least 8 h to empty the gastrointestinal tract and inject antispasmodic medication (Anisodamine, Minsheng, Hangzhou, China) before the MRI examination to reduce gastrointestinal artifacts. During the MRI scan, the patient was placed in the supine position, and the positioning line was located on the xiphoid process. All patients underwent a routine plain scan (T1WI, T2WI with fat suppression, T2WI, ADC, DWI) before the DCE-MRI scan and a multi-angle cross-sectional T1WI in the axial plane scan (repetition time/echo time, 3.48 ms/1.3 ms; layer thickness, 3 mm; field of view, 260 mm × 260 mm; matrix, 202 × 288; scan at multiple flip angles of 5°, 10°, and 15°). DCE-MRI adopts free breathing and is performed using a fast three-dimensional T1-weighted spoiled gradient recalled echo sequence. Multiphase dynamic enhanced scanning was performed with the following parameters: flip angle, 10°; and number of phases scanned, 35. The other acquisition parameters were the same as those above. Subsequently, a gadolinium contrast agent (Omniscan, GE Healthcare, China) was injected intravenously during phase 3 using a power injector at 0.1 mmol/kg and 3.5 mL/s. Finally, 20-mL saline was injected for flushing at the same flow rate. Contrast agent injection and data acquisition were performed simultaneously.

Image data analysis and processing

All sequences acquired from the DCE-MRI of eligible patients with LARC were imported into Omni Kinetics (GE Healthcare, China) software for post-processing. First, multi-flip angles of 5°, 10°, and 15° and corrected dynamic enhancement sequence scans were processed using Omni Kinetics software. Second, the external iliac artery was selected as the input artery. Third, the Tofts pharmacokinetic model was used to obtain three DCE-MRI pseudo-color images (Ktrans, Kep, and Ve). Furthermore, the region of interest (ROI) was manually delineated on each slice of the sagittal DCE pseudo-color images for calculation, using T2-weighted images as a guide. The ROI was placed in an area to avoid necrosis, calcification, and blood vessels on each slice (Figure 1). Two radiologists with 5 years (reader 1) and 8 years (reader 2) of specific clinical experience in rectal cancer imaging completed all image segmentations. The software automatically generated 231 radiomics features from three perfusion maps (Ktrans, Kep, and Ve), which included five categories: first-order, histogram, gray level co-occurrence matrix, Haralick, and run-length matrix.

Immunohistochemical evaluation of low-density lipoprotein receptor-related protein-1 and survivin

LARC pathological specimens were harvested during surgery or by enteroscopy biopsy. In order to avoid the influence of anti-tumor therapy on the expressions of LRP-1 and survivin, biopsy specimens were used in patients who received any antitumor treatment before surgery. Postoperative specimens were used only in patients treated with TME plus adjuvant chemotherapy. Accordingly, there were 36 biopsy specimens and 64 surgical specimens, respectively. The expressions of LRP-1 and survivin were determined in formalin-fixed, paraffin-embedded tumor tissues using immuno histochemistry (IHC). Serial sections were immunostained with antibodies against LRP-1 (1:4000; Gene Tech, Shanghai, China) and survivin (GT204821; Gene Tech, Shanghai, China). Immunohistochemical tests for LRP-1 and survivin were

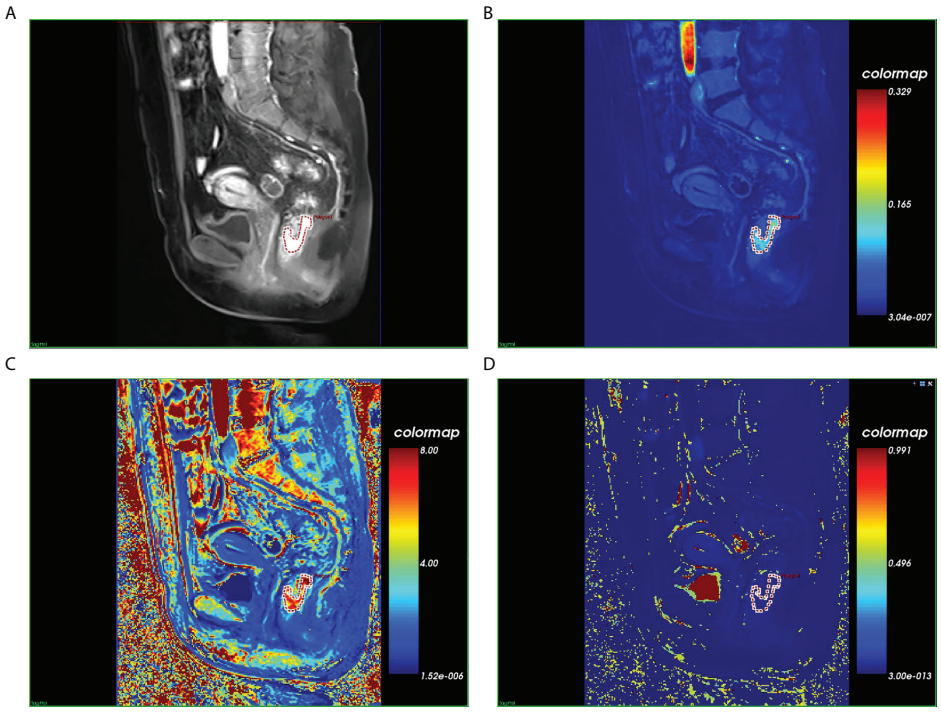

FIGURE 1
Magnetic resonance images of a histopathologically confirmed locally advanced rectal cancer in a 56-year-old woman. **(A)** Manual region of interest (ROI) placement in a contrast-enhanced sagittal T1-weighted image. **(B)** Color-coded Ktrans map of the ROI. **(C)** Color-coded Kep map of the ROI. **(D)** Color-coded Vp map of the ROI.

performed strictly according to the IHC protocol. The expression levels of LRP-1 and survivin in tumor cells were determined using the following scoring system: 1 (≤ 10%), 2 (10% to ≤ 50%), 3 (50% to ≤ 80%), or 4 (> 80%). Staining intensity was scored as 0 (no staining), 1 (weak staining), 2 (moderate staining), or 3 (intense staining). The score for the percentage of positively stained tumor cells and the score for staining intensity were then multiplied to obtain the immunoreactive score (IRS), which ranged from 0 to 12. There was no uniform opinion on the evaluation of LRP-1 and survivin expressions on IHC, considering the limited number of patients in this study. To facilitate further statistical analyses, the expression levels of LRP-1 and survivin were divided into two categories: low expression (IRS ≤ 4 points) and high expression (IRS > 4 points). An 80% agreement between the two pathologists participating in immunostaining evaluation was set as the standard. When the pathologists disagreed regarding an evaluation, they made decisions based on consultation.

Interobserver variability evaluation

To assess the intraobserver and interobserver reproducibilities of radiomics feature extraction, 30 patients were randomly selected and intraclass correlation coefficients (ICCs) were calculated for tumor segmentation performed 1 week later by readers 1 and 2. Subsequently, intragroup consistency analysis was performed on the features of the 30 patients drawn by reader 1, and intergroup consistency analysis was performed on the features of the same 30 patients drawn by readers 1 and 2. The reproducibility of radiomics features extracted from DCE-MRI was considered good, with intraobserver and interobserver ICC values both > 0.8. These features, with good reproducibility, were collected for subsequent radiomics analysis.

Feature selection and radiomics signature construction

For each extracted radiomic feature, the mean value was individually subtracted from the score, which was then divided by the respective standard deviation (Z-score normalization). Subsequently, two technical approaches (the maximum relevance minimum redundancy [mRMR] method (21) combined with the least absolute shrinkage and selection operator [LASSO] method) were used to select the most useful predictive features from the training data cohort. The LASSO logistic regression model was used with penalty parameter tuning, which was conducted using tenfold cross-validation. Lambda was selected according to the 1-standard

error of the minimum (1-SE) rule, where the coefficients are not rapidly changing, and the model is most parsimonious with the minimum prediction error. Multivariate logical regression was used to construct the predictive model using the selected features. A radiomics score (Rad-score) was calculated for each patient using a linear combination weighted by the respective coefficients (22).

Receiver operating characteristic (ROC) curves were used to assess the performance of the radiomics models for LRP-1 and survivin. The specificity, sensitivity, positive predictive value (PPV), negative predictive value (NPV), and area under the curve (AUC) were calculated to determine model performance. Calibration curves were used to investigate the predictive accuracy of the model graphically. The aforementioned operations were performed in both the training and validation cohorts. Finally, decision curve analysis (DCA) was used to determine the clinical usefulness of the radiomic models.

Pathological evaluation of the therapeutic response

Tumor regression grading (TRG) was assessed in postoperative pathological specimens according to the four-tier American Joint Committee on Cancer system (23): TRG 0, no residual tumor cells; TRG 1, single cell or small group of cells; TRG 2, residual cancer with a desmoplastic response; and TRG 3, minimal evidence of tumor response. Patients were then divided into 2 groups; patients with TRG scores of 0 and 1 classified as sensitive and those with TRG scores of 2 and 3 were classified as resistant.

Statistical analyses

All statistical analyses and figure creation were performed using R software (version 40.2; packages mainly included glmnet, pROC, rms, and rmda, Foundation for Statistical Computing, Vienna, Austria). To determine the clinical usefulness of the LRP-1 and survivin predictive model, DCA was performed by calculating the net benefits at different threshold probabilities in the test cohorts. The area under the ROC curve was calculated to measure the diagnostic efficacy of the models. Moreover, the sensitivity, specificity, PPV, NPV, and accuracy were assessed. All tests were two-tailed, and statistical significance was set at $p < 0.05$. Continuous variables (age) are presented as means and standard deviations, and an independent sample t-test was used to assess differences between high and low expression groups. Categorical variables (sex, location, mrT stage, mrN stage, CEA level, and CA199 level) were assessed using Fisher's exact test or chi-squared test, as appropriate.

Results

Characteristics of patients with locally advanced rectal cancer

This research's summary profile is shown in Figure 2. Of the 100 patients, 64 were male and 36 were female. The patients were randomly divided, in a 7:3 ratio, into training (70 patients) and validation cohorts (30 patients). According to LRP-1 and survivin expression groups, no statistically significant differences were observed between the training and validation cohorts in terms of sex, age, body mass index, location, mrT stage, mrN stage, CEA level, or CA199 level (all $p > 0.05$). Details regarding the clinical characteristics of patients with LARC with high/low expression (LRP-1 and survivin) in both cohorts are provided in Tables 1, 2.

Expressions of LRP-1 and survivin

LRP-1 and survivin expressions were identified by IHC. Examples of the IHC analysis of LRP-1 and survivin expressions are shown in Figure 3. A weak correlation between LRP-1 and survivin was observed ($r = 0.201$, $p = 0.045$). Furthermore, some patients with high LRP expression exhibited significantly low survivin expression.

Feature selection and radiomics model construction

In total, 231 features were extracted from the MRI data (67 features each from Ktrans, Kep, and Ve). The details of these selected features are provided in the Supplemental Material. Using the mRMR method, 20 features were identified as having high stability for predicting LRP-1 and survivin. The LASSO method with tenfold cross-validation was then used to select four potential predictive features each for LRP-1 and survivin, with non-zero coefficients, to construct the final model; the LASSO process is shown in Figure 4. The features were weighted according to their corresponding coefficients. The resulting Rad-score equation for the LRP-1 prediction (Rad-score1) is as follows:

$$\text{“}Rad-score1 = 2.351 \times sumAverage.Ktrans - 0.147 \times skewness.Kep + 2.023 \times RunLengthNonuniformity.Ve - 0.530 \times differenceEntropy.Ktrans + 1.265\text{”}$$

The resulting Rad-score equation for the survivin prediction (Rad-score2) is as follows::

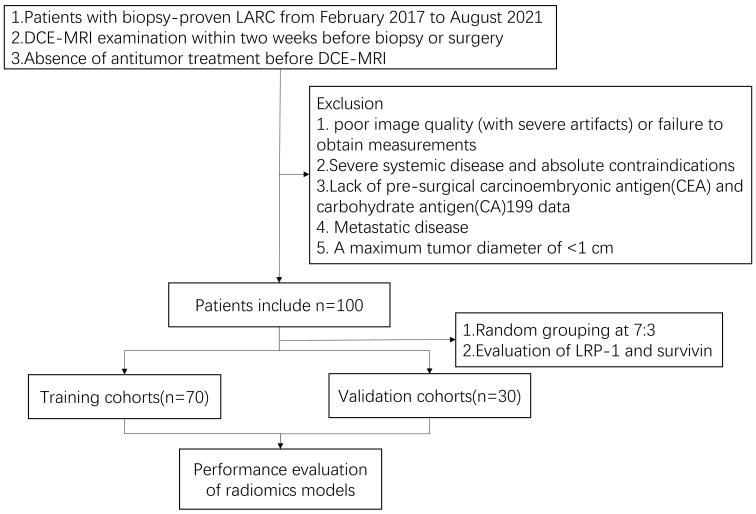

FIGURE 2
Patient inclusion and exclusion details and the patient recruitment flowchart.

TABLE 1 Characteristics of patients with locally advanced rectal cancer in the training and validation cohorts (low-density lipoprotein receptor-related protein-1).

Characteristic	Training cohorts(n = 70)		P	Validation cohorts(n = 30)		P
	High	Low		High	Low	
Sex			0.668			0.297
Male	26(65.00%)	18(60.00%)		10(58.82%)	10(76.92%)	
Female	14(35.00%)	12(40.00%)		7(41.18%)	3(23.08%)	
Age(years)			0.717			0.088
mean ± SD	68.75 ± 11.29	67.83 ± 9.13		65.47 ± 11.21	71.92 ± 7.89	
BMI(kg/m^2)	23.45 ± 3.58	22.90 ± 3.13	0.154	23.54 ± 3.47	22.77 ± 4.06	0.088
Location			0.254			0.237
Above	8(26.67%)	10(25.00%)		5(29.41%)	4(30.77%)	
Straddling	15(37.50%)	6(20.00%)		5(29.41%)	8(61.54%)	
Below	15(37.50%)	16(53.33%)		7(41.18%)	1(7.69%)	
mrT stage			0.571			0.785
T2	3(7.50%)	1(3.33%)		1(7.69%)	0(0.00%)	
T3	35(87.50%)	26(86.67%)		15(88.24%)	11(86.62%)	
T4	2(5.00%)	3(10.00%)		2(11.77%)	1(7.69%)	
mrN stage			0.843			0.758
N0	3(7.50%)	1(3.33%)		0(0.00%)	1(7.69%)	
N1	10(25.00%)	7(23.33%)		2(11.77%)	1(7.69%)	
N2	27(67.50%)	22(73.33%)		15(88.24%)	11(84.62%)	
CEA level			0.533			0.217
Normal	23(57.50%)	15(50.00%)		10(58.82%)	4(30.77%)	
Abnormal	17(42.50%)	15(50.00%)		7(41.18%)	9(69.23%)	
CA199 level			0.255			0.410
Normal	32(80.00%)	27(90.00%)		15(88.24%)	10(76.92%)	
Abnormal	8(20.00%)	3(10.00%)		3(11.77%)	2(23.08%)	

TABLE 2 Characteristics of patients with locally advanced rectal cancer in the training and test groups (survivin group).

Characteristic	Training cohorts(n = 70)		P	Validation cohorts(n = 30)		P
	High	Low		High	Low	
Sex			0.353			0.193
Male	27(67.50%)	17(56.67%)		13(76.47%)	7(53.85%)	
Female	13(32.50%)	13(43.33%)		4(23.53%)	6(46.15%)	
Age(years)			0.382			0.265
mean ± SD	66.43 ± 10.71	70.93 ± 9.43		66.41 ± 9.34	22.67 ± 3.92	
BMI	23.55 ± 3.55	22.76 ± 3.14	0.339	23.61 ± 3.57	23.00 ± 3.09	0.513
Location			0.706			0.200
Above	11(27.50%)	7(23.33%)		3(17.65%)	6(46.15%)	
Straddling	13(32.50%)	8(26.67%)		6(35.29%)	2(15.38%)	
Below	16(40.00%)	15(50.00%)		8(47.06%)	5(38.46%)	
mrT stage			0.046			0.371
T2	0(0.00%)	4(13.33%)		0(0.00%)	1(7.69%)	
T3	37(92.50%)	24(80.00%)		16(94.12%)	10(76.92%)	
T4	3(7.50%)	2(6.67%)		1(5.88%)	2(15.39%)	
mrN stage			0.019			0.151
	N0	0(0.00%)	4(13.33%)		0(0.00%)	1(7.69%)
N1	8(20.00%)	9(30.00%)		3(17.65%)	0(0.00%)	
N2	32(80.00%)	17(56.67%)		14(82.35%)	12(92.31%)	
CEA level			0.268			0.127
Normal	24(60.00%)	14(46.67%)		7(69.23%)	9(41.18%)	
Abnormal	16(40.00%)	16(53.33%)		10(58.82%)	4(30.77%)	
CA199 level			0.635			0.410
Normal	33(82.50%)	26(86.67%)		15(88.24%)	10(76.92%)	
Abnormal	7(17.50%)	4(13.33%)		2(11.77%)	3(23.08%)	

$$\text{“}Rad-score2 = -0.805 \times differenceEntropy.Kep + 1.564 \times Correlation.Ktrans - 0.069 \times Quantile95.Kep - 0.236 \times inverseDifferenceMoment.Ktrans + 0.565$$

Radiomics model evaluation

We compared Rad-scores between the LRP/survivin (high) and LRP/survivin (low) groups in the training and validation cohorts. There was a significant difference in Rad-scores between the LRP/survivin (high) and LRP/survivin (low) groups, as shown in Figure 5.

The discrimination performance of the Rad-scores for LRP-1 and survivin is summarized in Table 3. ROC curves of the Rad-score for predicting LRP-1 and survivin status are shown in Figure 6. The LRP-1 model yielded an AUC of 0.853, with a 95% confidence interval (CI), accuracy, sensitivity, and specificity of 0.760–0.945, 0.829, 0.900, and 0.733, respectively. This model was applied to the validation cohort, which generated an AUC, 95% CI, accuracy, sensitivity, and specificity of 0.747, 0.556–0.938, 0.767, 0.882, and 0.615, respectively. Correspondingly, in the training cohort, the survivin model yielded an AUC of 0.780 with 95% CI, accuracy, sensitivity, and specificity of 0.670–0.890, 0.757, 0.700, and 0.833, respectively. Analysis in the validation cohort generated an AUC, 95% CI, accuracy, sensitivity, and specificity of 0.800, 0.635–0.967, 0.800, 0.824, and 0.769, respectively.

The calibration curves of the two models demonstrated that the predicted probability fit well with the actual expression levels in both the training and validation cohorts, indicating excellent calibration of the radiomics models (Figure 7). The decision curve of the radiomics model is shown in Figure 8, and DCA revealed that using the radiomics models (LRP-1/survivin) added more net benefit than the treat-all or treat-none strategies, indicating the excellent performance of the radiomics models in terms of clinical application.

Rad-scores in resistant and sensitive groups

Among 15 patients who underwent radiotherapy (12 received neoadjuvant chemoradiotherapy followed by TME

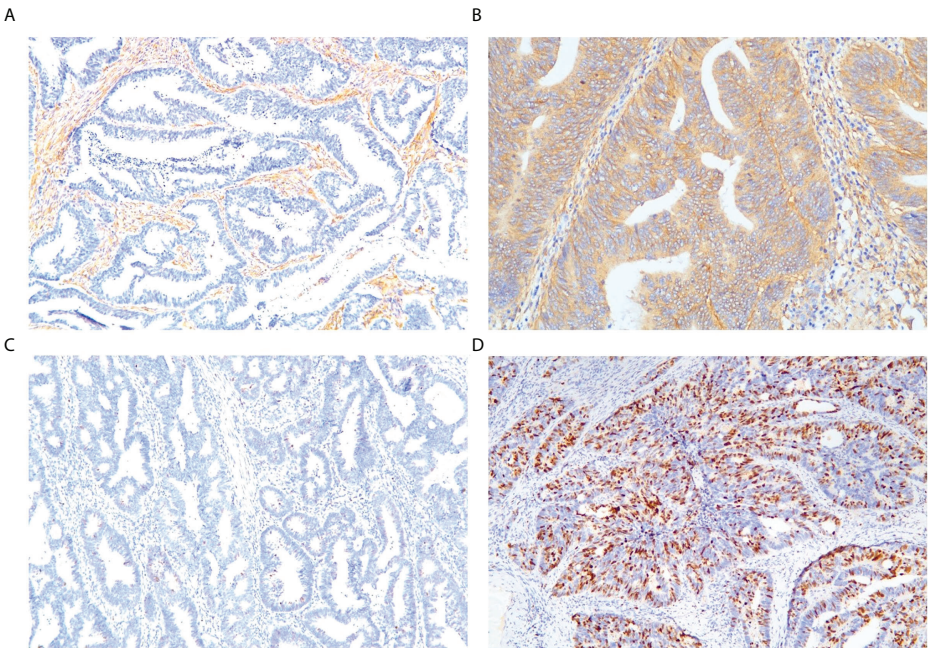

FIGURE 3
Representative immunohistochemical staining of markers. Low-density lipoprotein receptor-related protein-1: **(A)** low expression, **(B)** high expression. Survivin: **(C)** low expression, **(D)** high expression (magnification: ×10 20).

and 3 received neoadjuvant radiotherapy plus TME), Rad-score2 was not significantly different between sensitive and resistant groups ($p = 0.594$; Table 4). However, Rad-score1 was significantly higher in the resistant group (4.829 ± 3.459) than in the sensitive group (-0.210 ± 0.648, $p = 0.043$; Table 4).

Discussion

To the best of our knowledge, this study is the first attempt to propose and validate noninvasive radiomics models based on DCE-MRI for the preoperative prediction of LRP-1 and survivin expressions in patients with LARC. The predictive model for LRP-1 demonstrated favorable discrimination and yielded AUCs of 0.853 and 0.747 in the training and validation groups, respectively. In predicting survivin expression, the radiomics model achieved AUCs of 0.780 and 0.800 in the training and validation cohorts, respectively. The results suggest that the clinical use of radiomics is promising in terms of the preoperative prediction of LRP-1 and survivin. In addition, Rad-score1 was significantly higher in the resistant group than in the sensitive group, although Rad-score2 was not significantly different between the two groups. Thus, the predictive models may be helpful in guiding clinicians in identifying patients who are radiotherapy resistant and selecting appropriate treatment plans for patients with LARC.

In recent years, radioresistance has mainly been responsible for treatment failure and mortality in patients with LARC receiving radiation therapy. Furthermore, the current standard of care for LARC is to apply the same treatments to all patients, regardless of their individual responses to radiotherapy. This uniform treatment method inevitably leads to undertreatment or overtreatment for several patients with LARC (24). Currently, approximately 30%–50% of patients are reported to show radioresistance to ionizing radiation (IR); however, if these patients are identified before surgery, more intensive chemotherapy could be applied (25). In contrast, the complete response for tumors predicted to undergo invasive radical surgery may even be modified. Therefore, the development of new biomarkers capable of successfully assessing patients' radio-responsiveness status preoperatively is urgently needed to establish patient-specific treatment (26). Radioresistance is a complex process involving the alteration of several cellular mechanisms (27). Moreover, cell division phases profoundly influence the response to radiation in cancer (28, 29). Numerous studies have shown that LRP-1 and survivin play essential roles in regulating the cell cycle, which is significantly related to radiotherapy tolerance in LARC. Identifying LRP-1 and survivin expressions before surgery may improve prognostication and guide the selection of a clinical treatment plan. At present, a pathological examination is the gold standard for diagnosing LRP-1 and survivin expressions. However, results are influenced by sampling and may be inadequately comprehensive because of

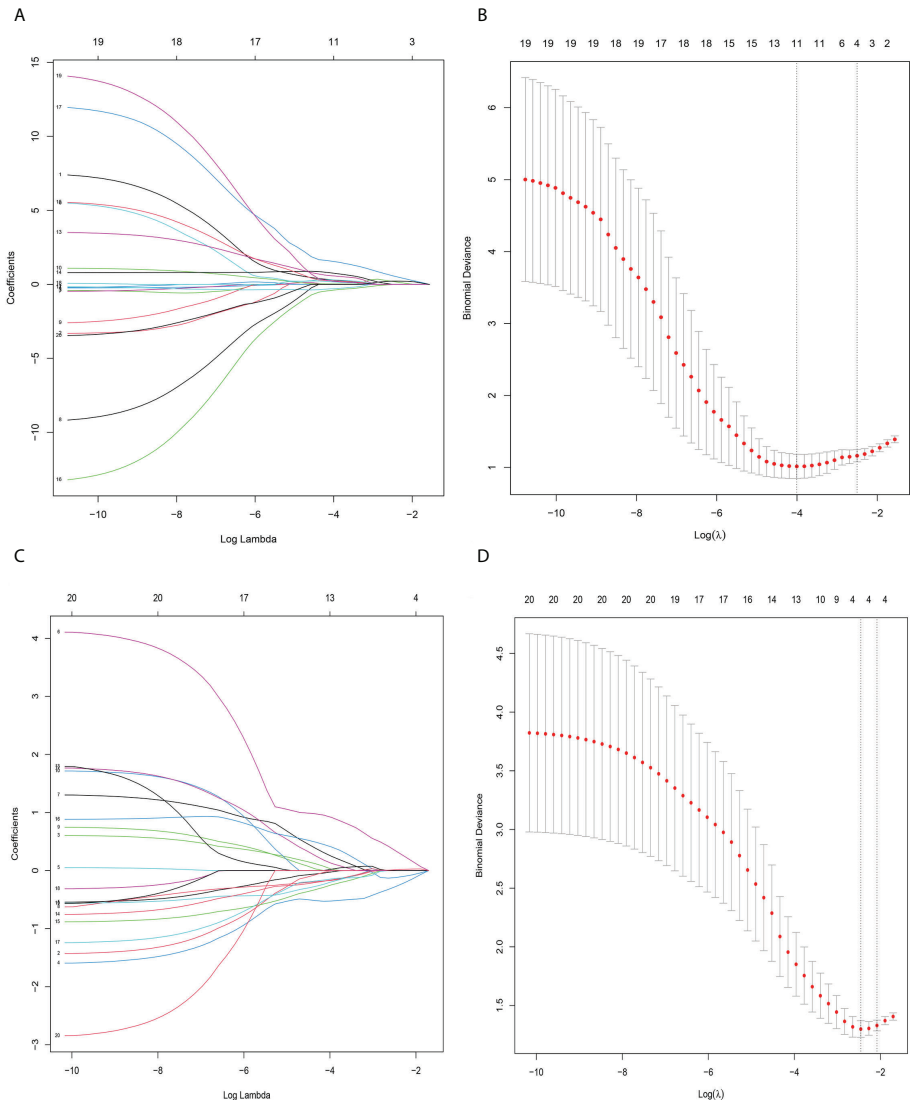

FIGURE 4
Radiomics feature selection using sthe least absolute shrinkage and selection operator (LASSO) binary logistic regression model. **(A)** LASSO coefficient profile, displaying 30 texture features. A coefficient profile plot was produced against the log (lambda) sequence. Each colored line represents the coefficient of an individual feature. **(B)** Tuning parameter (log lambda) selection in the LASSO model used tenfold cross –validation *via* 1-SE criteria. Vertical dotted lines were drawn at the selected λ values. **(A, C)** The error rate curve. **(B, D)** LASSO coefficient λ graph. Coefficient λ was selected in the LASSO using a tenfold cross-validation. We selected the coefficient λ according to the 1-SE rule.

tumor heterogeneity. With the advent of the precision medicine era, single-modality medical imaging is gradually evolving and cannot meet the requirements of individualized treatment (30, 31). Radiomics, an emerging technique in computational medical imaging, can extract information-rich imaging functions with high throughput and quantify imaging information that the human eye cannot detect (32, 33). Many prior studies have shown that radiomics can effectively predict the expression of multiple pathological biomarkers in various tumors based on quantitative image features derived from different MRI techniques (34, 35). In our study, we used DCE-MRI to construct a predictive model. Unlike conventional MRI imaging techniques, DCE-MRI has the advantage of estimating blood flow, blood volume, and vascular permeability and the tumor vascular microenvironment. DCE-MRI has been applied in several tumor studies and has yielded satisfactory results (36). However, no study has aimed to determine the expressions of LRP-1 and survivin. In view of this knowledge gap, we established radiomics models based on DCE-MRI to distinguish between LRP-1 and survivin expression levels, and obtained promising results.

LRP-1 is a multifunctional scavenger receptor that belongs to the low-density lipoprotein receptor family (37). Owing to its

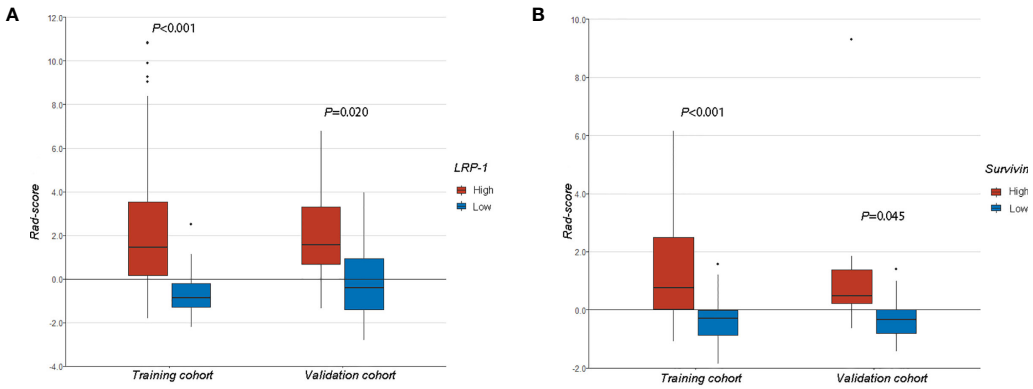

FIGURE 5
(A) A comparison of radiomics scores (Rad-scores) between different low-density lipoprotein receptor-related protein-1 expression levels in the training and validation cohorts. **(B)** A comparison of Rad-scores between different survivin expression levels in the training and validation cohorts.

TABLE 3 Performance summary of radiomics scores for predicting low-density lipoprotein receptor-related protein-1 and survivin status in each cohort.

	Cohort	Cut-off	AUC	ACC	SEN	SPE	PPV	NPV
LRP-1	Training	0.400	0.853	0.829	0.900	0.733	0.818	0.846
	Validation	0.445	0.747	0.767	0.882	0.615	0.750	0.800
Survivin	Training	0.557	0.780	0.757	0.700	0.833	0.848	0.676
	Validation	0.511	0.800	0.800	0.824	0.769	0.824	0.769

AUC, area under the receiver operating characteristic curve; ACC, accuracy; SEN, sensitivity; SPE, specificity; PPV, positive predictive value; NPV, negative predictive value.

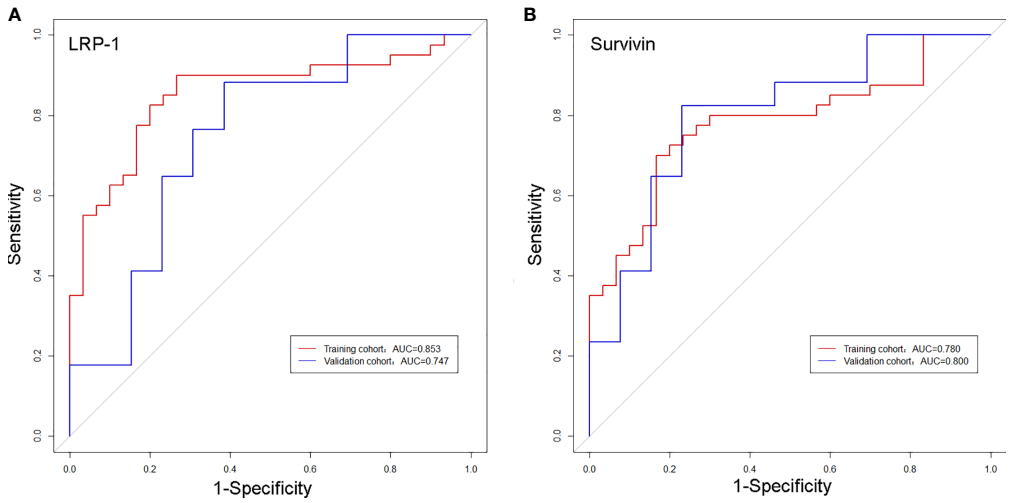

FIGURE 6
Receiver operating characteristic curves of the biomarkers for classifying low-density lipoprotein receptor-related protein-1 **(A)** and survivin **(B)** expression levels in the training and validation cohorts.

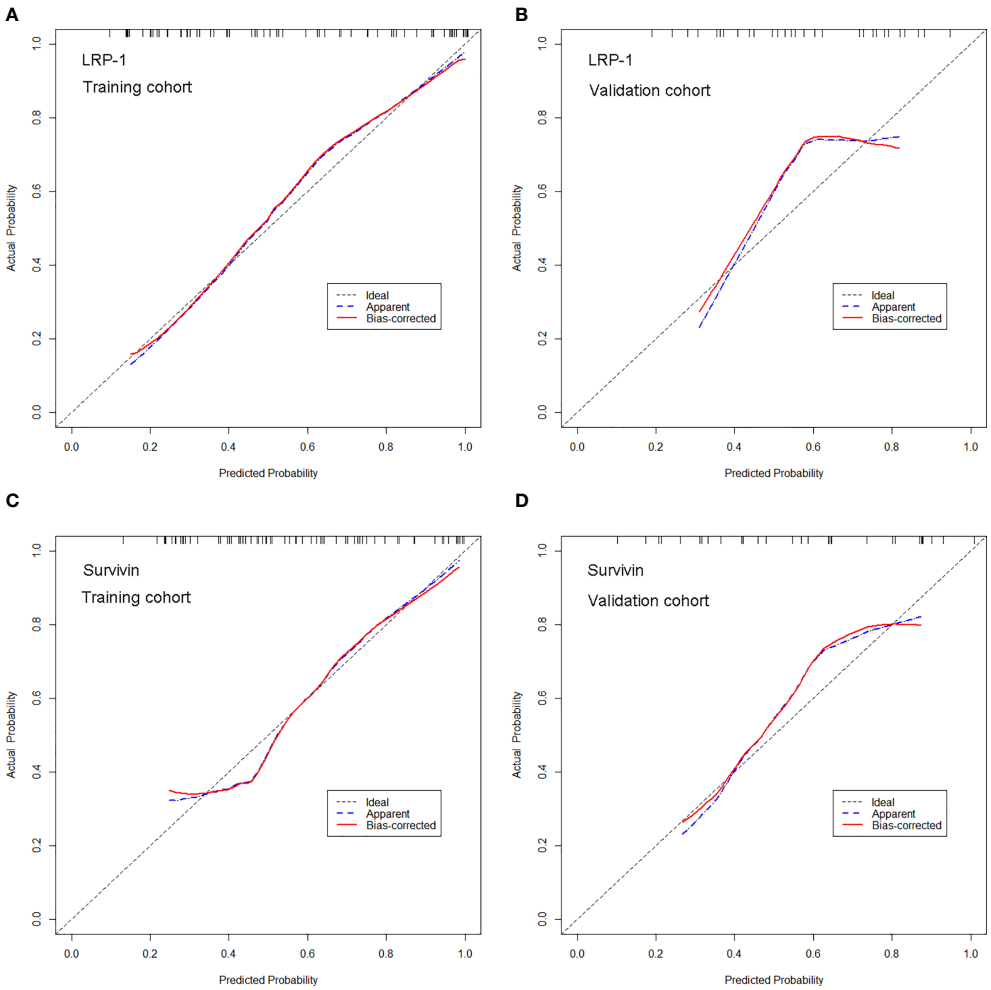

FIGURE 7
Calibration curves of the radiomics model for predicting low-density lipoprotein receptor-related protein-1 (LRP-1) and survivin expression levels in the training and validation cohorts. **(A, B)**. Calibration curves of the model for LRP-1 in **(A)** the training and **(B)** validation cohorts. **(C, D)** Calibration curves of the model for survivin in **(C)** the training and **(D)** validation cohorts. In the calibration plots, the 45° line represents marks the location of the ideal model. The blue line represents the predicted performance of the model, and the red line represents the bias correction in the model.

capacity to control the pericellular levels of various growth factors and proteases, LRP-1 plays a crucial role in tumor progression. Compared to untreated cells with LRP-1 inhibition, treated cells present an increase in the proportion of cells in the G1 phase and a decrease in the S phase cell population (8). Clinically, high LRP-1 expression in patients subjected to radiotherapy has a poor prognosis. Certainly, LRP-1 expression status has a crucial role in predicting radiotherapy resistance and prognosis in patients with LARC; however, few studies have used radiomics features extracted from pretreatment DCE-MRI to predict LRP-1 expression. In this study, four DCE-MRI radiomics features (Ktran. sum Average, Ktrans. difference entropy, Kep. skewness, and Ve. run length nonuniformity) were selected to construct the predictive model for LRP-1, which yielded a high AUC in both training (AUC = 0.853) and validation (AUC = 0.747) cohorts. Moreover, features from Ktrans were most commonly used in the optimal radiomics model (2/4). Previous studies have corroborated that Ktrans reflects vessel blood flow and is the product of vessel permeability and vessel surface area (38). Theoretically, the value of Ktrans is mainly determined by blood flow or elevated vessel permeability. Devy et al. (39) revealed that LRP-1 also plays an essential role in the angiogenic processes for tumor growth through its wide spectrum of interactions. Thus, the observed association between Ktrans (sum average) and LRP-1 expression is reasonable. Our radiomics model may

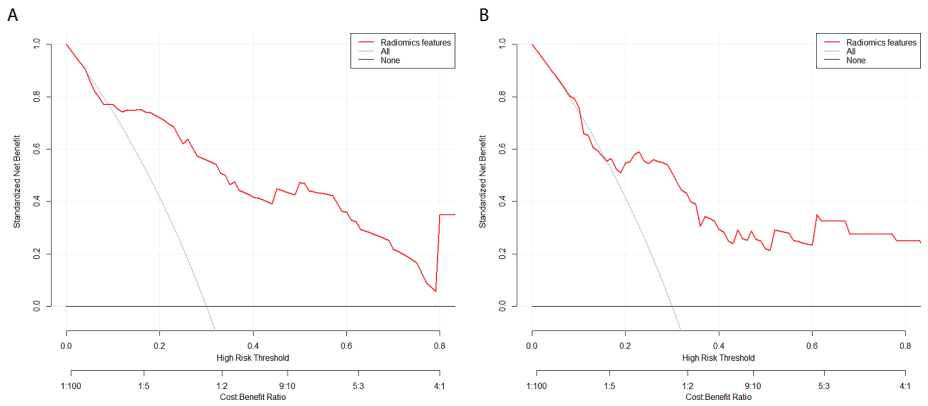

FIGURE 8
Decision curve analysis for the model for **(A)** low-density lipoprotein receptor-related protein-1 and **(B)** survivin in the test cohorts. The y-axis measures the standardized net benefit. The red curve represents the radiomics model. The gray curve represents the assumption that all patients were treated, and the straight black line at the bottom of the figure represents the assumption that no patient was treated.

TABLE 4 Radiomics scores between resistant and sensitive groups.

	Sensitive groups(n=10)	Resistant groups(n=5)	F value	P value
Rad-score1	-0.210 ± 0.648	4.829 ± 3.459	2.891	0.043
Rad-score2	1.771 ± 0.415	-0.083 ± 0.947	-0.547	0.594

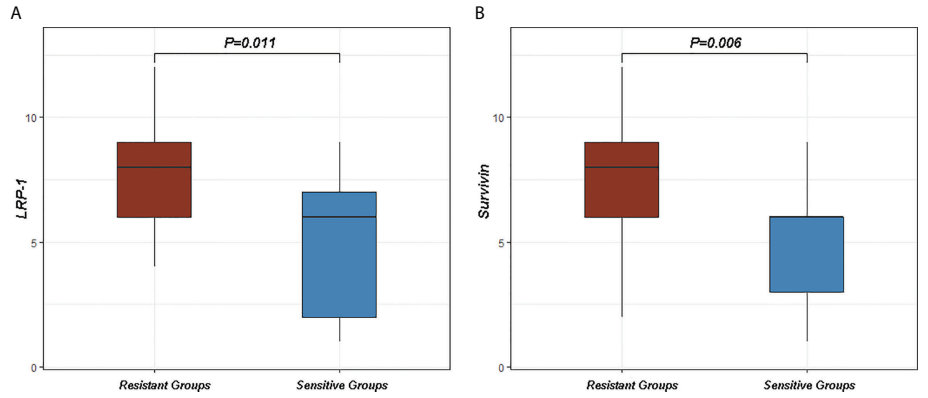

FIGURE 9
Differences in low-density lipoprotein receptor-related protein-1 (LRP-1) and survivin between sensitive and resistant groups. **(A)** The expression of LRP-1 was higher in the resistant group than in the sensitive group (p = 0.011). **(B)** The expression of survivin was higher in the resistant group than in the sensitive group (p = 0.006).

serve as a novel quantitative tool for individually predicting the expression of LRP-1 and selecting appropriate targeted therapies for patients with LARC.

In addition, we constructed a radiomics model to predict the expression of survivin and achieved excellent results, with sensitivities of 70.0% and 76.5%, specificities of 83.3% and 69.2%, and AUCs of 0.780 and 0.800 in the training and validation cohorts, respectively. Notably, the performance of the radiomics model in the test cohort was superior to that in the validation cohort (AUC, 0.800 vs. 0.780), which demonstrates

the robustness of our model. Survivin is a unique member of the inhibitor of apoptosis protein family that is expressed in most cancer cells but is barely detected in most normal adult tissues (40). Without doubt, survivin has attracted a great deal of interest as an anti-radiotherapy factor, and its overexpression in tumors has been shown to be associated with radioresistance, poor prognosis, and drug resistance (41, 42). Previous studies have shown that targeted inhibition of survivin in cancer cells can interfere with their DNA repair ability and increase their radiosensitivity to IR (12, 42). Two features from Ktrans were selected in the radiomics model for predicting survivin. In several studies, Ktrans has been considered as a robust and clinically useful biomarker of radiation resistance in some tumor types (43). These results demonstrate that Ktrans plays an essential role in reflecting the expression levels of LRP-1 and survivin. Our findings also highlighted a weak correlation between LRP-1 expression and survival ($r = 0.201$, $p = 0.045$). This correlation between LRP-1 and survivin suggests that they may play a synergistic role in radiotherapy resistance in LARC to some extent. LRP-1 or survivin may have a specific association with radiotherapy tolerance in rectal cancer, and targeted inhibition of LRP-1 or survivin can improve the prognosis of patients. However, as a puzzling part of our study, we found that some patients with high LRP-1 expression exhibited low survivin expression. These results are entirely contrary to our initial conjecture that the presentation of LRP-1 should be consistent with that of survivin to a certain extent. In our view, this inconsistency may originate from the heterogeneity of the tumor and the complex mechanisms of IR. Radiotherapy tolerance is a complex process involving many mechanisms. The biological behavior of LARC radioresistance may be reflected by multiple biomarkers rather than a single biomarker (LRP-1 or survivin). In the future, with further research on radiotherapy tolerance mechanisms, the inclusion of more tolerance factors may help improve the predictive model for radiotherapy tolerance. Further studies with larger sample sizes are required to investigate the clinical validation and additive values of the radiomics model for predicting the response to radiotherapy.

Furthermore, the calibration curve of the predictive radiomics models demonstrated good agreement between the predicted and actual probabilities in the training and validation cohorts, indicating that our models accurately evaluated the true values of LRP-1 and survivin expression. DCA showed a higher overall net benefit with the radiomics model, thus highlighting its value as an excellent tool, based on DCE-MRI, for assistance in clinical decision-making. Using the radiomics model, if a patient is predicted to have high LRP-1 or survivin expression, the administration of targeted therapy or more intensive chemotherapy should be recommended. In the future, patients with high LRP-1 and survivin-expressing LARC may serve as an ideal population for testing newer therapies.

In order to investigate the relationship between LRP-1 and survivin expression and resistance to neoadjuvant radiotherapy in patients with LARC, we collected additional LARC biopsy specimens from 27 patients who received neoadjuvant radiotherapy with/without DCE-MRI examinations from February 2017 to August 2021 at Shaoxing People's Hospital; these patients were not among the 100 patients in the main analyses. LRP-1 expression was significantly higher in the resistant group than in the sensitive group (7.813 ± 2.297 vs 5.000 ± 2.828, $p = 0.011$). In addition, survivin expression was significantly higher in the resistant group than in the sensitive group (7.500 ± 2.318 vs 4.636 ± 2.385, $p = 0.006$), as shown in Figure 9. These results further suggest that LRP-1 and survivin may be predictive markers clinically relevant to resistance to neoadjuvant radiotherapy in patients with LARC.

Regarding whether the effects of radiation therapy can be predicted using radiomics models, we find that although radiomics models based on DCE-MRI performed well, the present study has some limitations. First, this was a retrospective study from a single institution, which may lead to potential selection biases; also, the predictive model was not tested with external test data. Therefore, prospective and multicenter studies are encouraged in the future. Second, the number of patients was relatively small; therefore, it is necessary to incorporate more cases in future studies to determine the proposed model's reliability. Third, additional pathological, clinical, and radiological characteristics were not considered in our study. Finally, the present study was merely based on DCE-MRI, and several previous studies have shown that the combined application of more MRI sequences (e.g., T2WI, T1WI, and DWI) may improve the predictive ability of the radiomics model. Despite these limitations, the application of the radiomics models may have clinical prospects in terms of precision and personalized medicine for patients with LARC.

Conclusion

In conclusion, the present study demonstrated that radiomics analysis of DCE-MRI features facilitates the determination of LRP-1 and survivin expression levels in LARC before treatment. Our models have significant potential for the preoperative identification of patients with radiotherapy resistance and can serve as an essential reference for treatment planning.

Data availability statement

The original contributions presented in the study are included in the article/Supplementary Material. Further inquiries can be directed to the corresponding author.

Ethics statement

Ethical review and approval was not required for the study on human participants in accordance with the local legislation and institutional requirements. Written informed consent for participation was not required for this study in accordance with the national legislation and the institutional requirements.

Author contributions

ZXL and ZZ designed the study and helped to revise the manuscript. ZHL was involved in the study design, analyzed and interpreted the patient data regarding locally advanced rectal cancer, performed some image processing, and was the major contributor to the writing of the paper. CW, HM, DW, and WP collected the clinical data. HH, CW, YY, and FL performed the immunohistochemical analysis. All authors have read and approved the final manuscript.

Funding

This work was supported by the Key Laboratory of Functional Molecular Imaging of Tumor (Shaoxing People's Hospital, Shaoxing, Zhejiang, China), General Project of Zhejiang Province Health Science and Technology Plan (Grant Number: 2021KY1140), Medical and Health Science and Technology Platform Project of Zhejiang Province (Grant Number: 2018ZD047), General Project of Zhejiang Province Health Science and Technology Plan (Grant Number: 2022KY1296), General Project of Zhejiang Province Health Science and Technology Plan (Grant Number: 2022KY1291), and Medical and Health Science and Technology Plan Project of Zhejiang Province (Grant Number: 2020KY977). The funding sources had no role in the collection, analysis, or interpretation of the data or in the decision to submit the manuscript for publication.

Conflict of interest

The authors declare that the research was conducted in the absence of any commercial or financial relationships that could be construed as a potential conflict of interest.

Publisher's note

Supplementary material

The Supplementary Material for this article can be found online at: https://www.frontiersin.org/articles/10.3389/fonc.2022.881341/full#supplementary-material

References

1. Liu Z, Zhang XY, Shi YJ, Wang L, Zhu HT, Tang Z, et al. Radiomics analysis for evaluation of pathological complete response to neoadjuvant chemoradiotherapy in locally advanced rectal cancer. *Clin Cancer Res* (2017) 23 (23):7253–62. doi: 10.1158/1078-0432.CCR-17-1038

2. Wo JY, Anker CJ, Ashman JB, Bhadkamkar NA, Bradfield L, Chang DT, et al. Radiation therapy for rectal cancer: Executive summary of an astro clinical practice guideline. *Pract Radiat Oncol* (2021) 11(1):13–25. doi: 10.1016/j.prro.2020.08.004

3. Tang Z, Liu L, Liu D, Wu L, Lu K, Zhou N, et al. Clinical outcomes and safety of different treatment modes for local recurrence of rectal cancer. *Cancer Manag Res* (2020) 12:12277–86. doi: 10.2147/CMAR.S278427

4. Kirkby CJ, Gala de Pablo J, Tinkler-Hundal E, Wood HM, Evans SD, West NP. Developing a raman spectroscopy-based tool to stratify patient response to pre-operative radiotherapy in rectal cancer. *Analyst* (2021) 146(2):581–9. doi: 10.1039/d0an01803a

5. Amatatsu M, Arigami T, Uenosono Y, Yanagita S, Uchikado Y, Kijima Y, et al. Programmed death-ligand 1 is a promising blood marker for predicting tumor progression and prognosis in patients with gastric cancer. *Cancer Sci* (2018) 109 (3):814–20. doi: 10.1111/cas.13508

6. Pan W, Gong S, Wang J, Yu L, Chen Y, Li N, et al. A nuclear-targeted titanium dioxide radiosensitizer for cell cycle regulation and enhanced radiotherapy. *Chem Commun (Camb)* (2019) 55(56):8182–5. doi: 10.1039/c9cc01651a

7. Teyssier F, Bay JO, Dionet C, Verrelle P. Cell cycle regulation after exposure to ionizing radiation. *Bull Cancer* (1999) 86(4):345–57. doi: 10.1186/gb-2002-3-4-reports4009

8. Le CC, Bennasroune A, Collin G, Hachet C, Lehrter V, Rioult D, et al. Lrp-1 promotes colon cancer cell proliferation in 3d collagen matrices by mediating Ddr1 endocytosis. *Front Cell Dev Biol* (2020) 8:412. doi: 10.3389/fcell.2020.00412

9. Schaue D, McBride WH. Opportunities and challenges of radiotherapy for treating cancer. *Nat Rev Clin Oncol* (2015) 12(9):527–40. doi: 10.1038/nrclinonc.2015.120

10. Lee KJ, Ko EJ, Park YY, Park SS, Ju EJ, Park J, et al. A novel nanoparticle-based theranostic agent targeting lrp-1 enhances the efficacy of neoadjuvant radiotherapy in colorectal cancer. *Biomaterials* (2020) 255:120151. doi: 10.1016/j.biomaterials.2020.120151

11. Yoshikawa K, Shimada M, Higashijima J, Nakao T, Nishi M, Takasu C, et al. Ki-67 and survivin as predictive factors for rectal cancer treated with preoperative chemoradiotherapy. *Anticancer Res* (2018) 38(3):1735–9. doi: 10.21873/anticanres.12409

12. Zhou J, Guo X, Chen W, Wang L, Jin Y. Targeting survivin sensitizes cervical cancer cells to radiation treatment. *Bioengineered* (2020) 11(1):130–40. doi: 10.1080/21655979.2020.1717297

13. Aerts HJ, Velazquez ER, Leijenaar RT, Parmar C, Grossmann P, Carvalho S, et al. Decoding tumour phenotype by noninvasive imaging using a quantitative radiomics approach. *Nat Commun* (2014) 5:4006. doi: 10.1038/ncomms5006

14. Peeken JC, Nusslin F, Combs SE. "Radio-oncomics" : The potential of radiomics in radiation oncology. *Strahlenth Onkol* (2017) 193(10):767–79. doi: 10.1007/s00066-017-1175-0

15. Deng X, Liu M, Sun J, Li M, Liu D, Li L, et al. Feasibility of mri-based radiomics features for predicting lymph node metastases and vegf expression in cervical cancer. *Eur J Radiol* (2021) 134:109429. doi: 10.1016/j.ejrad.2020.109429

16. Shen FU, Lu J, Chen L, Wang Z, Chen Y. Diagnostic value of dynamic contrast-enhanced magnetic resonance imaging in rectal cancer and its correlation with tumor differentiation. *Mol Clin Oncol* (2016) 4(4):500–6. doi: 10.3892/mco.2016.762

17. O'Connor JP, Jackson A, Parker GJ, Roberts C, Jayson GC. Dynamic contrast-enhanced mri in clinical trials of antivascular therapies. *Nat Rev Clin Oncol* (2012) 9(3):167–77. doi: 10.1038/nrclinonc.2012.2

18. Reynolds HM, Parameswaran BK, Finnegan ME, Roettger D, Lau E, Kron T, et al. Diffusion weighted and dynamic contrast enhanced mri as an imaging biomarker for stereotactic ablative body radiotherapy (Sabr) of primary renal cell carcinoma. *PloS One* (2018) 13(8):e0202387. doi: 10.1371/journal.pone.0202387

19. Xie T, Ye Z, Pang P, Shao G. Quantitative multiparametric mri may augment the response to radiotherapy in mid-treatment assessment of patients with esophageal carcinoma. *Oncol Res Treat* (2019) 42(6):326–33. doi: 10.1159/000499322

20. Li C, Song L, Yin J. Intratumoral and peritumoral radiomics based on functional parametric maps from breast dce-mri for prediction of her-2 and ki-67 status. *J Magn Reson Imaging* (2021) 54(3):703–14. doi: 10.1002/jmri.27651

21. Peng H, Long F, Ding C. Feature selection based on mutual information: Criteria of max-dependency, max-relevance, and Min-redundancy. *IEEE Trans Pattern Anal Mach Intell* (2005) 27(8):1226–38. doi: 10.1109/TPAMI.2005.159

22. Wu S, Zheng J, Li Y, Yu H, Shi S, Xie W, et al. A radiomics nomogram for the preoperative prediction of lymph node metastasis in bladder cancer. *Clin Cancer Res* (2017) 23(22):6904–11. doi: 10.1158/1078-0432.CCR-17-1510

23. Trakarnsanga A, Gonen M, Shia J, Nash GM, Temple LK, Guillem JG, et al. Comparison of tumor regression grade systems for locally advanced rectal cancer after multimodality treatment. *J Natl Cancer Inst* (2014) 106(10):dju248. doi: 10.1093/jnci/dju248

24. Chen G, Yang Z, Eshleman JR, Netto GJ, Lin MT. Molecular diagnostics for precision medicine in colorectal cancer: Current status and future perspective. *BioMed Res Int* (2016) 2016:9850690. doi: 10.1155/2016/9850690

25. Tan Y, Shao R, Li J, Huang H, Wang Y, Zhang M, et al. Pitpnc1 fuels radioresistance of rectal cancer by inhibiting reactive oxygen species production. *Ann Transl Med* (2020) 8(4):126. doi: 10.21037/atm.2020.02.37

26. Yiu AJ, Yiu CY. Biomarkers in colorectal cancer. *Anticancer Res* (2016) 36 (3):1093–102. doi: 10.1002/sim.7149

27. McCann E, O'Sullivan J, Marcone S. Targeting cancer-cell mitochondria and metabolism to improve radiotherapy response. *Transl Oncol* (2021) 14(1):100905. doi: 10.1016/j.tranon.2020.100905

28. Tachon G, Cortes U, Guichet PO, Rivet P, Balbous A, Masliantsev K, et al. Cell cycle changes after glioblastoma stem cell irradiation: The major role of Rad51. *Int J Mol Sci* (2018) 19(10):3018. doi: 10.3390/ijms19103018

29. Zhou X, Liu H, Zheng Y, Han Y, Wang T, Zhang H, et al. Overcoming radioresistance in tumor therapy by alleviating hypoxia and using the hif-1 inhibitor. *ACS Appl Mater Interf* (2020) 12(4):4231–40. doi: 10.1021/acsami.9b18633

30. Saini A, Breen I, Pershad Y, Naidu S, Knuttinen MG, Alzubaidi S, et al. Radiogenomics and radiomics in liver cancers. *Diagnost (Basel)* (2018) 9(1):4. doi: 10.3390/diagnostics9010004

31. Li ZY, Wang XD, Li M, Liu XJ, Ye Z, Song B, et al. Multi-modal radiomics model to predict treatment response to neoadjuvant chemotherapy for locally advanced rectal cancer. *World J Gastroenterol* (2020) 26(19):2388–402. doi: 10.3748/wjg.v26.i19.2388

32. Gillies RJ, Kinahan PE, Hricak H. Radiomics: Images are more than pictures, they are data. *Radiology* (2016) 278(2):563–77. doi: 10.1148/radiol.2015151169

33. Wen X, Li Y, He X, Xu Y, Shu Z, Hu X, et al. Prediction of malignant acute middle cerebral artery infarction *Via* computed tomography radiomics. *Front Neurosci* (2020) 14:708. doi: 10.3389/fnins.2020.00708

34. Gao M, Huang S, Pan X, Liao X, Yang R, Liu J. Machine learning-based radiomics predicting tumor grades and expression of multiple pathologic biomarkers in gliomas. *Front Oncol* (2020) 10:1676. doi: 10.3389/fonc.2020.01676

35. Zhang Y, Zhu Y, Zhang K, Liu Y, Cui J, Tao J, et al. Invasive ductal breast cancer: Preoperative predict ki-67 index based on radiomics of adc maps. *Radiol Med* (2020) 125(2):109–16. doi: 10.1007/s11547-019-01100-1

36. Granata V, Grassi R, Fusco R, Izzo F, Brunese L, Delrio P, et al. Current status on response to treatment in locally advanced rectal cancer: What the radiologist should know. *Eur Rev Med Pharmacol Sci* (2020) 24(23):12050–62. doi: 10.26355/eurrev_202012_23994

37. May P, Woldt E, Matz RL, Boucher P. The ldl receptor-related protein (Lrp) family: An old family of proteins with new physiological functions. *Ann Med* (2007) 39(3):219–28. doi: 10.1080/07853890701214881

38. Tofts PS, Brix G, Buckley DL, Evelhoch JL, Henderson E, Knopp MV, et al. Estimating kinetic parameters from dynamic contrast-enhanced T(1)-weighted mri of a diffusable tracer: Standardized quantities and symbols. *J Magn Reson Imaging* (1999) 10(3):223–32. doi: 10.1002/(sici)1522-2586(199909)10:3<223::aid-jmri2>3.0.co;2-s

39. Campion O, Thevenard Devy J, Billottet C, Schneider C, Etique N, Dupuy JW, et al. Lrp-1 matricellular receptor involvement in triple negative breast cancer tumor angiogenesis. *Biomedicines* (2021) 9(10):1430. doi: 10.3390/biomedicines9101430

40. Altieri DC. Survivin and iap proteins in cell-death mechanisms. *Biochem J* (2010) 430(2):199–205. doi: 10.1042/BJ20100814

41. Tang TK, Chiu SC, Lin CW, Su MJ, Liao MH. Induction of survivin inhibition, G(2)/M cell cycle arrest and autophagic on cell death in human malignant glioblastoma cells. *Chin J Physiol* (2015) 58(2):95–103. doi: 10.4077/CJP.2015.BAC267

42. Hu S, Fu S, Xu X, Chen L, Xu J, Li B, et al. The mechanism of radiosensitization by Ym155, a novel small molecule inhibitor of survivin expression, is associated with DNA damage repair. *Cell Physiol Biochem* (2015) 37(3):1219–30. doi: 10.1159/000430245

43. Ellingsen C, Hompland T, Galappathi K, Mathiesen B, Rofstad EK. Dce-mri of the hypoxic fraction, radioresponsiveness, and metastatic propensity of cervical carcinoma xenografts. *Radioth Oncol* (2014) 110(2):335–41. doi: 10.1016/j.radonc.2013.10.018

frontiers | Frontiers in Oncology

TYPE Original Research
PUBLISHED 31 August 2022
DOI 10.3389/fonc.2022.929342

OPEN ACCESS

EDITED BY
Sona Vodenkova,
Institute of Experimental Medicine (ASCR), Czechia

REVIEWED BY
Pavel Soucek,
National Institute of Public Health (NIPH), Czechia
Klara Cervena,
Institute of Experimental Medicine (ASCR), Czechia

*CORRESPONDENCE
Weijie Zhang
fcczhangwj@zzu.edu.cn

†These authors have contributed equally to this work and share first authorship

SPECIALTY SECTION
This article was submitted to Gastrointestinal Cancers: Colorectal Cancer, a section of the journal Frontiers in Oncology

RECEIVED 26 April 2022
ACCEPTED 16 August 2022
PUBLISHED 31 August 2022

CITATION
Zhang W, Zhang Z, Lou S, Li D, Ma Z and Xue L (2022) Efficacy, safety and predictors of combined fruquintinib with programmed death-1 inhibitors for advanced microsatellite- stable colorectal cancer: A retrospective study. *Front. Oncol.* 12:929342. doi: 10.3389/fonc.2022.929342

Efficacy, safety and predictors of combined fruquintinib with programmed death-1 inhibitors for advanced microsatellite-stable colorectal cancer: A retrospective study

Weijie Zhang*†, Zhongyue Zhang†, Shitong Lou, Donghui Li, Zhijun Ma and Lei Xue

Department of Oncology, The First Affiliated Hospital of Zhengzhou University, Zhengzhou, China

Background: Research findings have revealed that combining anti-angiogenesis inhibitors with programmed death-1(PD-1) inhibitors can reverse the immunosuppressive tumor microenvironment and enhance the antitumor immune response. To explore the therapeutic options for breaking immune tolerance in microsatellite stability (MSS) or mismatch repair-proficiency (pMMR) advanced colorectal cancer (CRC), we assessed the efficacy, safety and predictors of the fruquintinib and PD-1 inhibitors combination in patients with MSS/pMMR advanced CRC in a real-world environment.

Methods: We conducted a single-center retrospective study by collecting relevant data on patients with MSS/pMMR advanced CRC who received fruquintinib coupled with PD-1 inhibitors in the First Affiliated Hospital of Zhengzhou University between August 2019 and November 2021, focusing on progression-free survival.

Results: We enrolled 110 eligible patients in this study between August 2019 and November 2021. At the deadline (January 20, 2022), 13 patients had objective responses. The objective response rate was 11.8% (13/110, 95% confidence interval [CI]: 6.4-18.2), the disease control rate was 70.0% (82/110, 95% CI: 60.9-78.2), and the progression-free survival was 5.4 months (95% CI: 4.0-6.8). Liver metastases (hazard ratio [HR]: 0.594, 95% CI: 0.363-0.973, P<0.05), alkaline phosphatase elevation (ALP>160U/L) (HR: 0.478, 95%CI: 0.241-0.948, P<0.05), fibrinogen elevation (FIB>4g/L) (HR: 0.517, 95% CI: 0.313-0.855, P<0.05), and an increase in the ALP level from the baseline after treatment (HR: 1.673, 95% CI: 1.040-2.690, P<0.05) were negative predictors of the progression-free survival. A total of 101 of 110 patients experienced treatment-related adverse events, including 14 who experienced grade 3 or above treatment-related adverse events, and no treatment-related deaths

occurred. Hypertension was the most frequently encountered grade 3 treatment-related adverse event.

Conclusion: Fruquintinib combined with PD-1 inhibitors has antitumor activity and manageable safety in treating patients with MSS/pMMR advanced CRC. Liver metastases, ALP level and FIB level might be a prediction of the patient response to this therapy.

KEYWORDS

fruquintinib, PD-1 inhibitors, microsatellite-stable (MSS), colorectal cancer (CRC), predictors, retrospective study

Introduction

Colorectal cancer (CRC) is the third most prevalent cancer and the second largest cause of mortality globally (1). Due to the lack of specificity in its early diagnosis, the majority of patients with the condition are diagnosed at an advanced stage. Chemotherapy remains the standard treatment for CRC despite its disadvantages such as apparent systemic adverse effects, low selectivity, and drug concentration at the tumor site. Immunotherapy has shown promising outcomes in treating various malignant tumors in recent years. The approved immune checkpoint inhibitors (ICIs) for CRC, pembrolizumab and nivolumab ± ipilimumab, are only suited for patients with microsatellite instability-high (MSI-H) or mismatch repair-deficient (dMMR) (2, 3), whereas 95% of CRC patients have microsatellite stability (MSS) or mismatch repair-proficiency (pMMR), and single-agent ICIs are ineffective. The objective response rate (ORR) of pembrolizumab in the MSS/pMMR CRC cohort in the KEYNOTE-016 study was 0% (4), and advanced patients have fewer options for later-line treatment.

Fruquintinib is a small-molecule tyrosine kinase inhibitor that targets the vascular endothelial growth factor receptor (VEGFR) 1, 2, and 3, and it is highly selective and potent. The FRESCO study found that fruquintinib extended the median overall survival (OS) (9.3 months vs. 6.6 months) and progression-free survival (PFS) (3.7 months vs. 1.8 months) when compared to placebo (5). The Food and Drug Administration has approved fruquintinib as a third-line treatment for metastatic CRC (mCRC).

According to growing evidence, anti-angiogenic therapy combined with immunotherapy strengthens the vascular normalization and immune reprogramming, reversing the immunosuppressive tumor microenvironment (TME) and inducing a long-lasting antitumor immune response in the body (6, 7). In a case report, after failing multiple lines of treatment, a late-stage patient who received fruquintinib plus sintilimab experienced a quick remission. The antitumor activity and the ability to reprogram the immunosuppressive TME of fruquintinib plus PD-1 inhibitors were confirmed in mouse experiments (8). According to an American Society of Clinical Oncology (ASCO) study published in 2020, the ORR of fruquintinib plus sintilimab in the treatment of mCRC was much higher than that of single-agent fruquintinib (15.4% vs. 4.9%) (9). The Phase Ib/II study of the fruquintinib and sintilimab combination for advanced CRC showed that the ORR was 27.3% and the PFS was 6.9 months in the fruquintinib 5 mg intermittent-treatment group according to the 2021 ASCO Meeting Abstract (10). These findings suggest that fruquintinib coupled with PD-1 inhibitors has a promising application in advanced CRC, providing compelling evidence of the clinical application of combined therapy.

These findings suggest novel approaches to treating MSS/pMMR advanced CRC. However, clinical trial data are limited due to the strict inclusion criteria that are implemented. In the real world, the efficacy and safety of fruquintinib coupled with PD-1 inhibitors in treating MSS/pMMR mCRC are unknown, and few studies have reported efficacy predictors for this treatment. Therefore, we designed this retrospective study.

Patients and methods

Patients

From August 2019 to November 2021, patients with MSS/pMMR advanced CRC receiving fruquintinib plus PD-1 inhibitors at the First Affiliated Hospital of Zhengzhou University were included in this single-center retrospective study. Out of the 141 eligible patients, 31 patients were excluded, 19 had no available follow-up data, 4 received treatment that was combined with other chemotherapy drugs, and 8 had severe underlying diseases or other tumor complications. The data of the remaining 110 patients were analyzed. A flow chart of the patient selection procedure is

shown in Figure 1. The main inclusion criteria were: 1. advanced or metastatic CRC confirmed by histology or cytology; 2. MSS/pMMR confirmed by tumor genetic testing in a local laboratory; 3. an Eastern Cooperative Oncology Group Performance Status (ECOG PS) score of <3; 4. the patient's disease progressed after ≥2nd-line therapy; 5. the presence of measurable lesions that meet the Response Evaluation Criteria for Solid Tumors Version 1.1 (RECIST V1.1); 6. sufficient reserves of the bone marrow, liver, kidney organ functions and the coagulation function. The key exclusion criteria were as follows: 1. active or previous chronic or recurring autoimmune illness; 2. severe comorbidity; 3. a definitive diagnosis of hereditary CRC syndrome. The data are all from the medical record system of the First Affiliated Hospital of Zhengzhou University. The patient's clinical features, gene status, laboratory results, tumor responses, and treatment-related adverse events (TRAEs) were collected and analyzed. Table 1 summarizes the baseline characteristics of the study participants.

Treatment methods

Patients received fruquintinib at a dose of 3–5 mg once a day for 14/21 days, every 28 days. Patients received PD-1 inhibitors including sintilimab, camrelizumab, toripalimab, tislelizumab, and pembrolizumab. Patients received fixed doses of sintilimab, camrelizumab, tislelizumab, and pembrolizumab (200 mg) every 3 weeks, and toripalimab (240 mg) every 3 weeks on the first day of fruquintinib application. To control TRAEs, the dose of fruquintinib was adjusted in some patients; however, the doses of PD-1 inhibitors were not.

Assessment

According to RECIST V1.1, tumor response was tested using computed tomography every 6–8 weeks. Tumor response to treatment was assessed as complete response (CR: all target lesions disappeared and no new lesions appeared), partial response (PR: the sum of the longest diameters of all target lesions is less than 30% of the baseline), progression (PD: a 20% increase in the longest diameter of all target lesions compared to the minimum, or the appearance of new lesions), and stable (SD: insufficient reduction to achieve PR but insufficient increase to achieve PD). The ORR is the proportion of patients achieving CR and PR, and the disease control rate (DCR) is the proportion of patients achieving CR, PR, and SD. PFS was defined as the time from treatment initiation to either disease progression or death. The time from the treatment of the study until death from any cause was defined as the OS. TRAEs were assessed by the National Cancer Institute Common Terminology Criteria for Adverse Events Version 5.0 (NCI CTCAE V5.0).

Statistical analysis

The baseline characteristics of CRC patients were described using percentages and median values. Pearson's chi-square test was used to analyze the effects of patients' baseline characteristics on the efficacy of combination therapy for statistical analysis. $P<0.05$ was considered statistically significant. The Kaplan-Meier survival analysis was used to calculate the PFS, and the log-rank test was used to compare subgroups to each other. Hazard ratios (HRs) and confidence

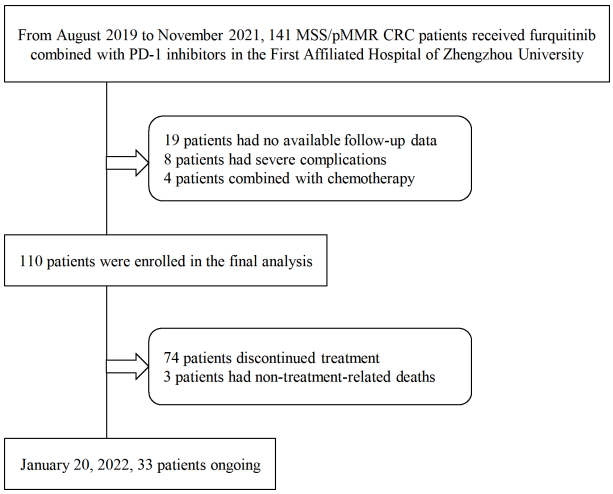

FIGURE 1
The patient selection process for the retrospective cohort. MSS/pMMR, microsatellite stability or mismatch repair-proficiency; CRC, colorectal cancer; PD-1, programmed death-1.

intervals (CIs) were calculated using the Cox proportional hazards regression model for variables with P<0.05 in univariate analysis. Statistical Product Service Solutions Version 21.0 and GraphPad Prism Version 9.0 were used for statistical analysis.

Results

Patients characteristics and treatment strategies

A total of 110 patients were enrolled from August 2019 to November 2021. The median age was 53 years (range: 22–81). A total of 91 (82.7%) patients were less than 65 years old, and 38 (34.5%) patients were early-onset (<50 years). At the beginning of treatment, 12 (10.9%) patients had an ECOG PS score of 2. At the initial diagnosis, the tumors of 86 (78.2%) patients were located in the left side (distal 1/3 of transverse colon, descending colon, sigmoid colon and rectum) and those of 24 (21.8%) patients were located in the right side (proximal 2/3 transverse colon, cecum, ascending colon). At the start of treatment, 60 (54.5%) patients had liver metastases, 64 (58.2%) had lung metastases, 47 (42.7%) had other organs metastases (23 had pelvic metastases, 12 had bone metastases, 3 brain metastases, 5 kidney metastases, 4 bladder metastases, 5 ureteral metastases, 2 spleen metastases, 1 gallbladder metastases, 3 soft tissue metastases, 1 penis metastases, 1 chest wall metastases), and 89 (80.9%) had at least two metastases. Treatment methods varied, and all patients received ≥2 lines of prior chemotherapy, 98 (89.1%) received anti-angiogenic therapy (mostly bevacizumab and cetuximab), 11 (10.0%) received PD-1 inhibitors, 9 (8.2%) patients received anti-angiogenic drugs combined with PD-1 inhibitors, 85 (77.3%) underwent surgery (including primary tumor and metastases resection), 10 (9.1%) received radiotherapy. All patients had histologically or cytologically confirmed CRC, and the gene test results were MSS/pMMR. A total of 54 (49.1%) patients had a *RAS* mutation, and 6 (5.4%) patients had a *BRAF* mutation. Thirty-three of the 110 patients were tested for tumor mutational burden (TMB), 8 (7.3%) patients showed high-TMB (TMB-H, TMB-H was defined as≥10mut/Mb), and 25 (22.7%) showed low-TMB (TMB-L). We collected the ALP, glutamyl transpeptidase (GGT), lactate dehydrogenase (LDH), D-Dimer, FIB values of 110 patients at baseline and divided patients into two groups using the upper limits of normal values as cutoff values. The baseline characteristics of study participants are shown in Table 1.

In this study, a total of five PD-1 inhibitors were used in 110 patients, with the most common ones being sintilimab (46.4%), camrelizumab (35.5%), and toripalimab (13.6%). In all patients, these molecules were combined with fruquintinib, and most of them (92.7%) received fruquintinib at a dose of 5 mg (Table 2).

Clinical efficacy

As of January 20, 2022, 110 patients who received the combination of fruquintinib and PD-1 inhibitors underwent at least one tumor imaging assessment. Table 3 summarizes the patients' best responses from the baseline. None of the patients achieved CR, 13 (11.8%) of them achieved PR, and 64 (58.2%) were rated as SD. The ORR was 11.8% (13/110, 95% CI: 6.4-18.2), and the DCR was 70.0% (82/110, 95% CI: 60.9–78.2). The median PFS was 5.4 months (95% CI: 4.0–6.8) (Figure 2). The median OS was not determined in our study (Figure 3).

No factors, including age, gender, location of the primary tumor, ECOG score, treatment lines, previous treatment methods, the presence or absence of metastases (liver, lung, peritoneum, pelvic, bone), gene mutation status, some biochemical and coagulation indicators (ALP, GGT, LDH, D-Dimer, and FIB) at baseline, were found to have a significant impact on the effectiveness of the fruquintinib and PD-1 inhibitors combination.

The Kaplan-Meier survival analysis found that the PFS of patients with liver metastases was significantly shorter than that of patients without them (PFS: 3.4 [95% CI: 2.3–4.5] months vs. 7.6 [95% CI: 5.3–9.9] months, P<0.05, Figure 4A). The patients with ALP>160 U/L had a substantially shorter PFS than those without them (PFS: 3.3 [95% CI: 3.0-3.7] months vs. 6.1 [95% CI: 4.6-7.6] months, P<0.05, Figure 4B). The PFS of patients with FIB>4g/L was significantly shorter than that of patients without them (3.4 [95% CI:2.5-4.3] months vs. 6.8 [95%CI:5.8-7.8] months, P<0.05, Figure 4C). Patients with D-dimer ≤0.3 mg had longer PFS (PFS: 6.3[95% CI: 4.8–7.8] months vs. 4.1[95% CI: 3.9–4.2] months, P<0.05, Figure 4D). The PFS was extended in patients with peritoneum metastases (P=0.976, Figure 4E), primary lesions located in the left side (P=0.396, Figure 4F), RAS wild (P=0.343, Figure 4G), BRAF-mutated (P=0.090, Figure 4H) and patients without lung metastases (P=0.995, Figure 4I) compared with their corresponding subgroups. In comparison to the TMB-L group, the PFS in the TMB-H group was longer (5.0 [95%CI: 2.0-8.0] months vs. 6.1 [95%CI: 0.0-12.2] months, P=0.979, Figure 4J). The comparison of the efficacy of each subgroup is shown in Figure 5.

Patients were assessed for ALP and FIB after two cycles of combination therapy and compared with pre-treatment values. The ALP level was decreased in 42 (38.9%) patients and increased in 66 (61.1%) patients. The PFS was 7.0 (95% CI: 5.9-8.0) months and 3.4 (95% CI: 2.2-4.8) months in the decreased and increased ALP level groups (P<0.05, Figure 4K). The FIB level was decreased in 43 (40.6%) patients and increased in 63 (59.4%) patients. The PFS was 5.4 (95% CI: 2.8–8.0) months and 5.0 (95% CI: 3.6–6.5) months in the FIB-lowering and FIB-raising groups (P=0.578, Figure 4L).

The multivariate Cox proportional hazards regression analysis results showed that liver metastases, ALP level, FIB level, and changes in ALP level after treatment were associated with PFS in fruquintinib coupled with PD-1 inhibitors in MSS/pMMR CRC (P<0.05, Table 4).

10.3389/fonc.2022.929342

TABLE 1 Baseline Characteristics.

Characteristic	Patients (n=110)
Age (years)	
Median age (range)	53.0 (22–81)
<65 years	91 (82.7%)
≥65 years	19 (17.3%)
Gender	
Male	63 (57.3%)
Female	47 (42.7%)
Baseline ECOG PS	
0	31 (28.2%)
1	67 (60.9%)
2	12 (10.9%)
Site of primary tumor	
Left-side	86 (78.2%)
Right-side	24 (21.8%)
Site of metastases	
Liver	60 (54.5%)
Lung	64 (58.2%)
Lymph node	79 (71.8%)
Peritoneum	25 (22.7%)
Other	47 (42.7%)
Number of organs with metastases	
<2	21 (19.1%)
≥2	89 (80.9%)
Previous therapies	
Fluoropyrimidines	109 (99.1%)
Platinum agents	107 (97.3%)
Irinotecan	91 (82.7%)
Antiangiogenic therapy	98 (89.1%)
Immunotherapy	11 (10.0%)
Antiangiogenic plus immunotherapy	9 (8.2%)
Surgery	85 (77.3%)
Radiotherapy	10 (9.1%)
Prior treatment lines	
≤3	32 (29.1%)
>3	78 (70.9%)
Gene mutation status	
RAS/BRAF wild	28 (25.5%)
RAS mutant	54 (49.1%)
BRAF mutant	6 (5.4%)
Unknown	22 (20.0%)
ALP	
> 160U/L	12 (10.9%)
≤ 160U/L	98 (89.1%)
GGT	
> 50U/L	43 (39.1%)
≤ 50U/L	67 (60.9%)
LDH	
> 245U/L	55 (50.0%)
≤ 245U/L	55 (50.0%)
D-Dimer	
> 0.3mg/L	55 (50.0%)
≤ 0.3 mg/L	55 (50.0%)
FIB	
> 4g/L	31 (28.2%)
≤ 4g/L	79 (71.8%)
TMB	
TMB-H	8 (7.3%)
TMB-L	25 (22.7%)
Unknow	77 (70.0%)

ECOG PS, Eastern Cooperative Oncology Group Performance Status; ALP, alkaline phosphatase; GGT, glutamyl transpeptidase; LDH, lactate dehydrogenase; FIB, fibrinogen; TMB, tumor mutational burden; TMB-H, high tumor mutational burden; TMB-L, low tumor mutational burden.
Site of primary tumor, Left-side: distal 1/3 of transverse colon, descending colon, sigmoid colon and rectum, Right-side: proximal 2/3 transverse colon, cecum, ascending colon.
Site of metastases, others: 23 had pelvic metastases, 12 had bone metastases, 3 brain metastases, 5 kidney metastases, 4 bladder metastases, 5 ureteral metastases, 2 spleen metastases, 1 gallbladder metastases, 3 soft tissue metastases, 1 penis metastases, 1 chest wall metastases.
Biochemical and coagulation indicators used the upper limit of normal as the cutoff value.
TMB-H defined as ≥10 mut/Mb.

Considering that the difference in PFS caused by ALP and FIB levels may be caused by the metastatic site, we compared the clinical characteristics of ALP>160U/L group and ALP ≤ 160U/L group, FIB>0.4g/L group and FIB<0.4 g/L group, and found that patients with liver metastases had a higher incidence of the elevated ALP level than those without liver metastases (16.7% vs. 4.0%, P=0.034), while none of the characteristics assessed between FIB subgroups were significantly different. In patients without liver metastases, the PFS of ALP>160U/L group and ALP ≤ 160U/L group were 7.7 months and 3.2 months (P=0.052).

There was no significant difference in the efficacy of different PD-1 inhibitors and fruquintinib combinations (sintilimab: PFS: 4.1 [95% CI: 2.5-5.6] months, ORR: 7.8%, DCR: 68.6%; camrelizumab: PFS: 5.6 [95% CI: 3.3-7.9] months, ORR: 7.7%, DCR: 69.2%; tislelizumab: PFS: 6.8 [95% CI: 3.8-9.8] months, ORR: 33.3%, DCR: 73.3%), and no significant difference between different doses of the fruquintinib and PD-1 inhibitors combination (fruquintinib 3mg: PFS: 4.1 [95% CI: 2.5-5.7] months, ORR: 0%, DCR: 85.7%; fruquintinib 5mg: PFS: 5.4 [95% CI: 3.7-7.1] months, ORR: 12.7%, DCR: 68.6%).

Safety

As of January 20, 2022, 98 (89.1%) of 110 patients had at least 1 TRAE. Table 5 presents the TRAEs associated with fruquintinib coupled with PD-1 inhibitors. A total of 13

TABLE 2 Programmed death-1 inhibitors and fruquintinib combination strategies.

Drug	n (%)
Programmed death-1 inhibitors	
Sintilimab	51 (46.4%)
Camrelizumab	39 (35.5%)
Toripalimab	15 (13.6%)
Tislelizumab	4 (3.6%)
Pembrolizumab	1 (0.9%)
Fruquintinib	
Fruquintinib 3mg	7 (6.4%)
Fruquintinib 4mg	1 (0.9%)
Fruquintinib 5mg	102 (92.7%)

(11.9%) patients suffered TRAEs of grade 3, and two patients suffered TRAE of grade 4. Two patients experienced two types of TRAEs of grade 3 or higher (one patient continued the fruquintinib dose reduction to 4 mg [hand-foot syndrome and hypertension], the other improved after symptomatic treatment and continued to receive the combination therapy [leukopenia and neutropenia]). The following were the most common TRAEs: thrombocytopenia (32.7%), elevated aspartate aminotransferase (AST) levels (28.2%), elevated alanine aminotransferase (ALT) levels (24.5%), diarrhea (23.7%), elevated thyroid-stimulating hormone (TSH) levels (22.7%), proteinuria (21.8%), hypothyroidism (20.0%), hyperlipidemia (19.1%), anemia (18.2%), leukopenia (16.4%), hypertension (15.5%), hand-foot syndrome (14.5%), elevated lactate dehydrogenase levels (14.5%), constipation (12.7%), nausea or vomiting (11.8%), and elevated bilirubin levels (10.9%). The most frequent grade 3 TRAE was hypertension. No deaths occurred as a result of the treatment.

Eleven patients discontinued treatment due to TRAEs: proteinuria (2), rash (2), hypertension, hand-foot syndrome, oral mucositis, thrombocytopenia, diarrhea, arrhythmia, adrenal cortex hypofunction, and immune-associated pneumonia. Three patients experienced fruquintinib dose reduction: two with the hand-foot syndrome and one with hypertension.

As of January 20, 2022, 33 patients were still on treatment, and three were assessed to continue benefiting from the combination therapy and continued treatment after disease progression. Six patients discontinued treatment due to TRAEs, and 71 patients discontinued treatment due to disease progression.

TABLE 3 Curative effect evaluation.

	n=110 (%)
Partial response	13 (11.8%)
Stable disease	64 (58.2%)
Progressive disease	33 (30.0%)
Objective response	13 (11.8%) [95%CI:6.4~18.2]
Disease control	82 (70.0%) [95%CI:60.9~78.2]

CI, confidence interval.

Discussion

MSI-H/dMMR CRC stimulates tumor antigen synthesis by increasing TMB, resulting in increased T-cell infiltration in the TME and responding well to ICIs (11, 12). In contrast, MSS/pMMR CRC with a TMB-L and limited T-cell infiltration were resistant to ICIs. The ORR of pembrolizumab in MSI-H mCRC was 40% in the KEYNOTE-016 study; however, it was 0% for MSS mCRC (4). Only 1 of 20 MSS/pMMR CRC patients treated with nivolumab plus ipilimumab showed an objective response in CHECKMATE 142 (13). New treatments to break through immunological resistance in MSS/pMMR CRC are urgently needed.

Tumor angiogenesis promotes tumor growth and metastasis while also constructing an immunosuppressive TME resistant to immunotherapy (7). By inhibiting VEGFR, fruquintinib normalizes tumor blood vessels, improves the TME's hypoxic environment, and stimulates T-cell infiltration, all of which help reverse the immunosuppressive microenvironment. Fruquintinib shown significant selectivity for tumor cells and good antitumor activity in both preclinical and clinical studies (5, 14). Many studies have confirmed the mutual synergy of anti-angiogenesis inhibitors and ICIs in recent years. In a case report, fruquintinib combined with sintilimab in a patient with MSS/pMMR CRC who progressed on multiple lines of therapy brought about rapid remission. In mouse models, fruquintinib combined with a PD-1 inhibitor efficiently suppressed tumor growth in a syngeneic MSS-CRC model, enhancing antitumor immune response by decreasing the number of Treg cells and increasing tumor cell immunogenicity and T-cell infiltration (8). The ORR of regorafenib with nivolumab in MSS/pMMR CRC patients was 33.3%, and the PFS was 7.9 months in the REGONIVO study (15). Basic experiments and clinical trials have given us confidence in exploring combination therapy strategies for MSS/pMMR CRC; however, real-world evidence on combination therapy is still rare.

Our study included 110 MSS/pMMR CRC patients who received the combination regimen of fruquintinib and PD-1 inhibitors. At the deadline (January 20, 2022), 13 patients had objective responses, and 64 were rated as SD. The ORR was 11.8% (95% CI: 6.4–18.2), the DCR was 70.0% (95% CI: 60.9–78.2), and the PFS of all patients was 5.4 months (95% CI: 4.0-6.8). Because of the short follow-up time, we could not judge the OS, which was one of our study's shortcomings.

Clinical trials of the MSS/pMMR CRC combination therapy have been conducted to explore therapeutic strategies for breaking immune tolerance based on the surprising outcomes of the REGONIVO study (15). The ORR of regorafenib combined with toripalimab was 15.2% (5/33) in MSS/pMMR

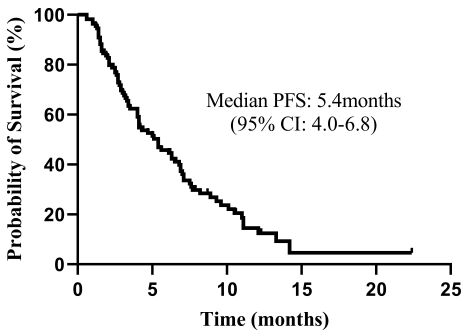

FIGURE 2
Kaplan–Meier plot for the total population (n = 110). The progression-free survival (PFS) from the beginning of the Fruquintinib and programmed death-1 (PD-1) inhibitors combination therapy. CI, confidence interval.

CRC patients in the REGOTORI study (16). The ORR was 25% (4/16) in another retrospective study of fruquintinib/regorafenib combined with camrelizumab (17). No promising combination therapy is without its challenges. The ORR of regorafenib combined with avelumab was 0% (0/40) in the REGOMUNE study (18). In another retrospective study, regorafenib combined with PD-1 inhibitors had no objective response in 23 MSS/pMMR CRC patients (19). The above indicates that selecting the right combination therapy is crucial for patients to benefit from it.

Although our ORR and PFS were lower than those in the REGONIVO study, we believe that attaining such results in the real world is gratifying and represents a significant breakthrough in the treatment of MSS/pMMR CRC. We suspect this is related to discrepancies between clinical trials' rigorous inclusion criteria and the actual clinical population included. It is worth noting that in our study, a patient with liver and lung metastases and a *KRAS* mutation had continuous PR for 8.5 months before the medication was discontinued owing to a suspected malignant arrhythmia. The patient's status was stable at the cutoff date, and the follow-up period was 22.4 months. Comparing the efficacy of ICI monotherapy and fruquintinib monotherapy in MSS/pMMR CRC (4, 5), the combined therapy significantly improved treatment efficacy; so, we are eagerly awaiting the benefits of fruquintinib coupled with PD-1 inhibitors for more cancer patients.

Previous research has revealed that patients without liver metastases have a higher incidence of CD8+ T-cell infiltration than those with them, implying that patients with liver metastases benefit less from ICIs due to a weakened antitumor immune response (20). In our study, we found that patients with liver metastases had significantly shorter PFS durations than those without liver metastases, which also confirms the abovementioned finding. Notably, patients with lung metastases had greater ORR than those with liver metastases and those without lung metastases. This is consistent with the

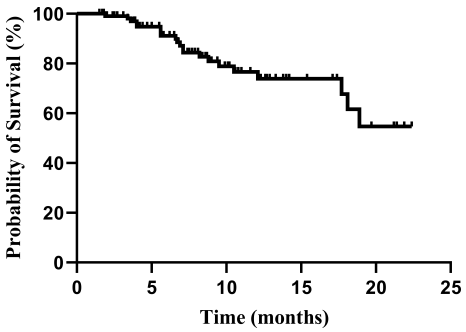

FIGURE 3
Kaplan–Meier plot for the total population (n = 110). The overall survival (OS) from the beginning of the Fruquintinib and programmed death-1 (PD-1) inhibitors combination therapy.

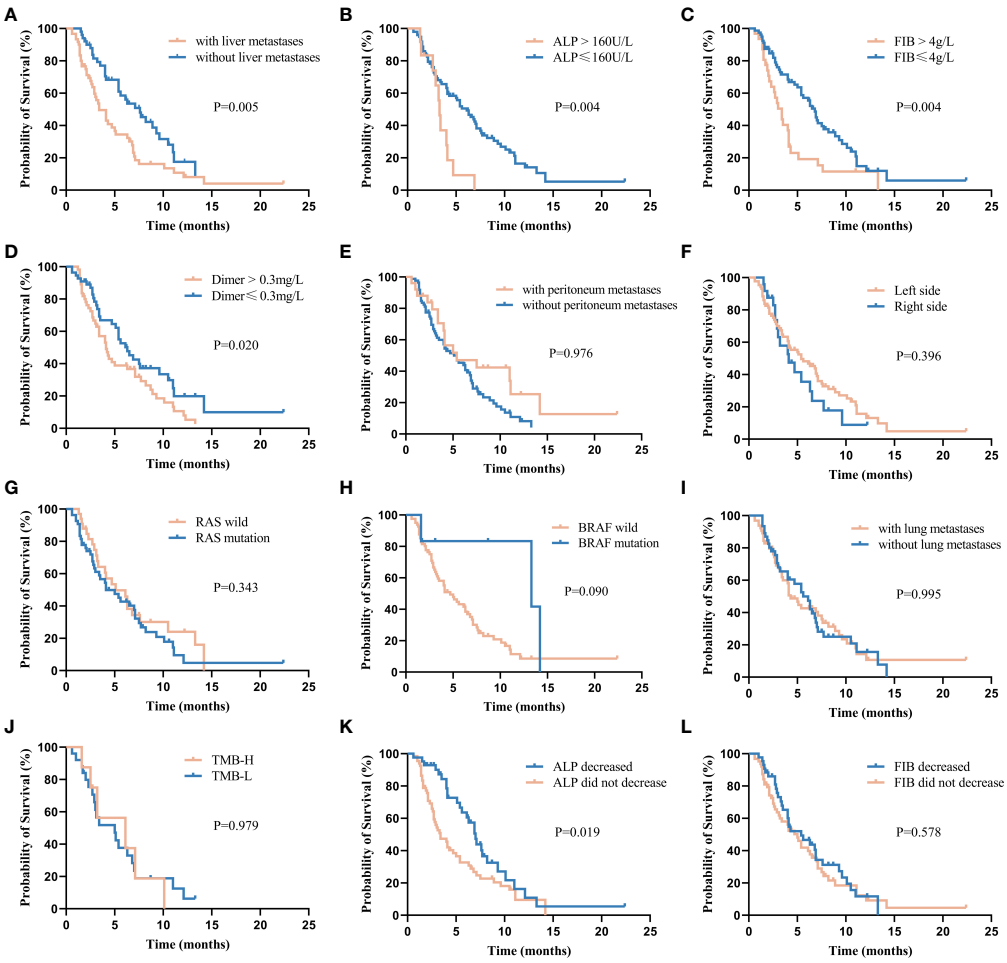

FIGURE 4
Kaplan–Meier plot for progression-free survival (PFS) stratified by clinical factors, including **(A)** liver metastases, **(B)** alkaline phosphatase (ALP), **(C)** fibrinogen (FIB), **(D)** D-Dimer, **(E)** peritoneum metastases, **(F)** Left-side: distal 1/3 of transverse colon, descending colon, sigmoid colon and rectum, Right-side: proximal 2/3 transverse colon, cecum, ascending colon, **(G)** RAS wild/mutant, **(H)** BRAF wild/mutant, **(I)** lung metastases, **(J)** high tumor mutational burden (TMB-H, ≥10 mut/Mb) / low tumor mutational burden (TMB-L, < 10 mut/Mb), **(K)** changes from baseline in ALP levels after treatment, **(L)** changes from baseline in FIB levels after treatment.

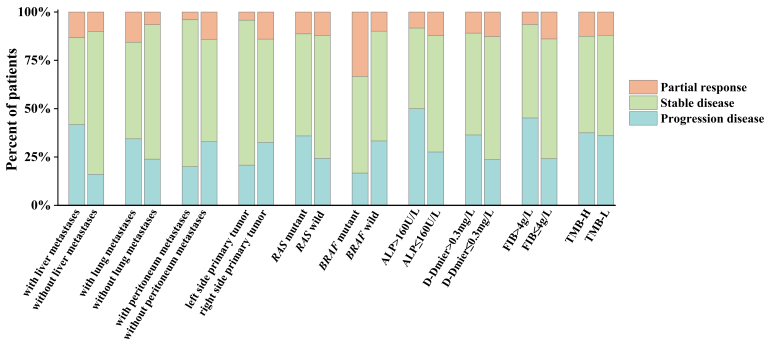

FIGURE 5
Efficacy in selected subgroups. ALP, alkaline phosphatase; FIB, fibrinogen; TMB-H, high tumor mutational burden (≥10 mut/Mb), TMB-L, low tumor mutational burden (<10 mut/Mb).

TABLE 4 Influence of clinical factors on progression-free survival.

	Univariate analysis HR (95% CI)	P value	Multivariate analysis HR (95% CI)	P value
Age (<65/≥65years)	1.662 (0.904-3.054)	0.096		
Gender (Male/Female)	1.131 (0.722-1.772)	0.587		
Baseline ECOG PS (0/1/2)	1.324 (0.903-1.941)	0.342		
Site of primary tumor (Left side/Right side)	1.262 (0.733-2.171)	0.396		
Liver metastases (yes/no)	**0.531 (0.337-0.838)**	**0.005**	**0.594 (0.363-0.973)**	**0.038**
Lung metastases (yes/no)	0.999 (0.639-1.561)	0.995		
Peritoneum metastases (yes/no)	0.992 (0.589-1.672)	0.976		
Pelvic metastases (yes/no)	1.601 (0.908-2.826)	0.098		
Bone metastases (yes/no)	0.817 (0.403-1.653)	0.569		
Number of organs with metastases (≥2/<2)	1.012 (0.582-1.761)	0.966		
Treatment lines (3/>3)	2.280 (0.706-7.366)	0.154		
RAS status (wild/mutant)	1.281 (0.764 -2.148)	0.343		
BRAF status (wild/mutant)	0.372 (0.113-1.222)	0.090		
Prior antiangiogenic therapy (yes/no)	0.422 (0.170-1.046)	0.052		
Prior immunotherapy (yes/no)	0.945 (0.452-1.978)	0.880		
Prior antiangiogenic plus immunotherapy (yes/no)	0.724 (0.346-1.511)	0.382		
ALP (>160U/L/≤160U/L)	**0.390 (0.200-0.757)**	**0.004**	**0.478 (0.241-0.948)**	**0.035**
GGT (>50U/L/≤50U/L)	0.788 (0.329-1.888)	0.475		
LDH (>245U/L/≤245U/L)	1.534 (0.643-3.675)	0.213		
D-Dimer (>0.3mg/L/≤0.3mg/L)	**0.584 (0.371-0.918)**	**0.020**	0.783 (0.491-1.247)	0.302
FIB (>4g/L/≤4g/L)	**0.503 (0.314-0.807)**	**0.004**	**0.517 (0.313-0.855)**	**0.010**
TMB (TMB-H/TMB-L)	0.988 (0.391-2.493)	0.979		
Changes in ALP levels (decreased/did not decreased)	**1.743 (1.091-2.785)**	**0.019**	**1.673 (1.040-2.690)**	**0.034**
Changes FIB levels (decreased/did not decreased)	1.138 (0.723-1.790)	0.578		

ECOG PS, Eastern Cooperative Oncology Group Performance Status; ALP, alkaline phosphatase; GGT, glutamyl transpeptidase; LDH, lactate dehydrogenase; FIB, fibrinogen; TMB, tumor mutational burden; TMB-H, high tumor mutational burden (≥10 mut/Mb); TMB-L, low tumor mutational burden (<10 mut/Mb).
Site of primary tumor, Left-side: distal 1/3 of transverse colon, descending colon, sigmoid colon and rectum, Right-side: proximal 2/3 transverse colon, cecum, ascending colon.
The bold values represent P<0.05, and the difference is statistically significant.

findings of the REGONIVO and REGOTORI studies (15, 16). Before patients receive combination therapy, we think the presence or absence of liver metastases can be used as a predictor of treatment efficacy.

TMB is a biomarker for immunotherapy in multiple solid tumors. TMB-H is a biomarker for pembrolizumab-treated solid tumors that may inadvertently reflect the tumors' capacity to produce neoantigens (21, 22). Our study showed that TMB-H patients had a longer PFS, but this difference was not statistically significant. Perhaps TMB≥10mut/Mb is not a reliable predictor of immunotherapy efficacy for all solid tumors. There is still debate on the TMB-H threshold for MSS/pMMR CRC. Critical issues with reliably detecting TMB in a particular cancer type and then determining an ideal TMB threshold (if one exists) must be resolved in order to better adopt TMB-H as a reliable clinical biomarker. It also has to be determined whether TMB-H can be utilized as a biomarker for immunotherapy in conjunction with targeted therapy.

In clinical practice, ICIs are routinely administered with other drugs. However, few clinical trials have revealed predictors of the success of combination therapy. We won't be able to choose patients who will benefit from combination therapy and maximize patient effectiveness unless we can identify the appropriate predictors. For this, we did some exploration. In 1878, Billroth discovered that tumor cells were wrapped in the thrombus formed by FIB through the body's coagulation system to escape the killing effect of the body's immune system (23). High levels of plasma FIB and D-Dimer have been associated with cancer metastasis, recurrence, and poor prognosis in a number of studies (24). The strongest associations of D-Dimer and FIB with poor prognosis in CRC were observed in a meta-analysis (25). In our study, it was determined that the level of FIB was associated with the PFS of combination therapy. However, the effect of D-Dimer level on efficacy is only meaningful in univariate analysis, we think it may be due to insufficient sample size. ALPase is highly expressed in tumor cells and can stimulate tumor cell growth, the elevated ALP levels in preoperative CRC patients are related to a poor prognosis (26). ALP levels were observed to correlate with PFS in MSS/pMMR CRC receiving

10.3389/fonc.2022.929342

TABLE 5 Treatment-related adverse events.

Adverse events	Any grade	Grade 1	Grade 2	Grade 3	Grade 4
Hand-foot syndrome	16 (14.5%)	9 (8.2%)	5 (4.5%)	2 (1.8%)	0 (0.0%)
Rash	3 (2.7%)	0 (0.0%)	3 (2.7%)	0 (0.0%)	0 (0.0%)
Hoarseness	3 (2.7%)	0 (0.0%)	3 (2.7%)	0 (0.0%)	0 (0.0%)
Nausea/vomiting	13 (11.8%)	13 (11.8%)	0 (0.0%)	0 (0.0%)	0 (0.0%)
Diarrhea	26 (23.7%)	8 (7.3%)	18 (16.4%)	0 (0.0%)	0 (0.0%)
Constipation	14 (12.7%)	10 (9.1%)	4 (3.6%)	0 (0.0%)	0 (0.0%)
Hypertension	17 (15.5%)	4 (3.6%)	10 (9.0%)	3 (2.7%)	0 (0.0%)
Leukopenia	18 (16.3%)	11 (10.0%)	5 (4.5%)	2 (1.8%)	0 (0.0%)
Neutropenia	6 (5.4%)	2 (1.8%)	2 (1.8%)	2 (1.8%)	0 (0.0%)
Thrombocytopenia	36 (32.7%)	24 (21.8)	10 (9.1%)	1 (0.9%)	1 (0.9%)
Anemia	20 (18.1%)	15 (13.6%)	4 (3.6%)	1 (0.9%)	0 (0.0%)
Proteinuria	24 (21.8%)	9 (8.2%)	14 (12.7%)	1 (0.9%)	0 (0.0%)
alanine aminotransferase elevated	27 (24.5%)	23 (20.9%)	4 (3.6%)	0 (0.0%)	0 (0.0%)
aminotransferase elevated	31 (28.1%)	27 (24.5%)	2 (1.8%)	2 (1.8%)	0 (0.0%)
Bilirubin elevated	12 (10.9%)	10 (9.1%)	1 (0.9%)	1 (0.9%)	0 (0.0%)
Hyperlipidemia	21 (19.1%)	21 (19.1%)	0 (0.0%)	0 (0.0%)	0 (0.0%)
Fatigue	7 (6.4%)	7 (6.4%)	0 (0.0%)	0 (0.0%)	0 (0.0%)
Oral mucositis	6 (5.4%)	2 (1.8%)	4 (3.6%)	0 (0.0%)	0 (0.0%)
Creatinine elevated	6 (5.4%)	6 (5.4%)	0 (0.0%)	0 (0.0%)	0 (0.0%)
Arrhythmia	1 (0.9%)	0 (0.0%)	1 (0.9%)	0 (0.0%)	0 (0.0%)
Lactate dehydrogenase elevated	16 (14.5%)	16 (14.5%)	0 (0.0%)	0 (0.0%)	0 (0.0%)
Hypothyroidism	22 (20.0%)	16 (14.5%)	6 (5.5%)	0 (0.0%)	0 (0.0%)
thyroid-stimulating hormone elevated	25 (22.7%)	20 (18.2%)	5 (4.5%)	0 (0.0%)	0 (0.0%)
Hyperthyroidism	2 (1.8%)	1 (0.9%)	1 (0.9%)	0 (0.0%)	0 (0.0%)
Adrenal cortex hypofunction	1 (0.9%)	0 (0.0%)	1 (0.9%)	0 (0.0%)	0 (0.0%)
Immune-associated pneumonia	1 (0.9%)	0 (0.0%)	1 (0.9%)	0 (0.0%)	0 (0.0%)
Joint pain	3 (2.7%)	3 (2.7%)	0 (0.0%)	0 (0.0%)	0 (0.0%)
Bleeding	6 (5.4%)	6 (5.4%)	0 (0.0%)	0 (0.0%)	0 (0.0%)
Hyperuricemia	10 (9.1%)	10 (9.1%)	0 (0.0%)	0 (0.0%)	0 (0.0%)

combination therapy in our study. It is possible that liver injury caused by liver metastases caused us to observe such differences, but patients with elevated ALP levels in the without liver metastases group had poorer prognosis. ALP levels have been shown to be associated with radiologic undetectable occult metastasis in liver or bone tissue (27), and we think it still has value in judging the prognosis of MSS/pMMR CRC receiving combination therapy. Unfortunately, we are unable to study the underlying mechanism. In clinical practice, the detection of ALP and FIB is convenient, fast and economical, and we believe that it is feasible as a predictor of the efficacy of combined therapy.

In addition to the DNA mismatch-repair system, the other most important pathway involved in CRC development is the epidermal growth factor receptor (EGFR) signaling pathway including *KRAS* and *BRAF* mutations (28). *RAS* mutations are associated with a poor prognosis with EGFR inhibitor therapy (29). There was no significant difference in the PFS between *RAS* mutant patients and *RAS* wild patients in our study (4.1 months vs. 5.1 months, P>0.05). It remains to be seen if anti-EGFR therapy combined with ICIs can conquer *RAS* resistance to anti-EGFR therapy. According to previous studies, patients with *BRAF* mutations who progress after first-line therapy are less likely to receive later-line therapy and have a worse prognosis (30). Although only six patients had *BRAF* mutations in our study, two patients achieved PR, and the remaining four achieved disease control. The ORR was 33.3%, the DCR was 83.3%, and the PFS was 13.3 months. A high response rate of 50% was also observed in two patients with *BRAF* mutations in the REGOTORI study (16). According to previous reports, this may be related to PD-1 inhibitors altering *BRAF* abundance and increasing *BRAF* mutation-associated tumor-associated lymphocytes *via* the mitogen-activated protein kinase (MAPK) pathway (31, 32). Our study, despite its small sample size, proposes a novel therapeutic strategy for *BRAF*-mutant patients in the late stage. More large-scale

randomized controlled studies are needed to substantiate the efficacy of fruquintinib coupled with PD-1 inhibitors in *BRAF*-mutant patients.

Safety was evaluated as a secondary endpoint in our study. Only 11 of the 110 patients discontinued treatment due to TRAEs, and the majority of them were able to continue treatment once the TRAEs were attenuated. The dose of fruquintinib was modified in three patients due to TRAEs, and all of them continued treatment after the dose of the drug was decreased. Although 89% of patients experienced TRAEs, the majority of these TRAEs were of grade 2 or lower (87%). It is worth noting that 10 patients developed hyperuricemia and six developed bleeding in our study; however, all of them recovered after symptomatic treatment. Due to suspected malignant arrhythmia, immune-related pneumonia, and immune-related adrenal insufficiency, three patients discontinued treatment. Immune-related adrenal insufficiency resolved with glucocorticoid therapy. The most common TRAEs are consistent with those seen with single-drug fruquintinib and single-drug PD-1 inhibitors (33, 34). Compared with the REGONIVO study, the overall incidence of TRAEs (100% vs. 89.1%) and the incidence of grade 3 TRAEs (20% vs. 11.8%) were lower (15). The following are some plausible explanations: 1. Doctors will adjust the dosage and usage of the drug in time according to the patient's tolerance in the process of clinical management, which minimizes the risk of TRAEs to a certain extent; 2. In retrospective studies, the limitations of restricted data collection and incomplete data may decrease the incidence of TRAEs. 3. The dose expansion of regorafenib may have increased the incidence of TRAEs in the REGONIVO study.

This study had some limitations. First, being a retrospective study, it was prone to biases due to limited data collection and incomplete data, resulting in biased results. Second, the OS could not be determined because of the short follow-up duration and inadequate data collected. Third, infiltration of cytotoxic T-cells in tumors has been shown to predict immunotherapy response in different studies. Most patients have not been checked for PD-1/PD-L1 expression levels or T-lymphocyte values to reduce the burden of clinical treatment; as such, we could not investigate whether they can be used as biomarkers associated with combination therapy. Fourth, although we preliminarily identified liver metastases, ALP level, and FIB level as efficacy predictors for fruquintinib coupled with PD-1 inhibitors in MSS/pMMR CRC, the underlying mechanisms were not investigated. Fifth, our study used a variety of PD-1 inhibitors and was unable to determine the best medication combination. However, this may imply that we can select a more appropriate medicine combination for the patient based on their financial situation and tolerance without worrying about the drug's effectiveness. Further large-scale randomized controlled trials are needed to determine the best combination therapy regimen.

In conclusion, MSS/pMMR CRC resistant to immunotherapy can benefit from combination therapy, and liver metastases, ALP levels, and FIB levels may indicate prognosis.

Data availability statement

The original contributions presented in the study are included in the article/supplementary material. Further inquiries can be directed to the corresponding author.

Ethics statement

The studies involving human participants were reviewed and approved by The First Affiliated Hospital of Zhengzhou University, Research and Clinical Experiment Ethics Office. Written informed consent for participation was not required for this study in accordance with the national legislation and the institutional requirements.

Author contributions

WZ conceived the idea, designed, and supervised the study. ZZ, SL, DL, ZM, and LX conducted the study. WZ, ZZ, and SL analyzed the data. WZ and ZZ wrote the manuscript. All authors have read and agreed on the published version of the manuscript.

Funding

This study was funded by Henan Province Medical Science and Technology Research Program (Provincial and Ministry Co-construction) Project (grant number SBGJ202003026) and Beijing Xisike Clinical Oncology Research Foundation.

Acknowledgments

We thank Prof. Shuiling Jin for the insightful suggestions. We would like to thank Charlesworth (https://www.cwauthors.com.cn/) for English language editing. We also sincerely thank the editors and reviewers for their careful review and valuable opinions that helped to greatly improve the manuscript.

Conflict of interest

The authors declare that this study was conducted in the absence of any commercial or financial relationships that could be construed as a potential conflict of interest.

Publisher's note

References

1. Siegel RL, Miller KD, Jemal A. Cancer statistics, 2020. *CA: A Cancer J Clin* (2020) 70(1):7–30. doi: 10.3322/caac.21590

2. Golshani G, Zhang Y. Advances in immunotherapy for colorectal cancer: a review. *Ther Adv Gastroenterol* (2020) 13:175628482091752. doi: 10.1177/1756284820917527

3. Sahin IH, Akce M, Alese O, Shaib W, Lesinski GB, El-Rayes B, et al. Immune checkpoint inhibitors for the treatment of MSI-H/MMR-D colorectal cancer and a perspective on resistance mechanisms. *Br J Cancer* (2019) 121(10):809–18. doi: 10.1038/s41416-019-0599-y

4. Le DT, Uram JN, Wang H, Bartlett BR, Kemberling H, Eyring AD, et al. PD-1 blockade in tumors with mismatch-repair deficiency. *N Engl J Med* (2015) 372 (26):2509–20. doi: 10.1056/NEJMoa1500596

5. Li J, Qin S, Xu RH, Shen L, Xu J, Bai Y, et al. Effect of fruquintinib vs placebo on overall survival in patients with previously treated metastatic colorectal cancer: The FRESCO randomized clinical trial. *JAMA* (2018) 319(24):2486–96. doi: 10.1001/jama.2018.7855

6. Kammertoens T, Friese C, Arina A, Idel C, Briesemeister D, Rothe M, et al. Tumour ischaemia by interferon-gamma resembles physiological blood vessel regression. *Nature* (2017) 545(7652):98–102. doi: 10.1038/nature22311

7. Yi M, Jiao D, Qin S, Chu Q, Wu K, Li A. Synergistic effect of immune checkpoint blockade and anti-angiogenesis in cancer treatment. *Mol Cancer* (2019) 18(1):60. doi: 10.1186/s12943-019-0974-6

8. Wang Y, Wei B, Gao J, Cai X, Xu L, Zhong H, et al. Combination of fruquintinib and anti-PD-1 for the treatment of colorectal cancer. *J Immunol* (2020) 205(10):2905–15. doi: 10.4049/jimmunol.2000463

9. Gou M, Yan H, Liu TE, Wang Z, Dai G. Fruquintinib combination with sintilimab in refractory metastatic colorectal cancer patients in China. *J Clin Oncol* (2020) 38(15_suppl):4028–8. doi: 10.1200/JCO.2020.38.15_suppl.4028

10. Guo Y, Zhang W, Ying J, Zhang Y, Pan Y, Qiu W, et al. Preliminary results of a phase 1b study of fruquintinib plus sintilimab in advanced colorectal cancer. *J Clin Oncol* (2021) 39(15_suppl):2514–4. doi: 10.1200/JCO.2021.39.15_suppl.2514

11. Mlecnik B, Bindea G, Angell HK, Maby P, Angelova M, Tougeron D, et al. Integrative analyses of colorectal cancer show immunoscore is a stronger predictor of patient survival than microsatellite instability. *Immunity* (2016) 44(3):698–711. doi: 10.1016/j.immuni.2016.02.025

12. Giannakis M, Mu XJ, Shukla SA, Qian ZR, Cohen O, Nishihara R, et al. Genomic correlates of immune-cell infiltrates in colorectal carcinoma. *Cell Rep* (2016) 15(4):857–65. doi: 10.1016/j.celrep.2016.03.075

13. Overman MJ, Kopetz S, Mcdermott RS, Leach J, Andre T. Nivolumab ± ipilimumab in treatment (tx) of patients (pts) with metastatic colorectal cancer (mCRC) with and without high microsatellite instability (MSI-h): CheckMate-142 interim results. *J Clin Oncol* (2016) 34(15_suppl):3501–1. doi: 10.1200/JCO.2016.34.15_suppl.3501

14. Sun Q, Zhou J, Zhang Z, Guo M, Liang J, Zhou F, et al. Discovery of fruquintinib, a potent and highly selective small molecule inhibitor of VEGFR 1, 2, 3 tyrosine kinases for cancer therapy. *Cancer Biol Ther* (2014) 15(12):1635–45. doi: 10.4161/15384047.2014.964087

15. Fukuoka S, Hara H, Takahashi N, Kojima T, Kawazoe A, Asayama M, et al. Regorafenib plus nivolumab in patients with advanced gastric or colorectal cancer: An open-label, dose-escalation, and dose-expansion phase ib trial (REGONIVO, EPOC1603). *J Clin Oncol* (2020) 38(18):2053–61. doi: 10.1200/JCO.19.03296

16. Wang F, He MM, Yao YC, Zhao X, Wang ZQ, Jin Y, et al. Regorafenib plus toripalimab in patients with metastatic colorectal cancer: a phase Ib/II clinical trial and gut microbiome analysis. *Cell Rep Med* (2021) 2(9):100383. doi: 10.1016/j.xcrm.2021.100383

17. Jiang FE, Zhang HJ, Yu CY, Liu AN. Efficacy and safety of regorafenib or fruquintinib plus camrelizumab in patients with microsatellite stable and/or proficient mismatch repair metastatic colorectal cancer: an observational pilot study. *Neoplasma* (2021) 68(4):861–6. doi: 10.4149/neo_2021_201228n1415

18. Cousin S, Bellera CA, Guégan JP, Gomez-Roca CA, Metges J-P, Adenis A, et al. REGOMUNE: A phase II study of regorafenib plus avelumab in solid tumors–results of the non-MSI-H metastatic colorectal cancer (mCRC) cohort. *J Clin Oncol* (2020) 38(15_suppl):4019–9. doi: 10.1200/JCO.2020.38.15_suppl.4019

19. Li J, Cong L, Liu J, Peng L, Wang J, Feng A, et al. The efficacy and safety of regorafenib in combination with anti-PD-1 antibody in refractory microsatellite stable metastatic colorectal cancer: A retrospective study. *Front Oncol* (2020) 10:594125. doi: 10.3389/fonc.2020.594125

20. Tumeh PC, Hellmann MD, Hamid O, Tsai KK, Loo KL, Gubens MA, et al. Liver metastasis and treatment outcome with anti-PD-1 monoclonal antibody in patients with melanoma and NSCLC. *Cancer Immunol Res* (2017) 5(5):417–24. doi: 10.1158/2326-6066.CIR-16-0325

21. Chalmers ZR, Connelly CF, Fabrizio D, Gay L, Ali SM, Ennis R, et al. Analysis of 100,000 human cancer genomes reveals the landscape of tumor mutational burden. *Genome Med* (2017) 9(1):34. doi: 10.1186/s13073-017-0424-2

22. Schumacher TN, Schreiber RD. Neoantigens in cancer immunotherapy. *Science* (2015) 348(6230):69–74. doi: 10.1126/science.aaa4971

23. Kwaan HC, Lindholm PF. Fibrin and fibrinolysis in cancer. *Semin Thromb Hemost* (2019) 45(4):413–22. doi: 10.1055/s-0039-1688495

24. Dirix LY, Salgado R, Weytjens R, Colpaert C, Benoy I, Huget P, et al. Plasma fibrin d-dimer levels correlate with tumour volume, progression rate and survival in patients with metastatic breast cancer. *Br J Cancer* (2002) 86(3):389–95. doi: 10.1038/sj.bjc.6600069

25. Lin Y, Liu Z, Qiu Y, Zhang J, Wu H, Liang R, et al. Clinical significance of plasma d-dimer and fibrinogen in digestive cancer: A systematic review and meta-analysis. *Eur J Surg Oncol* (2018) 44(10):1494–503. doi: 10.1016/j.ejso.2018.07.052

26. Hung HY, Chen JS, Chien Y, Tang R, Hsieh PS, Wen S, et al. Preoperative alkaline phosphatase elevation was associated with poor survival in colorectal cancer patients. *Int J Colorectal Dis* (2017) 32(12):1775–8. doi: 10.1007/s00384-017-2907-4

27. Li X, Mortensen B, Rushfeldt C, Huseby NE. Serum gamma-glutamyltransferase and alkaline phosphatase during experimental liver metastases. detection of tumour-specific isoforms and factors affecting their serum levels. *Eur J Cancer* (1998) 34(12):1935–40. doi: 10.1016/s0959-8049(98)00196-8

28. Gallo G, Sena G, Vescio G, Sacco R, Sammarco G. The prognostic value of KRAS and BRAF in stage I-III colorectal cancer. a systematic review. *Annali Italiani di Chirurgia* (2019) 90:127–37.

29. Douillard JY, Oliner KS, Siena S, Tabernero J, Burkes R, Barugel M, et al. Panitumumab-FOLFOX4 treatment and RAS mutations in colorectal cancer. *N Engl J Med* (2013) 369(11):1023–34. doi: 10.1056/NEJMoa1305275

30. Seligmann JF, Fisher D, Smith CG, Richman SD, Middleton G. Investigating the poor outcomes of BRAF-mutant advanced colorectal cancer: Analysis from 2530 patients in randomised clinical trials. *Ann Oncol* (2017) 28(3):562–8. doi: 10.1093/annonc/mdw645

31. Bastman JJ, Serracino HS, Zhu Y, Koenig MR, Mateescu V, Sams SB, et al. Tumor-infiltrating T cells and the PD-1 checkpoint pathway in advanced differentiated and anaplastic thyroid cancer. *J Clin Endocrinol Metab* (2016) 101 (7):2863–73. doi: 10.1210/jc.2015-4227

32. Zhao J, Chen AX, Gartrell RD, Silverman AM, Aparicio L, Chu T, et al. Immune and genomic correlates of response to anti-PD-1 immunotherapy in glioblastoma. *Nat Med* (2019) 25(3):462–9. doi: 10.1038/s41591-019-0349-y

33. Martins F, Sofiya L, Sykiotis GP, Lamine F, Maillard M, Fraga M, et al. Adverse effects of immune-checkpoint inhibitors: epidemiology, management and surveillance. *Nat Rev Clin Oncol* (2019) 16(9):563–80. doi: 10.1038/s41571-019-0218-0

34. Shirley M. Fruquintinib: First global approval. *Drugs* (2018) 78(16):1757–61. doi: 10.1007/s40265-018-0998-z

frontiers | Frontiers in Oncology

TYPE Original Research
PUBLISHED 17 October 2022
DOI 10.3389/fonc.2022.959407

OPEN ACCESS

EDITED BY
Aditi Banerjee,
University of Maryland, United States

REVIEWED BY
Xin-Hua Cheng,
Shanghai Jiao Tong University, China
Zhenzhen Gao,
Second Hospital of Jiaxing City, China

*CORRESPONDENCE
Alena Opattova
alena.opattova@iem.cas.cz
Pavel Vodicka
pavel.vodicka@iem.cas.cz

†These authors share senior authorship

SPECIALTY SECTION
This article was submitted to Gastrointestinal Cancers: Colorectal Cancer, a section of the journal Frontiers in Oncology

RECEIVED 01 June 2022
ACCEPTED 01 September 2022
PUBLISHED 17 October 2022

CITATION
Horak J, Dolnikova A, Cumaogullari O, Cumova A, Navvabi N, Vodickova L, Levy M, Schneiderova M, Liska V, Andera L, Vodicka P and Opattova A (2022) MiR-140 leads to MRE11 downregulation and ameliorates oxaliplatin treatment and therapy response in colorectal cancer patients. *Front. Oncol.* 12:959407. doi: 10.3389/fonc.2022.959407

MiR-140 leads to MRE11 downregulation and ameliorates oxaliplatin treatment and therapy response in colorectal cancer patients

Josef Horak[1,2], Alexandra Dolnikova[1,3], Ozge Cumaogullari[4,5], Andrea Cumova[1,3], Nazila Navvabi[1,6], Ludmila Vodickova[1,3,6], Miroslav Levy[7], Michaela Schneiderova[8], Vaclav Liska[6,9], Ladislav Andera[10], Pavel Vodicka[1,3,6*†] and Alena Opattova[1,3,6*†]

[1]Department of Molecular Biology of Cancer, Institute of Experimental Medicine Czech Academy of Sciences (CAS), Prague, Czechia, [2]Third Faculty of Medicine, Charles University, Prague, Czechia, [3]First Faculty of Medicine, Charles University, Prague, Czechia, [4]Eastern Mediterranean University, Dr. Fazıl Küçük Faculty of Medicine, North Cyprus, Turkey, [5]Gazimağusa State Hospital, Molecular Genetics Research Laboratory, North Cyprus, Turkey, [6]Biomedical Center in Pilsen, Charles University, Pilsen, Czechia, [7]Surgical Department, 1.st Medical Faculty, Charles University and Thomayer Hospital , Prague, Czechia, [8]Department of Surgery, University Hospital Kralovske Vinohrady and 3rd Faculty of Medicine, Charles University, Prague, Czechia, [9]Department of Surgery, Medical Faculty in Pilsen, Charles University, Pilsen, Czechia, [10]Institute of Biotechnology, Czech Academy of Sciences (CAS), Vestec, Czechia

Cancer therapy failure is a fundamental challenge in cancer treatment. One of the most common reasons for therapy failure is the development of acquired resistance of cancer cells. DNA-damaging agents are frequently used in first-line chemotherapy regimens and DNA damage response, and DNA repair pathways are significantly involved in the mechanisms of chemoresistance. MRE11, a part of the MRN complex involved in double-strand break (DSB) repair, is connected to colorectal cancer (CRC) patients' prognosis. Our previous results showed that single-nucleotide polymorphisms (SNPs) in the 3′ untranslated region (3′UTR) microRNA (miRNA) binding sites of *MRE11* gene are associated with decreased cancer risk but with shorter survival of CRC patients, which implies the role of miRNA regulation in CRC. The therapy of colorectal cancer utilizes oxaliplatin (oxalato(trans-l-1,2-diaminocyclohexane) platinum), which is often compromised by chemoresistance development. There is, therefore, a crucial clinical need to understand the cellular processes associated with drug resistance and improve treatment responses by applying efficient combination therapies. The main aim of this study was to investigate the effect of miRNAs on the oxaliplatin therapy response of CRC patients. By the *in silico* analysis, miR-140 was predicted to target MRE11 and modulate CRC prognosis. The lower expression of miR-140 was associated with the metastatic phenotype ($p < 0.05$) and poor progression-free survival (odds ratio (OR) = 0.4, $p < 0.05$). In the *in vitro* analysis, we used miRNA mimics to increase the level of miR-140 in the CRC cell line. This resulted in decreased proliferation of CRC cells ($p < 0.05$). Increased levels of miR-140 also led to

increased sensitivity of cancer cells to oxaliplatin ($p < 0.05$) and to the accumulation of DNA damage. Our results, both *in vitro* and *in vivo*, suggest that miR-140 may act as a tumor suppressor and plays an important role in DSB DNA repair and, consequently, CRC therapy response.

KEYWORDS

miR-140, colorecal cancer, *MRE11*, oxaliplatin, therapy response, DNA damage, DNA repair, miRNA

Introduction

Treatment failure of colorectal cancer (CRC) therapy, represented by the development of drug resistance or outgrowth of metastasis, is a major complication for CRC patients. There is a crucial clinical need for predictive biomarkers that indicate the success or failure of cancer treatment. A better understanding of the cellular processes associated with drug resistance will eventually lead to improved treatment response by applying more effective combination therapies (1).

Cancer cells react toward chemotherapeutics in different modes, such as by modifying DNA repair pathways. DNA repair plays a major role in the cancer therapy response, as chemotherapeutics usually induce various types of DNA damage in cancer cells (2). The overexpression of DNA repair genes in the tumor may confer more efficient repair of induced damage and thus contribute to chemoresistance and impaired therapy response (3). However, downregulation of the DNA repair genes may confer a better therapy response but may also give a basis for the appearance of new mutations and cancer progression (4).

Oxaliplatin (oxalato(trans-l-1,2-diaminocyclohexane) platinum; OX) belongs to the most used chemotherapeutics in CRC treatment. OX is a genotoxic drug that induces the formation of DNA crosslinks, thus directly impairing the structure of DNA, inhibiting DNA replication and RNA synthesis, and inducing apoptosis (5). One of the most crucial repair pathways to deal with DNA crosslinks is homologous recombination (HR), a constituent of double-strand break (DSB) repair (6).

MRN complex, a protein complex consisting of MRE11-RAD50-NBS1, plays an important role in the initial processing of DSB repair. The impaired function of the MRN complex leads to gene instability and DNA damage accumulation, a prerequisite of malignant transformation (7). Mutations in *MRE11* predispose to CRC and are frequent in primary CRC with mismatch repair deficiency (8). Patients with the decreased expression of MRE11 were more sensitive to OX treatment, with more significant tumor mass reduction and more prolonged progression-free survival (9). Moreover, single-nucleotide polymorphisms (SNPs) in the 3′ untranslated region (3′UTR) of *MRE11* gene are associated with decreased cancer risk but with shorter survival in CRC patients, which implies the role of microRNA (miRNA) regulation in CRC (10).

MiRNAs are signaling molecules in various cell processes functioning mainly as the suppressors of gene expression through interaction with 3′UTRs of target mRNAs. However, miRNAs have also been shown to interact with other regions of mRNA and can even activate gene expression under certain conditions (11). There are several mechanisms by which the deregulation of miRNAs can influence malignant transformation (for review, see (12)). Regardless of the mechanism, miRNA dysregulation can potentiate CRC development by acquiring one or more hallmarks of cancer (13). Despite some evidence of miRNAs influencing the CRC sensitivity to the therapy, there is a scarcity of miRNAs associated with OX therapy response (14).

The main aim of this study was to investigate the effect of miRNAs on the OX therapy response of CRC patients. Based on our previous published study, where we observed an association of SNPs in the 3′UTR of the *MRE11* gene with decreased CRC risk (10), we performed *in silico* analysis of miRNAs associated with MRE11 and found 187 miRNAs with *MRE11* as a predicted target. By additional analysis using The Cancer Genome Atlas (TCGA) database, we have identified miR-140 as the best candidate for further investigation. Our results suggest that the miR-140/MRE11 axis is associated with improved therapeutic response in oxaliplatin-treated CRC patients.

Materials and methods

Patient characteristics and samples

Paired tumor and non-malignant adjacent mucosa samples were obtained from 50 patients who underwent surgery between the years 2011 and 2015 and in whom all information was followed and updated in 2021 (patients' characteristics in Table 1 and Supplementary Table 1). All the patients provided signed consent for participation and their medical

TABLE 1 Patients' characteristics.

		Number of patients (N = 50)
Gender, N	Male	26
	Female	24
Age of diagnosis	Median	65
	Range	37-82
Smoker, N	Smokers	16
	Non-smokers	16
	Ex-smokers	18
TNM stage, N	I	2
	II	13
	III	25
	IV	10
Metastasis	Yes	26
	No	24

documentation for research. The design of the study was approved by the Ethical Committee of the Institute of Experimental Medicine, Prague, Czech Republic. RNA was isolated from tissues by miRNeasy® Mini Kit (50) (Qiagen, Hilden, Germany).

Bioinformatics analysis

Data from TargetScan (15) were extracted by multiMiR R package (16).

All miRNA-Seq transcriptional profiles and detailed clinical information were downloaded from TCGA (https://portal.gdc.cancer.gov) using the TCGAbiolinks R package (17). For the present study, data from the project TCGA-READ (rectal adenocarcinoma, n = 155) and TCGA-COAD (colon adenocarcinoma, n = 476) for every miRNA were separately analyzed and filtered according to the following criteria: 1) analyses were performed on CRC patients who had miRNA expression level data available, and 2) clinical data including survival data were also available. Finally, for miR-140, a total of 570 patients presented expression levels.

Cell cultures

Human colorectal cancer cell lines HCT116, DLD1, and HT29 were obtained from Merck (Darmstadt, Germany). Cell lines were cultured in Dulbecco's modified Eagle's medium (DMEM) (Merck, Germany) with 10% fetal bovine serum (Merck, Germany), 1 mM of l-glutamine (Biosera, Nuaille, France), 1 mM of sodium pyruvate (Biosera, Nuaille, France), and 1 mM of penicillin/streptomycin (Biosera, Nuaille, France). All cells were cultured in a humidified incubator at 37°C, with 5% CO2.

Transient transfection

Cells were transfected in 6-well plates at 60%–80% confluency with 2.5 pmol of MISSION miRNA hsa-miR-140-3p miRNA Mimics (Ambion, Austin, TX, USA) or with Negative Control miRNA Mimics (Ambion, USA) with no homology to the human genome using Lipofectamine® RNAiMAX 2000 (Invitrogen™) according to the manufacturer's protocol. All the experiments in cell lines were performed in three independent repeats. The efficiency of transfection was analyzed by qPCR measuring expression levels of transfected miRNAs as compared to negative controls.

Isolation and reverse transcription of RNA from cell culture samples

Forty-eight hours after transfection, total RNA (including miRNAs) was extracted from cells using Qiagen miReasy Mini Kit (Qiagen, Germany) according to the manufacturer's protocol. The concentration of the total RNA was measured by Nanodrop™ 8000 Spectrophotometer (Thermo Fisher Scientific, Waltham, MA, USA), and the integrity of mRNA (RNA integrity number (RIN)) of each sample was determined by Agilent RNA 6000 Nano Kit by Agilent Bioanalyzer 2100 (Agilent Technologies, Santa Clara, CA, USA). Reverse transcription was performed using the High-Capacity cDNA Reverse Transcription Kit (Thermo Fisher Scientific, USA), according to the manufacturer's protocol.

Quantitative PCR of cell culture samples

Expression levels of miR-140 were measured using TaqMan MicroRNA Assays at 7500 Real Time PCR System (Thermo Fisher Scientific, USA). The reaction contained 2 µl of a sample with 40 ng of cDNA, 10 µl of TaqMan™ Universal PCR Master Mix, 1 µl of the assay, and 7 µl of RNAse-free water. The thermal protocol was as follows: 50°C for 2 min, 95°C for 10 min, 40 cycles of 95°C for 15 s, and 60°C for 60 s plus melting curve analysis. MiRNA expression was normalized to RNU6B, and all data were subsequently analyzed by the 2−ΔΔCt method.

Oxaliplatin treatment

Oxaliplatin, obtained from Merck (Germany), was dissolved in dimethyl sulfoxide (DMSO; Merck, Germany) at the concentration of 100 mM and stored at 4°C. To assess the chemosensitivity of CRC cells with overexpressed miR-140 and control cells, both cells were treated with a 6 µM concentration

of oxaliplatin 24 h after miRNA mimics transfection and analyzed for cell viability.

Viability and proliferation assays

For clonogenicity formation assay (CFA), 48 h after cell transfection with miRNA mimics, 500 cells per well were plated for colony formation assay onto 6-well plates and cultured in DMEM. Twelve days later, colonies were fixed with 3% formaldehyde, stained with 1% crystal violet, and counted.

For proliferation assay, cells were plated onto 96-well plates at a density of 3 × 104 cells per well. The metabolic activity of the cells was measured 24 h after plating by adding WST-1 solution into the media as recommended by the manufacturer (Merck, Germany). Absorbance at 450 and 690 nm was measured on BioTek ELx808 absorbance microplate reader (BioTek, Winooski, VT, USA).

Cell cycle analysis

Cells were seeded on 12 well plates (5 × 105 cells/ml), harvested, washed with PBS, and centrifuged at 1,000 rpm for 10 min. Then, 1 ml of propidium iodide (PI) staining solution (0.02 μg/μl of PI, 0.02 mg/ml of RNase, and 0.05% Triton X-100) was added to the cell pellet, and cells were incubated for 30 min at 37°C in the dark. After incubation, samples were analyzed using a flow cytometer (Apogee A-50 micro, Apogee, Hertfordshire, UK). Measured data were evaluated with FlowLogic software (Inivai Technologies, Mentone, VIC, Australia).

Sodium dodecyl sulfate–polyacrylamide gel electrophoresis and Western blotting analysis

Proteins (20 μg) were loaded and separated in 10% sodium dodecyl sulfate–polyacrylamide gel electrophoresis (SDS-PAGE) gels at 15 mA for 60 min. Then, the separated proteins were transferred to 0.45 μm Amersham Protran Nitrocellulose Blotting Membrane (GE Healthcare, Life Sciences, Marlborough, MA, USA) in methanol transfer buffer using Mini Trans-Blot Cell (Bio-Rad Laboratories, Hercules, CA, USA). The membranes were blocked with 5% bovine serum albumin (BSA) in Tris-buffered saline containing Tween 20 (TBST; 20 mM of Tris–HCl, pH 7.4, 0.15 M of NaCl, and 0.1% Tween 20) for 1 h and incubated with anti-MRE11, anti-γH2AX, anti-RAD51 (Cell Signaling, Leiden, the Netherlands) and anti-GAPDH antibodies (Abcam, Cambridge, UK) at 4°C overnight, followed by incubation with goat anti-rabbit secondary antibody conjugated with horseradish peroxidase (Abcam, Cambridge, UK). The membranes were then incubated with Immobilon Western Chemiluminescent HRP Substrate (EMD Millipore Corporation, Billerica, MA, USA) and visualized by Azure c600 (Azure Biosystems, Dublin, CA, USA).

Preparation and application of recombinant lentiviruses for MRE11 silencing

For the preparation of recombinant lentiviruses expressing MRE11 shRNAs, HEK293FT cells (Thermo Fisher, Waltham, MA, USA) seeded in 6-well plates were co-transfected with pLKO1 mission MRE11 shRNA plasmids and helper plasmids psPax2 and pMD2.g (Addgene, Cambridge, MA, USA) using Lipofectamine 3000 (Thermo Fisher, Massachusetts, USA). Six hours later, the medium was replaced with fresh DMEM without antibiotics. After 48 h, the recombinant lentivirus-containing culture medium was harvested and centrifuged at 15 min, 3,000 rpm, and 4°C to remove any floating cells and cell debris. The cleared media containing lentiviruses were at 1:3 and 1:10 v/v ratios, added to HCT116 cells and plated in a 12-well plate, and after 24 h; the media were replaced with the fresh cultivation medium; cell cultures containing integrated lentiviruses were selected by using 2 μg/ml of puromycin for 4–5 days. Transfected cells were then tested using genomic PCR and Western blotting analysis for the genetic elimination/loss of expression of the *MRE11* gene.

Statistical analysis

Statistical analyses were performed using pairwise comparison by Student's t-test and two-way ANOVA (GraphPad Prism8, GraphPad Software, La Jolla, CA, USA; www.graphpad.com). The results represent the mean value of three independent experiments ± SD; the significance level was set at $p \leq 0.05$. Statistical analysis for TCGA data was performed using the R environment using the dplyr and survival, survminer, and ggplot2 packages. The survival significance was measured by a log-rank test.

Results

In silico analysis of miRNAs targeting MRE11

Using TargetScan (15), we found 187 miRNAs with *MRE11* as a predicted target (Supplementary Table 2) with 111 miRNAs with data sufficient for progression-free survival (PFS) calculation in the TCGA database. Out of these 111 miRNAs, eight had a statistically significant impact on PFS ($p < 0.05$, Supplementary Table 3). We identified miR-140 as the candidate for further investigation, as it displayed the strongest statistically

significant association with PFS (Figure 1, $p < 0.01$) in the group of analyzed miRNAs supported by data from more than 500 patients.

MiR-140 is downregulated in colorectal cancer and associated with progression-free survival and with the metastatic phenotype in colorectal cancer patients' samples

We investigated the expression levels of MRE11 and miR-140 in 50 CRC tumor tissues and adjacent non-malignant mucosa samples (Table 1 and Supplementary Table 1). The levels of miR-140 were significantly lower in tumor tissue (Figure 2A, $p < 0.01$) compared to adjacent mucosa. MRE11 levels were moderately, but not significantly, higher in tumor tissues (Figure 2B, $p = 0.11$). A significant decrease in miR-140 in patients' CRC samples led only to a moderate non-significant increase in MRE11, which might be due to broader regulation, mixed phenotype, or complex treatment.

The Kaplan–Meier analysis showed, in concordance with TCGA results, that lower expression of miR-140 in tumor tissue is associated with poor PFS (Figure 2C, $p < 0.05$).

Because metastatic CRC has a higher mortality rate and treatment is much more challenging, we have also investigated the association between miR-140 and metastatic formation. Our data showed that decreased expression of miR-140 is associated with the metastatic phenotype of CRC (Figure 2D, $p < 0.05$).

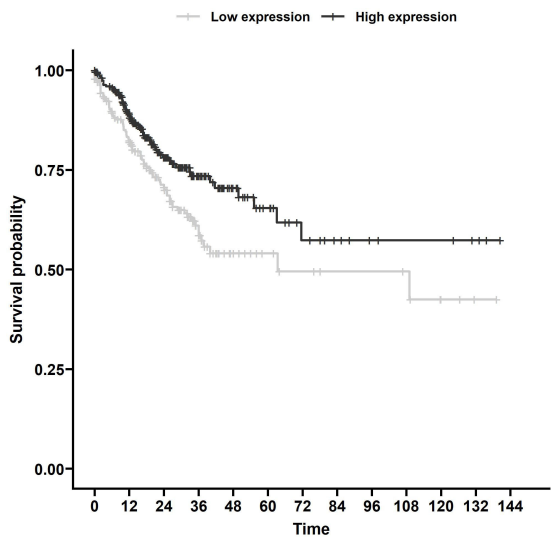

FIGURE 1
Survival analysis of TCGA samples. PFS associated with miR-140 expression of CRC patients from TCGA database. Kaplan–Meier analysis of the TCGA dataset showed that lower miR-140 expression is associated with poor PFS ($p = 0.006$). TCGA, The Cancer Genome Atlas; PFS, progression-free survival; CRC, colorectal cancer.

MiR-140 represses MRE11 expression

To select the appropriate colorectal cell line for transient transfection, we measured the expression levels of miR-140 in different CRC cell lines (Supplementary Figure 1A), and we decided on DLD1 by transient transfection of miR-140 by miRNA mimics. We have reached a significant increase in miR-140 levels stable up to 72 h (Supplementary Figure 1B). Our data showed that overexpression of miR-140 using miRNA mimics decreased the protein levels of MRE11 (Figure 3A) as well as mRNA levels of MRE11 (Figure 3B).

Overexpression of miR-140 leads to the accumulation of DNA damage

MRE11 is a crucial component of the MRN complex associated with DSB repair (18). Therefore, we evaluated the effect of miRNA mimic-induced miR-140 overexpression on one of the markers of DSB DNA damage and γH2AX protein accumulation (19). Western blotting analysis showed higher levels of γH2AX after miR-140 miRNA mimics in the CRC cell line (Figure 4).

Overexpression of miR-140 decreases colorectal cancer cell proliferation

The effect of miR-140 overexpression induced by miRNA mimics on CRC cell proliferation was measured using the WST-1 assay. Figure 5A shows that overexpression of miR-140 leads to decreased cell proliferation, pronounced 24 h after transfection ($p = 0.05$). However, miR-140 overexpression does not affect clonogenic potential (Figure 5B). In addition, flow cytometry analysis of the cell cycle showed that overexpression of miR-140 leads to moderate accumulation of cells in the G1 phase (Figure 5C).

MiR-140 enhances the chemotherapeutic sensitivity of colorectal cancer cells

Oxaliplatin is a third-generation platinum compound with an important role in CRC treatment. Therefore, we have investigated miR-140 in relation to the oxaliplatin sensitivity of CRC cells. Cell proliferation after oxaliplatin treatment in DLD1 cells overexpressing miR-140 significantly decreased after 48 and 72 h (Figure 6A, $p < 0.05$). The clonogenic potential of the cells (CFA) revealed a significant decrease in colony numbers (Figure 6B, $p <$

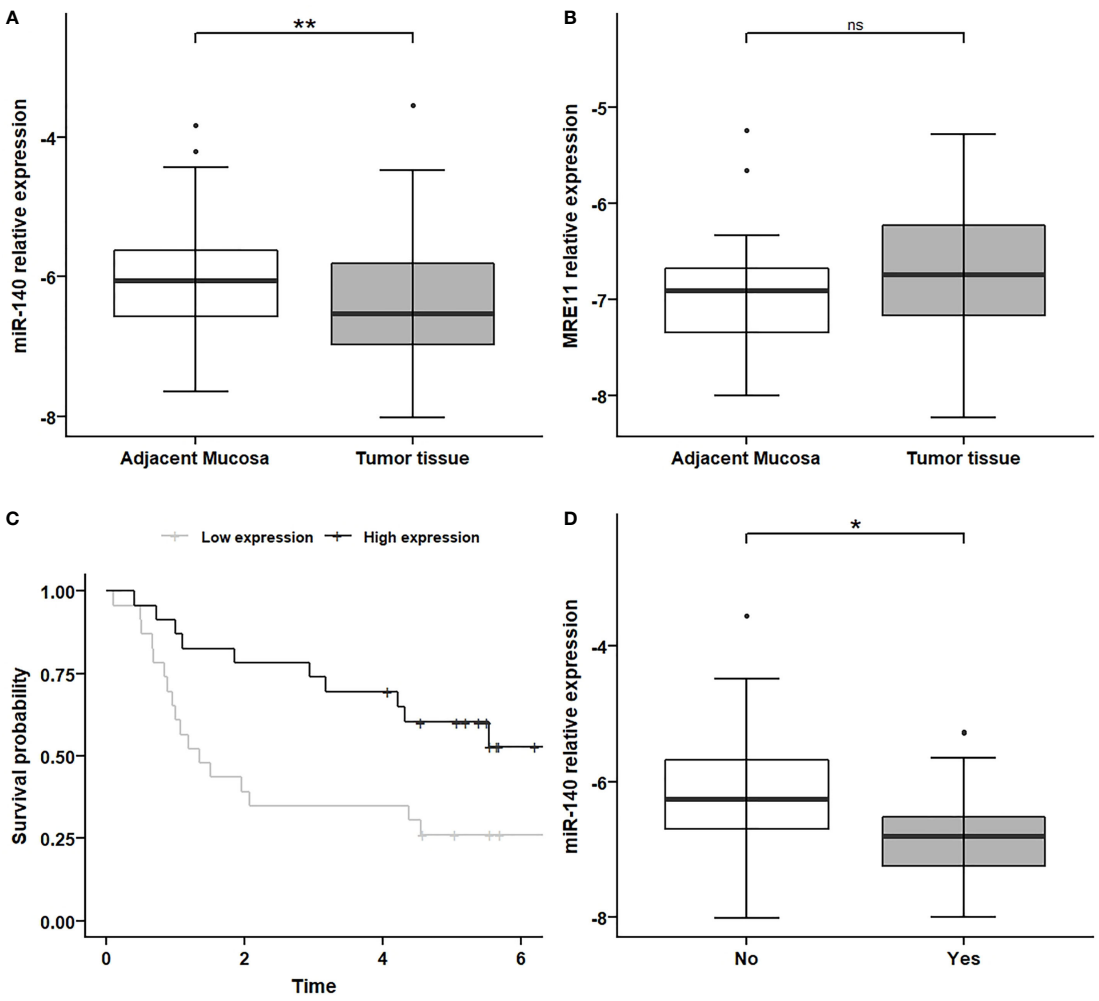

FIGURE 2
MiR-140 downregulation and association with PFS and metastatic CRC phenotype. **(A)** Relative expression of miR-140 is decreased in tumor tissues compared to non-adjacent mucosa (p = 0.009). **(B)** Relative expression of MRE11 in non-significantly increased in tumor tissue (p = 0.11). **(C)** Kaplan–Meier analysis showed that lower expression of miR-140 in tumor tissue is associated with poor PFS (p = 0.017). **(D)** Decreased relative expression of miR-140 is associated with the metastatic phenotype of CRC (p = 0.023). *p ≤ 0.05, **p ≤ 0.01. PFS, progression-free survival; CRC, colorectal cancer. ns = p>0.05 = non-significant

0.05). Cell cycle analysis of oxaliplatin-treated cells showed that overexpression of miR-140 leads to an increase in cells in the G1 phase and a decrease in those in the S phase (Figure 6C).

MiR-140 did not affect oxaliplatin sensitivity in shMRE11 cell lines

Our *in silico* analysis proposed a potential connection between miR-140 and MRE11. To further analyze the effect of miR-140 on oxaliplatin sensitivity through MRE11, we used recombinant lentiviruses expressing MRE11 shRNAs and established CRC cell lines with suppressed levels of MRE11 (Figure 7A). Cellular growth after miR-140 overexpression was not changed in parental and shMRE11 cell lines (Figures 7B, C). The measurement of cellular growth of HCT116 with overexpression of miR-140 and oxaliplatin treatment showed decreased cellular growth (p = 0.05) (Figure 7D). However, the analysis of cell growth did not show increased oxaliplatin sensitivity of shMRE11 cells with overexpressed miR-140 (Figure 7E).

Discussion

Poor therapy response and chemoresistance pose significant complications in CRC treatment, leading to ineffective therapy, tumor progression, metastasis, relapse of disease, and impaired patient survival.

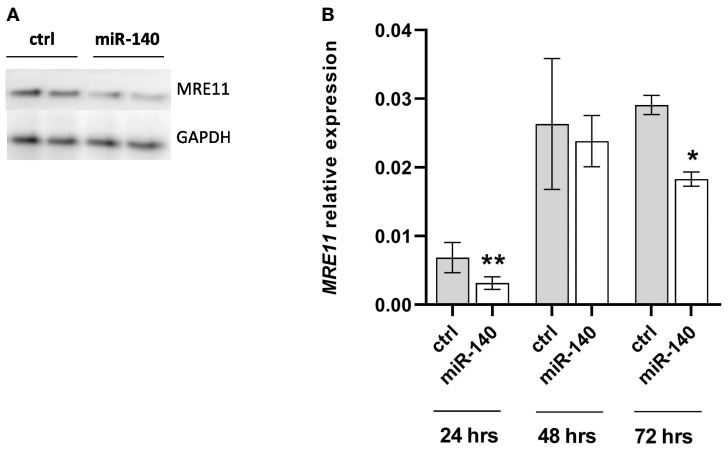

FIGURE 3
Increased levels of miR-140 led to the downregulation of MRE11. **(A)** Western blotting analysis of cells after transient transfection of miR-140 in the DLD1 cell line showed decreased protein level of MRE11. **(B)** qPCR analysis of cells showed decreased MRE11 mRNA level. The results represent the mean value of three independent experiments ± SD. *p ≤ 0.05, **p ≤ 0.01.

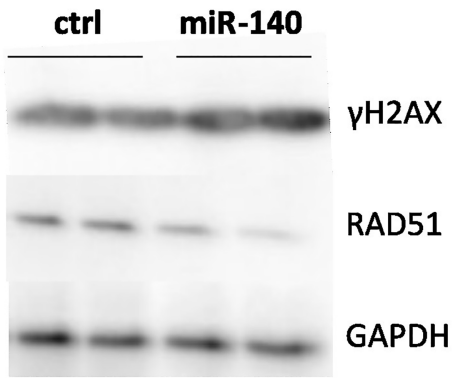

FIGURE 4
Effect of miR-140 on markers of DSBs. Western blotting analysis of cells transiently transfected with miR-140 showed decreased protein levels of RAD51 and increased levels of γH2AX. DSBs, double-strand breaks.

Based on our previous evidence that miRSNPs in the *MRE11* gene influence CRC risks and survival (10), in the present study, we investigated the effect of the miRNA/MRE11 axis on the oxaliplatin therapy response of CRC patients.

Despite the multidisciplinary approach and chemotherapy improvement, there is a considerable percentage of patients with inadequate response to treatments and a poor prognosis. Currently, there is a lack of properly validated predictive factors for CRC treatment response, and the emergence of resistant clones is a non-negligible reason for therapeutic failure and potential metastasis development (20). In our study, we defined the association of miR-140 expression with PFS, where lower miR-140 expression is associated with poor survival. Furthermore, our results showed lower levels of miR-140 in tumor tissue. MiR-140 expression has been previously studied mainly in association with cancer development and recurrence. Zheng et al. performed a meta-analysis and found a strong correlation between high expression of miR-140 and better overall survival (OS) in several cancers. Conversely, low expression is associated with advanced stages, worse histologic type, and lymph node metastasis (21). MiR-140 could also remarkably reduce the tumor size in gastric cancer xenograft mice (22). Yuan et al. found that miR-140 is significantly downregulated in non-small lung carcinoma (NSCLC) tissues and cell lines (23). In recent years, there has been increasing evidence of

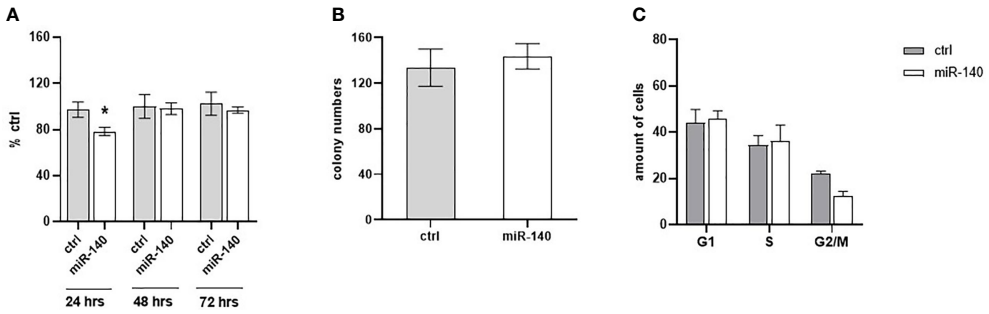

FIGURE 5
Effect of miR-140 on colorectal cancer cells. **(A)** Proliferation analysis showed a decreased level of proliferation in cells overexpressed miR-140 after 24 h ($p = 0.05$). **(B)** miR-140 overexpression did not affect the clonogenic potential of the cells. **(C)** Analysis of cell cycle content showed moderate accumulation of cells in the G1 phase. The results represent the mean value of three independent experiments ± SD. *$p \leq 0.05$.

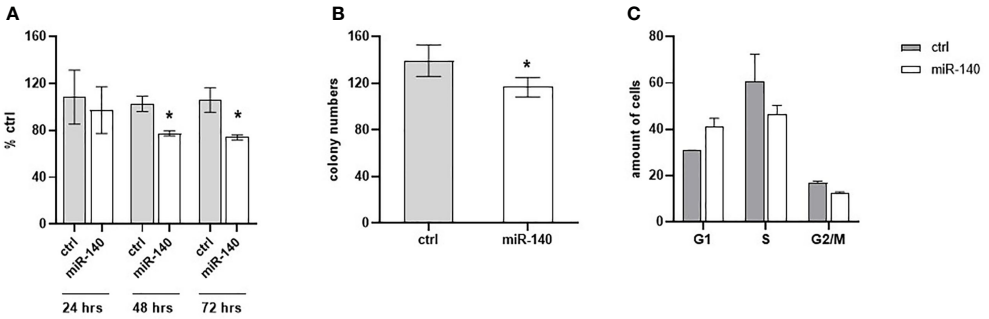

FIGURE 6
MiR-140 enhances the oxaliplatin sensitivity of CRC cells. **(A)** CRC cell proliferation after miR-140 and oxaliplatin treatment is decreased after 48 h ($p < 0.05$) and 72 h ($p < 0.05$). **(B)** Analysis of cell clonogenicity potential showed a significant decrease in CFA ($p < 0.05$). **(C)** Analysis of cell cycles showed an accumulation of cells in the G1 phase and a decrease in the S phase. The results represent the mean value of three independent experiments ± SD. *$p \leq 0.05$. CRC, colorectal cancer; CFA, clonogenicity formation assay.

a miR-140 role in the response to platinum derivative treatment in different cancers. Meng et al. described that miR-140 promoted autophagy mediated by HMGN5 and sensitized osteosarcoma cells to chemotherapy (24). Furthermore, miR-140 acts as a tumor suppressor in breast cancer by inhibiting FEN1 from repressing DNA damage repair. The authors of the published work reveal miR-140 to be a new anti-tumorigenesis factor for adjuvant breast cancer therapy (25). These results suggest a therapeutic potential of miR-140 in cancer treatment. Lui et al. demonstrated that plasma exosomal miR-140 in CRC patients was lower than in healthy controls, and their work supports our findings that miR-140 exerts a tumor suppressor ability (26).

Moreover, we found that decreased expression of miR-140 was associated with metastatic CRC phenotype. Our findings are consistent with a study by Shahabi et al. (2020). The authors showed that low expression of miR-140 is associated with lymph node metastasis in breast cancer (27).

Our *in vitro* analysis revealed an association of miR-140 overexpression with decreased CRC cell survival and accumulation of DNA damage. Moreover, overexpression of miR-140 enhances the sensitivity of colorectal cells to oxaliplatin. The important role of miRNA in oxaliplatin resistance in CRC was also proven by Wang et al. (28). They published evidence that overexpression of miR-29b re-sensitized OR-SW480 cells to oxaliplatin treatment. MiR-140 also re-sensitizes cisplatin-resistant NSCLC cells to cisplatin treatment through the SIRT1/ROS/JNK pathway (29).

Direct or indirect induction of DNA damage is the main goal of most cancer treatment regimens. Therefore, the process of DNA damage repair plays an important role in therapy response and chemotherapy resistance. Unfortunately, cancer cells can initiate DNA repair, which plays a role in therapy response (3) and chemotherapy resistance (2). The clinical importance of HR for cancer therapy, mainly of MRE11, RAD50, and, NBS, has

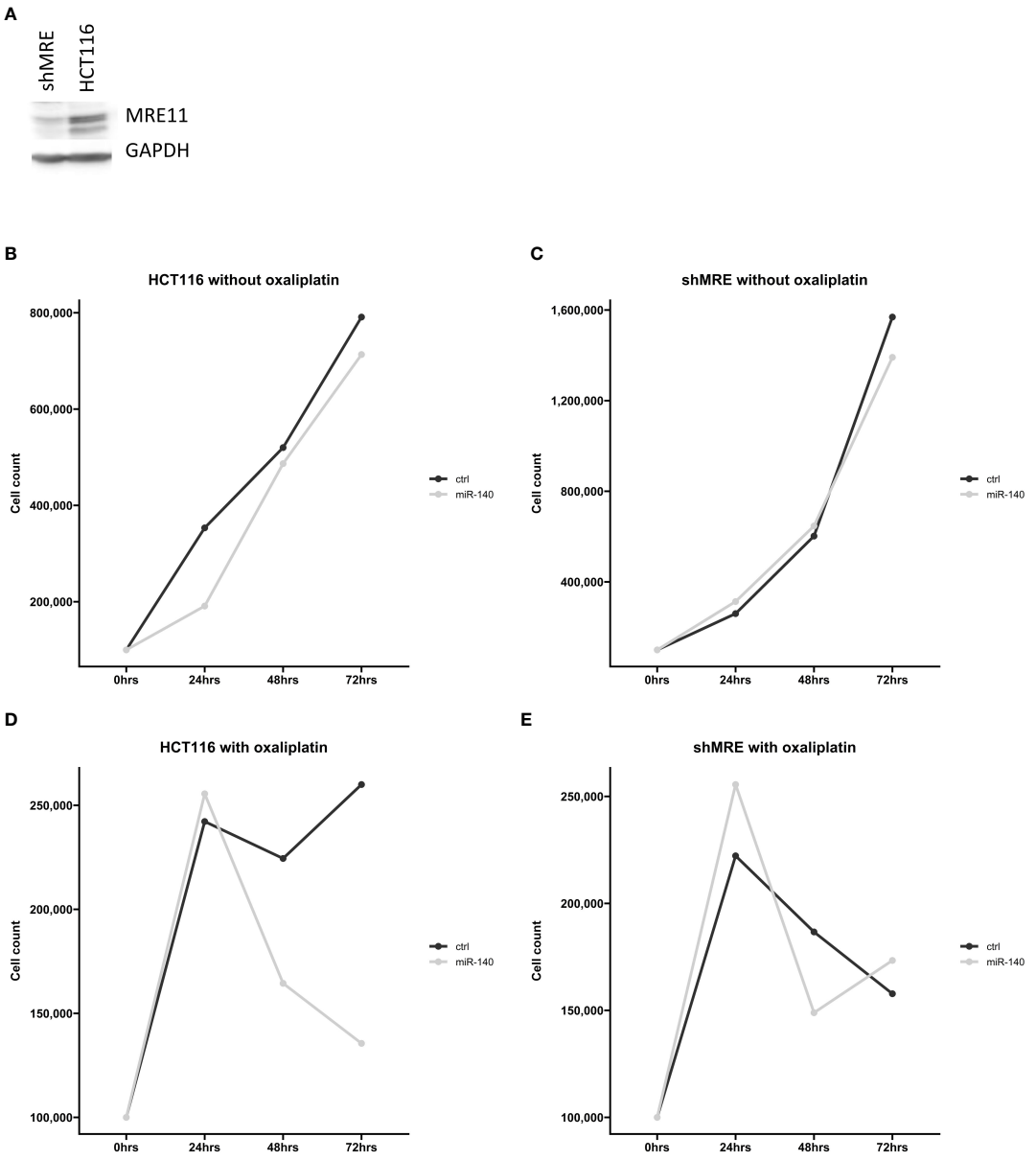

FIGURE 7
MiR-140 did not affect oxaliplatin sensitivity in shMRE11 cell lines. **(A)** Western blotting analysis of novel established cell line expressing recombinant lentiviruses MRE11 shRNA. **(B)** Cellular growth of parental cells HCT116 after overexpression of miR-140 was not changed. **(C)** Cellular growth of shMRE11 cells after overexpression of miR-140 was not changed. **(D)** Analysis of cellular growth of HCT116 with overexpression of miR-140 and oxaliplatin treatment showed decreased growth ($p = 0.05$). **(E)** Cellular growth of shMRE11 cells with miR-140 overexpression after oxaliplatin treatment was not changed. The results represent the mean value of three independent experiments.

already been reported (30). According to Pavelitz et al., deficient MRE11 protein is a marker of better prognosis for CRC patients irrespective of treatment in the long term (31). We previously described the significant influence of miRNA binding sites (miRSNPs) in the *MRE11* gene on CRC risks and survival (10). The importance of SNPs in miRSNPs of DNA repair genes has been also described in other types of cancer (32). MiR-140 was predicted as a potential interacting partner for MRE11 by TargetScan (15). *In vitro* overexpression of miR-140 causes the decrease of MRE11 protein levels. We did not observe any effect of miR-140 on cell proliferation and oxaliplatin sensitivity in the cells with inhibited MRE11 (shMRE11). Based on this data, we hypothesize that miR-140 affects oxaliplatin sensitivity in CRC cells *via* MRE11, or miR-140 may cooperate with MRE11 and may affect oxaliplatin sensitivity in tested cells. MRE11 downregulation may lead to

impairment of MRN complex and thus to inefficient HR and subsequent damage accumulation (33). That is in accordance with our results, as we observed the accumulation of γH2AX, a marker of DNA damage, following overexpression of miR-140.

Despite intensive research, the efficiency of CRC therapy remains low. Searching for novel prognostic and predictive biomarkers may lead to better therapy responses. The presence of miRNAs in blood plasma gives miRNAs a solid potential to be easily accessible biomarkers. However, their use may be compromised by the interindividual variability of cancer patients and large intratumor heterogeneity. Our results indicate miR-140 as a tumor suppressor and potential predictive biomarker for oxaliplatin treatment. We believe that identifying and validating novel biomarkers will ultimately lead to more personalized cancer therapy and improve the quality of a CRC patient's life.

Data availability statement

The raw data supporting the conclusions of this article will be made available by the authors, without undue reservation.

Ethics statement

This study was reviewed and approved by the Ethical Committee of the Institute of Experimental Medicine, Prague, Czech Republic. The patients/participants provided written informed consent to participate in this study.

Author contributions

JH, AD, AC, OC, and AO performed the experiments. LA coordinated the cell line establishment. ML, LV, and MS were responsible for the collection of patients' samples. PV reviewed the manuscript and discussed the results. AO coordinated the study and wrote a manuscript, JH wrote the manuscript. All authors contributed to the article and approved the submitted version.

Funding

The study was supported by the Grant Agency of Charles University (GAUK 784120), the Czech Science Foundation (20-03997S, 21-27902S, and 21-04607X), the Czech Health Research Council (grants AZV NV18/03/00199), Charles University grant Unce/Med/006, the Charles University Research Fund (Cooperation No. 43—Surgical Disciplines and the Cooperation Program, research area Oncology and Haematology), EFRR [project No. CZ.02.1.01/0.0/0.0/16_019/0000787 "Fighting INfectious Diseases", awarded by the MEYS CR], and the National Operation Programme: National Institute for Cancer Research LX22NPO05102.

Acknowledgments

The results shown in the section "*In silico* analysis of miRNAs targeting MRE11" are in part based upon data generated by TCGA Research Network: https://www.cancer.gov/tcga.

Conflict of interest

The authors declare that the research was conducted in the absence of any commercial or financial relationships that could be construed as a potential conflict of interest.

Publisher's note

Supplementary material

The Supplementary Material for this article can be found online at: https://www.frontiersin.org/articles/10.3389/fonc.2022.959407/full#supplementary-material

SUPPLEMENTARY FIGURE 1
(A) relative expression of miR-140 in different colorectal cell lines **(B)** optimization of the transfection with miR-140 mimics. The results represent the mean value of three independent experiments ± SD *p ≤ 0.05, **p ≤ 0.01, ***p ≤ 0.001

References

1. Dahlmann M, Werner R, Kortum B, Kobelt D, Walther W, Stein U. Restoring treatment response in colorectal cancer cells by targeting MACC1-dependent ABCB1 expression in combination therapy. *Front Oncol* (2020) 10:599. doi: 10.3389/fonc.2020.00599

2. Li LY, Guan YD, Chen XS, Yang JM, Cheng Y. DNA Repair pathways in cancer therapy and resistance. *Front Pharmacol* (2020) 11:629266. doi: 10.3389/fphar.2020.629266

3. Vodenkova S, Jiraskova K, Urbanova M, Kroupa M, Slyskova J, Schneiderova M, et al. Base excision repair capacity as a determinant of prognosis and therapy response in colon cancer patients. *DNA Repair (Amst)* (2018) 72:77–85. doi: 10.1016/j.dnarep.2018.09.006

4. Kiwerska K, Szyfter K. DNA Repair in cancer initiation, progression, and therapy-a double-edged sword. *J Appl Genet* (2019) 60(3-4):329–34. doi: 10.1007/s13353-019-00516-9

5. Wang D, Lippard SJ. Cellular processing of platinum anticancer drugs. *Nat Rev Drug Discovery* (2005) 4(4):307–20. doi: 10.1038/nrd1691

6. Hashimoto S, Anai H, Hanada K. Mechanisms of interstrand DNA crosslink repair and human disorders. *Genes Environ* (2016) 38:9. doi: 10.1186/s41021-016-0037-9

7. Situ Y, Chung L, Lee CS, Ho V. MRN (MRE11-RAD50-NBS1) complex in human cancer and prognostic implications in colorectal cancer. *Int J Mol Sci* (2019) 20(4). doi: 10.3390/ijms20040816

8. Giannini G, Rinaldi C, Ristori E, Ambrosini MI, Cerignoli F, Viel A, et al. Mutations of an intronic repeat induce impaired MRE11 expression in primary human cancer with microsatellite instability. *Oncogene.* (2004) 23(15):2640–7. doi: 10.1038/sj.onc.1207409

9. Ihara K, Yamaguchi S, Ueno N, Tani Y, Shida Y, Ogata H, et al. Expression of DNA double-strand break repair proteins predicts the response and prognosis of colorectal cancer patients undergoing oxaliplatin-based chemotherapy. *Oncol Rep* (2016) 35(3):1349–55. doi: 10.3892/or.2015.4488

10. Naccarati A, Rosa F, Vymetalkova V, Barone E, Jiraskova K, Di Gaetano C, et al. Double-strand break repair and colorectal cancer: gene variants within 3' UTRs and microRNAs binding as modulators of cancer risk and clinical outcome. *Oncotarget.* (2016) 7(17):23156–69. doi: 10.18632/oncotarget.6804

11. O'Brien J, Hayder H, Zayed Y, Peng C. Overview of MicroRNA biogenesis, mechanisms of actions, and circulation. *Front Endocrinol (Lausanne)* (2018) 9:402. doi: 10.3389/fendo.2018.00402

12. Shah V, Shah J. Recent trends in targeting miRNAs for cancer therapy. *J Pharm Pharmacol* (2020) 72(12):1732–49. doi: 10.1111/jphp.13351

13. Forterre A, Komuro H, Aminova S, Harada M. A comprehensive review of cancer MicroRNA therapeutic delivery strategies. *Cancers (Basel)* (2020) 12(7). doi: 10.3390/cancers12071852

14. Ahadi A. The significance of microRNA deregulation in colorectal cancer development and the clinical uses as a diagnostic and prognostic biomarker and therapeutic agent. *Noncoding RNA Res* (2020) 5(3):125–34. doi: 10.1016/j.ncrna.2020.08.003

15. McGeary SE, Lin KS, Shi CY, Pham TM, Bisaria N, Kelley GM, et al. The biochemical basis of microRNA targeting efficacy. *Science* (2019) 366(6472). doi: 10.1126/science.aav1741

16. Ru Y, Kechris KJ, Tabakoff B, Hoffman P, Radcliffe RA, Bowler R, et al. The multiMiR r package and database: integration of microRNA-target interactions along with their disease and drug associations. *Nucleic Acids Res* (2014) 42(17):e133. doi: 10.1093/nar/gku631

17. Colaprico A, Silva TC, Olsen C, Garofano L, Cava C, Garolini D, et al. TCGAbiolinks: an R/Bioconductor package for integrative analysis of TCGA data. *Nucleic Acids Res* (2016) 44(8):e71. doi: 10.1093/nar/gkv1507

18. Lamarche BJ, Orazio NI, Weitzman MD. The MRN complex in double-strand break repair and telomere maintenance. *FEBS Lett* (2010) 584(17):3682–95. doi: 10.1016/j.febslet.2010.07.029

19. Mah LJ, El-Osta A, Karagiannis TC. gammaH2AX: a sensitive molecular marker of DNA damage and repair. *Leukemia.* (2010) 24(4):679–86. doi: 10.1038/leu.2010.6

20. Gherman A, Balacescu L, Gheorghe-Cetean S, Vlad C, Balacescu O, Irimie A, et al. Current and new predictors for treatment response in metastatic colorectal cancer. the role of circulating miRNAs as biomarkers. *Int J Mol Sci* (2020) 21(6). doi: 10.3390/ijms21062089

21. Zheng M, Liu J, Meng C, Tang K, Liao J. Prognostic and clinicopathological importance of microRNA-140 expression in cancer patients: a meta-analysis. *World J Surg Oncol* (2021) 19(1):266. doi: 10.1186/s12957-021-02380-6

22. Fang Z, Yin S, Sun R, Zhang S, Fu M, Wu Y, et al. miR-140-5p suppresses the proliferation, migration and invasion of gastric cancer by regulating YES1. *Mol Cancer* (2017) 16(1):139. doi: 10.1186/s12943-017-0708-6

23. Yuan Y, Shen Y, Xue L, Fan H. miR-140 suppresses tumor growth and metastasis of non-small cell lung cancer by targeting insulin-like growth factor 1 receptor. *PloS One* (2013) 8(9):e73604. doi: 10.1371/journal.pone.0073604

24. Meng Y, Gao R, Ma J, Zhao J, Xu E, Wang C, et al. MicroRNA-140-5p regulates osteosarcoma chemoresistance by targeting HMGN5 and autophagy. *Sci Rep* (2017) 7(1):416. doi: 10.1038/s41598-017-00405-3

25. Lu X, Liu R, Wang M, Kumar AK, Pan F, He L, et al. MicroRNA-140 impedes DNA repair by targeting FEN1 and enhances chemotherapeutic response in breast cancer. *Oncogene.* (2020) 39(1):234–47. doi: 10.1038/s41388-019-0986-0

26. Liu D, Chen C, Cui M, Zhang H. miR-140-3p inhibits colorectal cancer progression and its liver metastasis by targeting BCL9 and BCL2. *Cancer Med* (2021) 10(10):3358–72. doi: 10.1002/cam4.3840

27. Shahabi A, Naghili B, Ansarin K, Montazeri V, Zarghami N. miR-140 and miR-196a as potential biomarkers in breast cancer patients. *Asian Pac J Cancer Prev* (2020) 21(7):1913–8. doi: 10.31557/APJCP.2020.21.7.1913

28. Wang W, Wang M, Xu J, Long F, Zhan X. Overexpressed GATA3 enhances the sensitivity of colorectal cancer cells to oxaliplatin through regulating MiR-29b. *Cancer Cell Int* (2020) 20:339. doi: 10.1186/s12935-020-01424-3

29. Lin Z, Pan J, Chen L, Wang X, Chen Y. MiR-140 resensitizes cisplatin-resistant NSCLC cells to cisplatin treatment through the SIRT1/ROS/JNK pathway. *Onco Targets Ther* (2020) 13:8149–60. doi: 10.2147/OTT.S261799

30. Altan B, Yokobori T, Ide M, Bai T, Yanoma T, Kimura A, et al. High expression of MRE11-RAD50-NBS1 is associated with poor prognosis and chemoresistance in gastric cancer. *Anticancer Res* (2016) 36(10):5237–47.

31. Pavelitz T, Renfro L, Foster NR, Caracol A, Welsch P, Lao VV, et al. MRE11-deficiency associated with improved long-term disease free survival and overall survival in a subset of stage III colon cancer patients in randomized CALGB 89803 trial. *PloS One* (2014) 9(10):e108483. doi: 10.1371/journal.pone.0108483

32. Cumova A, Vymetalkova V, Opattova A, Bouskova V, Pardini B, Kopeckova K, et al. Genetic variations in 3'UTRs of SMUG1 and NEIL2 genes modulate breast cancer risk, survival and therapy response. *Mutagenesis.* (2021) 36(4):269–79. doi: 10.1093/mutage/geab017

33. Bian L, Meng Y, Zhang M, Li D. MRE11-RAD50-NBS1 complex alterations and DNA damage response: implications for cancer treatment. *Mol Cancer* (2019) 18(1):169. doi: 10.1186/s12943-019-1100-5

frontiers | Frontiers in Oncology

TYPE Original Research
PUBLISHED 27 October 2022
DOI 10.3389/fonc.2022.1046143

OPEN ACCESS

EDITED BY
Veronika Vymetalkova,
Academy of Sciences of the Czech Republic (ASCR), Czechia

REVIEWED BY
Xuming Ji,
Zhejiang Chinese Medical University, China
Monika Sramkova,
Slovak Academy of Sciences, Slovakia

*CORRESPONDENCE
Chunze Zhang
chunze.zhang@nankai.edu.cn
Shiwu Zhang
zhangshiwu666@aliyun.com
Yijia Wang
yijiawang_1980@163.com

†These authors have contributed equally to this work and share first authorship

SPECIALTY SECTION
This article was submitted to Gastrointestinal Cancers: Colorectal Cancer, a section of the journal Frontiers in Oncology

RECEIVED 16 September 2022
ACCEPTED 13 October 2022
PUBLISHED 27 October 2022

CITATION
Liu Y, Tian S, Yi B, Feng Z, Chu T, Liu J, Zhang C, Zhang S and Wang Y (2022) Platycodin D sensitizes *KRAS*-mutant colorectal cancer cells to cetuximab by inhibiting the PI3K/Akt signaling pathway.
Front. Oncol. 12:1046143.
doi: 10.3389/fonc.2022.1046143

Platycodin D sensitizes *KRAS*-mutant colorectal cancer cells to cetuximab by inhibiting the PI3K/Akt signaling pathway

Yanfei Liu[1,2†], Shifeng Tian[3†], Ben Yi[1,2], Zhiqiang Feng[1,2], Tianhao Chu[1,2], Jun Liu[4], Chunze Zhang[2*], Shiwu Zhang[5*] and Yijia Wang[5*]

[1]School of Integrative Medicine, Tianjin University of Traditional Chinese Medicine, Tianjin, China, [2]Department of Colorectal Surgery, Tianjin Union Medical Center, Tianjin, China, [3]Tianjin Union Medical Center, Tianjin Medical University, Tianjin, China, [4]Department of Radiology, The Fourth Central Hospital Affiliated to Nankai University, Tianjin, China, [5]Laboratory of Oncologic Molecular Medicine, Tianjin Union Medical Center, Tianjin, China

Cetuximab is a monoclonal antibody against epidermal growth factor receptor that blocks downstream signaling pathways of receptor tyrosine kinases, including Ras/Raf/MAPK and PI3K/Akt, thereby inhibiting tumor cell proliferation and inducing cancer cell apoptosis. Owing to *KRAS* mutations, the effectiveness of cetuximab is usually limited by intrinsic drug resistance. Continuous activation of the PI3K/Akt signaling pathway is another reason for cetuximab resistance. Platycodin-D, a bioactive compound isolated from the Chinese herb *Platycodon grandiflorum*, regulates Akt in different trends based on tissue types. To investigate whether platycodin-D can sensitize *KRAS*-mutant colorectal cancer cells to cetuximab by inhibiting the PI3K/Akt signaling pathway, HCT116 and LoVo cells were treated with cetuximab and platycodin-D. LY294002 and SC79 were used to regulate Akt to further evaluate whether platycodin-D sensitizes cells to cetuximab by inhibiting Akt. Our results confirmed that platycodin-D increased the cytotoxic effects of cetuximab, including inhibition of growth, migration, and invasion, *via* downregulation of PI3K and Akt phosphorylation in HCT116 and LoVo cells both *in vitro* and *in vivo*. Given these data, platycodin-D may sensitize KRAS-mutant colorectal cancer cells to cetuximab *via* inhibition of the PI3K/Akt signaling pathway.

KEYWORDS

Akt, cetuximab, colorectal cancer, platycodin D, resistance

Introduction

Epidermal growth factor receptor (EGFR) is a member of the human epidermal growth factor receptor (HER) family of receptor tyrosine kinases, and its abnormal expression is associated with the etiology of various cancers. When EGFR binds to its ligands, it activates the PI3K/Akt pathway, promotes the growth and proliferation of tumor cells, inhibits apoptosis, promotes invasion and metastasis, and regulates tumor angiogenesis (1). Cetuximab (CTX), a clinically recommended EGFR inhibitor, mainly binds to the extracellular ligand-binding domain of EGFR with high affinity and interferes with the binding of other endogenous ligands to EGFR, thereby inhibiting the activity of EGFR downstream signaling and tumor cell proliferation as well as inducing apoptosis in cancer cells (2). Wild-type *KRAS* is the gold standard for identifying cancer patients and is suitable for CTX therapy, which ensures that the Ras/Raf/MAPK pathway is effectively inhibited by CTX (3). Therefore, the effectiveness of CTX is limited by drug resistance due to downstream *KRAS* mutations (4). In addition, the continuous activation of Akt independent of EGFR is also an important reason for the emergence of resistance to CTX therapy (1); therefore, Akt inhibition is a strategy to sensitize cancer cells to CTX (5). As a downstream pathway of EGFR, the PI3K/Akt signaling pathway is dysregulated in many cancer cells. In addition to the direct regulation of this pathway by EGFR, various proteins affect Akt activation (1, 6). Therefore, there is an urgent need to develop new treatments targeting Akt to enhance the sensitivity of *KRAS*-mutant colorectal cancer (CRC) cells to CTX.

Platycodon grandiflorum saponin D (platycodin D, PD) is a triterpenoid saponin-like ingredient extracted from the Chinese herb *Platycodon grandiflorum*, with various biological effects. It exhibits immunostimulatory (7), anti-inflammatory (8), anti-obesity (9), and anti-atherosclerotic activities (10). In addition, PD exhibits anticancer effects against various cancer cell lines, mainly by inhibiting cell proliferation, inducing cell cycle arrest, and promoting apoptosis (11–15). It has been shown that PD up- or downregulates PI3K/Akt signaling in various types of cancer. For example, PD inhibits the proliferation of human glioma U251 cells by inhibiting PI3K/Akt signaling activation, reducing Akt phosphorylation, inducing apoptosis, and causing cell cycle arrest (16). In addition, PD significantly inhibits the expression of p-Akt in NCI-H460 and A549 cells in a dose- and time-dependent manner and induces autophagy in the two cell types by inhibiting the PI3K/Akt/mTOR signaling pathway (17). PD inhibits the migration, invasion, and growth of MDA-MB-231 human breast cancer cells by suppressing the EGFR-mediated Akt and MAPK pathways and by inhibiting the phosphorylation of Akt and mTOR (18). However, contradictory reports (19) have revealed that PD could promote p-Akt ubiquitination by increasing p-Akt levels. It has also been shown that PD is involved in the activation of extracellular signal-regulated kinases in hepatoma cells to trigger autophagy by upregulating the expression of p-Akt. Furthermore, PD can activate PI3K/Akt signaling in HEK-293 cells, promoting the phosphorylation of p-PI3K and p-Akt, but has no effect on the expression of PI3K and Akt (20). To the best of our knowledge, studies on cancer treatment with a combination of PD and CTX or other EGFR tyrosine kinase inhibitors (EGFR-TKIs) are still lacking.

In this study, two *KRAS*-mutant CRC cell lines, HCT116 and LoVo, were used to investigate the effect of PD treatment on the cytotoxicity of CTX *in vitro* and *in vivo*. The effect of PD on p-PI3K and p-Akt in CRC cells and whether the regulation of the PI3K/Akt signaling pathway affects CTX resistance were examined in this study. Our research provides a potentially reliable theory for the improvement of CTX chemotherapy efficacy with PD treatment.

Materials and methods

Reagents and antibodies

All cell culture media, trypsin, and antibiotics were purchased from Gibco (Grand Island, NY, USA), and fetal bovine serum (FBS) was purchased from Quacell (Zhongshan, China). PI3 Kinase p85 (19H8) Rabbit mAb, Phospho-PI3 Kinase p85 (Tyr458)/p55 (Tyr199) Antibody, Akt (pan) (C67E7) Rabbit mAb, Phospho-Akt (Ser473) (D9E) XP® Rabbit mAb were obtained from Cell Signaling Technology (Danvers, MA, USA). Rabbit a beta-Actin (Loading Control), Goat anti-rabbit IgG/HRP, Phenylmethanesulfonyl fluoride (PMSF) and RIPA Lysis Buffer were purchased from Bioss (greater Boston, MA, USA). CTX was purchased from TargetMol (Boston, MA, USA). PD was purchased from Topscience (Shanghai, China). LY294002 and SABC-HRP Kit with Anti-Rabbit IgG (IHC&ICC) were obtained from Beyotime (Shanghai, China). Cell Counting Kit-8 (CCK-8), Rabbit anti-

Abbreviations: EGFR, epidermal growth factor receptor; Ras, Rat sarcoma protein; Raf, Raf protein kinase; MAPK, mitogen-activated protein kinase; PI3K, phosphoinositide 3-kinase; Akt, serine/threonine kinase; PD, Platycodin-D; CTX, cetuximab; CRC, colorectal cancer; HER, human epidermal growth factor receptor; mTOR, mammalian target of rapamycin; TKIs, tyrosine kinase inhibitors; FBS, fetal bovine serum; PMSF, phenylmethanesulfonyl fluoride; CCK-8, Cell Counting Kit-8; TUNEL, terminal deoxynucleotidyl transferase-mediated dUTP nick-end labeling; DAB, diaminobenzidine; BCA, Bichinoline acid; PBS, phosphate buffer solution; TBST, Tris Buffered Saline with Tween-20; GSK3β, Glycogen Synthase Kinase 3β; EGF, Epidermal Growth Factor; GPCR, G Protein-Coupled Receptor. ALT, alanine aminotransferase; AST, aspartate aminotransferase.

Ki67 Polyclonal Antibody and terminal deoxynucleotidyl transferase-mediated dUTP nick-end labeling (TUNEL) Apoptosis Detection Kit-diaminobenzidine (DAB) were purchased from absin (Shanghai, China).

Cell lines

The *KRAS* mutant human colon cancer cell lines HCT116 and LoVo were purchased from the Shanghai Institutes for Biological Sciences, Chinese Academy of Sciences (Shanghai, China). All cells were cultured in an RPMI 1640 medium supplemented with 10% FBS, 100 μg/ml streptomycin, and 100 U/ml penicillin and incubated at 37°C in a humidified atmosphere containing 5% CO_2.

Measurement of cell viability

Cells were seeded in 96-well flat-bottom microtiter plates at a density of 5000 cells per well and treated with different concentrations of PD and CTX in four different groups: (1) cells without drug treatment as the control group; (2) cells treated with PD alone for 48 h; (3) cells treated with CTX alone for 48 h; and (4) cells treated with a mixture of PD and CTX for 48 h. Cell viability was measured using the Cell Counting Kit-8 (CCK-8) after treatment, according to the manufacturer's instructions. Absorbance was measured at 450 nm using a microplate reader (Synergy HT; Bio-Tek, USA).

Colony formation assay

For colony formation assay with monolayer cultures, cells were seeded in 6-well plates, and 300 cells/well were seeded in each experimental group for 2 weeks. After fixing in methanol for 15 min, the cells were stained with GIMSA application stain for 30 min, and the colonies were imaged and counted.

Wound healing assay

Cells were cultured in 6-well plates to form a monolayer and serum-starved overnight. Then, the cells were scratched with a 10-μl sterile pipette tip to create an artificial scratch wound, washed three times with phosphate buffer solution (PBS), and incubated with serum-free medium for 48 h. Photographs of random fields from three replicate wells were captured using a light microscope (Nikon Corporation; Tokyo, Japan). The following equation was used to calculate percent wound closure: percent wound closure (%) = [1 − (Lt/L0)] × 100, where Lt represents the width of the scratch at time t, and L0 represents the initial scratch width.

Cell invasion assay

Cells with a subconfluent growth density were serum-starved for 24 h. Next, the cells were trypsinized and seeded into the upper chamber of 24-well Transwell plates (8 μm pore size; Corning; NY, USA) at a density of 2×10^5cells/ml in 200 μl of serum-free medium, and 600 μl of medium with 10% FBS was added to the lower chambers. After 24 h of incubation, the cells on the upper surface of the membrane were removed using cotton swabs, and those on the lower surface were fixed in methanol and stained with 0.1% crystal violet. The stained cells were counted under a light microscope. Images of randomly selected fields across three replicate wells were captured for analysis.

Western blotting analysis

Cells were harvested from culture dishes and lysed in RIPA lysis buffer containing 1 mM phenylmethylsulfonyl fluoride and 1 mM protease inhibitors. The lysates were centrifuged, and the protein concentration was determined using a BCA protein assay kit (Solarbio; Beijing, China). Protein samples were suspended in the SDS loading buffer. After boiling for 10 min, cell protein samples (25μg protein/line) were separated on a 6–10% gel SDS-PAGE (Bio-Rad; CA, USA) and then transferred to Immobilon PVDF membranes(Immobilon; Darmstadt, Germany), which were then blocked with 5% skim milk for 1 h and probed with primary antibodies (1:1000 dilution in tris buffered saline with tween-20 (TBST); Akt antibody was used at 1:2000 dilution in TBST). Immunoreactive bands were visualized by enhanced chemiluminescence using horseradish peroxidase-conjugated goat anti-rabbit IgG secondary antibody (1:10000 dilution in TBST). Band density was quantified using ImageJ (Wayne Rasband, et al. Bethesda, MD, USA) and normalized to an indicated sample in an identical membrane. Each assay was performed in triplicate.

Subcutaneous tumor model

A subcutaneous tumor model was used to evaluate the inhibitory effects of PD and CTX on the tumors *in vivo*. Briefly, 6-week-old male BALB/c nude mice were purchased from Beijing Hfkbio Co., Ltd (Beijing, China). HCT116 and LoVo cells were digested and washed twice with cold PBS to a final concentration of 2.5×10^7 cells/ml in cold PBS. A 200-μl cell suspension was injected subcutaneously into one side of the armpit area of nude mice. When the tumor reached a certain size (4–5 mm) after 7 days, the mice were randomly grouped into four groups: control, PD, CTX, and combined groups (five mice in each group). The mean tumor volume and body weight were well balanced between the groups. The control group received an

intraperitoneal injection of 200 µl normal saline every day; the CTX group was injected with 200 µl CTX (2 mg/kg); the PD group was intragastrically administered PD (20 mg/kg); and the combined group received PD plus CTX every day. The mice were sacrificed 14 days after dosing. Blood of mice in each group was collected from the retroorbital sinus for the measurement of serum biochemical indices. Tumors were removed from mice of the different treatment groups, and weight was measured using an electronic balance. All animal-related procedures were approved by the Animal Care and Use Committee of Tianjin Union Medical Center.

Detection of serum biochemical parameters

Blood samples were centrifuged at 4500× g and 4°C for 15 min to collect the serum. Then, the serum concentrations of alanine aminotransferase (ALT) and aspartate aminotransferase (AST) were detected using respective commercial test kits (Solarbio, Beijing, China), according to the manual instructions.

Immunohistochemical staining analysis

Tumor tissues were fixed in 10% buffered formalin. After 48 h of fixation, tissue samples were embedded in paraffin and sectioned into 4-µm-thick slices.

For immunohistochemical staining, tumor sections were dissolved in 10 mM sodium citrate solution (pH 6) after deparaffinization. Next, the samples were incubated overnight at 4°C with the primary antibody (dilution 1:200). The sections were then washed and incubated with a secondary antibody (dilution 1:100) for 2 h. The color was developed using DAB substrate kits. Images were captured using a Nikon microscope paired with the SPOT Advanced software (Diagnostic Instruments, Inc., MI, USA) (magnification, ×100). The ImageJ software was used to count the number of cells in each slice. Color deconvolution was used to determine positive/negative staining and was thresholded across all image samples.

TUNEL staining analysis

For TUNEL staining, tumor sections were stained with terminal deoxynucleotidyl transferase-mediated dUTP nick-end labeling (TUNEL) to detect apoptotic cells using the TUNEL Apoptosis Detection Kit-DAB according to the manufacturer's instructions. The slides were incubated with the TUNEL reaction cocktail and streptavidin-HRP reaction cocktail at 37°C separately for 2 h and 30 min in the dark and counterstained with DAB at 20°C for 30 min. Specimens were observed under a Nikon microscope (magnification, ×100). The TUNEL-positivity index was calculated by dividing the number of TUNEL-positive cells by the total number of cells.

Hematoxylin and eosin staining

The lung, liver, and kidney tissues of sacrificed mice were fixed with 10% buffered formalin. Following 48 h of fixation, the samples were embedded in paraffin and sectioned into 4-µm-thick slices. The sections were stained with hematoxylin solution for 15 min and incubated with eosin for 3 min. The tissue structure and cell morphology were observed under a light microscope (magnification, ×100).

Statistical analysis

All data are represented as the mean ± S.D. One-way analysis of variance was used to evaluate the significance of differences between different groups using the SPSS software (SPSS Inc., Chicago, IL, USA). *Statistical significance was set at $P < 0.05$.*

Results

Combined treatment with platycodin D increased the sensitivity of *KRAS*-mutant colorectal cancer cells to cetuximab

Figure 1 shows the cytotoxicity of PD and/or CTX treatment on *KRAS*-mutant (HCT116 and LoVo) CRC cell lines. The cells were treated with different concentrations of PD and/or CTX for 48 h, and their viability was assessed *via* the CCK-8 assay. The results shown in Figure 1A indicate that both CTX and PD exert considerable cytotoxicity to the two cell lines. The IC50 of PD on HCT116 and LoVo cells was 27.62 µM and 33.78 µM, respectively, whereas the IC50 of CTX on both cell lines was 46.57 µg/ml and 105.11 µg/ml, respectively. Furthermore, combination index (CI) analysis using the CalcuSyn software showed that the combination of CTX and PD had an obvious synergistic effect on HCT116 and LoVo cells (CI<1) (Figure 1B).

A colony formation assay was performed to evaluate the antiproliferative effect of PD in combination with CTX. HCT116 cells were treated with 5 µM PD and 10 µg/ml CTX, and LoVo cells were treated with 6 µM PD and 20 µg/ml CTX for 48 h. The results showed that these two drugs had only a slight inhibitory effect on the cells when used alone at the indicated concentrations, but the combination treatment significantly reduced cell viability (Figure 1C). Taken together, the results of CCK-8 and colony formation assays both showed that PD sensitized these two cell lines to CTX. Therefore, the two drugs were used at these concentrations in all subsequent *in vitro* experiments.

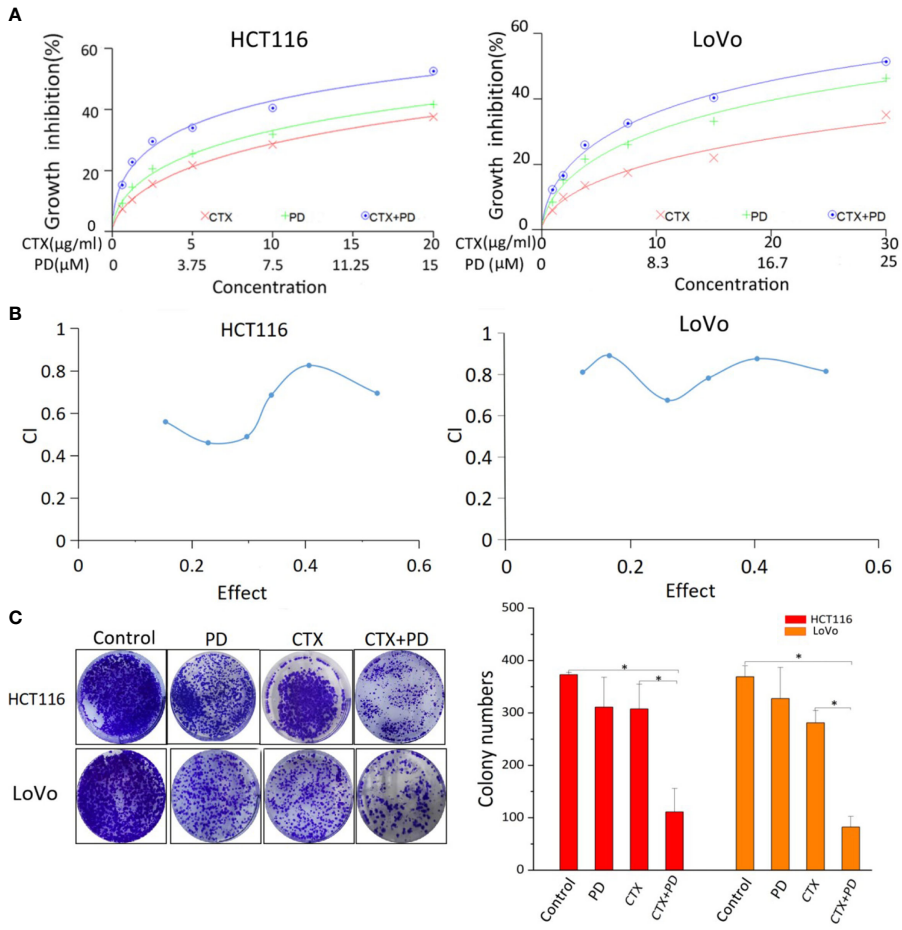

FIGURE 1
Results of CCK-8 and colony formation assays of PD- and CTX-treated cells. **(A)** The inhibitory effects of PD and/or CTX treatment in HCT116 and LoVo cells were examined by CCK-8 assay after treatment for 48 h. **(B)** The results of CCK-8 assay were analyzed with the CalcuSyn software. Combination Index (CI) was calculated by the Calcusyn software. CI < 1 was considered synergistic, CI = 1 additive, and CI > 1 antagonistic cytotoxicity. **(C)** The colony-formation assay was performed, and the results are displayed as colony numbers. Columns showed mean ± S.D. 'Control' was compared with the other groups, 'CTX' was compared with 'CTX+PD' using one-way ANOVA. *$P < 0.05$ represents a significant difference.

Platycodin D inhibits the PI3K/Akt signaling pathway in *KRAS*-mutant colorectal cancer cells with or without cetuximab treatment

It has been reported that p-Akt is upregulated or remains unchanged after CTX treatment in some CTX-resistant cancer cells, and some drug treatments inhibit p-Akt to sensitize these cells to CTX (1, 21). PD was found to inhibit the PI3K/Akt signaling pathway and the proliferation and migration of other types of cancer cells (16). The PI3K/Akt signaling pathway is known to play an important role in the occurrence and drug resistance of cancer. Therefore, we investigated whether PD could enhance the sensitivity of *KRAS*-mutant CRC cells to CTX by acting on the PI3K/Akt signaling pathway. Western blotting analysis (Figure 2) indicated that CTX did not effectively decrease the phosphorylation levels of PI3K and Akt. PI3K and Akt phosphorylation in cells was significantly suppressed by a single treatment with PD or combined treatment with PD and CTX. However, there was little change in the total levels of PI3K and Akt. To further determine the role of PI3K/Akt inhibition by PD in CTX resistance, experiments were performed using LY294002 (10 μM, 48 h), a selective inhibitor specific for this signaling pathway, and SC-79 (4 μg/ml, 48 h), an Akt phosphorylation activator. These two regulators did not have detectable inhibitory effects on cells at this concentration, as confirmed by the CCK-8 assay (data not shown).

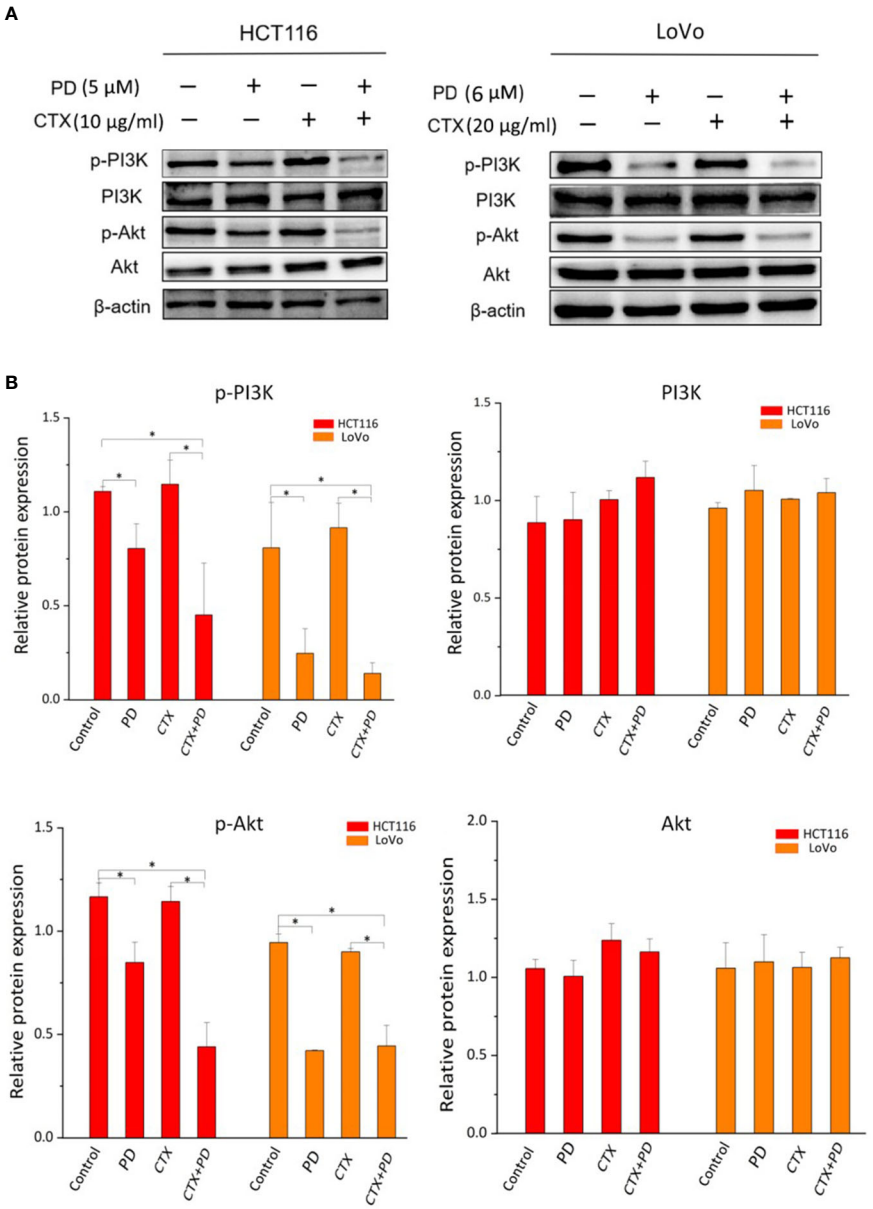

FIGURE 2
Western blotting analysis of PI3K and Akt in PD- and CTX-treated cells. **(A)** Western blot images. The left column shows protein names, including p-PI3K, PI3K, p-Akt, Akt, and β-actin, which was used as loading control. The top row shows two cell lines HCT116 and LoVo, and drug treatment with different combinations. **(B)** Bar plots of densitometric analysis. Protein expression levels are normalized to that of the loading control. Columns show the mean ± S.D. One-way ANOVA was used to analyze *P* values between groups. All groups are compared with the 'Control' group, the 'CTX' group is compared with the 'CTX+PD' group. **P* < 0.05 represents a significant difference.

Figure 3 shows that LY294002 decreased the phosphorylation levels of PI3K and Akt when administered alone or in combination with CTX. The combination treatment of PD and SC-79 did not decrease p-Akt effectively, suggesting that SC-79 rescued the inhibitory effect of p-Akt by PD. These results indicate that these two Akt regulators can be used to further investigate the influence of PD-induced Akt inhibition caused by PD on CTX resistance.

Akt regulators affect cetuximab resistance

The CCK-8 assay was used to investigate the effect of PI3K/Akt signaling on CTX resistance and the synergistic effects of PD and CTX. Figure 4A shows that CTX-induced cell growth inhibition was enhanced by the PI3K selective inhibitor

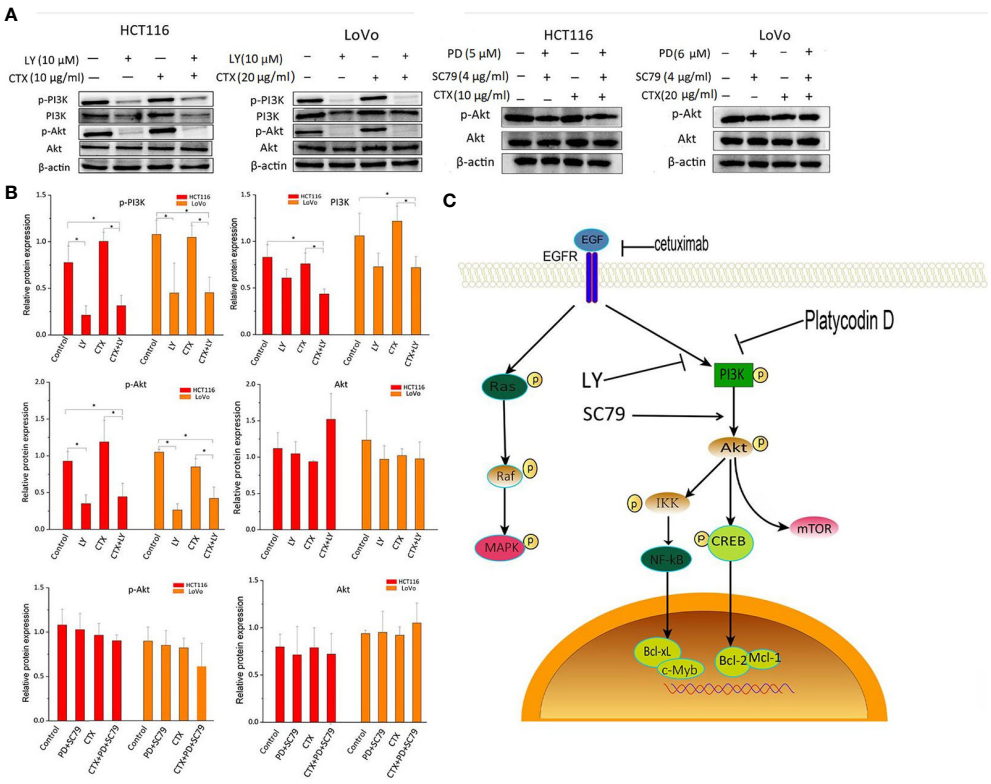

FIGURE 3
Western blot analysis of PI3K and Akt in cells treated with LY294002 and SC-79. **(A)** Western blot images. The left column shows protein names, including p-PI3K, PI3K, p-Akt, Akt, and β-actin, which was used as loading control. The top row shows two cell lines HCT116 and LoVo, and drug treatment with different combinations. 'LY' represents LY294002. **(B)** Bar plots of densitometric analysis. Protein expression levels are normalized to that of the loading control. Columns show the mean ± S.D. One-way ANOVA was used to analyze *P* values between groups. All groups are compared with the 'Control' group, the 'CTX' group is compared with the 'CTX+LY' or 'CTX+PD+SC79' group. $*P < 0.05$ represents a significant difference. **(C)** The signaling pathway by which PD enhances the cytotoxicity of CTX. A PI3K inhibitor and an Akt activator were used to confirm the inhibitory effect of PD on PI3K.

LY294002, which suggests that Akt inhibition is a critical factor in CTX sensitization. In addition, when the Akt activator SC-79 was used to offset Akt inhibition by PD, the synergistic effect between PD and CTX was lost (Figures 4B, C). The results of the colony formation assay (Figure 4D) also showed that LY294002 further inhibited the growth of cells treated with CTX, and when Akt inhibition by PD was offset by SC-79, the cell growth-inhibitory effect of PD and CTX combination decreased.

Platycodin D and Cetuximab both inhibit the migration and invasive abilities of *KRAS*-mutant colorectal cancer cells

The PI3K/Akt signaling pathway contributes to the migration and invasion abilities of cancer cells during CTX treatment, and inhibition of p-Akt reduces cancer cell migration and invasion (22, 23). Considering our finding that PD inhibited p-Akt, scratch wound healing, and cell invasion assays were conducted to investigate the effects of PD and CTX treatment on the migration and invasion abilities of cancer cells, respectively. Figure 5 shows that low concentrations of PD and CTX significantly decreased cancer cell migration and invasion, and the combination of these two drugs further decreased cancer cell migration and invasion.

Combinative treatment with platycodin D and cetuximab exerted the strongest inhibition of tumorigenicity in *KRAS*-mutant colorectal cancer cells *in vivo*

A subcutaneous tumor model of HCT116 and LoVo cells in BALB/c nude mice was used to investigate the therapeutic efficacy of the combination treatment of PD and CTX *in vivo*. As shown in Figure 6, according to the comparison of the tumor weight, CTX treatment exerted considerable inhibitory effect on HCT116 and LoVo tumor growth. PD treatment only inhibited

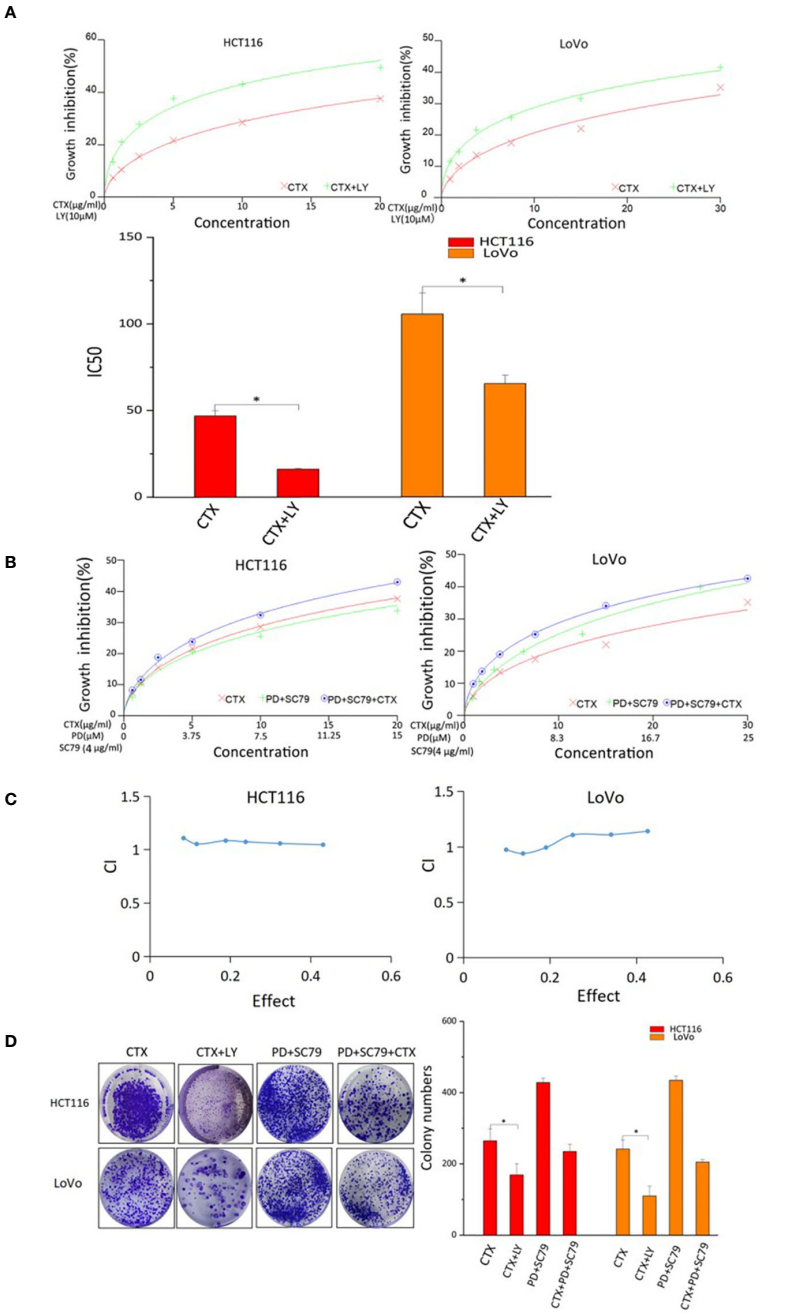

FIGURE 4
CCK-8 and colony-formation assay results of cells treated with PD, CTX, and Akt regulators. **(A)** The inhibitory effects of CTX and LY294002 treatment in HCT116 and LoVo cells were examined by CCK-8 assay after treatment for 48 h. 'LY' represents LY294002. The inhibitory effect of 'CTX+LY' is significantly higher than that of 'CTX' at all concentrations, as determined by one-way ANOVA ($P<0.05$). **(B)** SC79 (4 μg/ml) was administered concomitantly with PD. The inhibitory effects of PD+SC79 and/or CTX treatment in HCT116 and LoVo cells were examined by CCK-8 assay after treatment for 48 h. **(C)** The CCK-8 assay results of PD+SC79 and/or CTX treatment were analyzed with the CalcuSyn software. Combination Index (CI) was calculated by the Calcusyn software. CI < 1 was considered synergistic, CI = 1 Tadditive, and CI > 1 antagonistic cytotoxicity. **(D)** The colony-formation assay was performed, and the results are displayed as colony numbers in the column diagram. HCT116 cells were treated with 5 μM PD and 10 μg/ml CTX, whereas LoVo cells were treated with 6 μM PD and 20 μg/ml CTX. Cells were treated with 4 μg/ml SC-79 and 10 μM LY294002. 'LY' represents LY294002. Columns showed mean ± S.D. 'CTX' was compared with 'CTX+LY' or 'CTX+PD+SC79' using one-way ANOVA. *$P < 0.05$ represents a significant difference.

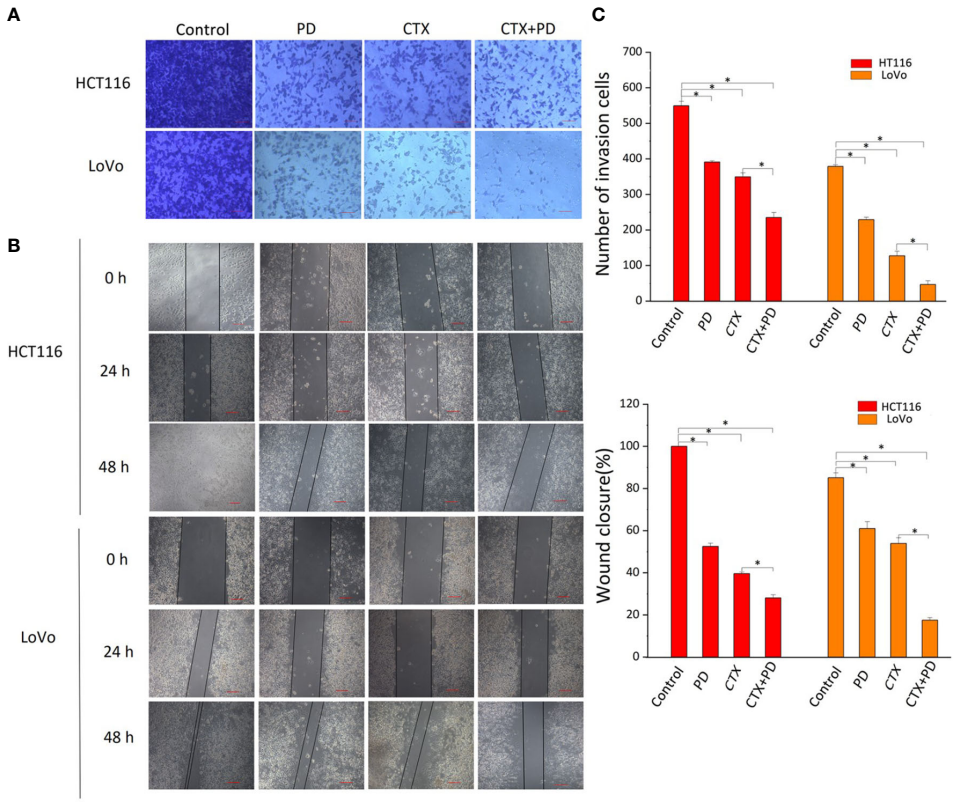

FIGURE 5
Results of Transwell and scratch wound-healing assays. **(A)** Invasion of HCT116 and LoVo cells were both measured by Transwell assay. The top row shows various drug treatments. Scale bars, 100 μm. **(B)** Migration of HCT116 and LoVo cells were both measured by scratch wound-healing assay. The top row shows various drug treatments. The left column shows the type of cells and time of measurement. **(C)** Bar diagrams of Transwell (C1) and scratch wound-healing (C2) assays. Columns show the mean ± S.D. One-way ANOVA was conducted to analyze *P* values between groups. All groups are compared with the 'Control' group, and the 'CTX' group is compared with the 'CTX+PD' group. **P* < 0.05 represents a significant difference.

tumor growth in HCT116 cells at the statistical level. The combination of PD and CTX showed the strongest inhibitory effect among all treatments. These *in vivo* results indicated a synergistic effect of PD and CTX, similar to the *in vitro* results. Survival curves showed that all mice ultimately died owing to tumor burden. Single treatment with PD or CTX prolonged survival time compared with the control, and the combination treatment further increased survival time.

Combination treatment of cetuximab and platycodin D decreased proliferation and enhance apoptosis *via* PI3K/Akt inhibition *in vivo*

To further investigate the mechanism by which PD sensitized CTX, we examined the expression of a cell proliferation marker (Ki-67) and the rate of apoptosis in tumor tissues from each group, as shown in Figure 7. Compared with that in the control groups, Ki67 expression was decreased in the CTX group, but not in the PD group, and the combination treatment further decreased the expression level of Ki67 (Figure 7A, Ki67 panels). To further analyze the effects of CTX and PD on tumor apoptosis, a TUNEL assay was performed on tumor samples. Histopathological staining revealed massive necrotic sheets in the combination treatment group, compared with the control group. The results of this experiment indicated a significant increase in apoptosis following the combination treatment, compared with that after single CTX treatment (Figure 7A, TUNEL assay panels). Furthermore, PD alone did not induce obvious tumor apoptosis. Collectively, the series of experiments revealed that the combination of CTX and PD effectively decreased tumor growth by decreasing cell proliferation (Ki67) and increasing cell death (apoptosis) in *KRAS*-mutant CRC cell lines.

Next, we detected the expression of p-PI3K and p-Akt using immunohistochemical staining. As shown in Figure 8, the lowest expression of p-PI3K and p-Akt was found in HCT116 and LoVo subcutaneous tumors in the combination treatment group; moreover, PD treatment also significantly decreased these two phosphorylated proteins, but CTX treatment did not. These results indicated that CTX did not inhibit the PI3K/Akt signaling pathway in HCT116 and LoVo subcutaneous tumor Balb/c mouse models, and co-treatment with PD compensated for this deficiency of CTX treatment. This mechanism explains how PD sensitizes these subcutaneous tumors to CTX.

Platycodin D decreases cetuximab-induced liver damage *in vivo*

Tissue damage in the lung, liver, and kidney were analyzed by hematoxylin and eosin staining, as shown in Figure 9. The results indicated that PD and CTX did not exert obvious damaging effects on the lung and kidney. Furthermore, CTX decreased the number and vessel diameter of central veins in the hepatic lobules when administered alone, but these effects were reduced when CTX was administered in combination with PD (Figure 9B). We next investigated the serum biochemical indicators in mice. The findings revealed that the concentration of serum AST and ALT in the CTX group were increased compared with the normal group. In the combination treatment group, serum levels of AST and ALT were significantly decreased compared with the CTX group (Figure 9C). These data suggested that PD effectively suppressed the activities of liver functional enzymes increased by CTX in mice.

Discussion

It is estimated that approximately 30–40% of CRC patients have *KRAS* mutation (24). Owing to *KRAS* mutations, many patients do not benefit from CTX therapy. Inhibition of Akt/PI3K, another downstream signaling pathway of EGFR, is a strategy to overcome resistance to CTX (25). Our results showed that PD reduced the CTX resistance of two *KRAS*-mutant CRC cell lines, HCT116 and LoVo. PD significantly increased the cytotoxicity of CTX when administered at a low concentrations, which only had a slight inhibitory effect on cells. Further

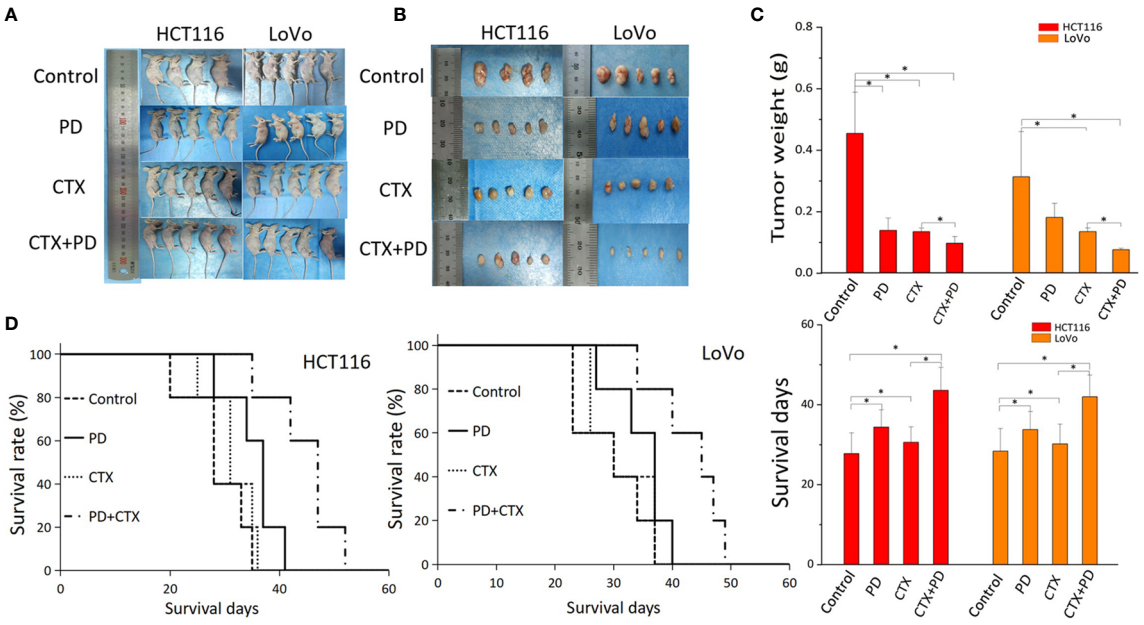

FIGURE 6
The antitumor efficacy of co-treatment with PD and CTX in subcutaneous tumor models. **(A)** Subcutaneous tumor models of HCT116 and LoVo cells were collected after the mice were sacrificed. Each group contained five mice, but one mouse of the HCT116 control group died during the experiment. **(B)** After sacrifice, subcutaneous tumors were removed and photographed. **(C)** Tumor weight was measured using an electronic balance. The mean ± S.D. is shown. One-way ANOVA was performed used to analyze P values between groups. All groups are compared with the 'control' group, the 'CTX' group is compared with the 'CTX+PD' group. *P < 0.05 represents a significant difference. **(D)** Survival curves of each group. Survival days of other groups are compared with those of the control group; the 'CTX' group is compared with the 'CTX+PD' group. *P<0.05 represents a significant difference.

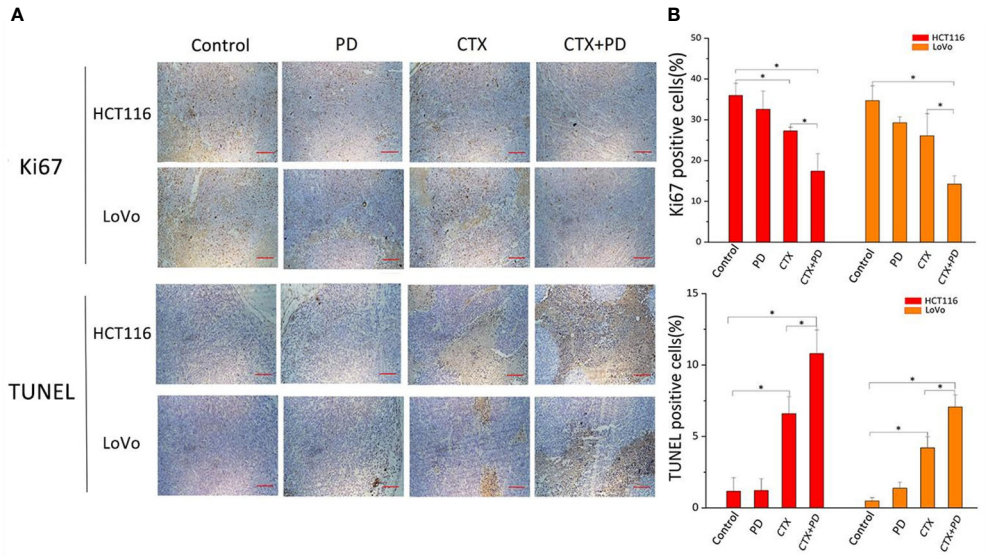

FIGURE 7
Combination treatment of CTX and PD decreases proliferation and enhance apoptosis *in vivo*. **(A)** Images of Ki67 immunohistochemical analysis and TUNEL staining assay in subcutaneous tumor models. Scale bars, 100 μm. **(B)** Quantitation of positive immunohistochemical staining for Ki67 and TUNEL staining in every group. Graph of percentage of positive cells for Ki67 and TUNEL staining (three random fields). ImageJ was used to quantify positive immunohistochemical staining results (n=3). Data are shown as the mean ± S.D. One-way ANOVA was used to analyze *P* values between groups. All groups are compared with the 'Control' group, and the 'CTX' group is compared with the 'CTX+PD' group. **P* < 0.05 represents a significant difference.

experiments showed that Akt was not effectively inhibited by CTX in *KRAS*-mutant CRC cells, but was inhibited by PD. Therefore, two Akt regulators, LY294002 and SC79, were used to investigate whether PD could enhance CTX efficacy through Akt inhibition. As an Akt inhibitor, LY294002 was combined with CTX to determine whether Akt inhibition increased CTX efficacy. The results indicated that LY294002 enhanced CTX efficacy similar to that of PD. SC-79 is an Akt activator, and western blotting results showed that SC-79 treatment rescued Akt inhibition by PD. Therefore, the synergistic effect of SC-79 and PD combination (PD+SC-79) with CTX was evaluated by CCK-8 and colony formation assays. CI calculation indicated that although the combination treatment had the highest growth inhibition effect, PD+SC-79 had no synergistic effect with CTX. *In vitro* experiments showed that the inhibitory effect of CTX on cancer cell proliferation, migration, and invasion was negatively correlated with p-Akt levels. This implies that some downstream components of Akt that are related to migration and invasion, such as mTOR (26)or Glycogen Synthase Kinase 3β (GSK3β)/Snail (27), may be inhibited by PD. In addition, CTX itself decreases CRC cell migration and invasion to a certain degree, which may interfere with other downstream pathways of EGF/EGFR (28).

PD is a triterpenoid saponin present in the roots of *P. grandiflorum*. Increasing evidence suggests that PD has a wide spectrum of antitumor activity, exhibiting significant growth inhibitory effects and strong cytotoxicity against various cancers (29–33). Our *in vitro* and *in vivo* experiments also showed that PD exerted an antitumor effect on *KRAS*-mutant CRC cells. PD has different regulatory effects on p-Akt in various tissue types (17–20), and our *in vitro* results confirmed that low concentration of PD (about 0.2 IC50) inhibited p-Akt in *KRAS*-mutant CRC cells. This suggests that PD with low cytotoxicity can be used as an auxiliary agent to enhance CTX efficacy. *In vivo* experiments using a subcutaneous tumor model also showed that PD with a low toxic concentration had an inhibitory effect on p-Akt. The proliferation inhibition and apoptosis promotion effects were not obvious with PD treatment alone, but PD co-treatment significantly enhanced the therapeutic efficacy of CTX in subcutaneous tumors. In addition, PD had no obvious damaging effects on the lungs, liver, and kidneys of these mice, and reduced the liver damage caused by CTX treatment.

Akt inhibition contributes to antitumor effects and enhances the efficacy of antitumor drugs; therefore, many strategies involving Akt inhibition have been developed to inhibit tumor proliferation and overcome drug resistance (34, 35). In addition to acting on the Ras/Raf/MAPK pathway, CTX can exert an antitumor effect if the PI3K/Akt pathway is effectively inhibited. However, in addition to EGF/EGFR, other upstream molecules, such as integrin (36)and G protein-coupled receptor (GPCR) (37), also regulate the PI3K/Akt pathway. Therefore, the PI3K/

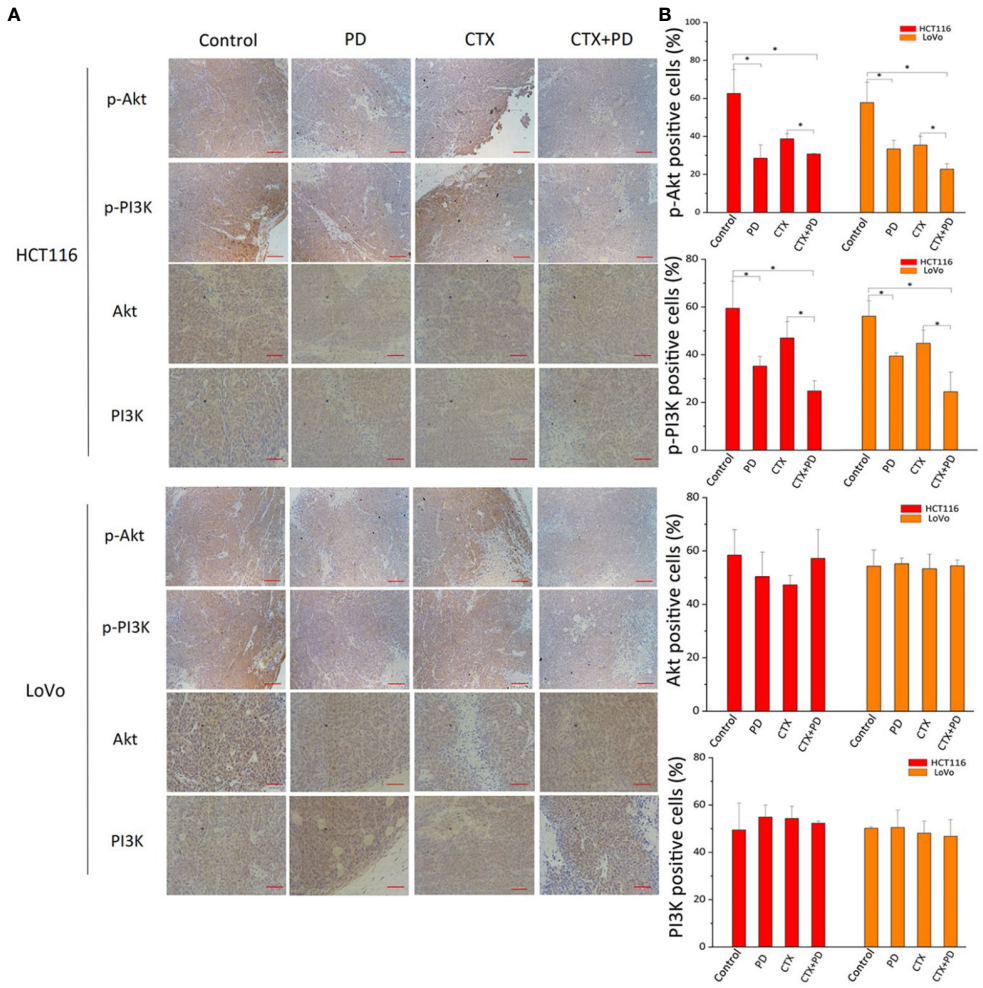

FIGURE 8
Immunohistochemical analysis of PI3K and Akt in tumor tissues treated with PD and/or CTX. **(A)** Images of immunohistochemically stained tissues. The left column shows proteins in each tumor type. The top row shows drug treatments with different combinations. Scale bars, 100 μm. **(B)** Quantitation of positive staining for p-Akt, p-PI3K, Akt, and PI3K in every group. Graph of percentage of positive cells for immunohistochemical staining (three random fields). ImageJ was used to quantify the positive immunohistochemical staining results (n=3). Data are shown as the mean ± S.D. One-way ANOVA was used to analyze *P* values between groups. All groups are compared with the 'Control' group, and the 'CTX' group is compared with the 'CTX+PD' group. **P* < 0.05 represents a significant difference.

Akt pathway may be activated by other upstream molecules owing to the feedback mechanism that occurs when EGF/EGFR is blocked by CTX. Our results showed that CTX did not effectively inhibit the PI3K/Akt pathway in *KRAS*-mutant CRC cells and that it was significantly inhibited by combination treatment with PD and CTX. This effect suggests that PD inhibited PI3K/Akt independent of EGF/EGFR to a certain degree. Therefore, the combination treatment showed tumor suppression through Akt inhibition, even in *KRAS*-mutant CRC cells.

In addition to the inhibition of downstream pathways of EGFR, CTX has other antitumor effects. For example, the interaction between CTX and the tumor microenvironment is an important factor for its therapeutic efficacy. CTX is a monoclonal antibody containing a human IgG Fc fragment. CTX triggers antibody-dependent cell-mediated cytotoxicity through Fcγ receptors in immunologic effector cells (38). Therefore, effective inhibition of Akt through combination with PD can help CTX to block the downstream pathways of EGFR, although CTX still has other antitumor effects. The combination treatment of PD and CTX may be a potential therapy for *patients with KRAS*-mutant CRC.

In this study, the potential role of PD in the sensitivity of *KRAS*-mutant CRC cells to CTX treatment was evaluated. *In vitro* and *in vivo* experimental results confirmed that PD enhanced the sensitivity of HCT116 and LoVo cells to CTX

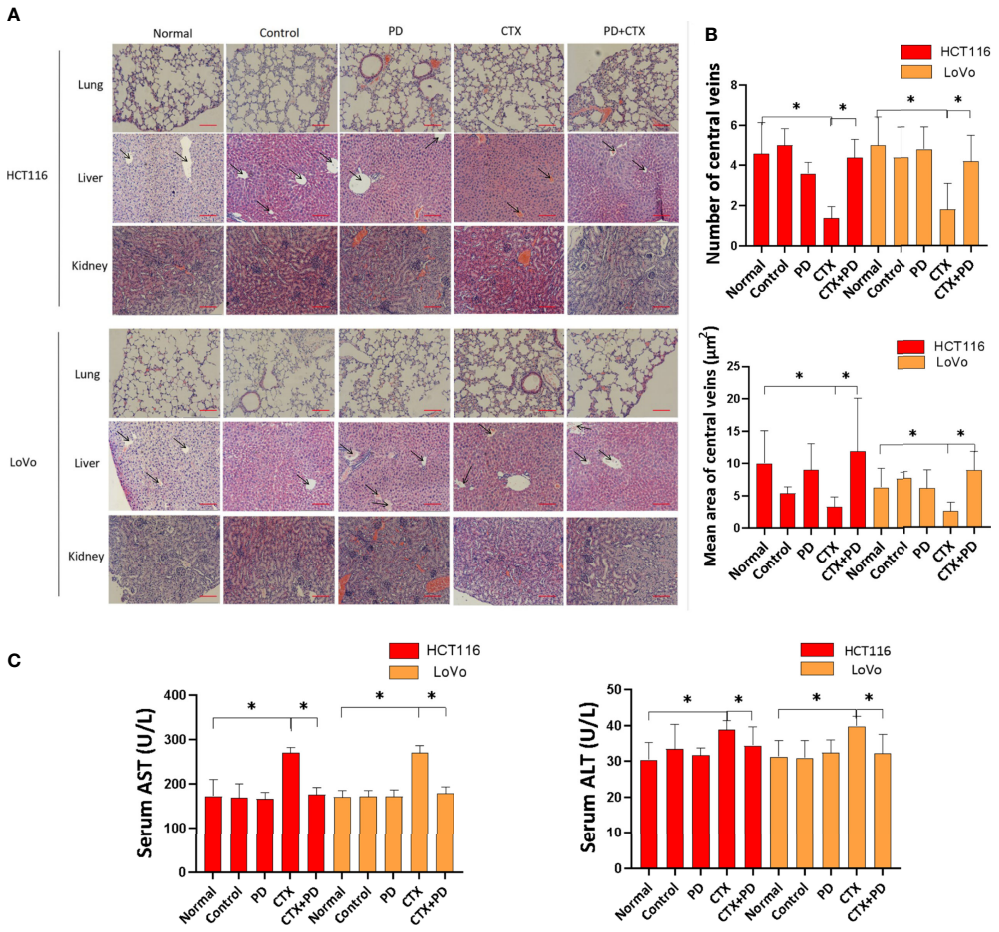

FIGURE 9
Hematoxylin and eosin staining assay of the lung, liver, and kidney. **(A)** Images of hematoxylin and eosin stained tissues. The left column shows cell types of subcutaneous tumor and types of stained tissue. The top line shows drug treatments, where 'Normal' represents healthy mice, and 'Control' represents tumor-burdened mice without drug treatment. Scale bars, 100 μm. **(B)** Quantitation of the number and vessel area of central veins in the hepatic lobules in every group. ImageJ was used to quantify the vessel diameter of central veins. Five pictures of the liver used in the column diagram were added as Figure S3 in Supplementary Materials. **(C)** Concentrations of serum AST and ALT were determined in mice in different groups. Data are shown as the mean ± S.D. One-way ANOVA was used to analyze *P* values between groups. All groups are compared with the 'Normal' group, and the 'CTX' group is compared with the 'CTX+PD' group. $^*P < 0.05$ represents a significant difference.

through PI3K/Akt inhibition. Our results showed that PD inhibited PI3K and Akt phosphorylation in these cells, but did not affect the expression levels of these two proteins. This conclusion will hopefully provide a prospective therapeutic strategy for patients with CRC with *KRAS* mutations.

Data availability statement

The original contributions presented in the study are included in the article/Supplementary Material. Further inquiries can be directed to the corresponding authors.

Ethics statement

The animal study was reviewed and approved by Animal Care and Use Committee of Tianjin Union Medical Center.

Author contributions

YW, SZ, and CZ conceived and designed the experiment. YL, ST, BY, ZF, TC, and JL performed the experiments. YL and YW wrote the paper. YW, SZ, and CZ reviewed the manuscript. All authors contributed to the article and approved the submitted version.

Funding

This work was partially supported by the Natural Science Foundation of China Grant number 81972826 and 12174203, Natural Science Foundation of Tianjin, 21JCYBJC00180, Key R&D Projects in the Tianjin Science and Technology Pillar Program, 19YFZCSY00420, and Tianjin Key Medical Discipline (Specialty) Construction Project (NO: TJYXZDXK-044A).

Conflict of interest

The authors declare that the research was conducted in the absence of any commercial or financial relationships that could be construed as a potential conflict of interest.

Publisher's note

Supplementary material

The Supplementary Material for this article can be found online at: https://www.frontiersin.org/articles/10.3389/fonc.2022.1046143/full#supplementary-material

References

1. Takata M, Chikumi H, Miyake N, Adachi K, Kanamori Y, Yamasaki A, et al. Lack of AKT activation in lung cancer cells with EGFR mutation is a novel marker of cetuximab sensitivity. *Cancer Biol Ther* (2012) 13(6):369–78. doi: 10.4161/cbt.19238

2. Vincenzi B, Schiavon G, Silletta M, Silletta M, Santini D, Tonini G. The biological properties of cetuximab. *Crit Rev Oncol Hematol* (2008) 68(2):93–106. doi: 10.1016/j.critrevonc.2008.07.006

3. Chen P, Li X, Zhang R, Liu S, Xiang Y, Zhang M, et al. Combinative treatment of beta-elemene and cetuximab is sensitive to KRAS mutant colorectal cancer cells by inducing ferroptosis and inhibiting epithelial-mesenchymal transformation. *Theranostics* (2020) 10(11):5107–19. doi: 10.7150/thno.44705

4. Serebriiskii IG, Connelly C, Frampton G, Newberg J, Cooke M, Miller V, et al. Comprehensive characterization of RAS mutations in colon and rectal cancers in old and young patients. *Nat Commun* (2019) 10(1):3722. doi: 10.1038/s41467-019-11530-0

5. Wang Y, Wang W, Wu X, Li C, Huang Y, Zhou H, et al. Resveratrol sensitizes colorectal cancer cells to cetuximab by connexin 43 upregulation-induced akt inhibition. *Front Oncol* (2020) 10:383. doi: 10.3389/fonc.2020.00383

6. Frattini M, Saletti P, Romagnani E, Martin V, Molinari F, Ghisletta M, et al. PTEN loss of expression predicts cetuximab efficacy in metastatic colorectal cancer patients. *Br J Cancer* (2007) 97(8):1139–45. doi: 10.1038/sj.bjc.6604009

7. Xie Y, Deng W, Sun H, Li D. Platycodin D2 is a potential less hemolytic saponin adjuvant eliciting Th1 and Th2 immune responses. *Int Immunopharmacol* (2008) 8(8):1143–50. doi: 10.1016/j.intimp.2008.04.006

8. Ahn KS, Noh EJ, Zhao HL, Jung SH, Kang SS, Kim YS. Inhibition of inducible nitric oxide synthase and cyclooxygenase II by platycodon grandiflorum saponins *via* suppression of nuclear factor-kappaB activation in RAW 264.7 cells. *Life Sci* (2005) 76(20):2315–28. doi: 10.1016/j.lfs.2004.10.042

9. Lee H, Kang R, Kim YS, Chung SI, Yoon Y. Platycodin d inhibits adipogenesis of 3T3-L1 cells by modulating kruppel-like factor 2 and peroxisome proliferator-activated receptor gamma. *Phytother Res* (2010) 24 Suppl 2:S161–7. doi: 10.1002/ptr.3054

10. Wu J, Yang G, Zhu W, Wen W, Zhang F, Yuan J, et al. Anti-atherosclerotic activity of platycodin d derived from roots of platycodon grandiflorum in human endothelial cells. *Biol Pharm Bull* (2012) 35(8):1216–21. doi: 10.1248/bpb.b-y110129

11. Chun J, Joo EJ, Kang M, Kim YS. Platycodin d induces anoikis and caspase-mediated apoptosis *via* p38 MAPK in AGS human gastric cancer cells. *J Cell Biochem* (2013) 114(2):456–70. doi: 10.1002/jcb.24386

12. Kim MO, Moon DO, Choi YH, Lee JD, Kim ND, Kim GY. Platycodin d induces mitotic arrest *in vitro*, leading to endoreduplication, inhibition of proliferation and apoptosis in leukemia cells. *Int J Cancer* (2008) 122(12):2674–81. doi: 10.1002/ijc.23442

13. Qin H, Du X, Zhang Y, Wang R. Platycodin d, a triterpenoid saponin from platycodon grandiflorum, induces G2/M arrest and apoptosis in human hepatoma HepG2 cells by modulating the PI3K/Akt pathway. *Tumour Biol* (2014) 35(2):1267–74. doi: 10.1007/s13277-013-1169-1

14. Tang ZH, Li T, Gao HW, Sun W, Chen XP, Wang YT, et al. Platycodin d from platycodonis radix enhances the anti-proliferative effects of doxorubicin on breast cancer MCF-7 and MDA-MB-231 cells. *Chin Med* (2014) 9:16. doi: 10.1186/1749-8546-9-16

15. Li T, Xu XH, Tang Z H, Wang YF, Leung CH, Ma DL, et al. Platycodin d induces apoptosis and triggers ERK- and JNK-mediated autophagy in human hepatocellular carcinoma BEL-7402 cells. *Acta Pharmacol Sin* (2015) 36(12):1503–13. doi: 10.1038/aps.2015.99

16. Xu C, Sun G, Yuan G, Wang R, Sun X. Effects of platycodin d on proliferation, apoptosis and PI3K/Akt signal pathway of human glioma U251 cells. *Molecules* (2014) 19(12):21411–23. doi: 10.3390/molecules191221411

17. Zhao R, Chen M, Jiang Z, Zhao F, Xi B, Zhang X, et al. Platycodin-d induced autophagy in non-small cell lung cancer cells *via* PI3K/Akt/mTOR and MAPK signaling pathways. *J Cancer* (2015) 6(7):623–31. doi: 10.7150/jca.11291

18. Chun J, Kim YS. Platycodin d inhibits migration, invasion, and growth of MDA-MB-231 human breast cancer cells *via* suppression of EGFR-mediated akt and MAPK pathways. *Chem Biol Interact* (2013) 205(3):212–21. doi: 10.1016/j.cbi.2013.07.002

19. Lu Z, Song W, Zhang Y, Wu C, Zhu M, Wang H, et al. Combined anti-cancer effects of platycodin d and sorafenib on androgen-independent and PTEN-deficient prostate cancer. *Front Oncol* (2021) 11:648985. doi: 10.3389/fonc.2021.648985

20. Hu JN, Leng J, Shen Q, Liu Y, Li XD, Wang SH, et al. Platycodin d suppresses cisplatin-induced cytotoxicity by suppressing ROS-mediated oxidative damage, apoptosis, and inflammation in HEK-293 cells. *J Biochem Mol Toxicol* (2021) 35(1):e22624. doi: 10.1002/jbt.22624

21. D'Amato V, Rosa R, D'Amato C, Formisano L, Marciano R, Nappi L, et al. The dual PI3K/mTOR inhibitor PKI-587 enhances sensitivity to cetuximab in EGFR-resistant human head and neck cancer models. *Br J Cancer* (2014) 110(12):2887–95. doi: 10.1038/bjc.2014.241

22. Shimizu R, Ibaragi S, Eguchi T, Kuwajima D, Kodama S, Nishioka T, et al. Nicotine promotes lymph node metastasis and cetuximab resistance in head and neck squamous cell carcinoma. *Int J Oncol* (2019) 54(1):283–94. doi: 10.3892/ijo.2018.4631

23. Lu H, Zhang H, Weng ML, Zhang J, Jiang N, Cata JP, et al. Morphine promotes tumorigenesis and cetuximab resistance *via* EGFR signaling activation in human colorectal cancer. *J Cell Physiol* (2021) 236(6):4445–54. doi: 10.1002/jcp.30161

24. Dunn EF, Iida M, Myers RA, Campbell DA, Hintz KA, Armstrong EA, et al. Dasatinib sensitizes KRAS mutant colorectal tumors to cetuximab. *Oncogene* (2011) 30(5):561–74. doi: 10.1038/onc.2010.430

25. Zaryouh H, De Pauw I, Baysal H, Pauwels P, Peeters M, Vermorken JB, et al. The role of akt in acquired cetuximab resistant head and neck squamous cell

carcinoma: An *In vitro* study on a novel combination strategy. *Front Oncol* (2021) 11:697967. doi: 10.3389/fonc.2021.697967

26. Gao H, Wang W, Li Q. GANT61 suppresses cell survival, invasion and epithelial-mesenchymal transition through inactivating AKT/mTOR and JAK/STAT3 pathways in anaplastic thyroid carcinoma. *Cancer Biol Ther* (2022) 23 (1):369–77. doi: 10.1080/15384047.2022.2051158

27. Hu Y, Bai J, Zhou D, Zhang L, Chen X, Chen L, et al. The miR-4732-5p/XPR1 axis suppresses the invasion, metastasis, and epithelial-mesenchymal transition of lung adenocarcinoma *via* the PI3K/Akt/GSK3β/Snail pathway. *Mol Omics* (2022) 18(5):417–29. doi: 10.1039/d1mo00245g

28. Quadri M, Comitato A, Palazzo E, Tiso N, Rentsch A, Pellacani G, et al. Activation of cGMP-dependent protein kinase restricts melanoma growth and invasion by interfering with the EGF/EGFR pathway. *J Invest Dermatol* (2022) 142 (1):201–11. doi: 10.1016/j.jid.2021.06.011

29. Zhang X, Zhai T, Hei Z, Zhou D, Jin L, Han C, et al. Effects of platycodin d on apoptosis, migration, invasion and cell cycle arrest of gallbladder cancer cells. *Oncol Lett* (2020) 20(6):311. doi: 10.3892/ol.2020.12174

30. Hsu WC, Ramesh S, Shibu MA, Chen MC, Wang TF, Day CH, et al. Platycodin d reverses histone deacetylase inhibitor resistance in hepatocellular carcinoma cells by repressing ERK1/2-mediated cofilin-1 phosphorylation. *Phytomedicine* (2021) 82:153442. doi: 10.1016/j.phymed.2020.153442

31. Zhang Z, Zhao M, Zheng W, Liu Y, Platycodin D. A triterpenoid saponin from platycodon grandiflorum, suppresses the growth and invasion of human oral squamous cell carcinoma cells *via* the NF-kappaB pathway. *J Biochem Mol Toxicol* (2017) 31(9):e21934. doi: 10.1002/jbt.21934

32. Ye Y, Han X, Guo B, Sun Z, Liu S. Combination treatment with platycodin d and osthole inhibits cell proliferation and invasion in mammary carcinoma cell lines. *Environ Toxicol Pharmacol* (2013) 36(1):115–24. doi: 10.1016/j.etap.2013.03.012

33. Chen D, Chen T, Guo Y, Wang C, Dong L, Lu C. Suppressive effect of platycodin d on bladder cancer through microRNA-129-5p-mediated PABPC1/PI3K/AKT axis inactivation. *Braz J Med Biol Res* (2021) 54(3):e10222. doi: 10.1590/1414-431X202010222

34. Yin J, Lang T, Cun D, Zheng Z, Huang Y, Yin Q, et al. pH-sensitive nano-complexes overcome drug resistance and inhibit metastasis of breast cancer by silencing akt expression. *Theranostics* (2017) 7(17):4204–16. doi: 10.7150/thno.21516

35. Xie Z, Li W, Ai J, Xie J, Zhang X. C2orf40 inhibits metastasis and regulates chemo-resistance and radio-resistance of nasopharyngeal carcinoma cells by influencing cell cycle and activating the PI3K/AKT/mTOR signaling pathway. *J Transl Med* (2022) 20(1):264. doi: 10.1186/s12967-022-03446-z

36. Sheta M, Hassan G, Afify SM, Monzur S, Kumon K, Abu Quora HA, et al. Chronic exposure to FGF2 converts iPSCs into cancer stem cells with an enhanced integrin/focal adhesion/PI3K/AKT axis. *Cancer Lett* (2021) 521:142–54. doi: 10.1016/j.canlet.2021.08.026

37. Hao F, Xu Q, Zhao Y, Stevens JV, Young SH, Sinnett-Smith J, et al. Insulin receptor and GPCR crosstalk stimulates YAP *via* PI3K and PKD in pancreatic cancer cells. *Mol Cancer Res* (2017) 15(7):929–41. doi: 10.1158/1541-7786

38. Zhou J, Ji Q, Li Q. Resistance to anti-EGFR therapies in metastatic colorectal cancer: underlying mechanisms and reversal strategies. *J Of Exp Clin Cancer Res* (2021) 40(1):328. doi: 10.1186/s13046-021-02130-2

frontiers | Frontiers in Oncology

TYPE Original Research
PUBLISHED 16 December 2022
DOI 10.3389/fonc.2022.1087778

OPEN ACCESS

EDITED BY
Veronika Vymetalkova,
Academy of Sciences of the Czech Republic (ASCR), Czechia

REVIEWED BY
Beatrice Mohelnikova-Duchonova,
Palacký University, Czechia
Ludmila Boublikova,
Charles University, Czechia
Stanislav Filip,
Charles University, Czechia

*CORRESPONDENCE
Ching-Chieh Yang
cleanclear0905@gmail.com

†These authors have contributed equally to this work

SPECIALTY SECTION
This article was submitted to Gastrointestinal Cancers: Colorectal Cancer, a section of the journal Frontiers in Oncology

RECEIVED 11 November 2022
ACCEPTED 01 December 2022
PUBLISHED 16 December 2022

CITATION
Kuo Y-H, Lin Y-T, Ho C-H, Chou C-L, Cheng L-C, Tsai C-J, Hong W-J, Chen Y-C and Yang C-C (2022) Adjuvant chemotherapy and survival outcomes in rectal cancer patients with good response (ypT0-2N0) after neoadjuvant chemoradiotherapy and surgery: A retrospective nationwide analysis.
Front. Oncol. 12:1087778.
doi: 10.3389/fonc.2022.1087778

Adjuvant chemotherapy and survival outcomes in rectal cancer patients with good response (ypT0-2N0) after neoadjuvant chemoradiotherapy and surgery: A retrospective nationwide analysis

Yu-Hsuan Kuo[1,2†], Yun-Tzu Lin[1†], Chung-Han Ho[3,4], Chia-Lin Chou[5,6], Li-Chin Cheng[5], Chia-Jen Tsai[7], Wei-Ju Hong[7], Yi-Chen Chen[3] and Ching-Chieh Yang[7,8*]

[1]Division of Hematology and Oncology, Department of Internal Medicine, Chi Mei Medical Center, Tainan, Taiwan, [2]Department of Cosmetic Science, Chia-Nan University of Pharmacy and Science, Tainan, Taiwan, [3]Department of Medical Research, Chi Mei Medical Center, Tainan, Taiwan, [4]Department of Information Management, Southern Taiwan University of Science and Technology, Tainan, Taiwan, [5]Division of Colorectal Surgery, Department of Surgery, Chi Mei Medical Center, Tainan, Taiwan, [6]Department of Medical Laboratory Science and Biotechnology, Chung Hwa University of Medical Technology, Tainan, Taiwan, [7]Department of Radiation Oncology, Chi Mei Medical Center, Tainan, Taiwan, [8]Department of Pharmacy, Chia-Nan University of Pharmacy and Science, Tainan, Taiwan

Background: For rectal cancer, it remains unclear how to incorporate tumor response to neoadjuvant chemoradiotherapy (nCRT) when deciding whether to give adjuvant chemotherapy. In this study, we aim to determinate the survival benefit of adjuvant chemotherapy for rectal cancer patients with good response (ypT0-2N0) after nCRT and surgery.

Methods: The study cohort included 720 rectal cancer patients who had good response (ypT0-2N0) after nCRT and surgery, who did or did not receive adjuvant chemotherapy between January 2007 and December 2017, from the Taiwan Cancer Registry and National Health Insurance Research database. The Kaplan–Meier method, log-rank tests, and Cox regression analysis were performed to investigate the effect of adjuvant chemotherapy on 5-year overall survival (OS) and disease-free survival (DFS).

Results: Of 720 patients, 368 (51.1%) received adjuvant chemotherapy and 352 (48.9%) did not. Patients who received adjuvant chemotherapy were more likely to be female, younger (≤ 65), with advanced clinical T (3-4)/N (1-2) classification and ypT2 classification. No significant difference in 5-year OS (p=0.681) or DFS (p=0.942) were observed by receipt of adjuvant chemotherapy or not. Multivariable analysis revealed adjuvant chemotherapy was not associated with better OS (adjusted hazard ratio [aHR], 1.03; 95% Confidence Interval [CI], 0.88-

1.21) or DFS (aHR, 1.05; 95% CI, 0.89-1.24). Stratified analysis for OS and DFS found no significant protective effect in the use of adjuvant chemotherapy, even for those with advanced clinical T or N classification.

Conclusion: Adjuvant chemotherapy may be omitted in rectal cancer patients with good response (ypT0-2N0) after nCRT and surgery.

KEYWORDS

rectal cancer, neoadjuvant chemoradiotherapy, surgery, adjuvant chemotherapy, survival

Background

Although mortality has steadily decreased since 1990, colorectal cancer remains one of the most frequent cancer-related death in the US (1). In addition, the incidence of colorectal cancer under the age of 50 increased from 1992 to 2012 at a rate of 2.1% annually, and continues to rise (2). According to the Taiwan Cancer Registry (TCR) database in recent two decades, male and female young-onset rectal cancer incidence rates rose from 4.0 to 8.3 and 3.8 to 6.4 per 100,000 (3).

Although radical resection is the cornerstone of management in rectal cancer, radiotherapy and chemotherapy has emerged as an important component of curative therapy, because local recurrence is more common in those types than with colon primaries (4, 5). Treatment for locally advanced rectal cancer (T3-4N0 or T1-4N1-2) consists of neoadjuvant chemoradiotherapy (nCRT) followed by total mesorectal excision and adjuvant chemotherapy with fluorouracil and oxaliplatin. The use of nCRT promotes greater sphincter preservation and facilitates tumor downstaging (6, 7). Most importantly, about 15% of these patients have a pathologic complete response (defined as ypT0N0), which is associated with an excellent long-term survival outcome (8, 9). A further 20% of patients downstage to ypT1/T2N0 (10). However, up to a third of contemporary patients who undergo surgical resection of rectal cancer patients still ultimately develop metastatic disease (11). Adjuvant chemotherapy after nCRT and resection has thus been proposed as a potential method of alleviating micrometastasis, hence reducing recurrence and enhancing survival. Currently, the use of adjuvant chemotherapy in rectal cancer patients remains controversial (12–14). National Comprehensive Cancer Network (NCCN) guidelines state that pre-treatment staging, not surgical pathology, should be used to guide decisions for adjuvant chemotherapy. It is unclear how to incorporate tumor response to nCRT when deciding to provide adjuvant chemotherapy; this uncertainty is reflected in the poor compliance with NCCN guidelines for adjuvant chemotherapy administration (15).

In this study, we sought to address the impact of adjuvant chemotherapy on survival in rectal cancer patients with good response (ypT0-2N0) after nCRT and surgery, by conducting an analysis from a large cohort of patients from the TCR and the National Health Insurance Research Database (NHIRD).

Abbreviations: LARC, Locally advanced rectal cancer; nCRT, Neoadjuvant chemoradiotherapy; pCR, Pathologic complete response; NCCN, National Comprehensive Cancer Network; TCR, Taiwan Cancer Registry; NHIRD, National Health Insurance Research database; AJCC, American Joint Committee on Cancer; ICD-O-3, International Classification of Diseases for Oncology, 3rd Edition; CCI, Charlson comorbidity index; OS, Overall survival; DFS, Disease free survival; HRs, Hazard ratios; CIs, Confidence intervals.

Materials and methods

Ethics approval and informed consent

The study was approved by the Ethics Committee of the Institutional Review Board of Chi Mei Medical Center (IRB: 10707–012). Informed consent was not obtained because the IRB waived the need for individual informed consent, as no personally identifiable information were used. This study had a non-interventional retrospective design, no human subjects used and all data were analyzed anonymously.

Data source and study cohort

We obtained data from the TCR and NHIRD, which cover more than 95% of the cancer cases in Taiwan. The TCR also has documented excellent data quality and completeness (16). The rectal cancer patients who underwent nCRT and surgical resection with or without adjuvant chemotherapy between January 2007 and December 2017 were included. Follow-up was completed on December 31, 2018. Exclusion criteria included: 1) a history of cancer or metastatic disease; 2) no clear coding on follow-up and treatment; or 3) patients received short course radiation. Rectal cancer diagnosis were defined by the International Classification of Disease for Oncology, third

edition (ICD-O-3) codes for location: rectum (code C20.9); and histologic type: adenocarcinoma (codes 8140, 8210, 8261, and 8263), mucinous adenocarcinoma (code 8480), or signet ring cell carcinoma (code 8490). These patients were all staged according to the 7th edition American Joint Committee on Cancer (AJCC) classification system. The variables from the TCR database used for analysis included age, gender, histology type, grade, stage, margin status, lymph node yield, comorbid conditions and cancer-related treatment. Here, Charlson Comorbidity Index (CCI) score were used to grade the severity of comorbid conditions (17). Finally, a total of 720 rectal cancer patients with good response " ypT0-2N0 " after nCRT and surgery were extracted (Figure 1).

Statistical analysis

In this study, all statistical analyses were performed using SAS 9.4 for Windows (SAS Institute, Inc., Cary, NC, USA) and Kaplan-Meier curves were plotted using STATA (version 12; Stata Corp., College Station, TX, USA). A p value ≤ 0.05 was considered statistically significant. The distribution difference between ypT0-2N0 rectal cancer patients treated with and without adjuvant chemotherapy was estimated using Pearson's chi-square test for categorical variables and the Wilcoxon rank sum test for continuous variables. The primary endpoints were the 5-year overall survival (OS) and disease-free survival (DFS) rates and were calculated *via* Kaplan-Meier method, comparing by log-rank statistics. The risk was presented as hazard ratios (HRs) with 95% confidence intervals (CIs) and calculated using the Cox proportional hazards model for factors associated with survival. We also performed stratified survival analyses for important prognostic characteristics such as age, cT/cN/ypN classification.

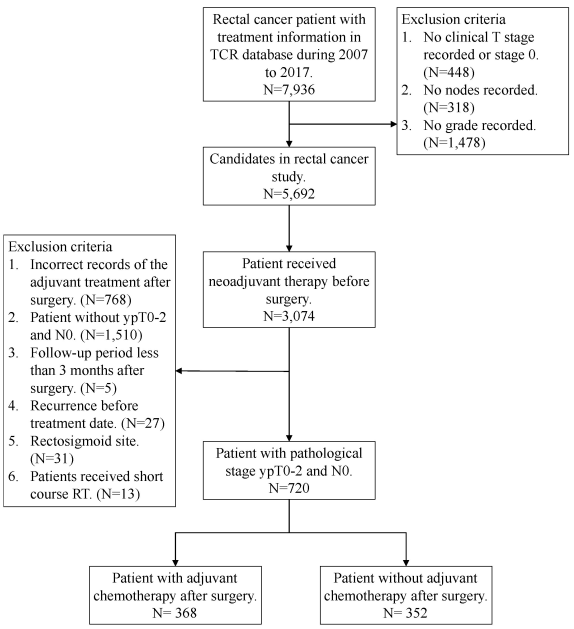

FIGURE 1
Flow chart.

Results

Between 2007 and 2017, a total of 720 rectal cancer patients were selected for analysis, including 368 patients receiving adjuvant chemotherapy and 352 patients without adjuvant chemotherapy (Figure 1). Baseline clinicopathological characteristics are summarized in Table 1. Among these patients, 498 were male (69.2%) and 222 were female (30.8%). The mean age at diagnosis was 61 ± 11 years, and the median (Q1-Q3) follow-up time was 4.22 years. The information of neoadjuvant treatment is summarized in Supplementary Table 1. The median (Q1-Q3) total dose of radiotherapy was 50.4 Gy in 27 fractions. Concurrent, neoadjuvant chemotherapy regimens included fluorouracil (5-FU), leucovorin, capecitabine, oxaliplatin and UFUR. Patients who received adjuvant chemotherapy were more likely to be female, younger (≤ 65), with advanced clinical T (3-4)/N (1-2) classification and ypT2 classification. The median (Q1-Q3) timing of adjuvant chemotherapy started after operation were 36 days. Adjuvant chemotherapy regimens used as follows: Leucovorin, Fluorouracil (5-FU), UFUR, oxaliplatin and capecitabine. Most patients (88.59%) received combined regimens instead of mono-therapy.

Kaplan-Meier survival curves were generated to compare the 5-year OS and DFS rates by receipt of adjuvant chemotherapy or not. As presented in Figure 2, there was no significant difference in 5-year OS (p=0.681) or DFS (p=0.942) between those who received adjuvant chemotherapy and those who did not. After adjustment for confounders (Table 2), multivariable analysis indicated that adjuvant chemotherapy was not significantly associated with better 5-year OS (adjusted hazard ratio [aHR], 1.03; 95% Confidence Interval [CI], 0.88-1.21) or DFS (aHR, 1.05; 95% CI, 0.89-1.224). Further stratified analysis for 5-year OS and DFS found no significant protective role in the use of adjuvant chemotherapy for these "good response" rectal cancer patients, even for those with advanced cT or cN classification (Table 2). In this study, we selected ypT1-2N0 patients without clinical metastases and there are some early stage (cT1-2N0) included into our analysis. As shown in Table 3, comparisons by different clinical and pathological T and N classifications revealed that the use of adjuvant chemotherapy provided limited survival benefit compared to not using it. Regarding to different adjuvant chemotherapy regimens, the related 5-year OS and DFS rate were presented in Table 4.

TABLE 1 Clinicopathological information of rectal cancer patients with good response (ypT0-2N0) after nCRT and surgery, n=720.

Variable	Adjuvant chemotherapy		*P*-value[b]
	Without	With	
Overall	N=352	N=368	
Age group			
≦65	200 (56.82)	246 (66.85)	0.006
>65	152 (43.18)	122 (33.15)	
Gender			
Male	258 (73.30)	240 (65.22)	0.019
Female	94 (26.70)	128 (34.78)	
Morphology			
Adenocarcinoma	349 (99.15)	364 (98.91)	1.000
Mucinous/signet	3 (0.85)	4 (1.09)	
Grade			
Well	319 (90.63)	336 (91.30)	0.751
Others	33 (9.38)	32 (8.70)	
cT classification			
1-2	78 (22.16)	62 (16.85)	0.072
3-4	274 (77.84)	306 (83.15)	
cN classification			
0	140 (39.77)	122 (33.15)	0.065
1-2	212 (60.23)	246 (66.85)	
ypT classification			
0	155 (44.03)	115 (31.25)	0.002
1	34 (9.66)	46 (12.50)	
2	163 (46.31)	207 (56.25)	
LN yield			
<12	172 (48.86)	167 (45.38)	0.349
≧12	180 (51.14)	201 (54.62)	
Surgery type			
LAR	246 (69.89)	255 (69.29)	0.966
APR	53 (15.06)	58 (15.76)	
Others	53 (15.06)	55 (14.95)	
CCI score			
0	216 (61.36)	231 (62.77)	0.739
1	83 (23.58)	89 (24.18)	
≧2	53 (15.06)	48 (13.04)	

(Continued)

TABLE 1 Continued

Variable	Adjuvant chemotherapy		*P*-value[b]
	Without	With	
Follow-up period[a], year			
Median (Q1-Q3)	4.22 (2.48-5.00)	4.24 (2.24-5.00)	0.956

a. The end of study was 2018.12.31 and the study period was defined as the patients were examined 5 years after 3 months of surgery.
b. P-value was derived from Pearson's Chi-square test for categorical variable and the Wilcoxon rank sum test for the difference in the median of follow-up period between two groups.
nCRT, neoadjuvant chemoradiotherapy; cT, clinical tumor; cN, clinical nodal; ypT, pathological tumor; LN, lymph node; LAR, low anterior resection; APR, abdominoperineal resection; CCI, Charlson Comorbidity Index.

Discussion

Treatment for clinical stage II or III rectal cancer patients consists of nCRT followed by total mesorectal excision and adjuvant chemotherapy with fluorouracil and oxaliplatin. However, the benefit of adjuvant chemotherapy for downstaged or good response (ypT0-2N0) rectal cancer after nCRT remains inconsistent (12–14). In this nationwide, population-based, cohort study, our results found no significant difference in 5-year OS or DFS between those who received adjuvant chemotherapy and those who did not. Moreover, there was no significantly difference in 5-year survival even in those with advanced cT or cN classification.

Our study offers a number of advantages over earlier studies from single institutions or several national datasets. First, we obtained data from the TCR and the NHIRD (18). This database covered more than 95% cancer cases in Taiwan. The follow-up period was long and the patient number was enough (N=764) to make our results convincing. Additionally, we included individuals with rectal cancer diagnosed between 2007 and 2018, which increased the relevance of our study. Second, this database had comprehensive information on patient characteristics, clinical staging, pathological staging, surgical methods and comorbidities enabling us to conduct in-depth analyses on the actual impact of adjuvant chemotherapy.

Adjuvant chemotherapy is recommended as standard treatment for those with high risk stage II and stage III colon cancer (19, 20). However, the precise benefit of adjuvant chemotherapy in rectal cancer remains unclear. According to NCCN guidelines, whether or not to give adjuvant chemotherapy depends on the pre-treatment clinical staging. The guidelines suggest all patients who underwent nCRT for locally advanced (T3/4 or node-positive) non-metastatic rectal cancer receive four months of adjuvant chemotherapy, regardless of the pathologic findings at the time of resection. However, in terms of the evidence level, four randomized phase III trials explored the benefit of adjuvant chemotherapy following nCRT for rectal cancer (6, 11, 21–23). None of the four found any advantage in the use of adjuvant chemotherapy, either in terms of recurrence rate or OS. However, all of these trials were flawed. For example, in the European Organisation for Research and Treatment of Cancer (EORTC) trial 22921 and the cooperative Italian study, the adjuvant chemotherapy regimen consisted of four to six cycles of postoperative bolus fluorouracil plus leucovorin, which was not consistent with the current standard regimen (24, 25). In these two studies, the rate of adherence to adjuvant chemotherapy was poor (43% in the EORTC 22921 study and 72% in the cooperative Italian study). In the Dutch colorectal PROCTOR/SCRIPT trials, the adjuvant chemotherapy regimens included fluorouracil/leucovorin or capecitabine (21). However, the trial did not reach full accrual.

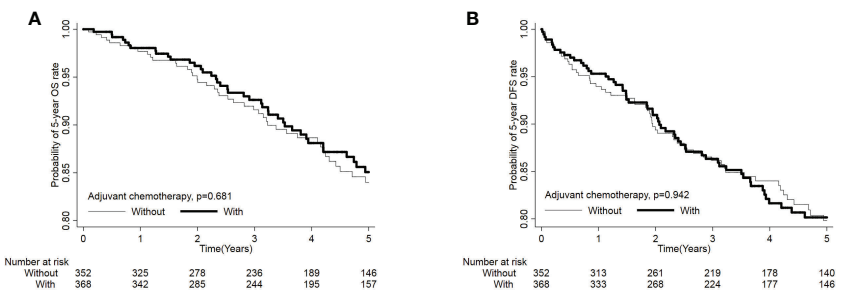

FIGURE 2
Probability of overall survival **(A)** and disease-free survival **(B)** in rectal cancer patients with good response (ypT0-2N0) after nCRT and surgery, n=720.

TABLE 2 Overall and stratified analysis of the use of adjuvant chemotherapy for 5-year OS and DFS in rectal cancer patients with good response (ypT0-2N0) after nCRT and surgery, n=720.

With adjuvant chemotherapy vs without	5-year OS				5-year DFS			
	Crude hazard ratio (95% C.I.)	P-value	Adjusted hazard ratio[c] (95% C.I.)	P-value	Crude hazard ratio (95% C.I.)	P-value	Adjusted hazard ratio[c] (95% C.I.)	P-value
Overall	1.00 (0.86-1.17)	0.988	1.03 (0.88-1.21)	0.711	1.01 (0.87-1.19)	0.862	1.05 (0.89-1.24)	0.556
Age group								
≦65	0.98 (0.81-1.19)	0.820	1.01 (0.83-1.24)	0.909	1.00 (0.82-1.21)	0.959	1.03 (0.84-1.27)	0.760
>65	1.03 (0.79-1.35)	0.806	1.09 (0.83-1.44)	0.529	1.05 (0.80-1.37)	0.750	1.11 (0.84-1.48)	0.463
cT classification								
1-2	1.04 (0.72-1.48)	0.846	0.99 (0.66-1.47)	0.944	1.07 (0.74-1.55)	0.730	1.06 (0.70-1.59)	0.798
3-4	0.99 (0.83-1.18)	0.914	1.04 (0.87-1.24)	0.693	1.00 (0.84-1.20)	0.973	1.05 (0.88-1.26)	0.592
cN classification								
0	0.84 (0.65-1.10)	0.199	0.83 (0.63-1.10)	0.195	0.83 (0.63-1.09)	0.183	0.82 (0.62-1.10)	0.184
1-2	1.08 (0.89-1.30)	0.464	1.15 (0.94-1.40)	0.184	1.11 (0.91-1.35)	0.299	1.18 (0.96-1.45)	0.116
ypT classification								
0	1.00 (0.78-1.29)	0.987	1.02 (0.79-1.33)	0.870	1.03 (0.80-1.33)	0.796	1.06 (0.81-1.38)	0.666
1-2	1.03 (0.85-1.27)	0.745	1.04 (0.84-1.27)	0.738	1.04 (0.85-1.28)	0.698	1.04 (0.84-1.29)	0.722

c. The relative risk between patient with or without adjuvant chemotherapy was calculated from Cox proportional hazard ratio model and adjusted for age, gender, cT/cN/ypT classification, surgery type, and CCI.
OS, overall survival; DFS, disease free survival; cT, clinical tumor; cN, clinical nodal; ypT, pathological tumor; CCI, Charlson Comorbidity Index.

TABLE 3 5-year OS and DFS comparison by different clinicopathological stage and the use of adjuvant chemotherapy of study patients, n =720.

ypT classification	cT/cN classification	Without adjuvant chemotherapy N = 352			With adjuvant chemotherapy N = 368			*P*-value[d]	
		N	5- year OS (%)	5- year DFS (%)	N	5- year OS (%)	5- year DFS (%)	5- year OS	5- year DFS
ypT0N0	T3-4,N1-2	84	79 (94.05)	77 (91.67)	74	71 (95.95)	68 (91.89)	0.648	0.966
	T3-4, N0	37	34 (91.89)	32 (86.49)	28	23 (82.14)	23 (82.14)	0.356	0.766
	T1-2, N1-2	17	17 (100.00)	17 (100.00)	10	10 (100.00)	9 (90.00)	–	–
	T1-2, N0	17	14 (82.35)	14 (82.35)	3	3 (100.00)	3 (100.00)	0.477	0.477
ypT1-2N0	T3-4, N1-1	95	81 (85.26)	75 (78.95)	138	123 (89.13)	115 (83.33)	0.484	0.509
	T3-4, N0	58	46 (79.31)	45 (77.59)	66	59 (89.39)	55 (83.33)	0.123	0.411
	T1-2, N1-2	16	13 (81.25)	13 (81.25)	24	22 (91.67)	21 (87.50)	0.266	0.595
	T1-2, N0	28	26 (92.86)	22 (78.57)	25	17 (68.00)	16 (64.00)	0.030	0.317

d. P-value was derived from the Log rank test.
OS, overall survival; DFS, disease free survival; cT, clinical tumor; cN, clinical nodal; ypT, pathological tumor.

The adjuvant chemotherapy regimen in the United Kingdom phase III Chronicle trial was capecitabine plus oxaliplatin (XELOX), which was the current standard chemotherapy regimen (22). Unfortunately, the study was also closed prematurely due to poor accrual. A meta-analysis of individual patient data from all four of these trials concluded that fluorouracil-based chemotherapy did not improve OS, DFS, or distant recurrence rates (26). Another systematic review published in 2017 identified eight phase III trials and one randomized phase II trial comparing adjuvant chemotherapy

TABLE 4 The distribution and 5-year survival among different adjuvant chemotherapy regimens groups, n =368.

Drug name	Number of patientN (%)	5- year OS N (%)	5- year DFS N (%)
5-FU	210 (57.07)	188 (89.52)	173 (82.38)
Capecitabine	53 (14.40)	42 (79.25)	32 (60.38)
Oxaliplatin	64 (17.39)	52 (81.25)	43 (67.19)
Leucovorin	297 (80.71)	266 (89.56)	250 (84.18)
UFUR	161 (43.75)	137 (85.09)	125 (77.64)
Combined			
L+F	210 (57.07)	188 (89.52)	173 (82.38)
FOLFOX	58 (15.76)	46 (79.31)	37 (63.79)
CAPEOX	20 (5.43)	15 (75.00)	9 (45.00)
F+O	58 (15.76)	46 (79.31)	37 (63.79)
Monotherapy,			
No	326 (88.59)	289 (88.65)	273 (83.74)
Yes	42 (11.41)	39 (92.86)	37 (88.10)

OS, overall survival; DFS, disease free survival; L+F, Leucovorin+5-FU; FOLFOX, Oxaliplatin+ Leucovorin+5-FU; CAPEOX, Oxaliplatin + Capecitabine; F+O, Oxaliplatin+ 5-FU.

with observation in patients with non-metastatic rectal cancer treated with nCRT. The authors reported that the data were not robust enough to warrant routine use of adjuvant therapy in this population (27). However, other meta-analyses have come to the opposite conclusion. A systematic review of the scientific literature from 1975 until March 2011 quantitatively summarized the available evidence regarding the impact of adjuvant chemotherapy on the survival of patients with surgically resectable rectal cancer (28). The authors supported the use of 5-FU based postoperative adjuvant chemotherapy, but available data did not allow them to define whether the efficacy of this treatment was greatest for one specific TNM stage. Consequently, conclusive data on the benefits of adjuvant therapy in rectal cancer patients remains lacking.

Our study focused on the benefit of adjuvant chemotherapy for patients with good response (ypT0-2N0) to nCRT and surgery. Patients who achieve a pathologic complete response after preoperative therapy have excellent outcomes (10). These findings raise concerns regarding the possibility of overtreatment in this group, when adding adjuvant chemotherapy. Other database studies have also failed to discover a significant benefit to adjuvant chemotherapy in this setting (29–31). However, three similar observational studies using the National Cancer Database, which looked only at patients achieving pathologic complete response, found that adjuvant chemotherapy did improve survival in this favorable subgroup (32–34).

Our study demonstrated that adjuvant chemotherapy is not beneficial for those rectal patients with good response to nCRT and surgery, even those with advanced clinical stage disease. However, our study showed that patients with clinical nodal positive status had worse OS and DSS. This finding implies that clinical stage might be a prognostic factor rather than a predictive factor. There are some potential explanations for the conflicting results, which are also the common limitations of nationwide cancer registry database analysis, including ours. First, it is challenging to accurately assess clinical stage, since the imaging tools used to determine stage differ by hospital. Some patients could be over-staged, which makes adjuvant chemotherapy appear to be of no benefit in this group. Second, the presence of perineural and extramural venous invasion, particularly after preoperative irradiation, is a significant negative prognostic factor for local recurrence, metastatic disease, and OS (35). However, this information was not recorded in our database. Third, due to treatment-related toxicity, patients receiving adjuvant chemotherapy may face interruption or dose reduction during the course of treatment. However, we could not assess the compliance with the administration of adjuvant chemotherapy (including prescribed dose, and cycles) (36, 37). Future work including the information about the compliance with the administration of chemotherapy may help us to investigate in depth about the role of adjuvant chemotherapy on survival. However, we could know the stop of neoadjuvant CRT course from the coding of total radiation dose. We found 20 (2.7%) patients received less than 45Gy during their neoadjuvant CRT. Fourth, patients with different molecular profiles, such as microsatellite instability, KRAS mutation, or BRAF mutation, may vary in their prognostic profiles and sensitivity to chemotherapeutic and biological agents. The microsatellite instability status also influences the decision to provide adjuvant chemotherapy, but

these molecular profiles were not available for our analysis (38). Finally, following nCRT and surgery, patients with a pathologic complete response or a clinically significant downstage to ypT1/T2N0 often have a good prognosis and are unlikely to benefit from additional adjuvant chemotherapy. Although no markers were available in our cancer registry database, we defined the good response from the pathological stage (yp) which is generally accepted and used. However, the response should be a dynamic process and is better evaluated by tumor regression grade (39).

Questions remain regarding how much downstaging is predictive of further benefit from adjuvant therapy. It is possible that adjuvant chemotherapy may not benefit patients at the two extremes of pathologic response: patients with good response and those with poor or minimal pathologic response to nCRT. Perhaps the intermediate group may benefit from further adjuvant chemotherapy. However, identifying this group remains challenging and more prospective studies are needed before this occurs.

Conclusion

In summary, our results demonstrated that adjuvant chemotherapy does not improve 5-year OS or DFS in rectal cancer patients with good response after nCRT and surgery. Moreover, there is no significantly difference in 5-year OS, even in those with advanced cT or cN classification. Therefore, adjuvant chemotherapy may be omitted in these good response patients. Prospective studies that include more patients and clinicopathological variables are necessary to valid our findings into clinical practice.

Data availability statement

The original contributions presented in the study are included in the article/Supplementary Material. Further inquiries can be directed to the corresponding author.

Author contributions

Study design: Y-HK, Y-TL, C-HH, C-LC, L-CC, C-JT, W-JH, Y-CC, C-CY. Data analysis: Y-HK, C-HH, Y-CC, C-CY. Manuscript writing: Y-HK, Y-TL, C-HH, C-CY. All authors contributed to the article and approved the submitted version.

Acknowledgments

We are grateful to Health Data Science Center, National Cheng Kung University Hospital for providing administrative and technical support.

Conflict of interest

The authors declare that the research was conducted in the absence of any commercial or financial relationships that could be construed as a potential conflict of interest.

Publisher's note

All claims expressed in this article are solely those of the authors and do not necessarily represent those of their affiliated organizations, or those of the publisher, the editors and the reviewers. Any product that may be evaluated in this article, or claim that may be made by its manufacturer, is not guaranteed or endorsed by the publisher.

Supplementary material

The Supplementary Material for this article can be found online at: https://www.frontiersin.org/articles/10.3389/fonc.2022.1087778/full#supplementary-material

References

1. Cronin KA, Scott S, Firth AU, Sung H, Henley SJ, Sherman RL, et al. Annual report to the nation on the status of cancer, part 1: National cancer statistics. *Cancer* (2022) 128(24):4251–84. doi: 10.1002/cncr.34479

2. Stoffel EM, Murphy CC. Epidemiology and mechanisms of the increasing incidence of colon and rectal cancers in young adults. *Gastroenterology* (2020) 158 (2):341–53. doi: 10.1053/j.gastro.2019.07.055

3. Sung JJY, Chiu HM, Jung KW, Jun JK, Sekiguchi M, Matsuda T, et al. Increasing trend in young-onset colorectal cancer in Asia: More cancers in men and more rectal cancers. *Am J Gastroenterol* (2019) 114(2):322–9. doi: 10.14309/ajg.0000000000000133

4. Sauer R, Becker H, Hohenberger W, Rodel C, Wittekind C, Fietkau R, et al. Preoperative versus postoperative chemoradiotherapy for rectal cancer. *N Engl J Med* (2004) 351(17):1731–40. doi: 10.1056/NEJMoa040694

5. Sebag-Montefiore D, Stephens RJ, Steele R, Monson J, Grieve R, Khanna S, et al. Preoperative radiotherapy versus selective postoperative chemoradiotherapy in patients with rectal cancer (Mrc Cr07 and ncic-ctg C016): A multicentre, randomised trial. *Lancet* (2009) 373(9666):811–20. doi: 10.1016/S0140-6736(09)60484-0

6. Collette L, Bosset JF, den Dulk M, Nguyen F, Mineur L, Maingon P, et al. Patients with curative resection of Ct3-4 rectal cancer after preoperative radiotherapy or radiochemotherapy: Does anybody benefit from adjuvant fluorouracil-based chemotherapy? A trial of the European organisation for research and treatment of cancer radiation oncology group. *J Clin Oncol* (2007) 25(28):4379–86. doi: 10.1200/JCO.2007.11.9685

7. Park IJ, You YN, Agarwal A, Skibber JM, Rodriguez-Bigas MA, Eng C, et al. Neoadjuvant treatment response as an early response indicator for patients with rectal cancer. *J Clin Oncol* (2012) 30(15):1770–6. doi: 10.1200/JCO.2011.39.7901

8. Fokas E, Strobel P, Fietkau R, Ghadimi M, Liersch T, Grabenbauer GG, et al. Tumor regression grading after preoperative chemoradiotherapy as a prognostic factor and individual-level surrogate for disease-free survival in rectal cancer. *J Natl Cancer Inst* (2017) 109(12). doi: 10.1093/jnci/djx095

9. Zhang JW, Cai Y, Xie XY, Hu HB, Ling JY, Wu ZH, et al. Nomogram for predicting pathological complete response and tumor downstaging in patients with locally advanced rectal cancer on the basis of a randomized clinical trial. *Gastroenterol Rep (Oxf)* (2020) 8(3):234–41. doi: 10.1093/gastro/goz073

10. Maas M, Nelemans PJ, Valentini V, Das P, Rodel C, Kuo LJ, et al. Long-term outcome in patients with a pathological complete response after chemoradiation for rectal cancer: A pooled analysis of individual patient data. *Lancet Oncol* (2010) 11(9):835–44. doi: 10.1016/S1470-2045(10)70172-8

11. Bosset JF, Calais G, Mineur L, Maingon P, Stojanovic-Rundic S, Bensadoun RJ, et al. Fluorouracil-based adjuvant chemotherapy after preoperative chemoradiotherapy in rectal cancer: Long-term results of the eortc 22921 randomised study. *Lancet Oncol* (2014) 15(2):184–90. doi: 10.1016/S1470-2045(13)70599-0

12. Chang GJ. Is there validity in propensity score-matched estimates of adjuvant chemotherapy effects for patients with rectal cancer? *JAMA Oncol* (2018) 4(7):921–3. doi: 10.1001/jamaoncol.2018.0227

13. Fokas E, Liersch T, Fietkau R, Hohenberger W, Beissbarth T, Hess C, et al. Tumor regression grading after preoperative chemoradiotherapy for locally advanced rectal carcinoma revisited: Updated results of the Cao/Aro/Aio-94 trial. *J Clin Oncol* (2014) 32(15):1554–62. doi: 10.1200/JCO.2013.54.3769

14. Rodel C, Martus P, Papadoupolos T, Fuzesi L, Klimpfinger M, Fietkau R, et al. Prognostic significance of tumor regression after preoperative chemoradiotherapy for rectal cancer. *J Clin Oncol* (2005) 23(34):8688–96. doi: 10.1200/JCO.2005.02.1329

15. Xu Z, Mohile SG, Tejani MA, Becerra AZ, Probst CP, Aquina CT, et al. Poor compliance with adjuvant chemotherapy use associated with poorer survival in patients with rectal cancer: An ncdb analysis. *Cancer* (2017) 123(1):52–61. doi: 10.1002/cncr.30261

16. Chiang CJ, Lo WC, Yang YW, You SL, Chen CJ, Lai MS. Incidence and survival of adult cancer patients in Taiwan, 2002-2012. *J Formos Med Assoc* (2016) 115(12):1076–88. doi: 10.1016/j.jfma.2015.10.011

17. Tian Y, Xu B, Yu G, Li Y, Liu H. Age-adjusted charlson comorbidity index score as predictor of prolonged postoperative ileus in patients with colorectal cancer who underwent surgical resection. *Oncotarget* (2017) 8(13):20794–801. doi: 10.18632/oncotarget.15285

18. Liang YH, Shao YY, Chen HM, Cheng AL, Lai MS, Yeh KH. Irinotecan and oxaliplatin might provide equal benefit as adjuvant chemotherapy for patients with resectable synchronous colon cancer and liver-confined metastases: A nationwide database study. *Anticancer Res* (2017) 37(12):7095–104. doi: 10.21873/anticanres.12183

19. Gill S, Loprinzi CL, Sargent DJ, Thome SD, Alberts SR, Haller DG, et al. Pooled analysis of fluorouracil-based adjuvant therapy for stage ii and iii colon cancer: Who benefits and by how much? *J Clin Oncol* (2004) 22(10):1797–806. doi: 10.1200/JCO.2004.09.059

20. Quasar Collaborative G, Gray R, Barnwell J, McConkey C, Hills RK, Williams NS, et al. Adjuvant chemotherapy versus observation in patients with colorectal cancer: A randomised study. *Lancet* (2007) 370(9604):2020–9. doi: 10.1016/S0140-6736(07)61866-2

21. Breugom AJ, Swets M, Bosset JF, Collette L, Sainato A, Cionini L, et al. Adjuvant chemotherapy after preoperative (Chemo)Radiotherapy and surgery for patients with rectal cancer: A systematic review and meta-analysis of individual patient data. *Lancet Oncol* (2015) 16(2):200–7. doi: 10.1016/S1470-2045(14)71199-4

22. Glynne-Jones R, Counsell N, Quirke P, Mortensen N, Maraveyas A, Meadows HM, et al. Chronicle: Results of a randomised phase iii trial in locally advanced rectal cancer after neoadjuvant chemoradiation randomising postoperative adjuvant capecitabine plus oxaliplatin (Xelox) versus control. *Ann Oncol* (2014) 25(7):1356–62. doi: 10.1093/annonc/mdu147

23. Swets M, Kuppen PJK, Blok EJ, Gelderblom H, van de Velde CJH, Nagtegaal ID. Are pathological high-risk features in locally advanced rectal cancer a useful selection tool for adjuvant chemotherapy? *Eur J Cancer* (2018) 89:1–8. doi: 10.1016/j.ejca.2017.11.006

24. Bosset JF, Collette L, Calais G, Mineur L, Maingon P, Radosevic-Jelic L, et al. Chemotherapy with preoperative radiotherapy in rectal cancer. *N Engl J Med* (2006) 355(11):1114–23. doi: 10.1056/NEJMoa060829

25. Sainato A, Cernusco Luna Nunzia V, Valentini V, De Paoli A, Maurizi ER, Lupattelli M, et al. No benefit of adjuvant fluorouracil leucovorin chemotherapy after neoadjuvant chemoradiotherapy in locally advanced cancer of the rectum (Larc): Long term results of a randomized trial (I-Cnr-Rt). *Radiother Oncol* (2014) 113(2):223–9. doi: 10.1016/j.radonc.2014.10.006

26. Breugom AJ, van Gijn W, Muller EW, Berglund A, van den Broek CBM, Fokstuen T, et al. Adjuvant chemotherapy for rectal cancer patients treated with preoperative (Chemo)Radiotherapy and total mesorectal excision: A Dutch colorectal cancer group (Dccg) randomized phase iii trial. *Ann Oncol* (2015) 26 (4):696–701. doi: 10.1093/annonc/mdu560

27. Carvalho C, Glynne-Jones R. Challenges behind proving efficacy of adjuvant chemotherapy after preoperative chemoradiation for rectal cancer. *Lancet Oncol* (2017) 18(6):e354–e63. doi: 10.1016/S1470-2045(17)30346-7

28. Petersen SH, Harling H, Kirkeby LT, Wille-Jorgensen P, Mocellin S. Postoperative adjuvant chemotherapy in rectal cancer operated for cure. *Cochrane Database Syst Rev* (2012) 3):CD004078. doi: 10.1002/14651858.CD004078.pub2

29. Garlipp B, Ptok H, Benedix F, Otto R, Popp F, Ridwelski K, et al. Adjuvant treatment for resected rectal cancer: Impact of standard and intensified postoperative chemotherapy on disease-free survival in patients undergoing preoperative chemoradiation-a propensity score-matched analysis of an observational database. *Langenbecks Arch Surg* (2016) 401(8):1179–90. doi: 10.1007/s00423-016-1530-0

30. Hu X, Li YQ, Li QG, Ma YL, Peng JJ, Cai SJ. Adjuvant chemotherapy seemed not to have survival benefit in rectal cancer patients with yptis-2n0 after preoperative radiotherapy and surgery from a population-based propensity score analysis. *Oncologist* (2019) 24(6):803–11. doi: 10.1634/theoncologist.2017-0600

31. Loree JM, Kennecke HF, Lee-Ying RM, Goodwin RA, Powell ED, Tang PA, et al. Impact of postoperative adjuvant chemotherapy following long-course chemoradiotherapy in stage ii rectal cancer. *Am J Clin Oncol* (2018) 41(7):643–8. doi: 10.1097/COC.0000000000000342

32. Dossa F, Acuna SA, Rickles AS, Berho M, Wexner SD, Quereshy FA, et al. Association between adjuvant chemotherapy and overall survival in patients with rectal cancer and pathological complete response after neoadjuvant chemotherapy and resection. *JAMA Oncol* (2018) 4(7):930–7. doi: 10.1001/jamaoncol.2017.5597

33. Polanco PM, Mokdad AA, Zhu H, Choti MA, Huerta S. Association of adjuvant chemotherapy with overall survival in patients with rectal cancer and pathologic complete response following neoadjuvant chemotherapy and resection. *JAMA Oncol* (2018) 4(7):938–43. doi: 10.1001/jamaoncol.2018.0231

34. Turner MC, Keenan JE, Rushing CN, Gulack BC, Nussbaum DP, Benrashid E, et al. Adjuvant chemotherapy improves survival following resection of locally advanced rectal cancer with pathologic complete response. *J Gastrointest Surg* (2019) 23(8):1614–22. doi: 10.1007/s11605-018-04079-8

35. Gosens MJ, Klaassen RA, Tan-Go I, Rutten HJ, Martijn H, van den Brule AJ, et al. Circumferential margin involvement is the crucial prognostic factor after multimodality treatment in patients with locally advanced rectal carcinoma. *Clin Cancer Res* (2007) 13(22 Pt 1):6617–23. doi: 10.1158/1078-0432.CCR-07-1197

36. Biagi JJ, Raphael MJ, Mackillop WJ, Kong W, King WD, Booth CM. Association between time to initiation of adjuvant chemotherapy and survival in colorectal cancer: A systematic review and meta-analysis. *JAMA* (2011) 305 (22):2335–42. doi: 10.1001/jama.2011.749

37. Gresham G, Cheung WY, Speers C, Woods R, Kennecke H. Time to adjuvant chemotherapy and survival outcomes among patients with stage 2 to 3 rectal cancer treated with preoperative chemoradiation. *Clin Colorectal Cancer* (2015) 14(1):41–5. doi: 10.1016/j.clcc.2014.11.004

38. Koenig JL, Toesca DAS, Harris JP, Tsai CJ, Haraldsdottir S, Lin AY, et al. Microsatellite instability and adjuvant chemotherapy in stage ii colon cancer. *Am J Clin Oncol* (2019) 42(7):573–80. doi: 10.1097/COC.0000000000000554

39. Dworak O, Keilholz L, Hoffmann A. Pathological features of rectal cancer after preoperative radiochemotherapy. *Int J Colorectal Dis* (1997) 12(1):19–23. doi: 10.1007/s003840050072

frontiers | Frontiers in Oncology

TYPE Review
PUBLISHED 13 March 2023
DOI 10.3389/fonc.2023.1132141

OPEN ACCESS

EDITED BY
Veronika Vymetalkova,
Academy of Sciences of the Czech Republic (ASCR), Czechia

REVIEWED BY
Monika Sramkova,
Biomedical Research Center SAS, Slovakia
Junmin Zhang,
Lanzhou University, China

*CORRESPONDENCE
Xuan Huang
huangxuan1976@163.com

SPECIALTY SECTION
This article was submitted to Gastrointestinal Cancers: Colorectal Cancer, a section of the journal Frontiers in Oncology

RECEIVED 26 December 2022
ACCEPTED 27 January 2023
PUBLISHED 13 March 2023

CITATION
Lin X, Yang X, Yang Y, Zhang H and Huang X (2023) Research progress of traditional Chinese medicine as sensitizer in reversing chemoresistance of colorectal cancer.
Front. Oncol. 13:1132141.
doi: 10.3389/fonc.2023.1132141

Research progress of traditional Chinese medicine as sensitizer in reversing chemoresistance of colorectal cancer

Xiang Lin[1,2], Xinyu Yang[1,2], Yushang Yang[1,2], Hangbin Zhang[1,2] and Xuan Huang[2]*

[1]The First Clinical College, Zhejiang Chinese Medical University, Hangzhou, China, [2]Department of Gastroenterology, The First Affiliated Hospital of Zhejiang Chinese Medical University, Hangzhou, China

In recent years, the incidences and mortalities from colorectal cancer (CRC) have been increasing; therefore, there is an urgent need to discover newer drugs that enhance drug sensitivity and reverse drug tolerance in CRC treatment. With this view, the current study focuses on understanding the mechanism of CRC chemoresistance to the drug as well as exploring the potential of different traditional Chinese medicine (TCM) in restoring the sensitivity of CRC to chemotherapeutic drugs. Moreover, the mechanism involved in restoring sensitivity, such as by acting on the target of traditional chemical drugs, assisting drug activation, increasing intracellular accumulation of anticancer drugs, improving tumor microenvironment, relieving immunosuppression, and erasing reversible modification like methylation, have been thoroughly discussed. Furthermore, the effect of TCM along with anticancer drugs in reducing toxicity, increasing efficiency, mediating new ways of cell death, and effectively blocking the drug resistance mechanism has been studied. We aimed to explore the potential of TCM as a sensitizer of anti-CRC drugs for the development of a new natural, less-toxic, and highly effective sensitizer to CRC chemoresistance.

KEYWORDS

traditional Chinese medicine, colorectal cancer, chemoresistance, sensitizer, chemotherapy

1 Introduction

As reported by Global Cancer 2020, colorectal cancer (CRC) ranks second and third in global cancer incidence and mortality (1, 2). It has become a great threat to human health. This high incidence rate can be attributed to the asymptomatic manifestations of early CRC and the lack of experience in endoscopic detection so that about 50% of all patients with CRC are at or above the local progressive stage at the time of their first diagnosis (3, 4). Reducing the incidence and mortality of digestive tract tumors and optimizing the treatment scheme of digestive tract tumors are some of the major public health issues that need to be addressed.

Presently, the treatment of CRC involves surgery, radiotherapy, immunotherapy, targeted therapy, and other comprehensive treatments (5). For patients with advanced

CRC, chemotherapy is one of the most important treatments. Efforts have been made to use 5-fluorouracil (5-FU) combined with calcium folinate or oxaliplatin (OXA) as the first-line treatment for metastatic CRC, with a drug resistance rate was >40% (6). Some studies have even pointed out that 90% of patients with metastatic CRC died because of chemoresistance (7). This finding depicts that clinical drug resistance and chemoresistance are the major obstacles to the successful cure of cancer. Reducing chemoresistance, minimizing side effects, improving the patient's prognosis, and quality of life are important factors to be taken into consideration during the development of new treatment options for advanced CRC.

Chemoresistance in CRC hampers the use of standard chemotherapy as a treatment option. Efforts have been made to develop treatment options relying on reversing chemoresistance by targeting newer cytotoxic drugs, regulating drug resistance to conventional drugs, and studying the changes of in tumor gene spectrum before and after chemotherapy. However, most of these strategies result in serious side effects, involve higher treatment costs, and face a crunch in technical expertise (8, 9). The benefits of natural products render them a promising alternative for treating cancer chemoresistance. It has been reported that 50% of the anti-cancer drugs approved by the Food Drug Administration (FDA) originate directly or indirectly from natural products or their derivatives (10). Traditional Chinese medicine (TCM) is multi-targeted and less toxic. TCM treatments are unique, safe, and effective for cancer therapy in China. It is also known to improve the quality of life, prevent metastasis and recurrence, resist chemoresistance, increase efficiency, reduce toxicity, and enhance immunity. Owing to these properties, TCM has gained tremendous research attention worldwide (11). Moreover, the synergistic effects of the TCM extracts and compounds (such as curcumin, berberine, *Sophora japonica*, and *Andrographis paniculate*) when combined with traditional chemotherapy could resist chemotherapy tolerance, which is noteworthy.

The present paper focuses on understanding the mechanism of chemoresistance of CRC and explores the potential of TCM and its active ingredients as chemosensitizers in reversing chemotherapy tolerance, reducing toxicity, and increasing the efficiency of CRC. Furthermore, the related mechanisms *in vivo* and *in vitro* have been summarized. Finally, based on the current research on the function mechanism of TCM, we believe that TCM as an anticancer treatment option seems promising in solving the difficulties of clinical anticancer treatment.

2 TCM reverses the chemoresistance of CRC and inhibits tumor growth *in vivo* and *in vitro*

2.1 Drug efflux

The chemical resistance of tumor cells is dependent on the outward transporter of the ATP-binding Cassette Family (ABC). Its increased expression often causes drug efflux, thereby leading to multiple drug resistance (MDR) (Figure 1). ABC transporter is a transmembrane protein that assists in transporting various substances across cell membranes. Upon substrate binding, ATP hydrolyzes and actively pumps drugs out of the cell, thereby preventing the accumulation of toxic substances within the cell. Similarly, in cancer cells, the efflux mechanism reduces the concentration of antitumor drugs within cancer cells, thereby protecting the cancer cells (12). It has been reported that the expression of ABC transporter is low in CRC cases, but significantly increased when drug resistance is induced in a variety of CRC cells (13–15).

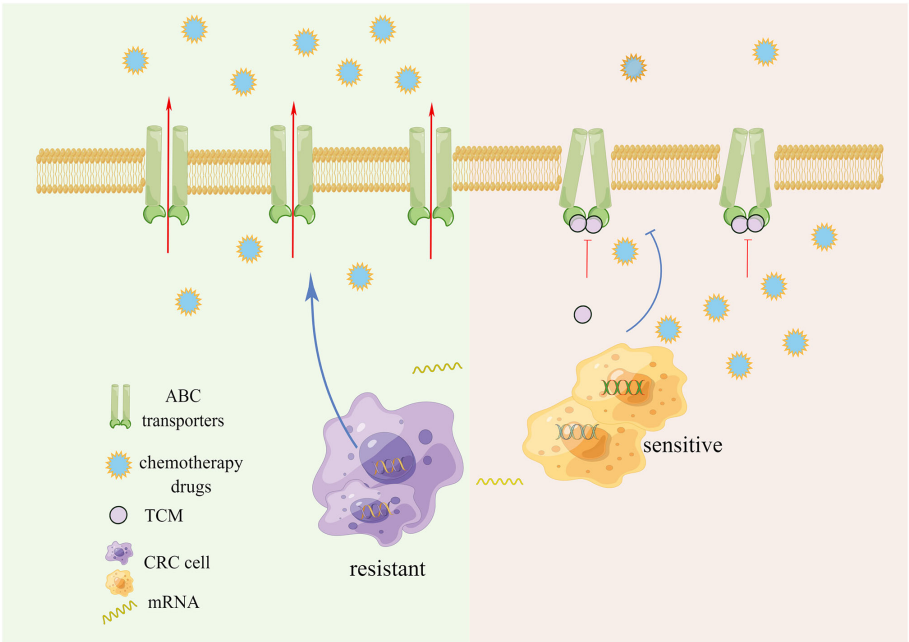

FIGURE 1
ABC transporters active drug efflux and chemotherapy resistance.

Anti-MDR strategies include P- glycoprotein (P-gp) inhibitors, RNA interference, nano-drugs and combination drugs, but these transporter inhibitors have not yet shown definite clinical benefits (16–19). The importance of developing new inhibitors with high efficiency and low side effects is self-evident. Several studies have reported that a variety of TCMs and their active ingredients can effectively inhibit the expression and efflux of transporters, reverse the chemoresistance of CRC, and act as chemical sensitizers while exerting cytotoxic effects. Our previous research found that Gegen Qinlian Decoction can inhibit the expression of ABC transporters *in vivo* and *in vitro*, and synergize with Oxaliplatin to treat OXA-resistant CRC, and restore the sensitivity to OXA (20).

Glycyrrhiza uralensis Fisch. inhibited the efflux function of transporter P-gp in a CRC cell model and played a therapeutic role with *Aconitum carmichaelii* Debeaux, enhancing its efficacy and reducing toxicity (21). The ethanol extract of *Scutellaria barbata* D. Don enhanced the retention of rhodamine, the substrate of ABC transporter in 5-FU-tolerant CRC cells, leading to the inhibition of cell proliferation and cell apoptosis (22). Cucurbitacin E can inhibit TFAP4/Wnt/β-Catenin signaling, down-regulate the expression of ABCC1 and MDR 1 to increase the chemosensitivity of colorectal cancer cells to 5-FU (23). Quercetin and kaempferol regulated the activity and expression of MRP2, thereby promoting the absorption of drugs in the intestinal tract and inhibiting drug efflux as well as downregulating the expression of ABCB1 (24, 25). Neferine, isolated from lotus seeds, combines with P-gp, and increases the retention of drugs in cancer cells (26). Lignans, a secondary metabolite of *Arctium lappa* L., regulates the efflux function of P-gp in multidrug-resistant cancer cells (27). *Pien Tze Huang*, a TCM preparation, decreased the proportion of stem cell-like lateral groups of CRC cells in a dose-dependent manner, affecting the morphology of cancer cells, and the mRNA levels of ABCB1 and ABCG2 (28). Evodiamine inhibits the p50/p65 NF-κB pathway and inhibits ABCG2-mediated oxaliplatin resistance (29). On the basis of homologous protein modeling and molecular docking technology, 837 TCMs were reported to have the potential to inhibit the activity of ABCG2 (30). TCM and its active ingredients have demonstrated a good ability to inhibit ABC transporters, making them favorable candidates for developing new inhibitors.

2.2 DNA damage and repair

DNA damage repair mechanisms include base excision repair (BER), mismatch repair (MMR), and homologous recombination (HR). These mechanisms identify and correct DNA damage caused by multiple factors such as reactive oxygen species (ROS), radiation, and chemicals (31, 32). DNA damage repair, not only removes the damaged cells but also assists in drug resistance (Figure 2) (33, 34).

For example, 5-FU induces a base mismatch in DNA, which is recognized by MMR protein, leading to programmed cell death. Defective MMR prevents cancer cell death. BER recognizes and removes 5-FU in DNA causing drug resistance (7, 35, 36). In addition, nuclear DNA is the main target of platinum-cytotoxic drugs. These drugs covalently bind to DNA to form a Pt-DNA adduct, which damages the normal transcription and replication functions of DNA. This event activates a variety of signal pathways leading to cell apoptosis. Once the process of platinum damaging

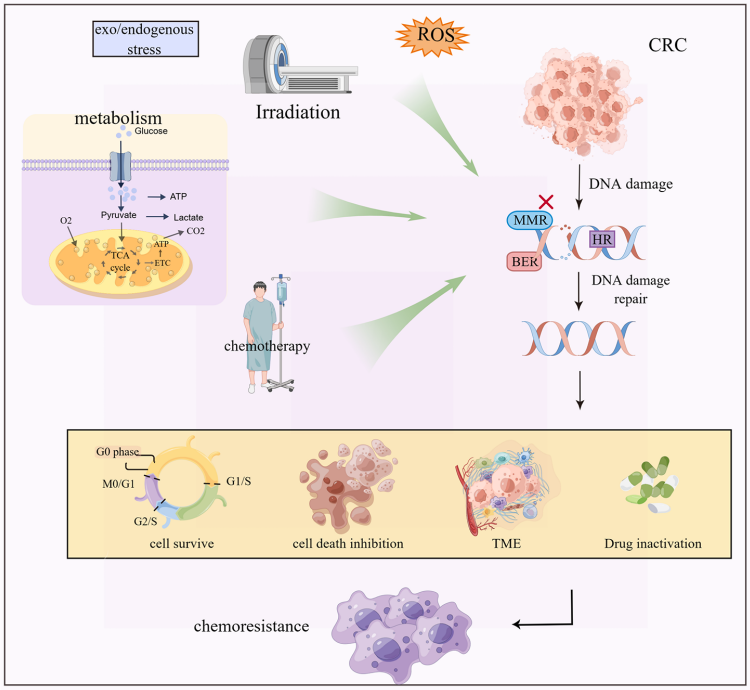

FIGURE 2
Exogenous and endogenous stresses such as radiotherapy and chemotherapy, metabolic reprogramming and ROS cause DNA damage and repair inhibition of CRC cells, which cause chemoresistance by regulating cell death, tumor microenvironment change and drug inactivation.

DNA is inhibited, the tendency of cell apoptosis will get weakened, resulting in drug resistance of the tumor (37–39). The challenges in anti-cancer platinum drugs are avoiding the precise and efficient DNA damage repair mechanisms, such as the HR repair mechanism of DNA double-strand breaks in cells. The mechanism of DNA damage combined with the inhibition of DNA repair results in sensitizing the cancer cells, thereby improving the therapeutic effect.

The use of TCM and prescriptions in DNA damage, the repair of cancer cells by reversing drug resistance, and alleviating the toxic side-effects of chemotherapeutic drugs are well documented (40–42). It has been reported that shikonin from the root of Lithospermum erythrorhizon enhances DNA damage caused by cisplatin by inducing intracellular oxidative stress and mitochondrial activation leading to the inhibition of HCT116 xenograft tumors in nude mice (43). Compound kushen injection led to the inhibition of cell cycle regulatory protein and DNA repair. It also promoted DNA double-strand break and induced cancer cell apoptosis through multiple pathways (44–46). Curcumin is known to regulate the expression of DNA repair-related genes, inhibit tumor growth, promote apoptosis, and enhance the chemosensitivity of MMR-deficient CRC to 5-FU (47–49). Berberine led to the downregulation of RRM1, RRM2, LIG1, and POLE2, participated in DNA repair and replication, and demonstrated the potential to inhibit DNA repair (50). Ginsenoside Rg3 responds to DNA damage by activating the VRK1/P53BP1 pathway, improving the efficiency of chemotherapy, reducing its side effects, and providing a new idea for cancer prevention and treatment (51). Cantharidin works by upregulating KDM4A and catalyzing the demethylation of histone H3K36me3 and inducing DNA damage, which in turn enhances the chemotherapy sensitivity (52). Cytotoxic drugs often result in serious neurotoxicity and other side effects while killing tumor cells, while Silibinin protects against cisplatin-induced neurotoxicity by reducing DNA damage and apoptosis (42, 53, 54).

2.3 Cell death

The programmed cell death pathway is necessary to maintain normal cellular development, which includes apoptosis, necrosis, cell scorch, iron death, and cell death modes related to autophagy and non-programmed necrosis (55, 56). Several studies have validated that apoptosis, autophagy, and other cell death modes are closely related to chemotherapy resistance (Figure 3). Multiple factors such as hunger and chemotherapy cause stress to the cancer cells. The uncontrolled growth of tumor cells leads to increased metabolic demand, which then activates autophagy, leading to the inhibition of tumors by the removal of damaged proteins/organelles (57). The rapid proliferation of cancer cells increases the nutrition and oxygen demand. Throughout treatment, cancer cells are in hypoxia and nutritionally deficient environments. For survival, the cancer cells are significantly dependent on autophagosomes for metabolism. Thus, autophagy fails to inhibit tumor growth, but instead results in chemotherapy resistance, thereby contributing to the development of MDR and protecting cancer cells from the attack of chemotherapy drugs (58–60).

Orderly death is called apoptosis, which is essential in maintaining the internal cell environment. Tumor cells lack the ability of apoptosis (20, 61). Tumor cells adapt to the induction of apoptosis by drugs, which leads to the development of drug resistance. An effective way to overcome drug resistance related to apoptosis of cancer cells is through stimulating and restoring the ability of tumor cells to undergo apoptosis and promoting the death mode independent of apoptosis (62–64).

Ferroptosis is a type of event that involves the accumulation of lipid-ROS (L-ROS) in an iron-dependent manner (65, 66). Glutathione (GSH) depletion inactivates GSH-dependent peroxidase (GPX4). Transferrin containing Fe^{3+} enters the cell and transforms into Fe2+ to participate in the Fenton reaction. The

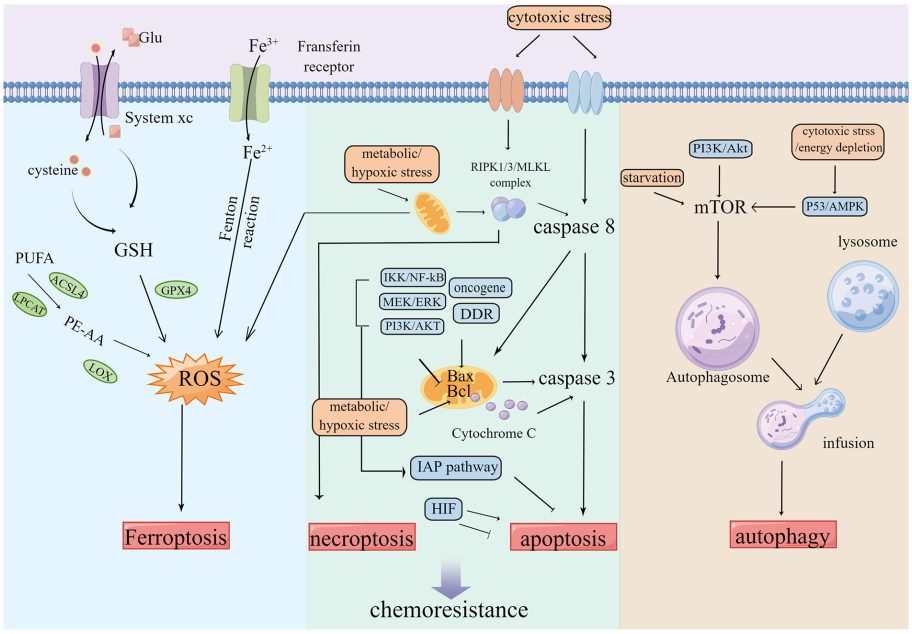

FIGURE 3
Tumors keep their sustained growth, metastasis and gain chemoresistance by escaping cell death such as ferroptosis, apoptosis and autophagy etc.

unsaturated fatty acids, such as arachidonic acid, are metabolized into PE-AA through ACSL4 and LPCAT, which are then oxidized by LOXs, all of which can lead to the accumulation of L-ROS and further ferroptosis of cells (67, 68). The inhibition of ferroptosis can promote the development of tumors, resulting in resistance to several types of chemotherapy (69–71).

Reversing the inhibited cell death mode, developing new cell death modes, and inducing cell death are important means to overcome chemoresistance. Various compounds from TCM have been proven to target a variety of cell death modes and reverse the drug resistance induced by chemotherapy drugs. For instance, the combination of artesunate and autophagy inhibition blocked the protective effect of artesunate-induced autophagy on CRC cells and enhanced the apoptosis induced by artesunate (72). *Zuojinwan* induced apoptosis of HCT116 cells by the PI3K-Akt-signaling pathway (73). Curcumin upregulates CDX2, thereby inhibiting the Wnt/β-catenin signaling pathway and downregulating the anti-apoptosis signaling. This event ultimately results in reduced cell viability and apoptosis of human colon adenocarcinoma cell SW620 (74–77). Pien Tze Huang inhibits STAT3 and the Notch1 pathways and promotes apoptosis of CRC cells (78, 79). *Sanguisorba officinalis L.* inhibits the Wnt/β-catenin pathway, downregulates Bcl-2 protein, upregulates pro-apoptotic proteins such as Bax, and inhibits the growth and metastasis of 5-FU-resistant CRC (80). Moreover, cisplatin is a known apoptosis inducer. The combined use of the compound kushen injection and cisplatin enhances cell death of SW480 by inducing exogenous apoptosis (46, 68).

Several studies have reported that Chinese medicinal compounds and their active ingredients are involved in the induction and inhibition of autophagy of cancer cells. Autophagy works by inhibiting tumor growth through the removal of damaged organelles and the induction of autophagy under appropriate conditions. *Reynoutria japonica* Houtt. extracts induce autophagy and promote the apoptosis of cisplatin-resistant cancer cells (81). *A. carmichaelii* Debeaux induces apoptosis and autophagy, thereby reversing multidrug resistance (82). The treatment of CRC cells with T33, a compound of Chinese medicine, caused changes in autophagy markers, the activation of autophagy, inhibition of tumor proliferation, and reduction in the transplanted tumor volume (83). At the same time, autophagy is also a protective response to DNA damage after drug treatment (84, 85). The increase in the expression of the autophagy gene enhances the vitality of cancer cells and prevents cancer cells from entering apoptosis (72, 86). Moreover, it exhibits a protective effect on cells, resulting in autophagy-dependent chemotherapy resistance (60). It has been reported that resveratrol and epigallocatechin gallate (EGCG), the active ingredient of green tea, enhanced cell death by blocking the drug-induced protective autophagy flux and demonstrated synergistic anticancer effect, thereby overcoming drug resistance (87–89). Flavonoids from *S. baicalensis* Georgi inhibited autophagy, promoted cell apoptosis, and exerted anti-CRC activity by regulating the ATF4/sestrin2 pathway (90). *Sophora flavescens* Aiton extract activated the AMPK/mTOR pathway, increased the autophagy flux of colon cancer, and induced apoptosis (91).

Ferroptosis-assisted reverse chemotherapy resistance can be achieved by regulating the GPX4 pathway, iron metabolism pathway, and lipid metabolism pathway (69, 92). Genome analysis revealed that HMOX1, TP53, and ACSL5 were significantly upregulated in activated ferroptosis. This phenomenon was recorded in *Andrographis paniculata*-mediated CRC chemical sensitivity to 5-FU (93). *Camellia nitidissima* C. W. Chi decreased the expression of GPX4 and increased the expression of HMOX1 *in vivo* and *in vitro*. It also induced ferroptosis to inhibit CRC progress (94). β-elemene, a zedoary turmeric extract, induced ferroptosis through iron-dependent ROS accumulation, GSH consumption, and upregulation of transferrin. The downregulation of negative regulatory proteins of ferroptosis such as GPX4 and GLS, when combined with cetuximab, sensitized KRAS mutant CRC cells (95). Auriculasin isolated from *Flemingia philippinensis* promoted ROS production, accumulated intracellular Fe^{2+}, and induced CRC ferroptosis in a concentration-dependent manner (96). MAP30 isolated from *Momordica charantia* seeds along with cisplatin stimulated cytoplasmic oxidative stress and ROS accumulation, induced ferroptosis, and mediated cancer cell death by increasing intracellular Ca^{2+}, thereby exhibiting effective anticancer and chemoresistance effects (97). Glycyrrhetinic acid nanoparticles increased the ROS level in CRC cells by downregulating GPX4 and enhancing Fe-dependent cytotoxicity to kill CRC cells by Fenton reaction (98).

2.4 Drug inactivation and target changes

5-FU is the cornerstone of first-line CRC therapy. However, clinical resistance to 5-FU and its derivatives remains a challenge in CRC treatment (36) (Figure 4). *In vivo*, 5-FU is transformed into FU deoxynucleotide (F-duMP) *via* the OPRT-RR and TP-TK pathways, inhibiting thymidylate synthase (TS), preventing dUMP methylation to dTMP, inhibiting DNA synthesis, and arresting the cell cycle in the S phase (7). Several studies have reported that gene polymorphism and TS upregulation in CRC are closely related to 5-FU tolerance (7, 99, 100). Thymidine phosphorylase (TP) is upregulated in CRC, which has a poor prognosis. Capecitabine is one of the most active oral fluoropyrimidines. Capecitabine has no cytotoxicity as a precursor of 5-FU, and it is activated by TP to become cytotoxic 5-FU; hence, its adverse reactions are mild and manageable (101). Increasing TP expression is required for chemotherapy drugs such as capecitabine to exert an anti-tumor effect. However, TP has significant angiogenic activities and anti-apoptosis properties, which promote tumor growth and metastasis (102, 103). A TP inhibitor eliminates the tumorigenic effect of TP and the activation of capecitabine. The dual nature of TP also affects chemical resistance. TAS-102 is an oral FU preparation composed of trifluoropyridine (TFT) and thymidine phosphorylation inhibitor (TPI) (104). TFT can inhibit TS from hindering DNA synthesis, but it can also induce DNA damage and demonstrate a cytotoxic effect by doping its metabolites into DNA. In addition, a TP inhibitor prevents TFT degradation by TP and ensures the TFT biological activity (105). This unique action mechanism makes it suitable for patients with CRC with 5-FU and OXA resistance, hence it can be employed in the clinical treatment of metastatic CRC (106).

5-FU is excreted before getting metabolized to dihydrofluorouracil by dihydropyrimidine dehydrogenase (DPD). A high DPD activity makes 5-FU inactive and tolerant (107, 108). Past studies have demonstrated that using DPD inhibitors to downregulate

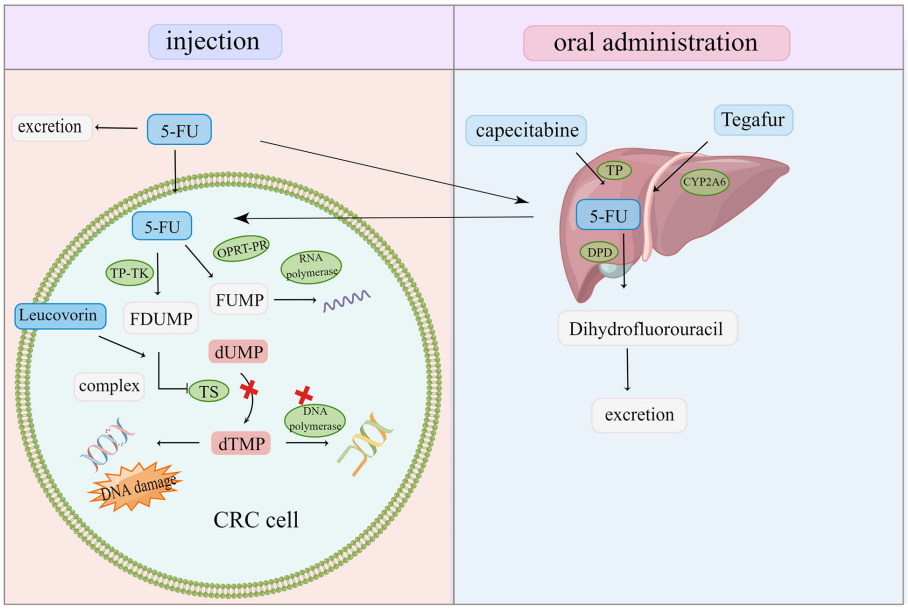

FIGURE 4
Oral and injected chemotherapeutic drugs are transformed into cytotoxic compounds after being activated and metabolized by various enzymes in the body. Once the target is changed and the drug is inactivated, CRC cells escape and become resistant to chemotherapy drugs.

DPD in CRC and increase 5-FU bioavailability can effectively reverse 5-FU resistance (109). However, the toxicity of 5-FU caused by low DPD activity renders chemotherapy unsustainable (110).

The CYP450 enzyme mediates the inactivation of several anticancer drugs and the activation of precursor drugs. The overexpression of CYP450 subtypes such as CYP3A4 and CYP3A5 in tumor cells renders chemotherapy drugs, such as irinotecan, ineffective, resulting in chemical resistance (111, 112). CYP1A2 and CYP2A6 were significantly upregulated in 5-FU-resistant CRC cells, while the combination of CYP450 inhibitors restored 5-FU cytotoxicity (113).

GSH-transferase (GST) catalyzes the combination of drugs with GSH and excretes it *via* bile/urine, causing it to detoxify and inactivate, thereby reducing the efficacy of chemotherapy drugs (7). GST overexpression and gene polymorphism are linked to cancer progression and resistance to chemotherapeutic drugs such as OXA (114, 115). Its inhibitor should therefore be administered to boost chemotherapy's curative effect and alleviate drug resistance.

The overexpression of TS desensitizes CRC to 5-FU drugs, and the overexpression of drug metabolic enzymes such as the CYP450 enzyme inactivates chemotherapeutic drug metabolism, allowing tumor cells to escape. Inhibiting drug target upregulation and lowering drug metabolic inactivation are essential approaches to increase chemotherapeutic sensitivity. Anti-tumor active ingredients derived from traditional Chinese medicinal plants and animals are gaining popularity. By inhibiting TS, formula HQGGT enhanced the toxic effect of 5-FU on 5-FU-resistant CRC cells and decreased tumor growth *in vivo* (116). *Venenum bufonis* extract degrades TS by the proteasome to limit TS expression, induce DNA damage, and hinder tumor cell proliferation (117). The expression of drug resistance-related genes TS and DPD in CRC cells was significantly downregulated after treatment with the formula GCFF, and 5-FU cooperated with the inhibition of cancer cell proliferation (118). *Coptidis rhizoma* extract can be utilized as an adjuvant to assist 5-FU in significantly inhibiting TS activity overexpressed in HCT116/R cells (119). Apigenin inhibited the TS expression and activity in 5-FU-resistant HCT116 cells as well as improved the 5-FU's therapeutic efficacy on CRC (100). Emodin exists in a variety of herbs. It has been reported that emodin may raise the expression of TP mRNA and protein in cancer cells treated with capecitabine, enhancing capecitabine activation, and downregulating Rad51 and ERCC1, as well as cooperating with capecitabine-induced cytotoxicity (120). *S. baicalensis Georgi*, *S. flavescens*, and *Schisandra chinensis* (Turcz.) Baill. extracts significantly inhibited cytochrome P450 subtype activity in human liver microsomes (121–124). *Curcumae rhizoma* and *Arisaematis Rhizoma Preparatum* are two Chinese medicinal plants that have considerate inhibitory effects on CYP3A4 (125).

2.5 Epithelial-mesenchymal transition

Epithelial-mesenchymal transition (EMT) is a reversible process in which polar epithelial cells lose the adhesion polarity of the basement membrane and the ability of the tight junction and cell adhesion due to the action of some factors, transforming the cells into mesenchymal cells that are capable of infiltration and migration (126). EMT in several physiological and pathological processes including wound healing, nerve development, and cancer cell metastasis. EMT is involved in several signaling pathways, which include the Notch, Wnt, and TGF-β signaling pathways (127).The changes in epithelial gene markers like E-cadherin and ZO-1 as well as mesenchymal gene markers such as N-cadherin indicate the occurrence of EMT. In recent years, the relationship between EMT and MDR has grown stronger (Figure 5). It was found that silencing

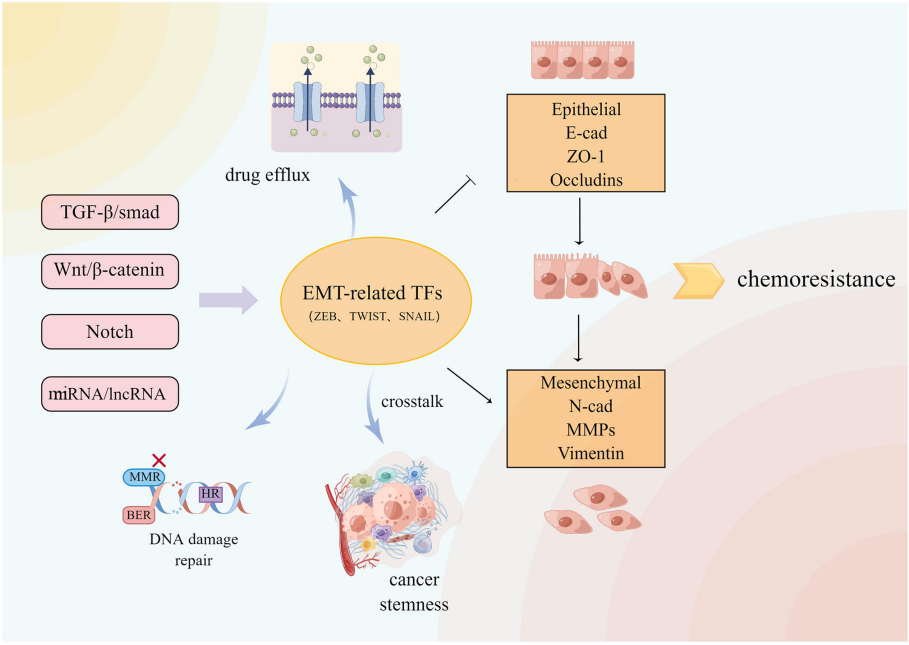

FIGURE 5
A variety of signal pathways regulate EMT-related transcription factors and downstream related pathways. EMT and crosstalk with TME, DNA damage repair and so on cause CRC resistance.

the E-cadherin expression altered the chemoresistance of various CRC cell lines to irinotecan and oxaliplatin (128). EMT induced by the hERG1 ion channel reduces cancer cell sensitivity to cisplatin (129). BMAL1 knockdown increases the expression of epithelial markers in CRC cell lines while decreasing the expression of mesenchymal markers, maintains the balance between epithelium and mesenchymal, stabilizes cancer cells in the epithelial characteristic state, inhibits EMT, and reduces the chemical resistance of colon cancer cells (130). Inhibiting the Wnt signaling pathway delays the progress of EMT and reverses CRC chemical resistance to 5-FU (41). The EMT-induced protein ZEB2 promotes oxaliplatin resistance in CRC by activating the nucleotide excision repair genes *ERCC1* and *ERCC4* (131).

Cancer chemoresistance is frequently accompanied by EMT, which generates chemical resistance either directly or indirectly, although the mechanism by which EMT drives chemoresistance remains elusive. EMT-mediated chemoresistance is closely related to ABC transporter, tumor microenvironment, and cancer stem cells (CSC). The ABC transporter gene promoter contains the binding sites for EMT transcription factors such as Snail and ZEB. The overexpression of these sites increases the transporter promoter activity in cancer cells, resulting in transporter overexpression and drug efflux (132). EMT cells contain stem cell-like characteristics similar to CSCs in signal pathways and chemoresistance phenotype (133). The FBXW7-ZEB2 axis connects EMT with the tumor microenvironment to promote stem cells and CRC chemoresistance (134). Cancer-associated fibroblasts (CAFs) in the tumor microenvironment can activate Wnt/β-catenin and promote CRC stemness and 5-FU/L-OHP resistance by secreting exosome miR-92a-3p and transferring it into CRC cells (135). Although it is unclear how EMT contributes to chemoresistance, it is evident that inhibiting EMT is an effective measure to reverse chemoresistance and inhibit tumor growth and metastasis.

TCM and its extracts have had a robust response in this regard. Curcumin can reverse 5-FU resistance in CRC cells by regulating the TET1-NKD-Wnt signaling pathway and inhibiting EMT progression, as well as inhibiting the TGF-β/Smad2/3 signaling pathway and reversing OXA resistance in CRC (136, 137). Curcumin can also sensitize 5-FU-resistant cells by upregulating EMT inhibitory miRNA and downregulating BMI1 and other *EMT* genes (138). Cinnamaldehyde, derived from *Cinnamomum cassia*, can inhibit the Wnt/β-catenin pathway induced by hypoxia in conjunction with oxaliplatin, reverse EMT and CRC cells dryness, and improve CRC sensitivity to OXA (139). *S. officinalis L.* blocked the Wnt pathway, which inhibited the proliferation and metastasis of 5-FU-resistant CRC by downregulating N-cadherin, vimentin, and snail protein and upregulating E-cadherin (80). Danshensu inhibits platelet-induced EMT transformation and chemoresistance in CRC cells (140). Jiedu Sangen Decoction inhibits the AKT/GSK-3β signaling pathway, thereby reversing EMT (141, 142). Resveratrol strongly inhibited the formation of EMT and CSC induced by TNF-β, downregulated cancer-promoting factors such as vimentin and slug, upregulated E-cadherin and claudin-2, increased the tight junction and cell adhesion, inhibited NF-κB activation, and increased 5-FU sensitivity in 5-FU-resistant CRC (143, 144). Resveratrol can also inhibit the EMT progression in LoVo cells *via* the TGF-β1/Smads pathway (145). Quercetin inhibits TGF-β1-induced EMT by inhibiting Twist1 and regulating E-cadherin (146). β-element combined with cetuximab promoted the epithelial marker expression, decreased mesenchymal gene marker expression, inhibited EMT, re-sensitized KRAS mutant CRC cells against EGFR antibody therapy, and inhibited cancer cell migration (95). By promoting the miR-134 expression, astragaloside IV could downregulate the CREB1 signaling pathway, inhibit EMT, and increase the sensitivity of CRC to OXA (147).

2.6 Tumor microenvironment

The mechanism of the tumor microenvironment (TME) in the MDR phenotype is becoming clearer. TME is an extremely complex ecosystem composed of tumor-associated macrophages (TAM), immune cells, cancer-associated fibroblasts (CAFs), and other non-cellular components such as secretory products and extracellular matrix (148). The cells and molecules in the tumor microenvironment can be exploited to maintain tumor immunosuppression and to promote immune escape, invasion, and treatment resistance. Cell components enhance tumor drug resistance by recruiting and secreting a variety of protective cytokines; non-cellular components, such as extracellular matrix (ECM) and hypoxia, can mediate drug resistance by building physical barriers and affecting tumor cell growth and metabolism (149–151). TAM secretes IL-6 and MFG-E8, respectively, activates the IL-6R/STAT3 and Hedgehog pathways, induces CSCs, and shields CSCs from the cytotoxic effects of 5-FU and cisplatin, resulting in treatment resistance and recurrence (152–154). CAFs transfer exosomes miR-92a-3p and lncRNA H19 into CRC cells, activate Wnt/β-catenin, mediate EMT, and promote CRC stemness and 5-FU/OXA resistance (135, 155). The hypoxic HOTAIR/miR-1277-5p/ZEB1 axis mediated oxaliplatin resistance in CRC (156, 157). Hypoxia can also interact with other mechanisms, such as activating cytochrome P450 subtype CYP3A6 and accelerating drug metabolism; it can also induce ABC transporter upregulation and promote drug efflux (158). Drugs' effects are opposed and limited due to the intricacy of the tumor microenvironment. The therapeutic scheme targeting tumor microenvironment is becoming one of the most promising anti-cancer strategies in the future as our understanding of it grows (Figure 6).

TCM has been proven in studies to regulate TME-related molecular mechanisms and serve an anti-tumor role (157). Curcumin can enhance the FOLFOX's cytotoxic effect on colon cancer by regulating EGFR and IGF-1R (159). Formula PHY906 can increase CPT-11's anti-tumor activity by reducing neutrophil or macrophage infiltration, TNF-α expression, and pro-inflammatory cytokine concentrations, inhibiting NF-κB and lowering irinotecan (CPT-11)'s gastrointestinal toxicity (160). Gegen Qinlian Decoction combined with PD-1 inhibitor could significantly increase CD8+T cells in the peripheral blood and tumor tissues, reshaped the tumor microenvironment, inhibited immune checkpoint, and effectively restored the T cell functions (161). Ginsenosides can regulate the quantity and function of bone marrow immunosuppressive agents, enhance the body's anti-cancer ability, and inhibit cancer cell growth, metastasis, and recurrence in a tumor microenvironment (162). When CRC cells are in the hypoxia microenvironment, tanshinone IIA inhibits angiogenesis by targeting TGF-β1 and inhibiting the HIF-1α/β-Catenin/VEGF pathway (163). Resveratrol inhibits tumor stem cell-like phenotype induced by TNF-β and increases chemotherapy sensitivity (144). Pien Tze Huang inhibited the Notch1 pathway *in vivo* to negatively regulate CSCs characteristics, prevent spheroid formation, and diminish tumorigenicity (78). The water extract of Huaier can inhibit the proliferation of CRC stem cells by downregulating the Wnt/β-catenin pathway (164). Berberine, an immunological checkpoint inhibitor, can enhance the immunity of tumor-infiltrating T cells, activate regulatory T cells, and diminish immunosuppressive myeloid-derived suppressor cells (MDSC) (165). Andrographolide, in combination with a PD-1 inhibitor, improved the function of CD4 and CD8 T cells, affected the expression of T cell-related markers, and inhibited the growth of CRC (166). Gallic acid combined with anti-PD-1 antibody can block PD-L1/PD-1 signal transduction, downregulate Foxp3 stability, inhibit regulatory T cells, promote CD8 T cells to secrete IFN-γ, and limit CRC (167). Nano-drugs containing ursolic acid and lentinan can destroy immunogenic cells, promote dendritic cell maturation, repolarize TAM into anti-

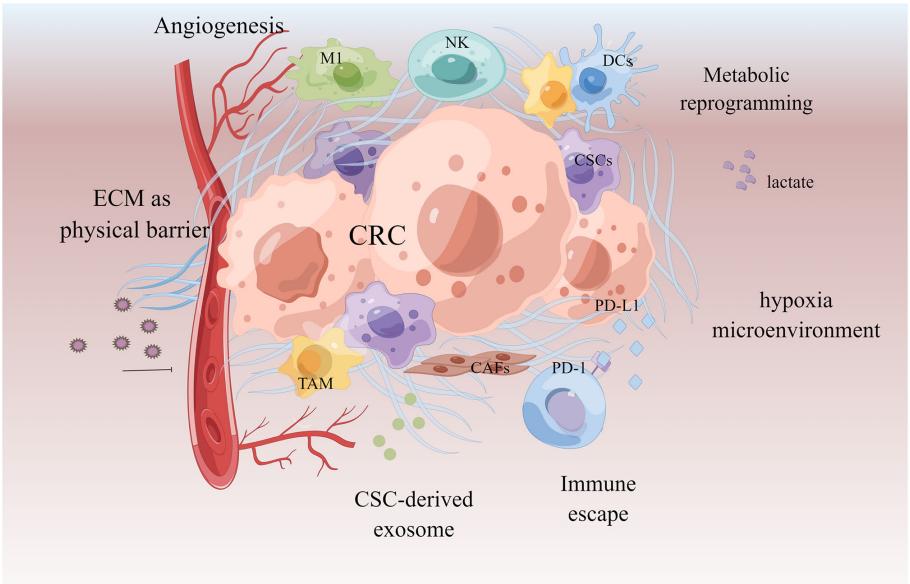

FIGURE 6
Tumor microenvironment in chemoresistant CRC. Extracellular matrix acts as a physical barrier to prevent drugs from entering. The microenvironment of the formation of new blood vessels, hypoxia and acidification contributes to chemoresistance. Cancer-associated fibroblasts (CAFs) and cancer stem cells (CSCs) promote tumor by secreting tumor growth factors and exosomes. Immune cells acquire immunosuppressive phenotype to make the tumor escape.

tumor M1 type, reshape immunosuppressive TME, and render it sensitive to immunotherapy (168).

2.7 Epigenetic modifications

Despite the continuous development of treatment modalities, chemoresistance remains the most significant barrier to the curative treatment of various cancers, while epigenetics modification also plays a key role in the occurrence and development of chemotherapy resistance in tumors (Figure 7). Epigenetic modification influences cancer cell proliferation, metabolism, and metastasis, leading to anti-cancer drug resistance (169, 170). Histone alteration, such as methylation and deacetylation, interferes with the efficacy of drugs by regulating the expression of multidrug efflux transporters, drug-metabolizing enzymes, and drug targets (171–178). In addition, by regulating DNA damage repair, cancer stem cells, and tumor microenvironment, epigenetic modification protects cells against drug-mediated cell death (179–181). Currently, the emergence of several epigenetic inhibitors, such as DNA methyltransferase inhibitors and histone methyltransferase inhibitors, may make epigenetics a viable treatment strategy for reversing CRC drug resistance. When compared to traditional chemotherapy drugs, epigenetics drugs offer certain hope, although several problems still need to be addressed. DNMT inhibitors azacytidine and decitabine can cause bone marrow suppression and trigger gastrointestinal reactions (182). The performance of natural compounds in inhibiting epigenetic changes attracts people's attention.

Curcumin has several epigenetic inhibitory activities. *In vivo* and *in vitro*, it can suppress the activity and expression of histone deacetylases in CRC, and reactivate the tumor suppressor gene *RARβ* (183, 184). Curcumin can be utilized to inhibit DNA methyltransferase, demethylate DNA, reverse decitabine tolerance in CRC (185). The combination of emodin and decitabine can significantly increase DNMT1 and DNMT3a expressions, improve the demethylation of tumor suppressor genes *P16*, *RASSF1A*, and *ppENK*, and play an anti-cancer role (186). Cinnamic acid derivatives inhibit histone deacetylase, which causes CRC cell death (187). Berberine lowered m6A *via* inhibiting β-catenin and increased FTO expression, which suppressed the stemness and tumorigenicity of CSCs in CRC (188). BBR binds to CSN5, blocking its ubiquitination activity, causing PD-L1 to be ubiquitinated and degraded, and preventing cancer cells from passing through immune checkpoints (165). Aidi injection inhibits ubiquitin-proteasome system activity, diminishes cytotoxic protein degradation, and targets mitochondrial apoptosis (189). TCM can target epigenetic modification, transform CRC into a therapeutic response, and prevent or overcome chemoresistance.

2.8 Other mechanisms

Tumor metabolic abnormalities are considered the new hallmark of cancer therapy (190). Metabolic reprogramming, which involves lipid metabolism, oxidative stress, mitochondrial metabolism, and glycolysis, is significant in cancer chemoresistance (191–194). Chemoresistance mediated by tumor metabolic changes is closely related to TME and epigenetic modifications. The high expression of the methylated protein YTHDF1 promotes the high expression and activity of transglutaminase 1, resulting in CRC's tolerance to cisplatin (177). The methylation of histone causes glutamine

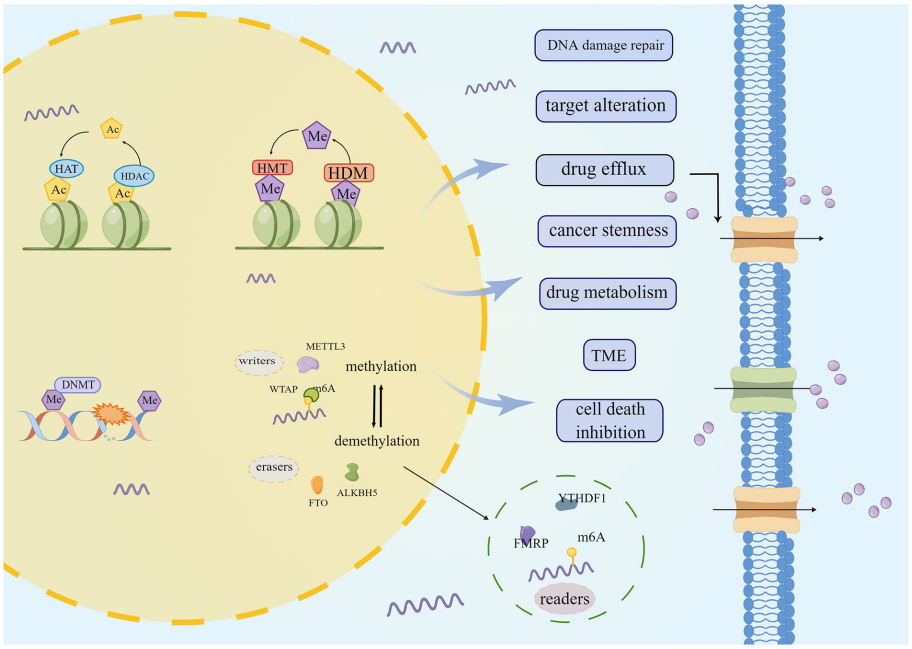

FIGURE 7
The role of epigenetic modification in chemoresistant CRC. DNA methylation, RNA methylation, histone methylation, deacetylation, etc., lead to CRC chemoesistance by promoting drug efflux, changing drug metabolism and cell death and other ways.

synthetase (GS) to be upregulated in adipocytes, and the resultant rise in the glutamine level is a potential resistance mechanism in patients with CRC to 5-FU (195). HIF-1α-induced glucose metabolism reprogramming confers 5-FU resistance to CRC cells (196). The application of drugs and small molecular compounds targeting the abnormal metabolism of tumors plays a decisive role in reversing the tolerance of traditional chemotherapy drugs and inhibiting the growth of tumors, which is the future of cancer treatment.

TCM, as an alternative and complementary medicine, has also demonstrated exceptional efficacy in regulating abnormal tumor metabolism. Moreover, natural compounds have fewer side effects while inhibiting the growth of cancer cells. By downregulating HIF-1α, Worenine and Matrine could reverse the Warburg effect and inhibit the growth of CRC cells (197, 198). Kaempferol upregulates miR-326-hnRNPA1, inhibits glycolysis mediated by PKM2, and reverses tolerance to 5-Fu in CRC (199). Jiedu Sangen decoction inhibits glycolysis in CRC by regulating the PI3K/AKT/HIF-1α signaling pathway and restoring 5-FU sensitivity (200). RA-XII is extracted from *Rubia yunnanensis* Diels and it inhibits CRC by inhibiting fatty acid synthesis (201).

The role of microbes in regulating drug metabolism is becoming increasingly clear with time. It is also established that microbes play an important role in cancer development and treatment resistance. UroA, a microbial metabolite, can inhibit ABC transporters by regulating the FOXO3-FOXM1 axis and sensitizing 5-FU-resistant CRC (202). *Lactobacillus plantarum* metabolites restored SMCT1 expression and function in 5-FU-resistant CRC cells, overcoming the double resistance of 5-FU and butyrate (203). The impairment of TGF-β signaling creates an intestinal flora imbalance and CRC resistance to 5-FU (204). Fusobacterium nucleatum promotes non-CSC lipid accumulation in CRC to achieve CSC characteristics, decreases lipid accumulation in CSC to allow it to self-renew, activates autophagy, and induces chemical resistance in CRC (205, 206). The intestinal flora can regulate the anticancer activity of oxaliplatin and cyclophosphamide and induce T-cell reaction and ROS production (207). The role of intestinal flora in chemical resistance is multifaceted, making it the guardian as well as the enemy.

Chinese herbal medicine is closely related to intestinal bacteria and plays a key role in cancer therapy. TCM influences the composition of intestinal flora, whereas intestinal microbes influence the metabolism of Chinese herbal medicines' active compounds. This interdependent relationship offers fresh possibilities for cancer treatment. Berberine has been demonstrated to inhibit *Fusobacterium nucleatum*, regulate intestinal flora composition, relieve immunosuppression, and inhibit CRC (208, 209). Wu pill can help prevent colitis-related CRC by regulating the intestinal microbiota (210). However, ferulic acid needs to be metabolized by intestinal flora, and its product has stronger anti-cancer activity than its mother, which is used to treat chemical resistance CRC (211). Yi-Yi-Fu-Zi-Bai-Jiang-San has no direct inhibitory effect on CRC, but it significantly improves the intestinal bacteria composition and tumor immune infiltration of CRC tumor-bearing mice and inhibits the tumor growth after fecal bacteria transplantation treatment with the intestinal flora regulated by this compound (212).

3 Discussion

Enhancing treatment sensitivity or overcoming chemoresistance is a pressing issue in the field of cancer. Several studies have reported that TCM participates in inhibiting tumor growth and metastasis, improving tumor microenvironment, regulating cell death, inhibiting CRC progression, increasing the response of drug-resistant CRC to drug treatment, reducing toxic and side effects, improving prognosis, prolonging patient survival time (Table 1). TCM's auxiliary sensitizing effect on chemotherapy sensitivity is becoming increasingly essential and evident. TCM used in combination with anticancer drugs can increase anticancer drug intracellular accumulation, prevent the original drug tolerance mechanism or mediate a new cell death mechanism, modify the tumor microenvironment, relieve the immunosuppression, erase methylation, and other reversible modifications. We thus believe that TCM has a promising future as an alternative and complementary therapy for clinical cancer treatment, whether used alone or as a sensitizer to other anticancer drugs.

However, the components of TCM and compound prescription are complex, and it is difficult to fully clarify its mechanism. Different from TCM, modern medicine mainly starts from the occurrence and development of cancer in the treatment of cancer, and the treatment mechanism and targeted path are clear. A variety of targeted inhibitors or small molecule drugs have been developed to overcome the chemical resistance of traditional chemotherapy drugs, such as ABC transports inhibitors, iron death inducers, autophagy inhibitors, DNA methylation inhibitors, histone deacetylase inhibitors, etc., and corresponding clinical trials have been carried out. Although these targeted preparations have shown some promising clinical results, their side effects that cannot be ignored also limit their real clinical application. ABC transports has not been approved for the treatment of malignant tumors due to its non-targeted selective inhibition and individual differences (213). The stability and dosage of epigenetic drugs also make their effects in solid tumors need to be improved (214). Under the development trend of precision medicine,TCM's effective components have become the research focus for Chinese medicine combined with chemotherapy to reverse MDR. Presently, most TCM research on active compounds for reversing CRC MDR is mostly concentrated in flavonoids and phenols, with the greatest study in CRC in combination with traditional drugs (215). In reversing CRC multidrug resistance, Chinese medicine and its active ingredients offer both considerable potential and controversy. Different from the precise targeting characteristics of modern medicine, TCM has the characteristics of multi-component, multi-target and multi-stage in nature. For example, curcumin can inhibit DNA damage repair, inhibit EMT, down-regulate the expression and activity of HDAC and cooperate with DNA demethylation of azacytidine to reverse the resistance of decitabine and 5-FU. This feature also makes it difficult for TCM to create secondary drug resistance or even multi-drug resistance. However, because of the complex components and numerous targets of TCM and compound prescription, as well as the thinking theory and compatibility of dialectical administration in TCM theory, it is difficult to specify the exact method. Presently, the research on compound prescription is limited to a single component and mechanism and is primarily concentrated in a single extract, which does not reflect the TCM's theory of syndrome differentiation

TABLE 1 The main mechanisms of TCM to increase the sensitivity of chemical drugs.

Mechanisms	Chemotherapy Drugs	Type	Cell line	*In vivo or in vitro*	TCM
inhibit ABC transposters	Oxaliplatin	formula	HCT116	*in vivo*; *in vitro*	Gegen Qinlian Decoction (20)
		extract	HCT116	*in vivo*; *in vitro*	Evodiamine (29)
			SW620	*in vivo*; *in vitro*	Danshensu (140)
	5-FU	herb	HCT8	*in vitro*	*Scutellaria barbata* D. Don (22)
		extract	DLD1;HCT8; HCT116; FHC	*in vivo; in vitro*	cucurbitacin E (23)
	Paclitaxel; Adriamycin	extract	HCT8	*in vitro*	Neferine (26)
	Doxorubicin	extract	CaCo2	*in vitro*	*Arctium lappa* (27)
promote DNA damage and inhibit repair	Cisplatin	extract	HCT116	*in vivo*; *in vitro*	Shikonin (43)
		formula	HCT116; SW480	*in vitro*	Compound Kushen Injection (46)
	5-FU	extract	HCT116	*in vitro*	Curcumin (47)
promote cell death	radiation	extract	HT29	*in vivo*; *in vitro*	Curcumin (48)
	autophagy inhibitor	extract	HCT116	*in vivo*; *in vitro*	Artesunate (72)
	5-FU	extract	HCT116	*in vitro*	Curcumin (74, 75)
			HCT116; SW480	*in vivo*; *in vitro*	Andrographis (93)
		formula	HCT-8	*in vivo*; *in vitro*	Jiedu Sangen decoction (200)
	Capecitabine	extract	HCT116	*in vitro*	Curcumin (76)
	γ-radiation	extract	HCT116	*In vivo*; *in vitro*	Curcumin (77)
	Cetuximab	extract	HCT116; Lovo	*in vivo*; *in vitro*	β-elemene (95)
	anti-PD-L1 antibody	nanoparticles	HT29; Caco2; SW480	*in vivo*	Glycyrrhetinic acid (98)
inactive chemotherapy drug and change target	5-FU	extract	HCT116,	*in vitro*	Apigenin (100)
			HCT116	*in vitro*	*Coptidis Rhizoma* (119)
		formula	H63; MC38	*in vivo*; *in vitro*	Huang Qin Ge Gen Tang (116)
			LoVo	*in vitro*	Guan Chang Fu Fang (118)
Inhibit EMT	5-FU	herb	RKO; HCT15	*in vivo*; *in vitro*	*Sanguisorba officinalis* Linn (80).
		extract	HCT116	*in vitro*	Curcumin (136)
			HCT116; SW480	*in vivo*; *in vitro*	Curcumin (138)
				in vitro	Resveratrol (143)
			HCT116	*in vitro*	Resveratrol (144)
	Oxaliplatin	extract	HCT116; SW480	*in vivo*; *in vitro*	Cinnamaldehyde (139)
			SW620	*in vivo*; *in vitro*	Danshensu (140)
			SW480	*in vitro*	astragaloside IV (147)
Improve tumor mircoenvironment	5-FU; Oxaliplatin	extract	HCT116; HT29	*in vitro*	Curcumin (159)
	PD-1 inhibitor	formula	CT26	*in vitro*	Gegen Qinlian decoction (151) (208)
		extract	CT26	*in vivo*; *in vitro*	Andrographolide (166)
			MC38	*in vivo*	gallic acid (167)

(Continued)

TABLE 1 Continued

Mechanisms	Chemotherapy Drugs	Type	Cell line	*In vivo or in vitro*	TCM
	angiogenesis inhibitor	extract	LoVo; HCT116; HT29; SW620	*in vivo*; *in vitro*	tanshinone IIA (163)
	anti-CD47 antibody	self-assembled nanomedicine	CT26	*in vivo*	Lentinan- ursolic acid (168)
target epigenetic modification	Decitabine	extract	HCT116	*in vitro*	Curcumin (185)
	5-FU; SN38	extract	HCT116; HT29	*in vivo*; *in vitro*	Berberine (188)
	5-FU	extract	HCT8	*in vitro*	Kaempferol (199)
		formula	HCT8	*in vivo*; *in vitro*	Jiedu Sangen decoction (200)

and treatment, and the principle of compatibility among the monarch, minister assistant, and guide. Some scholars studied the optimal proportion of the main active ingredients of Aidi injection, namely cantharidin, calycosin-7-O-β-D-glucoside, ginsenoside Rc, and ginsenoside Rd, and discovered that the latter three can inhibit the degradation of cytotoxic proteins by inhibiting the activity of the ubiquitin-proteasome system, which is enhanced by cantharidin. Synergistic cantharidin can activate PP2A, activate mitochondrial apoptosis, and promote CRC cell death (189). This report fully demonstrates the scientific nature of the compatibility theory of TCM. The reasonable compatibility of TCM is also the subject of TCM modernization research. TCM research as a chemical sensitizer mainly focuses on cell and animal experiments or is based on *in vitro* research. Although several clinical trials of TCM for CRC have been conducted, there is still a lack of evident clinical randomized controlled trials, and it has not yet become the first line of clinical medication. Weak absorption, low solubility, bioavailability, and unknown side effects have always limited the development of TCM's global expansion. However, with the development of nanotechnologies, such as liposomes, nanoparticles, and bionic drug delivery systems, the abovementioned defects of active ingredients of TCM have gradually been addressed (216–219). It is critical to accelerate the transformation of TCM experimental research findings into clinical applications by conducting evidence-based medicine and component research to assess efficacy and safety. Currently, the establishment of the State Key Laboratory of Traditional Chinese Medicine Components and its component bank and the Food and Drug Administration's approval of clinical TCM research have all accelerated the pace of modern TCM research and development.

4 Conclusion and perspective

With an increasing incidence rate of CRC morbidity and mortality, the concerns related to CRC treatment include improving drug sensitivity and reversing chemoresistance. TCM can work in conjunction with anticancer medications to lessen side effects and boost effectiveness, boost intracellular anticancer drug accumulation, block initial drug tolerance, mediate cell death, enhance tumor microenvironment, relieve immunosuppression, erase methylation and other reversible modifications, and produce significant anticancer efficacy. TCM has shown great advantages in the process of increasing chemotherapy sensitivity with its multi-component, multi-target and multi-stage treatment characteristics different from modern medicine. We believe TCM has a promising future as an alternative and complementary therapy for clinical CRC treatment in developing new sensitizers to other anticancer drugs.

Author contributions

XL and XH contributed into the writing and revision of the manuscript. XY, YY and HZ draw figures and tables. All authors contributed to the article and approved the submitted version.

Funding

This work was funded by grants from the Administration of Traditional Chinese Medicine of Zhejiang Province, China (No.2021ZZ013 and No.2022ZX006).

Acknowledgments

The authors would like to thank all workers who participated in the article, as well as MJEditor (www.mjeditor.com) for providing English editing services and the authorization of Figdraw.

Conflict of interest

The authors declare that the research was conducted in the absence of any commercial or financial relationships that could be construed as a potential conflict of interest.

Publisher's note

References

1. Wang L, Lo CH, He X, Hang D, Wang M, Wu K, et al. Risk factor profiles differ for cancers of different regions of the colorectum. *Gastroenterol* (2020) 159(1):241–56 e13. doi: 10.1053/j.gastro.2020.03.054

2. Sung H, Ferlay J, Siegel RL, Laversanne M, Soerjomataram I, Jemal A, et al. Global cancer statistics 2020: GLOBOCAN estimates of incidence and mortality worldwide for 36 cancers in 185 countries. *CA Cancer J Clin* (2021) 71(3):209–49. doi: 10.3322/caac.21660

3. Dekker E, Tanis PJ, Vleugels JLA, Kasi PM, Wallace MB. Colorectal cancer. *Lancet* (2019) 394(10207):1467–80. doi: 10.1016/S0140-6736(19)32319-0

4. Wang KW, Dong M. Potential applications of artificial intelligence in colorectal polyps and cancer: Recent advances and prospects. *World J Gastroenterol* (2020) 26 (34):5090–100. doi: 10.3748/wjg.v26.i34.5090

5. Garcia-Alfonso P, Torres G, Garcia G, Gallego I, Ortega L, Sandoval C, et al. FOLFOXIRI plus biologics in advanced colorectal cancer. *Expert Opin Biol Ther* (2019) 19 (5):411–22. doi: 10.1080/14712598.2019.1595580

6. Satapathy SR, Sjolander A. Cysteinyl leukotriene receptor 1 promotes 5-fluorouracil resistance and resistance-derived stemness in colon cancer cells. *Cancer Lett* (2020) 488:50–62. doi: 10.1016/j.canlet.2020.05.023

7. Vodenkova S, Buchler T, Cervena K, Veskrnova V, Vodicka P, Vymetalkova V. 5-fluorouracil and other fluoropyrimidines in colorectal cancer: Past, present and future. *Pharmacol Ther* (2020) 206:107447. doi: 10.1016/j.pharmthera.2019.107447

8. Baird RD, Kaye SB. Drug resistance reversal–are we getting closer? *Eur J Cancer* (2003) 39(17):2450–61. doi: 10.1016/S0959-8049(03)00619-1

9. Xu JF, Wan Y, Tang F, Chen L, Yang Y, Xia J, et al. Emerging significance of ginsenosides as potentially reversal agents of chemoresistance in cancer therapy. *Front Pharmacol* (2021) 12:720474. doi: 10.3389/fphar.2021.720474

10. Newman DJ, Cragg GM. Natural products as sources of new drugs from 1981 to 2014. *J Nat Prod* (2016) 79(3):629–61. doi: 10.1021/acs.jnatprod.5b01055

11. Huang YF, Niu WB, Hu R, Wang LJ, Huang ZY, Ni SH, et al. Correction: FIBP knockdown attenuates growth and enhances chemotherapy in colorectal cancer *via* regulating GSK3beta-related pathways. *Oncogenesis* (2022) 11(1):36. doi: 10.1038/s41389-022-00407-5

12. Wang Y, Wang Y, Qin Z, Cai S, Yu L, Hu H, et al. The role of non-coding RNAs in ABC transporters regulation and their clinical implications of multidrug resistance in cancer. *Expert Opin Drug Metab Toxicol* (2021) 17(3):291–306. doi: 10.1080/17425255.2021.1887139

13. Hsu HH, Chen MC, Baskaran R, Lin YM, Day CH, Lin YJ, et al. Oxaliplatin resistance in colorectal cancer cells is mediated *via* activation of ABCG2 to alleviate ER stress induced apoptosis. *J Cell Physiol* (2018) 233(7):5458–67. doi: 10.1002/jcp.26406

14. Theile D, Wizgall P. Acquired ABC-transporter overexpression in cancer cells: transcriptional induction or Darwinian selection? *Naunyn Schmiedebergs Arch Pharmacol* (2021) 394(8):1621–32. doi: 10.1007/s00210-021-02112-3

15. Zhu Y, Huang S, Chen S, Chen J, Wang Z, Wang Y, et al. SOX2 promotes chemoresistance, cancer stem cells properties, and epithelial-mesenchymal transition by beta-catenin and Beclin1/autophagy signaling in colorectal cancer. *Cell Death Dis* (2021) 12(5):449. doi: 10.1038/s41419-021-03733-5

16. Abdallah HM, Al-Abd AM, El-Dine RS, El-Halawany AM. P-glycoprotein inhibitors of natural origin as potential tumor chemo-sensitizers: A review. *J Adv Res* (2015) 6(1):45–62. doi: 10.1016/j.jare.2014.11.008

17. Li W, Zhang H, Assaraf YG, Zhao K, Xu X, Xie J, et al. Overcoming ABC transporter-mediated multidrug resistance: Molecular mechanisms and novel therapeutic drug strategies. *Drug Resist Updat* (2016) 27:14–29. doi: 10.1016/j.drup.2016.05.001

18. Robey RW, Pluchino KM, Hall MD, Fojo AT, Bates SE, Gottesman MM. Revisiting the role of ABC transporters in multidrug-resistant cancer. *Nat Rev Cancer* (2018) 18 (7):452–64. doi: 10.1038/s41568-018-0005-8

19. Mohammad IS, He W, Yin L. Insight on multidrug resistance and nanomedicine approaches to overcome MDR. *Crit Rev Ther Drug Carrier Syst* (2020) 37(5):473–509. doi: 10.1615/CritRevTherDrugCarrierSyst.2020025052

20. Lin X, Xu L, Tan H, Zhang X, Shao H, Yao L, et al. The potential effects and mechanisms of gegen qinlian decoction in oxaliplatin-resistant colorectal cancer based on network pharmacology. *Heliyon* (2022) 8(11):e11305. doi: 10.1016/j.heliyon.2022.e11305

21. He Y, Wei Z, Xie Y, Yi X, Zeng Y, Li Y, et al. Potential synergic mechanism of wutou-gancao herb-pair by inhibiting efflux transporter p-glycoprotein. *J Pharm Anal* (2020) 10(2):178–86. doi: 10.1016/j.jpha.2019.09.004

22. Lin J, Feng J, Yang H, Yan Z, Li Q, Wei L, et al. Scutellaria barbata d. don inhibits 5-fluorouracil resistance in colorectal cancer by regulating PI3K/AKT pathway. *Oncol Rep* (2017) 38(4):2293–300. doi: 10.3892/or.2017.5892

23. Yang P, Liu W, Fu R, Ding GB, Amin S, Li Z. Cucurbitacin e chemosensitizes colorectal cancer cells via mitigating TFAP4/Wnt/beta-catenin signaling. *J Agric Food Chem* (2020) 68(48):14148–60. doi: 10.1021/acs.jafc.0c05551

24. Zhang S, Morris ME. Effect of the flavonoids biochanin a and silymarin on the p-glycoprotein-mediated transport of digoxin and vinblastine in human intestinal caco-2 cells. *Pharm Res* (2003) 20(8):1184–91. doi: 10.1023/A:1025044913766

25. Xiao Y, Xin L, Li L, Li G, Shi X, Ji G, et al. Quercetin and kaempferol increase the intestinal absorption of isorhamnetin coexisting in elaeagnus rhamnoides (L.) a. nelson (Elaeagnaceae) extracts *via* regulating multidrug resistance-associated protein 2. *Phytomedicine* (2019) 53:154–62. doi: 10.1016/j.phymed.2018.09.028

26. Kadioglu O, Law BYK, Mok SWF, Xu SW, Efferth T, Wong VKW. Mode of action analyses of neferine, a bisbenzylisoquinoline alkaloid of lotus (Nelumbo nucifera) against multidrug-resistant tumor cells. *Front Pharmacol* (2017) 8:238. doi: 10.3389/fphar.2017.00238

27. Su S, Cheng X, Wink M. Natural lignans from arctium lappa modulate p-glycoprotein efflux function in multidrug resistant cancer cells. *Phytomedicine* (2015) 22(2):301–7. doi: 10.1016/j.phymed.2014.12.009

28. Wei L, Chen P, Chen Y, Shen A, Chen H, Lin W, et al. Pien tze Huang suppresses the stem-like side population in colorectal cancer cells. *Mol Med Rep* (2014) 9(1):261–6. doi: 10.3892/mmr.2013.1760

29. Sui H, Zhou LH, Zhang YL, Huang JP, Liu X, Ji Q, et al. Evodiamine suppresses ABCG2 mediated drug resistance by inhibiting p50/p65 NF-kappaB pathway in colorectal cancer. *J Cell Biochem* (2016) 117(6):1471–81. doi: 10.1002/jcb.25451

30. Le MT, Hoang VN, Nguyen DN, Bui TH, Phan TV, Huynh PN, et al. Structure-based discovery of ABCG2 inhibitors: A homology protein-based pharmacophore modeling and molecular docking approach. *Molecules* (2021) 26(11). doi: 10.3390/molecules26113115

31. Tomasini PP, Guecheva TN, Leguisamo NM, Pericart S, Brunac AC, Hoffmann JS, et al. Analyzing the opportunities to target DNA double-strand breaks repair and replicative stress responses to improve therapeutic index of colorectal cancer. *Cancers (Basel)* (2021) 13(13). doi: 10.3390/cancers13133130

32. Wang M, Xie C. DNA Damage repair and current therapeutic approaches in gastric cancer: A comprehensive review. *Front Genet* (2022) 13:931866. doi: 10.3389/fgene.2022.931866

33. Wiegering A, Matthes N, Muhling B, Koospal M, Quenzer A, Peter S, et al. Reactivating p53 and inducing tumor apoptosis (RITA) enhances the response of RITA-sensitive colorectal cancer cells to chemotherapeutic agents 5-fluorouracil and oxaliplatin. *Neoplasia* (2017) 19(4):301–9. doi: 10.1016/j.neo.2017.01.007

34. Marin JJG, Macias RIR, Monte MJ, Herraez E, Peleteiro-Vigil A, Blas BS, et al. Cellular mechanisms accounting for the refractoriness of colorectal carcinoma to pharmacological treatment. *Cancers (Basel)* (2020) 12(9). doi: 10.1016/j.neo.2017.01.007

35. de Castro EGH, Jesuino Nogueira L, Bencke Grudzinski P, da Costa Ghignatti PV, Guecheva TN, Motta Leguisamo N, et al. Olaparib-mediated enhancement of 5-fluorouracil cytotoxicity in mismatch repair deficient colorectal cancer cells. *BMC Cancer* (2021) 21(1):448. doi: 10.1186/s12885-021-08188-7

36. Sethy C, Kundu CN. 5-fluorouracil (5-FU) resistance and the new strategy to enhance the sensitivity against cancer: Implication of DNA repair inhibition. *BioMed Pharmacother* (2021) 137:111285. doi: 10.1016/j.biopha.2021.111285

37. Xian C, Chen H, Xiong F, Fang Y, Huang H, Wu J. Platinum-based chemotherapy *via* nanocarriers and co-delivery of multiple drugs. *Biomater Sci* (2021) 9(18):6023–36. doi: 10.1039/D1BM00879J

38. Koberle B, Schoch S. Platinum complexes in colorectal cancer and other solid tumors. *Cancers (Basel)* (2021) 13(9). doi: 10.3390/cancers13092073

39. Qu J, Sun Z, Peng C, Li D, Yan W, Xu Z, et al. C. tropicalis promotes chemotherapy resistance in colon cancer through increasing lactate production to regulate the mismatch repair system. *Int J Biol Sci* (2021) 17(11):2756–69. doi: 10.7150/ijbs.59262

40. Huang W, Tang H, Wen F, Lu X, Li Q, Shu P. Jianpi-yangwei decoction inhibits DNA damage repair in the drug resistance of gastric cancer by reducing FEN1 expression. *BMC Complement Med Ther* (2020) 20(1):196. doi: 10.1186/s12906-020-02983-8

41. Liu Y, Yang S, Wang K, Lu J, Bao X, Wang R, et al. Cellular senescence and cancer: Focusing on traditional Chinese medicine and natural products. *Cell Prolif* (2020) 53(10): e12894. doi: 10.1111/cpr.12894

42. Wang XL, Lin FL, Xu W, Wang C, Wang QQ, Jiang RW. Silybin b exerts protective effect on cisplatin-induced neurotoxicity by alleviating DNA damage and apoptosis. *J Ethnopharmacol* (2022) 288:114938. doi: 10.1016/j.jep.2021.114938

43. He G, He G, Zhou R, Pi Z, Zhu T, Jiang L, et al. Enhancement of cisplatin-induced colon cancer cells apoptosis by shikonin, a natural inducer of ROS *in vitro* and in vivo. *Biochem Biophys Res Commun* (2016) 469(4):1075–82. doi: 10.1016/j.bbrc.2015.12.100

44. Cui J, Qu Z, Harata-Lee Y, Nwe Aung T, Shen H, Wang W, et al. Cell cycle, energy metabolism and DNA repair pathways in cancer cells are suppressed by compound kushen injection. *BMC Cancer* (2019) 19(1):103. doi: 10.1186/s12885-018-5230-8

45. Zhang W, Gong W, He X, Wu C, Tu X. A systematic review and meta-analysis on the efficacy of compound kushen injection in 3 kinds of digestive tract tumor. *J Gastrointest Oncol* (2021) 12(6):2919–29. doi: 10.21037/jgo-21-774

46. Wu X, Lu Y, Qin X. Combination of compound kushen injection and cisplatin shows synergistic antitumor activity in p53-R273H/P309S mutant colorectal cancer cells through inducing apoptosis. *J Ethnopharmacol* (2022) 283:114690. doi: 10.1016/j.jep.2021.114690

47. Shakibaei M, Buhrmann C, Kraehe P, Shayan P, Lueders C, Goel A. Curcumin chemosensitizes 5-fluorouracil resistant MMR-deficient human colon cancer cells in high density cultures. *PloS One* (2014) 9(1):e85397. doi: 10.1371/journal.pone.0085397

48. Yang G, Qiu J, Wang D, Tao Y, Song Y, Wang H, et al. Traditional Chinese medicine curcumin sensitizes human colon cancer to radiation by altering the expression of DNA repair-related genes. *Anticancer Res* (2018) 38(1):131–6. doi: 10.21873/anticanres.12200

49. Li T, Pan DB, Pang QQ, Zhou M, Yao XJ, Yao XS, et al. Diarylheptanoid analogues from the rhizomes of zingiber officinale and their anti-tumour activity. *RSC Adv* (2021) 11 (47):29376–84. doi: 10.1039/D1RA03592D

50. Ni L, Li Z, Ren H, Kong L, Chen X, Xiong M, et al. Berberine inhibits non-small cell lung cancer cell growth through repressing DNA repair and replication rather than through apoptosis. *Clin Exp Pharmacol Physiol* (2022) 49(1):134–44. doi: 10.1111/1440-1681.13582

51. Liu T, Zuo L, Guo D, Chai X, Xu J, Cui Z, et al. Ginsenoside Rg3 regulates DNA damage in non-small cell lung cancer cells by activating VRK1/P53BP1 pathway. *BioMed Pharmacother* (2019) 120:109483. doi: 10.1016/j.biopha.2019.109483

52. Wei C, Deng X, Gao S, Wan X, Chen J. Cantharidin inhibits proliferation of liver cancer by inducing DNA damage *via* KDM4A-dependent histone H3K36 demethylation. *Evid Based Complement Alternat Med* (2022) 2022:2197071. doi: 10.1155/2022/2197071

53. Alberti P. Platinum-drugs induced peripheral neurotoxicity: Clinical course and preclinical evidence. *Expert Opin Drug Metab Toxicol* (2019) 15(6):487–97. doi: 10.1080/17425255.2019.1622679

54. Staff NP, Cavaletti G, Islam B, Lustberg M, Psimaras D, Tamburin S. Platinum-induced peripheral neurotoxicity: From pathogenesis to treatment. *J Peripher Nerv Syst* (2019) 24 Suppl 2:S26–39. doi: 10.1111/jns.12335

55. Su Z, Yang Z, Xu Y, Chen Y, Yu Q. Apoptosis, autophagy, necroptosis, and cancer metastasis. *Mol Cancer* (2015) 14:48. doi: 10.1186/s12943-015-0321-5

56. Bedoui S, Herold MJ, Strasser A. Emerging connectivity of programmed cell death pathways and its physiological implications. *Nat Rev Mol Cell Biol* (2020) 21(11):678–95. doi: 10.1038/s41580-020-0270-8

57. Li X, He S, Ma B. Autophagy and autophagy-related proteins in cancer. *Mol Cancer* (2020) 19(1):12. doi: 10.1186/s12943-020-1138-4

58. Ferro F, Servais S, Besson P, Roger S, Dumas JF, Brisson L. Autophagy and mitophagy in cancer metabolic remodelling. *Semin Cell Dev Biol* (2020) 98:129–38. doi: 10.1016/j.semcdb.2019.05.029

59. Li YJ, Lei YH, Yao N, Wang CR, Hu N, Ye WC, et al. Autophagy and multidrug resistance in cancer. *Chin J Cancer* (2017) 36(1):52. doi: 10.1186/s40880-017-0219-2

60. Zamame Ramirez JA, Romagnoli GG, Kaneno R. Inhibiting autophagy to prevent drug resistance and improve anti-tumor therapy. *Life Sci* (2021) 265:118745. doi: 10.1016/j.lfs.2020.118745

61. Kashyap D, Garg VK, Goel N. Intrinsic and extrinsic pathways of apoptosis: Role in cancer development and prognosis. *Adv Protein Chem Struct Biol* (2021) 125:73–120. doi: 10.1016/bs.apcsb.2021.01.003

62. Samanta D, Huang TY, Shah R, Yang Y, Pan F, Semenza GL. BIRC2 expression impairs anti-cancer immunity and immunotherapy efficacy. *Cell Rep* (2020) 32(8):108073. doi: 10.1016/j.celrep.2020.108073

63. Carneiro BA, El-Deiry WS. Targeting apoptosis in cancer therapy. *Nat Rev Clin Oncol* (2020) 17(7):395–417. doi: 10.1038/s41571-020-0341-y

64. Balaji S, Terrero D, Tiwari AK, Ashby CRJr., Raman D. Alternative approaches to overcome chemoresistance to apoptosis in cancer. *Adv Protein Chem Struct Biol* (2021) 126:91–122. doi: 10.1016/bs.apcsb.2021.01.005

65. Jiang X, Stockwell BR, Conrad M. Ferroptosis: Mechanisms, biology and role in disease. *Nat Rev Mol Cell Biol* (2021) 22(4):266–82. doi: 10.1038/s41580-020-00324-8

66. Zhang H, Deng T, Liu R, Ning T, Yang H, Liu D, et al. CAF secreted miR-522 suppresses ferroptosis and promotes acquired chemo-resistance in gastric cancer. *Mol Cancer* (2020) 19(1):43. doi: 10.1186/s12943-020-01168-8

67. Battaglia AM, Chirillo R, Aversa I, Sacco A, Costanzo F, Biamonte F. Ferroptosis and cancer: Mitochondria meet the "Iron maiden" cell death. *Cells* (2020) 9(6). doi: 10.3390/cells9061505

68. Su Y, Zhao B, Zhou L, Zhang Z, Shen Y, Lv H, et al. Ferroptosis, a novel pharmacological mechanism of anti-cancer drugs. *Cancer Lett* (2020) 483:127–36. doi: 10.1016/j.canlet.2020.02.015

69. Chaudhary N, Choudhary BS, Shah SG, Khapare N, Dwivedi N, Gaikwad A, et al. Lipocalin 2 expression promotes tumor progression and therapy resistance by inhibiting ferroptosis in colorectal cancer. *Int J Cancer* (2021) 149(7):1495–511. doi: 10.1002/ijc.33711

70. Zhang X, Sui S, Wang L, Li H, Zhang L, Xu S, et al. Inhibition of tumor propellant glutathione peroxidase 4 induces ferroptosis in cancer cells and enhances anticancer effect of cisplatin. *J Cell Physiol* (2020) 235(4):3425–37. doi: 10.1002/jcp.29232

71. Zhang Q, Deng T, Zhang H, Zuo D, Zhu Q, Bai M, et al. Adipocyte-derived exosomal MTTP suppresses ferroptosis and promotes chemoresistance in colorectal cancer. *Adv Sci (Weinh)* (2022) 9(28):e2203357. doi: 10.1002/advs.202203357

72. Jiang F, Zhou JY, Zhang D, Liu MH, Chen YG. Artesunate induces apoptosis and autophagy in HCT116 colon cancer cells, and autophagy inhibition enhances the artesunateinduced apoptosis. *Int J Mol Med* (2018) 42(3):1295–304. doi: 10.3892/ijmm.2018.3712

73. Huang S, Zhang Z, Li W, Kong F, Yi P, Huang J, et al. Network pharmacology-based prediction and verification of the active ingredients and potential targets of zuojinwan for treating colorectal cancer. *Drug Des Devel Ther* (2020) 14:2725–40. doi: 10.2147/DDDT.S250991

74. Shakibaei M, Kraehe P, Popper B, Shayan P, Goel A, Buhrmann C. Curcumin potentiates antitumor activity of 5-fluorouracil in a 3D alginate tumor microenvironment of colorectal cancer. *BMC Cancer* (2015) 15:250. doi: 10.1186/s12885-015-1291-0

75. Shakibaei M, Mobasheri A, Lueders C, Busch F, Shayan P, Goel A. Curcumin enhances the effect of chemotherapy against colorectal cancer cells by inhibition of NF-kappaB and src protein kinase signaling pathways. *PloS One* (2013) 8(2):e57218. doi: 10.1371/journal.pone.0057218

76. Kunnumakkara AB, Diagaradjane P, Anand P, Harikumar KB, Deorukhkar A, Gelovani J, et al. Curcumin sensitizes human colorectal cancer to capecitabine by modulation of cyclin D1, COX-2, MMP-9, VEGF and CXCR4 expression in an orthotopic mouse model. *Int J Cancer* (2009) 125(9):2187–97. doi: 10.1002/ijc.24593

77. Kunnumakkara AB, Diagaradjane P, Guha S, Deorukhkar A, Shentu S, Aggarwal BB, et al. Curcumin sensitizes human colorectal cancer xenografts in nude mice to gamma-radiation by targeting nuclear factor-kappaB-regulated gene products. *Clin Cancer Res* (2008) 14(7):2128–36. doi: 10.1158/1078-0432.CCR-07-4722

78. Qi F, Wei L, Shen A, Chen Y, Lin J, Chu J, et al. Pien tze Huang inhibits the proliferation, and induces the apoptosis and differentiation of colorectal cancer stem cells *via* suppression of the Notch1 pathway. *Oncol Rep* (2016) 35(1):511–7. doi: 10.3892/or.2015.4378

79. Zhuang Q, Hong F, Shen A, Zheng L, Zeng J, Lin W, et al. Pien tze Huang inhibits tumor cell proliferation and promotes apoptosis *via* suppressing the STAT3 pathway in a colorectal cancer mouse model. *Int J Oncol* (2012) 40(5):1569–74. doi: 10.1371/journal.pone.0057218

80. Zhang W, Peng C, Yan J, Chen P, Jiang C, Sang S, et al. Sanguisorba officinalis l. suppresses 5-fluorouracil-sensitive and-resistant colorectal cancer growth and metastasis *via* inhibition of the wnt/beta-catenin pathway. *Phytomedicine* (2022) 94:153844. doi: 10.1016/j.phymed.2021.153844

81. Wang YL, Horng CT, Hsieh MT, Chen HC, Huang YS, Yang JS, et al. Autophagy and apoptotic machinery caused by polygonum cuspidatum extract in cisplatinresistant human oral cancer CAR cells. *Oncol Rep* (2019) 41(4):2549–57.

82. Zhang W, Lu C, Cai S, Feng Y, Shan J, Di L. Aconiti lateralis radix praeparata as potential anticancer herb: Bioactive compounds and molecular mechanisms. *Front Pharmacol* (2022) 13:870282. doi: 10.3389/fphar.2022.870282

83. Liu YT, Tzang BS, Yow J, Chiang YH, Huang CY, Hsu TC. Traditional Chinese medicine formula T33 inhibits the proliferation of human colorectal cancer cells by inducing autophagy. *Environ Toxicol* (2022) 37(5):1007–17. doi: 10.1002/tox.23460

84. Chen LH, Loong CC, Su TL, Lee YJ, Chu PM, Tsai ML, et al. Autophagy inhibition enhances apoptosis triggered by BO-1051, an n-mustard derivative, and involves the ATM signaling pathway. *Biochem Pharmacol* (2011) 81(5):594–605. doi: 10.1016/j.bcp.2010.12.011

85. Xu J, Gewirtz DA. Is autophagy always a barrier to cisplatin therapy? *Biomolecules* (2022) 12(3). doi: 10.3390/biom12030463

86. Liu Y, Yang B, Zhang L, Cong X, Liu Z, Hu Y, et al. Ginkgolic acid induces interplay between apoptosis and autophagy regulated by ROS generation in colon cancer. *Biochem Biophys Res Commun* (2018) 498(1):246–53. doi: 10.1016/j.bbrc.2018.01.091

87. Lin CJ, Lee CC, Shih YL, Lin TY, Wang SH, Lin YF, et al. Resveratrol enhances the therapeutic effect of temozolomide against malignant glioma *in vitro* and *in vivo* by inhibiting autophagy. *Free Radic Biol Med* (2012) 52(2):377–91. doi: 10.1016/j.freeradbiomed.2011.10.487

88. Meng J, Chang C, Chen Y, Bi F, Ji C, Liu W. EGCG overcomes gefitinib resistance by inhibiting autophagy and augmenting cell death through targeting ERK phosphorylation in NSCLC. *Onco Targets Ther* (2019) 12:6033–43. doi: 10.2147/OTT.S209441

89. Rai G, Mishra S, Suman S, Shukla Y. Resveratrol improves the anticancer effects of doxorubicin *in vitro* and *in vivo* models: A mechanistic insight. *Phytomedicine* (2016) 23 (3):233–42. doi: 10.1016/j.phymed.2015.12.020

90. Liu L, Liu T, Tao W, Liao N, Yan Q, Li L, et al. Flavonoids from scutellaria barbata d. don exert antitumor activity in colorectal cancer through inhibited autophagy and promoted apoptosis *via* ATF4/sestrin2 pathway. *Phytomedicine* (2022) 99:154007. doi: 10.1016/j.phymed.2022.154007

91. Sun D, Tao W, Zhang F, Shen W, Tan J, Li L, et al. Trifolirhizin induces autophagy-dependent apoptosis in colon cancer *via* AMPK/mTOR signaling. *Signal Transduct Target Ther* (2020) 5(1):174. doi: 10.1038/s41392-020-00281-w

92. Zhang C, Liu X, Jin S, Chen Y, Guo R. Ferroptosis in cancer therapy: A novel approach to reversing drug resistance. *Mol Cancer* (2022) 21(1):47. doi: 10.1186/s12943-022-01530-y

93. Sharma P, Shimura T, Banwait JK, Goel A. Andrographis-mediated chemosensitization through activation of ferroptosis and suppression of beta-catenin/Wnt-signaling pathways in colorectal cancer. *Carcinogenesis* (2020) 41(10):1385–94. doi: 10.1093/carcin/bgaa090

94. Chen Y, Zhang F, Du Z, Xie J, Xia L, Hou X, et al. Proteome analysis of camellia nitidissima chi revealed its role in colon cancer through the apoptosis and ferroptosis pathway. *Front Oncol* (2021) 11:727130. doi: 10.3389/fonc.2021.727130

95. Chen P, Li X, Zhang R, Liu S, Xiang Y, Zhang M, et al. Combinative treatment of beta-elemene and cetuximab is sensitive to KRAS mutant colorectal cancer cells by inducing ferroptosis and inhibiting epithelial-mesenchymal transformation. *Theranostics* (2020) 10(11):5107–19. doi: 10.7150/thno.44705

96. Wang CX, Chen LH, Zhuang HB, Shi ZS, Chen ZC, Pan JP, et al. Auriculasin enhances ROS generation to regulate colorectal cancer cell apoptosis, ferroptosis,

oxeiptosis, invasion and colony formation. *Biochem Biophys Res Commun* (2022) 587:99–106. doi: 10.1016/j.bbrc.2021.11.101

97. Chan DW, Yung MM, Chan YS, Xuan Y, Yang H, Xu D, et al. MAP30 protein from momordica charantia is therapeutic and has synergic activity with cisplatin against ovarian cancer *in vivo* by altering metabolism and inducing ferroptosis. *Pharmacol Res* (2020) 161:105157. doi: 10.1016/j.phrs.2020.105157

98. Li Q, Su R, Bao X, Cao K, Du Y, Wang N, et al. Glycyrrhetinic acid nanoparticles combined with ferrotherapy for improved cancer immunotherapy. *Acta Biomater* (2022) 144:109–20. doi: 10.1016/j.actbio.2022.03.030

99. Durinikova E, Plava J, Tyciakova S, Skvara P, Vojs Stanova A, Kozovska Z, et al. Cytotoxic response of 5-fluorouracil-resistant cells to gene- and cell-directed enzyme/prodrug treatment. *Cancer Gene Ther* (2018) 25(11-12):285–99. doi: 10.1038/s41417-018-0030-5

100. Yang C, Song J, Hwang S, Choi J, Song G, Lim W. Apigenin enhances apoptosis induction by 5-fluorouracil through regulation of thymidylate synthase in colorectal cancer cells. *Redox Biol* (2021) 47:102144. doi: 10.1016/j.redox.2021.102144

101. Furukawa T, Tabata S, Yamamoto M, Kawahara K, Shinsato Y, Minami K, et al. Thymidine phosphorylase in cancer aggressiveness and chemoresistance. *Pharmacol Res* (2018) 132:15–20. doi: 10.1016/j.phrs.2018.03.019

102. Bronckaers A, Gago F, Balzarini J, Liekens S. The dual role of thymidine phosphorylase in cancer development and chemotherapy. *Med Res Rev* (2009) 29 (6):903–53. doi: 10.1002/med.20159

103. Zhang Q, Zhang Y, Hu X, Qin Y, Zhong W, Meng J, et al. Thymidine phosphorylase promotes metastasis and serves as a marker of poor prognosis in hepatocellular carcinoma. *Lab Invest* (2017) 97(8):903–12. doi: 10.1038/labinvest.2017.51

104. Cecchini M, Kortmansky JS, Cui C, Wei W, Thumar JR, Uboha NV, et al. A phase 1b expansion study of TAS-102 with oxaliplatin for refractory metastatic colorectal cancer. *Cancer* (2021) 127(9):1417–24. doi: 10.1002/cncr.33379

105. Chakrabarti S, Wintheiser G, Tella SH, Oxencis C, Mahipal A. TAS-102: A resurrected novel fluoropyrimidine with expanding role in the treatment of gastrointestinal malignancies. *Pharmacol Ther* (2021) 224:107823. doi: 10.1016/j.pharmthera.2021.107823

106. Yoshida Y, Yamada T, Kamiyama H, Kosugi C, Ishibashi K, Yoshida H, et al. Combination of TAS-102 and bevacizumab as third-line treatment for metastatic colorectal cancer: TAS-CC3 study. *Int J Clin Oncol* (2021) 26(1):111–7. doi: 10.1007/s10147-020-01794-8

107. Chai J, Dong W, Xie C, Wang L, Han DL, Wang S, et al. MicroRNA-494 sensitizes colon cancer cells to fluorouracil through regulation of DPYD. *IUBMB Life* (2015) 67 (3):191–201. doi: 10.1002/iub.1361

108. Salonga D, Danenberg KD, Johnson M, Metzger R, Groshen S, Tsao-Wei DD, et al. Colorectal tumors responding to 5-fluorouracil have low gene expression levels of dihydropyrimidine dehydrogenase, thymidylate synthase, and thymidine phosphorylase. *Clin Cancer Res* (2000) 6(4):1322–7.

109. Zhang YH, Luo DD, Wan SB, Qu XJ. S1PR2 inhibitors potently reverse 5-FU resistance by downregulating DPD expression in colorectal cancer. *Pharmacol Res* (2020) 155:104717. doi: 10.1016/j.phrs.2020.104717

110. Omura K. Clinical implications of dihydropyrimidine dehydrogenase (DPD) activity in 5-FU-based chemotherapy: Mutations in the DPD gene, and DPD inhibitory fluoropyrimidines. *Int J Clin Oncol* (2003) 8(3):132–8. doi: 10.1007/s10147-003-0330-z

111. Buck E, Sprick M, Gaida MM, Grullich C, Weber TF, Herpel E, et al. Tumor response to irinotecan is associated with CYP3A5 expression in colorectal cancer. *Oncol Lett* (2019) 17(4):3890–8. doi: 10.3892/ol.2019.10043

112. Olszewski U, Liedauer R, Ausch C, Thalhammer T, Hamilton G. Overexpression of CYP3A4 in a COLO 205 colon cancer stem cell model in vitro. *Cancers (Basel)* (2011) 3 (1):1467–79. doi: 10.3390/cancers3011467

113. Untereiner AA, Pavlidou A, Druzhyna N, Papapetropoulos A, Hellmich MR, Szabo C. Drug resistance induces the upregulation of H2S-producing enzymes in HCT116 colon cancer cells. *Biochem Pharmacol* (2018) 149:174–85. doi: 10.1016/j.bcp.2017.10.007

114. Pljesa-Ercegovac M, Savic-Radojevic A, Matic M, Coric V, Djukic T, Radic T, et al. Glutathione transferases: Potential targets to overcome chemoresistance in solid tumors. *Int J Mol Sci* (2018) 19(12). doi: 10.3390/ijms19123785

115. Singh RR, Reindl KM. Glutathione s-transferases in cancer. *Antioxid (Basel)* (2021) 10(5). doi: 10.3390/antiox10050701

116. Liu H, Liu H, Zhou Z, Parise RA, Chu E, Schmitz JC. Herbal formula Huang qin Ge gen tang enhances 5-fluorouracil antitumor activity through modulation of the E2F1/TS pathway. *Cell Commun Signal* (2018) 16(1):7. doi: 10.1186/s12964-018-0218-1

117. Yang A, Wu Q, Chen Q, Yang J, Li H, Tao Y, et al. Cinobufagin restrains the growth and triggers DNA damage of human hepatocellular carcinoma cells *via* proteasome-dependent degradation of thymidylate synthase. *Chem Biol Interact* (2022) 360:109938. doi: 10.1016/j.cbi.2022.109938

118. Yu C, Liu SL, Qi MH, Zou X, Wu J, Zhang J. Herbal medicine guan Chang fu fang enhances 5-fluorouracil cytotoxicity and affects drug-associated genes in human colorectal carcinoma cells. *Oncol Lett* (2015) 9(2):701–8. doi: 10.3892/ol.2014.2766

119. Kang YH, Lee JS, Lee NH, Kim SH, Seo CS, Son CG. Coptidis rhizoma extract reverses 5-fluorouracil resistance in HCT116 human colorectal cancer cells via modulation of thymidylate synthase. *Molecules* (2021) 26(7). doi: 10.3390/molecules26071856

120. Ko JC, Tsai MS, Kuo YH, Chiu YF, Weng SH, Su YC, et al. Modulation of Rad51, ERCC1, and thymidine phosphorylase by emodin result in synergistic cytotoxic effect in combination with capecitabine. *Biochem Pharmacol* (2011) 81(5):680–90. doi: 10.1016/j.bcp.2010.12.008

121. Chen L, Cai J, Wang S, Hu L, Yang X. Effect of radix sophorae flavescentis on activity of CYP450 isoforms in rats. *Int J Clin Exp Med* (2015) 8(11):21365–71.

122. Wang B, Yang S, Hu J, Li Y. Multifaceted interaction of the traditional Chinese medicinal herb schisandra chinensis with cytochrome P450-mediated drug metabolism in rats. *J Ethnopharmacol* (2014) 155(3):1473–82. doi: 10.1016/j.jep.2014.07.026

123. Yim D, Kim MJ, Shin Y, Lee SJ, Shin JG, Kim DH. Inhibition of cytochrome P450 activities by sophora flavescens extract and its prenylated flavonoids in human liver microsomes. *Evid Based Complement Alternat Med* (2019) 2019:2673769. doi: 10.1155/2019/2673769

124. Ueng YF, Shyu CC, Lin YL, Park SS, Liao JF, Chen CF. Effects of baicalein and wogonin on drug-metabolizing enzymes in C57BL/6J mice. *Life Sci* (2000) 67(18):2189–200. doi: 10.1016/S0024-3205(00)00809-2

125. Wei W, Li Z, Li HJ, An Y, Qu H, Yao C, et al. The inhibitory effect of 225 frequently-used traditional Chinese medicines for CYP3A4 metabolic enzyme by isoform-specific probe. *Fitoterapia* (2021) 152:104858. doi: 10.1016/j.fitote.2021.104858

126. Babaei G, Aziz SG, Jaghi NZZ. EMT. Cancer stem cells and autophagy; the three main axes of metastasis. *BioMed Pharmacother* (2021) 133:110909. doi: 10.1016/j.biopha.2020.110909

127. Cho ES, Kang HE, Kim NH, Yook JI. Therapeutic implications of cancer epithelial-mesenchymal transition (EMT). *Arch Pharm Res* (2019) 42(1):14–24. doi: 10.1007/s12272-018-01108-7

128. Skarkova V, Skarka A, Manethova M, Stefanidi AA, Rudolf E. Silencing of e-cadherin expression leads to increased chemosensitivity to irinotecan and oxaliplatin in colorectal cancer cell lines. *Hum Exp Toxicol* (2021) 40(12):2063–73. doi: 10.1177/09603271211021479

129. Fortunato A. The role of hERG1 ion channels in epithelial-mesenchymal transition and the capacity of riluzole to reduce cisplatin resistance in colorectal cancer cells. *Cell Oncol (Dordr)* (2017) 40(4):367–78. doi: 10.1007/s13402-017-0328-6

130. Zhang Y, Devocelle A, Desterke C, de Souza LEB, Hadadi E, Acloque H, et al. BMAL1 knockdown leans epithelial-mesenchymal balance toward epithelial properties and decreases the chemoresistance of colon carcinoma cells. *Int J Mol Sci* (2021) 22(10). doi: 10.3390/ijms22105247

131. Sreekumar R, Al-Saihati H, Emaduddin M, Moutasim K, Mellone M, Patel A, et al. The ZEB2-dependent EMT transcriptional programme drives therapy resistance by activating nucleotide excision repair genes ERCC1 and ERCC4 in colorectal cancer. *Mol Oncol* (2021) 15(8):2065–83. doi: 10.1002/1878-0261.12965

132. Erin N, Grahovac J, Brozovic A, Efferth T. Tumor microenvironment and epithelial mesenchymal transition as targets to overcome tumor multidrug resistance. *Drug Resist Updat* (2020) 53:100715. doi: 10.1016/j.drup.2020.100715

133. Roy S, Sunkara RR, Parmar MY, Shaikh S, Waghmare SK. EMT imparts cancer stemness and plasticity: new perspectives and therapeutic potential. *Front Biosci (Landmark Ed)* (2021) 26(2):238–65. doi: 10.2741/4893

134. Li N, Babaei-Jadidi R, Lorenzi F, Spencer-Dene B, Clarke P, Domingo E, et al. An FBXW7-ZEB2 axis links EMT and tumour microenvironment to promote colorectal cancer stem cells and chemoresistance. *Oncogenesis* (2019) 8(3):13. doi: 10.1038/s41389-019-0125-3

135. Hu JL, Wang W, Lan XL, Zeng ZC, Liang YS, Yan YR, et al. CAFs secreted exosomes promote metastasis and chemotherapy resistance by enhancing cell stemness and epithelial-mesenchymal transition in colorectal cancer. *Mol Cancer* (2019) 18(1):91. doi: 10.1186/s12943-019-1019-x

136. Lu Y, Zhang R, Zhang X, Zhang B, Yao Q. Curcumin may reverse 5-fluorouracil resistance on colonic cancer cells by regulating TET1-NKD-Wnt signal pathway to inhibit the EMT progress. *BioMed Pharmacother* (2020) 129:110381. doi: 10.1016/j.biopha.2020.110381

137. Yin J, Wang L, Wang Y, Shen H, Wang X, Wu L. Curcumin reverses oxaliplatin resistance in human colorectal cancer *via* regulation of TGF-beta/Smad2/3 signaling pathway. *Onco Targets Ther* (2019) 12:3893–903. doi: 10.2147/OTT.S199601

138. Toden S, Okugawa Y, Jascur T, Wodarz D, Komarova NL, Buhrmann C, et al. Curcumin mediates chemosensitization to 5-fluorouracil through miRNA-induced suppression of epithelial-to-mesenchymal transition in chemoresistant colorectal cancer. *Carcinogenesis* (2015) 36(3):355–67. doi: 10.1093/carcin/bgv006

139. Wu CE, Zhuang YW, Zhou JY, Liu SL, Wang RP, Shu P. Cinnamaldehyde enhances apoptotic effect of oxaliplatin and reverses epithelial-mesenchymal transition and stemnness in hypoxic colorectal cancer cells. *Exp Cell Res* (2019) 383(1):111500. doi: 10.1016/j.yexcr.2019.111500

140. Cao Y, Lu K, Xia Y, Wang Y, Wang A, Zhao Y. Danshensu attenuated epithelial-mesenchymal transformation and chemoresistance of colon cancer cells induced by platelets. *Front Biosci (Landmark Ed)* (2022) 27(5):160. doi: 10.31083/j.fbl2705160

141. Yuan L, Zhang K, Zhou MM, Wasan HS, Tao FF, Yan QY, et al. Jiedu sangen decoction reverses epithelial-to-mesenchymal transition and inhibits invasion and metastasis of colon cancer *via* AKT/GSK-3beta signaling pathway. *J Cancer* (2019) 10 (25):6439–56. doi: 10.7150/jca.32873

142. Zhang K, Peng T, Yan Q, Sun L, Miao H, Yuan L, et al. Jiedu sangen decoction inhibits migration and invasion of colon cancer SW480 cells *via* suppressing epithelial mesenchymal transition. *Evid Based Complement Alternat Med* (2018) 2018:1495768. doi: 10.1155/2018/1495768

143. Buhrmann C, Shayan P, Kraehe P, Popper B, Goel A, Shakibaei M. Resveratrol induces chemosensitization to 5-fluorouracil through up-regulation of intercellular

junctions, epithelial-to-mesenchymal transition and apoptosis in colorectal cancer. *Biochem Pharmacol* (2015) 98(1):51–68. doi: 10.1016/j.bcp.2015.08.105

144. Buhrmann C, Yazdi M, Popper B, Shayan P, Goel A, Aggarwal BB, et al. Resveratrol Chemosensitizes TNF-β-Induced Survival of 5-FU-Treated Colorectal Cancer Cells. *Resveratrol Chemosensitizes TNF-beta-Induced Survival 5-FU-Treated Colorectal Cancer Cells Nutrients* (2018) 10(7):888. doi: 10.3390/nu10070888

145. Ji Q, Liu X, Han Z, Zhou L, Sui H, Yan L, et al. Resveratrol suppresses epithelial-to-mesenchymal transition in colorectal cancer through TGF-beta1/Smads signaling pathway mediated Snail/E-cadherin expression. *BMC Cancer* (2015) 15:97. doi: 10.1186/s12885-015-1119-y

146. Feng J, Song D, Jiang S, Yang X, Ding T, Zhang H, et al. Quercetin restrains TGF-beta1-induced epithelial-mesenchymal transition by inhibiting Twist1 and regulating e-cadherin expression. *Biochem Biophys Res Commun* (2018) 498(1):132–8. doi: 10.1016/j.bbrc.2018.02.044

147. Ye Q, Su L, Chen D, Zheng W, Liu Y. Astragaloside IV induced miR-134 expression reduces EMT and increases chemotherapeutic sensitivity by suppressing CREB1 signaling in colorectal cancer cell line SW-480. *Cell Physiol Biochem* (2017) 43 (4):1617–26. doi: 10.1159/000482025

148. Jarosz-Biej M, Smolarczyk R, Cichon T, Kulach N. Tumor microenvironment as a "Game changer" in cancer radiotherapy. *Int J Mol Sci* (2019) 20(13). doi: 10.3390/ijms20133212

149. Riera-Domingo C, Audige A, Granja S, Cheng WC, Ho PC, Baltazar F, et al. Immunity, hypoxia, and metabolism-the menage a trois of cancer: Implications for immunotherapy. *Physiol Rev* (2020) 100(1):1–102. doi: 10.1152/physrev.00018.2019

150. Roma-Rodrigues C, Mendes R, Baptista PV, Fernandes AR. Targeting tumor microenvironment for cancer therapy. *Int J Mol Sci* (2019) 20(4). doi: 10.3390/ijms20040840

151. Zhang S, Ji WW, Wei W, Zhan LX, Huang X. Long noncoding RNA Meg3 sponges miR-708 to inhibit intestinal tumorigenesis *via* SOCS3-repressed cancer stem cells growth. *Cell Death Dis* (2021) 13(1):25. doi: 10.1038/s41419-021-04470-5

152. Bharti R, Dey G, Mandal M. Cancer development, chemoresistance, epithelial to mesenchymal transition and stem cells: A snapshot of IL-6 mediated involvement. *Cancer Lett* (2016) 375(1):51–61. doi: 10.1016/j.canlet.2016.02.048

153. Chen Y, Tan W, Wang C. Tumor-associated macrophage-derived cytokines enhance cancer stem-like characteristics through epithelial-mesenchymal transition. *Onco Targets Ther* (2018) 11:3817–26. doi: 10.2147/OTT.S168317

154. Jinushi M, Chiba S, Yoshiyama H, Masutomi K, Kinoshita I, Dosaka-Akita H, et al. Tumor-associated macrophages regulate tumorigenicity and anticancer drug responses of cancer stem/initiating cells. *Proc Natl Acad Sci U S A* (2011) 108 (30):12425–30. doi: 10.1073/pnas.1106645108

155. Ren J, Ding L, Zhang D, Shi G, Xu Q, Shen S, et al. Carcinoma-associated fibroblasts promote the stemness and chemoresistance of colorectal cancer by transferring exosomal lncRNA H19. *Theranostics* (2018) 8(14):3932–48. doi: 10.7150/thno.25541

156. Weng X, Liu H, Ruan J, Du M, Wang L, Mao J, et al. HOTAIR/miR-1277-5p/ZEB1 axis mediates hypoxia-induced oxaliplatin resistance *via* regulating epithelial-mesenchymal transition in colorectal cancer. *Cell Death Discovery* (2022) 8(1):310. doi: 10.1038/s41420-022-01096-0

157. Zhang Y, Lou Y, Wang J, Yu C, Shen W. Research status and molecular mechanism of the traditional Chinese medicine and antitumor therapy combined strategy based on tumor microenvironment. *Front Immunol* (2020) 11:609705. doi: 10.3389/fimmu.2020.609705

158. Duan Y, Zhu J, Yang J, Gu W, Bai X, Liu G, et al. A decade's review of miRNA: A center of transcriptional regulation of drugmetabolizing enzymes and transporters under hypoxia. *Curr Drug Metab* (2021) 22(9):709–25. doi: 10.2174/1389200222666210514011313

159. Patel BB, Sengupta R, Qazi S, Vachhani H, Yu Y, Rishi AK, et al. Curcumin enhances the effects of 5-fluorouracil and oxaliplatin in mediating growth inhibition of colon cancer cells by modulating EGFR and IGF-1R. *Int J Cancer* (2008) 122(2):267–73. doi: 10.1002/ijc.23097

160. Lam W, Bussom S, Guan F, Jiang Z, Zhang W, Gullen EA, et al. The four-herb Chinese medicine PHY906 reduces chemotherapy-induced gastrointestinal toxicity. *Sci Transl Med* (2010) 2(45):45ra59. doi: 10.1126/scitranslmed.3001270

161. Lv J, Jia Y, Li J, Kuai W, Li Y, Guo F, et al. Gegen qinlian decoction enhances the effect of PD-1 blockade in colorectal cancer with microsatellite stability by remodelling the gut microbiota and the tumour microenvironment. *Cell Death Dis* (2019) 10(6):415. doi: 10.1038/s41419-019-1638-6

162. Liu J, Wang Y, Qiu Z, Lv G, Huang X, Lin H, et al. Impact of TCM on tumor-infiltrating myeloid precursors in the tumor microenvironment. *Front Cell Dev Biol* (2021) 9:635122. doi: 10.3389/fcell.2021.635122

163. Sui H, Zhao J, Zhou L, Wen H, Deng W, Li C, et al. Tanshinone IIA inhibits beta-catenin/VEGF-mediated angiogenesis by targeting TGF-beta1 in normoxic and HIF-1alpha in hypoxic microenvironments in human colorectal cancer. *Cancer Lett* (2017) 403:86–97. doi: 10.1016/j.canlet.2017.05.013

164. Zhang T, Wang K, Zhang J, Wang X, Chen Z, Ni C, et al. Huaier aqueous extract inhibits colorectal cancer stem cell growth partially *via* downregulation of the wnt/beta-catenin pathway. *Oncol Lett* (2013) 5(4):1171–6. doi: 10.3892/ol.2013.1145

165. Liu Y, Liu X, Zhang N, Yin M, Dong J, Zeng Q, et al. Berberine diminishes cancer cell PD-L1 expression and facilitates antitumor immunity *via* inhibiting the deubiquitination activity of CSN5. *Acta Pharm Sin B* (2020) 10(12):2299–312. doi: 10.1016/j.apsb.2020.06.014

166. Liu W, Fan T, Li M, Zhang G, Guo W, Yang X, et al. Andrographolide potentiates PD-1 blockade immunotherapy by inhibiting COX2-mediated PGE2 release. *Int Immunopharmacol* (2020) 81:106206. doi: 10.1016/j.intimp.2020.106206

167. Deng B, Yang B, Chen J, Wang S, Zhang W, Guo Y, et al. Gallic Acid induces T-helper-1-like treg cells and strengthens immune checkpoint blockade efficacy. *J Immunother Cancer* (2022) 10(7). doi: 10.1136/jitc-2021-004037

168. Mao Q, Min J, Zeng R, Liu H, Li H, Zhang C, et al. Self-assembled traditional Chinese nanomedicine modulating tumor immunosuppressive microenvironment for colorectal cancer immunotherapy. *Theranostics* (2022) 12(14):6088–105. doi: 10.7150/thno.72509

169. Crea F, Nobili S, Paolicchi E, Perrone G, Napoli C, Landini I, et al. Epigenetics and chemoresistance in colorectal cancer: An opportunity for treatment tailoring and novel therapeutic strategies. *Drug Resist Updat* (2011) 14(6):280–96. doi: 10.1016/j.drup.2011.08.001

170. Li B, Jiang J, Assaraf YG, Xiao H, Chen ZS, Huang C. Surmounting cancer drug resistance: New insights from the perspective of N(6)-methyladenosine RNA modification. *Drug Resist Updat* (2020) 53:100720. doi: 10.1016/j.drup.2020.100720

171. Isono M, Nakano M, Fukami T, Nakajima M. Adenosine N(6)-methylation upregulates the expression of human CYP2B6 by altering the chromatin status. *Biochem Pharmacol* (2022) 205:115247. doi: 10.1016/j.bcp.2022.115247

172. Yang Z, Zhao F, Gu X, Feng L, Xu M, Li T, et al. Binding of RNA m6A by IGF2BP3 triggers chemoresistance of HCT8 cells *via* upregulation of ABCB1. *Am J Cancer Res* (2021) 11(4):1428–45.

173. Uddin MB, Roy KR, Hosain SB, Khiste SK, Hill RA, Jois SD, et al. An N(6)-methyladenosine at the transited codon 273 of p53 pre-mRNA promotes the expression of R273H mutant protein and drug resistance of cancer cells. *Biochem Pharmacol* (2019) 160:134–45. doi: 10.1016/j.bcp.2018.12.014

174. Ye P, Xing H, Lou F, Wang K, Pan Q, Zhou X, et al. Histone deacetylase 2 regulates doxorubicin (Dox) sensitivity of colorectal cancer cells by targeting ABCB1 transcription. *Cancer Chemother Pharmacol* (2016) 77(3):613–21. doi: 10.1007/s00280-016-2979-9

175. Hirukawa A, Singh S, Wang J, Rennhack JP, Swiatnicki M, Sanguin-Gendreau V, et al. Reduction of global H3K27me(3) enhances HER2/ErbB2 targeted therapy. *Cell Rep* (2019) 29(2):249–57 e8. doi: 10.1016/j.celrep.2019.08.105

176. Ma Y, Yang Y, Wang F, Moyer MP, Wei Q, Zhang P, et al. Long non-coding RNA CCAL regulates colorectal cancer progression by activating wnt/beta-catenin signalling pathway *via* suppression of activator protein 2alpha. *Gut* (2016) 65(9):1494–504. doi: 10.1136/gutjnl-2014-308392

177. Chen P, Liu XQ, Lin X, Gao LY, Zhang S, Huang X. Targeting YTHDF1 effectively re-sensitizes cisplatin-resistant colon cancer cells by modulating GLS-mediated glutamine metabolism. *Mol Ther Oncolytics* (2021) 20:228–39. doi: 10.1016/j.omto.2021.01.001

178. Chen Z, Wu L, Zhou J, Lin X, Peng Y, Ge L, et al. N6-methyladenosine-induced ERRgamma triggers chemoresistance of cancer cells through upregulation of ABCB1 and metabolic reprogramming. *Theranostics* (2020) 10(8):3382–96. doi: 10.7150/thno.40144

179. Gao Y, Wang H, Chen S, An R, Chu Y, Li G, et al. Single-cell N(6)-methyladenosine regulator patterns guide intercellular communication of tumor microenvironment that contribute to colorectal cancer progression and immunotherapy. *J Transl Med* (2022) 20(1):197. doi: 10.1186/s12967-022-03395-7

180. Straussman R, Morikawa T, Shee K, Barzily-Rokni M, Qian ZR, Du J, et al. Tumour micro-environment elicits innate resistance to RAF inhibitors through HGF secretion. *Nature* (2012) 487(7408):500–4. doi: 10.1038/nature11183

181. Wu Y, Wang Z, Han L, Guo Z, Yan B, Guo L, et al. PRMT5 regulates RNA m6A demethylation for doxorubicin sensitivity in breast cancer. *Mol Ther* (2022) 30(7):2603–17. doi: 10.1016/j.ymthe.2022.03.003

182. Giri AK, Aittokallio T. DNMT inhibitors increase methylation in the cancer genome. *Front Pharmacol* (2019) 10:385. doi: 10.3389/fphar.2019.00385

183. Guo Y, Shu L, Zhang C, Su ZY, Kong AN. Curcumin inhibits anchorage-independent growth of HT29 human colon cancer cells by targeting epigenetic restoration of the tumor suppressor gene DLEC1. *Biochem Pharmacol* (2015) 94(2):69–78. doi: 10.1016/j.bcp.2015.01.009

184. Jiang A, Wang X, Shan X, Li Y, Wang P, Jiang P, et al. Curcumin reactivates silenced tumor suppressor gene RARbeta by reducing DNA methylation. *Phytother Res* (2015) 29(8):1237–45. doi: 10.1002/ptr.5373

185. Hosokawa M, Seiki R, Iwakawa S, Ogawara KI. Combination of azacytidine and curcumin is a potential alternative in decitabine-resistant colorectal cancer cells with attenuated deoxycytidine kinase. *Biochem Biophys Res Commun* (2021) 578:157–62. doi: 10.1016/j.bbrc.2021.09.041

186. Pan FP, Zhou HK, Bu HQ, Chen ZQ, Zhang H, Xu LP, et al. Emodin enhances the demethylation by 5-Aza-CdR of pancreatic cancer cell tumor-suppressor genes P16, RASSF1A and ppENK. *Oncol Rep* (2016) 35(4):1941–9. doi: 10.3892/or.2016.4554

187. Anantharaju PG, Reddy DB, Padukudru MA, Chitturi CMK, Vimalambike MG, Madhunapantula SV. Induction of colon and cervical cancer cell death by cinnamic acid derivatives is mediated through the inhibition of histone deacetylases (HDAC). *PloS One* (2017) 12(11):e0186208. doi: 10.1371/journal.pone.0186208

188. Zhao Z, Zeng J, Guo Q, Pu K, Yang Y, Chen N, et al. Berberine suppresses stemness and tumorigenicity of colorectal cancer stem-like cells by inhibiting m(6)A methylation. *Front Oncol* (2021) 11:775418. doi: 10.3389/fonc.2021.775418

189. An P, Lu D, Zhang L, Lan H, Yang H, Ge G, et al. Synergistic antitumor effects of compound-composed optimal formula from aidi injection on hepatocellular carcinoma and colorectal cancer. *Phytomedicine* (2022) 103:154231. doi: 10.1016/j.phymed.2022.154231

190. Pavlova NN, Zhu J, Thompson CB. The hallmarks of cancer metabolism: Still emerging. *Cell Metab* (2022) 34(3):355–77. doi: 10.1016/j.cmet.2022.01.007

191. Tan Y, Li J, Zhao G, Huang KC, Cardenas H, Wang Y, et al. Metabolic reprogramming from glycolysis to fatty acid uptake and beta-oxidation in platinum-resistant cancer cells. *Nat Commun* (2022) 13(1):4554. doi: 10.1038/s41467-022-32101-w

192. Yang R, Yi M, Xiang B. Novel insights on lipid metabolism alterations in drug resistance in cancer. *Front Cell Dev Biol* (2022) 10:875318. doi: 10.3389/fcell.2022.875318

193. Chen X, Chen S, Yu D. Metabolic reprogramming of chemoresistant cancer cells and the potential significance of metabolic regulation in the reversal of cancer chemoresistance. *Metabolites* (2020) 10(7). doi: 10.3390/metabo10070289

194. Shi T, Ma Y, Cao L, Zhan S, Xu Y, Fu F, et al. B7-H3 promotes aerobic glycolysis and chemoresistance in colorectal cancer cells by regulating HK2. *Cell Death Dis* (2019) 10(4):308. doi: 10.1038/s41419-019-1549-6

195. Zhang X, Li Q, Du A, Li Y, Shi Q, Chen Y, et al. Adipocytic glutamine synthetase upregulation *via* altered histone methylation promotes 5FU chemoresistance in peritoneal carcinomatosis of colorectal cancer. *Front Oncol* (2021) 11:748730. doi: 10.3389/fonc.2021.748730

196. Dong S, Liang S, Cheng Z, Zhang X, Luo L, Li L, et al. ROS/PI3K/Akt and wnt/beta-catenin signalings activate HIF-1alpha-induced metabolic reprogramming to impart 5-fluorouracil resistance in colorectal cancer. *J Exp Clin Cancer Res* (2022) 41(1):15. doi: 10.1186/s13046-021-02229-6

197. Hong X, Zhong L, Xie Y, Zheng K, Pang J, Li Y, et al. Matrine reverses the warburg effect and suppresses colon cancer cell growth *via* negatively regulating HIF-1alpha. *Front Pharmacol* (2019) 10:1437. doi: 10.3389/fphar.2019.01437

198. Ji L, Shen W, Zhang F, Qian J, Jiang J, Weng L, et al. Worenine reverses the warburg effect and inhibits colon cancer cell growth by negatively regulating HIF-1alpha. *Cell Mol Biol Lett* (2021) 26(1):19. doi: 10.1186/s11658-021-00263-y

199. Wu H, Du J, Li C, Li H, Guo H, Li Z. Kaempferol can reverse the 5-fu resistance of colorectal cancer cells by inhibiting PKM2-mediated glycolysis. *Int J Mol Sci* (2022) 23(7). doi: 10.3390/ijms23073544

200. Sun LT, Zhang LY, Shan FY, Shen MH, Ruan SM. Jiedu sangen decoction inhibits chemoresistance to 5-fluorouracil of colorectal cancer cells by suppressing glycolysis *via* PI3K/AKT/HIF-1alpha signaling pathway. *Chin J Nat Med* (2021) 19(2):143–52. doi: 10.1016/S1875-5364(21)60015-8

201. Wang Y, Guo D, He J, Song L, Chen H, Zhang Z, et al. Inhibition of fatty acid synthesis arrests colorectal neoplasm growth and metastasis: Anti-cancer therapeutical effects of natural cyclopeptide RA-XII. *Biochem Biophys Res Commun* (2019) 512(4):819–24. doi: 10.1016/j.bbrc.2019.03.088

202. Ghosh S, Singh R, Vanwinkle ZM, Guo H, Vemula PK, Goel A, et al. Microbial metabolite restricts 5-fluorouracil-resistant colonic tumor progression by sensitizing drug transporters *via* regulation of FOXO3-FOXM1 axis. *Theranostics* (2022) 12(12):5574–95. doi: 10.7150/thno.70754

203. Kim HJ, An J, Ha EM. Lactobacillus plantarum-derived metabolites sensitize the tumor-suppressive effects of butyrate by regulating the functional expression of SMCT1 in 5-FU-resistant colorectal cancer cells. *J Microbiol* (2022) 60(1):100–17. doi: 10.1007/s12275-022-1533-1

204. Wang Z, Hopson LM, Singleton SS, Yang X, Jogunoori W, Mazumder R, et al. Mice with dysfunctional TGF-beta signaling develop altered intestinal microbiome and colorectal cancer resistant to 5FU. *Biochim Biophys Acta Mol Basis Dis* (2021) 1867 (10):166179. doi: 10.1016/j.bbadis.2021.166179

205. Liu H, Du J, Chao S, Li S, Cai H, Zhang H, et al. Fusobacterium nucleatum promotes colorectal cancer cell to acquire stem cell-like features by manipulating lipid droplet-mediated numb degradation. *Adv Sci (Weinh)* (2022) 9(12):e2105222. doi: 10.1002/advs.202105222

206. Yu T, Guo F, Yu Y, Sun T, Ma D, Han J, et al. Fusobacterium nucleatum promotes chemoresistance to colorectal cancer by modulating autophagy. *Cell* (2017) 170(3):548–63 e16. doi: 10.1016/j.cell.2017.07.008

207. Roy S, Trinchieri G. Microbiota: A key orchestrator of cancer therapy. *Nat Rev Cancer* (2017) 17(5):271–85. doi: 10.1038/nrc.2017.13

208. Li Y, Li ZX, Xie CY, Fan J, Lv J, Xu XJ, et al. Gegen qinlian decoction enhances immunity and protects intestinal barrier function in colorectal cancer patients *via* gut microbiota. *World J Gastroenterol* (2020) 26(48):7633–51. doi: 10.3748/wjg.v26.i48.7633

209. Yu YN, Yu TC, Zhao HJ, Sun TT, Chen HM, Chen HY, et al. Berberine may rescue fusobacterium nucleatum-induced colorectal tumorigenesis by modulating the tumor microenvironment. *Oncotarget* (2015) 6(31):32013–26. doi: 10.18632/oncotarget.5166

210. Jiang F, Liu M, Wang H, Shi G, Chen B, Chen T, et al. Wu Mei wan attenuates CAC by regulating gut microbiota and the NF-kB/IL6-STAT3 signaling pathway. *BioMed Pharmacother* (2020) 125:109982. doi: 10.1016/j.biopha.2020.109982

211. Luo Y, Wang CZ, Sawadogo R, Yuan J, Zeng J, Xu M, et al. 4-vinylguaiacol, an active metabolite of ferulic acid by enteric microbiota and probiotics, possesses significant activities against drug-resistant human colorectal cancer cells. *ACS Omega* (2021) 6 (7):4551–61. doi: 10.1021/acsomega.0c04394

212. Sui H, Zhang L, Gu K, Chai N, Ji Q, Zhou L, et al. YYFZBJS ameliorates colorectal cancer progression in Apc(Min/+) mice by remodeling gut microbiota and inhibiting regulatory T-cell generation. *Cell Commun Signal* (2020) 18(1):113. doi: 10.1186/s12964-020-00596-9

213. Engle K, Kumar G. Cancer multidrug-resistance reversal by ABCB1 inhibition: A recent update. *Eur J Med Chem* (2022) 239:114542. doi: 10.1016/j.ejmech.2022.114542

214. Hogg SJ, Beavis PA, Dawson MA, Johnstone RW. Targeting the epigenetic regulation of antitumour immunity. *Nat Rev Drug Discovery* (2020) 19(11):776–800. doi: 10.1038/s41573-020-0077-5

215. de Oliveira Junior RG, Christiane Adrielly AF, da Silva Almeida JRG, Grougnet R, Thiery V, Picot L. Sensitization of tumor cells to chemotherapy by natural products: A systematic review of preclinical data and molecular mechanisms. *Fitoterapia* (2018) 129:383–400. doi: 10.1016/j.fitote.2018.02.025

216. Zheng Y, Wang Y, Xia M, Gao Y, Zhang L, Song Y, et al. The combination of nanotechnology and traditional Chinese medicine (TCM) inspires the modernization of TCM: review on nanotechnology in TCM-based drug delivery systems. *Drug Delivery Transl Res* (2022) 12(6):1306–25. doi: 10.1007/s13346-021-01029-x

217. Wei D, Yang H, Zhang Y, Zhang X, Wang J, Wu X, et al. Nano-traditional Chinese medicine: a promising strategy and its recent advances. *J Mater Chem B* (2022) 10 (16):2973–94. doi: 10.1039/D2TB00225F

218. Song JW, Liu YS, Guo YR, Zhong WX, Guo YP, Guo L. Nano-liposomes double loaded with curcumin and tetrandrine: Preparation, characterization, hepatotoxicity and anti-tumor effects. *Int J Mol Sci* (2022) 23(12). doi: 10.3390/ijms23126858

219. Ma Z, Fan Y, Wu Y, Kebebe D, Zhang B, Lu P, et al. Traditional Chinese medicine-combination therapies utilizing nanotechnology-based targeted delivery systems: a new strategy for antitumor treatment. *Int J Nanomed* (2019) 14:2029–53. doi: 10.2147/IJN.S197889

frontiers | Frontiers in Pharmacology

TYPE Original Research
PUBLISHED 30 March 2023
DOI 10.3389/fphar.2023.1072033

OPEN ACCESS

EDITED BY
Veronika Vymetalkova,
Academy of Sciences of the Czech Republic (ASCR), Czechia

REVIEWED BY
Chuangyu Wen,
Southern Medical University, China
Radka Václavíková,
National Institute of Public Health (NIPH), Czechia
Shuiping Liu,
Hangzhou Normal University, China
Katarina Kozics,
Slovak Academy of Sciences, Slovakia

*CORRESPONDENCE
Jianguo Sun,
sjg19840902@163.com
Jianwei Wang,
sypzju@zju.edu.cn

†These authors have contributed equally to this work

SPECIALTY SECTION
This article was submitted to Pharmacology of Anti-Cancer Drugs, a section of the journal Frontiers in Pharmacology

RECEIVED 17 October 2022
ACCEPTED 09 March 2023
PUBLISHED 30 March 2023

CITATION
Zheng Z, Luan N, Tu K, Liu F, Wang J and Sun J (2023), The roles of protocadherin-7 in colorectal cancer cells on cell proliferation and its chemoresistance. *Front. Pharmacol.* 14:1072033. doi: 10.3389/fphar.2023.1072033

The roles of protocadherin-7 in colorectal cancer cells on cell proliferation and its chemoresistance

Zhibao Zheng[1†], Na Luan[2†], Kai Tu[3], Feiyan Liu[3], Jianwei Wang[2*] and Jianguo Sun[1*]

[1]Department of Surgical Oncology, Taizhou Central Hospital (Taizhou University Hospital), Taizhou, Zhejiang, China, [2]Department of Colorectal Surgery and Oncology, The Second Affiliated Hospital, Zhejiang University School of Medicine, Hangzhou, China, [3]College of Life Sciences, Zhejiang University, Hangzhou, China

Despite the high mutation frequencies of *KRAS*, *NRAS*, and *BRAF* in colorectal cancer (CRC), there are no effective and reliable inhibitors for these biomarkers. Protocadherin-7 (PCDH7) is regarded as a potentially targetable surface molecule in cancer cells and plays an important role in their proliferation, metastasis, and drug resistance. However, the roles and underlying mechanisms of PCDH7 in CRC remain unclear. In the current study, we found that different colorectal cancer cells expressed PCDH7 over a wide range. The levels of PCDH7 expression were positively associated with cell proliferation and drug resistance in CRC cells but negatively correlated with the potential for cell migration and invasion. Our data indicated that PCDH7 mediated the resistance of CRC cells to ABT-263 (a small-molecule Bcl-2 inhibitor that induces apoptosis) by inhibiting cell apoptosis, which was supported by the downregulation of caspase-3, caspase-9, and PARP cleavage. We found that PCDH7 effectively promoted Mcl-1 expression at both mRNA and protein levels. Furthermore, PCDH7 activated the Wnt signaling pathway, which was confirmed by the increase in β-catenin and c-Myc expression. Finally, and notably, S63845, a novel Mcl-1 inhibitor, not only effectively attenuated the inhibitory effect of PCDH7 on cell apoptosis induced by ABT-263 *in vitro* but also sensitized PCDH7-overexpressed CRC cell-derived xenografts to ABT-263 *in vivo*. Taken together, although PCDH7 inhibited the migration and invasion of CRC cells, it could facilitate the development of drug resistance in colorectal cancer cells by positively modulating Mcl-1 expression. The application of the Mcl-1 inhibitor S63845 could be a potential strategy for CRC chemotherapy, especially in CRC with high levels of PCDH7.

KEYWORDS

protocadherin-7, Mcl-1, chemoresistance, Wnt/beta-catenin, colorectal cancer

Abbreviations: ATCC, American Type Culture Collection; DMEM, Dulbecco's modified Eagle's medium; EMT, epithelial-to-mesenchymal transition; FBS, fetal bovine serum; protocadherin-7, PCDH7.

1 Introduction

Colorectal cancer (CRC) is one of the most lethal malignancies worldwide (Bray et al., 2018). In the United States, CRC has been the second-most common cause of cancer-related death for years because of the aging population and dietary habits (Siegel et al., 2020).

Although apparent declining trends in the incidence and mortality in the older population in high-income countries seem to be from a nationwide screening program and the wide application of colonoscopy in general (Connell et al., 2017), the rapid increase in both CRC incidence and mortality is ongoing in several developing countries, particularly in Eastern Europe, Asia, and South America (Dekker et al., 2019). Thus far, surgery is still the cornerstone of colorectal cancer treatment, and the combination of chemotherapy and molecular targeted therapy gradually contributes significantly to the improvement of patients' overall survival and quality of life (Kopetz, 2019). Numerous studies have demonstrated that overexpression of EGFR and alteration of signaling pathways could trigger and/or accelerate the progression of CRC, which assists in the treatment against EGFR using monoclonal antibodies (e.g., cetuximab and panitumumab) in CRC-targeted therapies. Although high mutation frequencies of *KRAS*, *NRAS*, and *BRAF* are present in CRC, there are no effective and reliable inhibitors of these biomarkers. Monotherapy with a *BRAF* inhibitor only yields a response in approximately 5% of CRC patients with the $BRAF^{V600E}$ mutation, which is one of the prominent mutations in approximately 10% of CRC patients (Venderbosch et al., 2014). RAS (including *KRAS* and *NRAS*) inhibitors have also been investigated for decades and, unfortunately, are still so elusive that RAS is charted as an undruggable target (Moore et al., 2020). Therefore, discovery of the underlying molecular mechanisms facilitating the development and metastatic progression of CRC would benefit the exploration of novel therapeutic targets.

Protocadherin-7 (PCDH7) belongs to the protocadherin family and was first found to be prominently expressed in brain tissue (Yoshida et al., 1998). Recently, it has been demonstrated that PCDH7 can regulate osteoclastogenesis by promoting cell–cell fusion and maintenance of bone homeostasis (Kim et al., 2020). Furthermore, PCDH7 has multiple biological functions in various cancers. PCDH7 was identified as one of the top-ranking genes associated with breast cancer metastasis to the brain. Reduction of PCDH7 in the metastatic breast cancer cell line MDA-MB-231 effectively inhibits cell proliferation, migration, and invasion *in vitro* (Li et al., 2013). In lung cancer, the enforced PCDH7 expression significantly accelerates lung tumorigenesis in mice harboring the $Kras^{G12D}$ mutation and potentiates MAPK pathway activation (Zhou et al., 2017; Zhou et al., 2019). In contrast to the promotive effects of PCDH7 in breast and lung cancer, downregulated PCDH7 correlates with advanced grade, larger tumor size, and poorer overall survival in bladder cancer and gastric cancer patients (Lin et al., 2016; Chen et al., 2017).

In the present study, we found that PCDH7 conferred higher cell proliferation potential and stronger chemoresistance in colorectal cancer cells both *in vitro* and *in vivo* by promoting MCL-1 expression. Our data provide novel insights into the underlying mechanism of the functions of PCDH7 in CRC progression, which might also help us in developing a new therapeutic strategy for CRC by targeting this molecule.

2 Methods and materials

2.1 Bioinformatics analysis of PCDH7 in colorectal cancer

Sequencing data of colorectal cancer in the TCGA database were downloaded. The correlation between PCDH7 expression and its clinical parameters in CRC patients was analyzed using two-sample *t*-test.

2.2 Cell lines and cell cultures

The colorectal cancer cell lines in this study, including LS411N (colorectal carcinoma), DLD1 (colon adenocarcinoma), RKO (colon carcinoma), HCT116 (colon adenocarcinoma), SW620 (Caucasian colon adenocarcinoma), HT29 (Caucasian colon adenocarcinoma), and SW480 (colon adenocarcinoma), were purchased from American Type Culture Collection (ATCC), and all cell lines are *KRAS* mutants. All cells were cultured in Dulbecco's modified Eagle's medium (DMEM) (HyClone) supplemented with 10% fetal bovine serum (FBS) (HyClone), 1% penicillin (100 units/mL), and streptomycin (100 μg/mL) (Sigma). These cells were placed in a cell culture incubator supplied with 5% CO_2, maintained at 37°C, and passaged at ≥80% confluence by trypsinization (Gibco). All experiments were performed when the cells were in the logarithmic growth phase.

2.3 Western blotting and the antibodies

Cells were lysed with RIPA buffer containing 50 mM Tris-HCl (pH 8.0), 150 mM NaCl, 2 mM EDTA (pH 8.0), 0.1% Triton-X 100, 0.5% sodium deoxycholate, 0.1% sodium dodecyl sulfate, and 1% protease inhibitor (Sigma). The lysate was incubated on ice for 10 min, the supernatant was collected after centrifugation at high speed, and the cell lysate was prepared with 2× SDS loading buffer after denaturation. Gel electrophoresis was performed on an 8%–15% gradient acrylamide gel to separate the proteins, which were then transferred onto a PVDF membrane (Millipore). After blocking with 5% fat-free milk in PBST for 2 h at room temperature, the PVDF membranes were incubated with the corresponding primary antibodies at 4°C overnight. The predicted proteins were detected using the corresponding secondary antibody-conjugated HRP. Protein bands were detected using an ECL chemiluminescence reaction kit (Thermo Fisher Scientific). ImageJ software was used for quantitative analysis.

Antibodies for immunoblotting included anti-PCDH7 (Santa Cruz, sc-517042, 1:500), anti-PARP (CST, 9532S, 1:1,000), anti-caspase 9 (CST, 9502, 1:1,000), anti-caspase 3 (CST, 9668, 1:1,000), anti-Mcl-1 (CST, 5453, 1:1,000), anti-β-catenin (CST, 8480, 1:1,000), anti-p-GSK-3β (CST, 9421, 1:1,000), anti-c-Myc (CST, 5605, 1:1,000), and mouse anti-β-actin (Sigma, A5441) diluted at 1:5,000.

2.4 Generation of PCDH7 knockdown cell lines and PCDH7 overexpression cell lines

PCDH7-siRNAs were purchased from GemmaPharma Bio. (Shanghai, China), and the human PCDH7 overexpression plasmid was purchased from Molecular Detection Bio (Hangzhou, China). The plasmid sequences were verified by sequencing. Transfection of siRNA or the PCDH7 overexpression plasmid was performed using Lipofectamine 3000 (Invitrogen) according to the manufacturer's protocol. Prior to transfection, the cells were seeded into 6-well plates at appropriate densities and cultured for 24 h in a complete medium. For PCDH7 cells stably overexpressing LS411N for animal experiments, G418 was used for cell selection. Cells were collected in the experiments designed to perform the corresponding experiments. The efficiency of overexpression or knockdown was evaluated by Western blotting of transfected cells after 48 h of transfection.

2.5 MTT assay

Cell proliferation was evaluated using the Cell Proliferation Kit I (MTT) (Roche) according to the manufacturer's protocol. Briefly, different colorectal cancer cells overexpressing PCDH7 or PCDH7 knockdown were collected 24 h after transfection, seeded into 96-well plates at an appropriate density (3 × 103/well), and cultured overnight to allow cell adherence. At the indicated time points, the corresponding cells were treated with 50 μL MTT reagent (final concentration 0.5 mg/mL) and incubated at 37°C for up to 4 h, followed by the addition of 150 μL of DMSO. Cell viability was checked by measuring the absorbance at 570 nm using a microplate reader (Molecular Devices).

For cytotoxicity detection, cancer cells were seeded into 96-well plates at a suitable density and treated with the indicated concentrations of ABT-263 or cisplatin for 24 and 48 h prior to performing the MTT assay. ABT-263 was diluted in DMSO to prepare the mother solution at 100 mg/mL and then diluted into the actual working concentration with the culture medium. Cisplatin was diluted in DMSO to prepare the mother solution at 5 mg/mL and then diluted into the actual working concentration with the culture medium.

Cell proliferation rate % = (experimental group OD value−0 day OD value)/(control group OD value−0 day OD value) * 100%; cell relative survival rate % = experimental group OD value/control group OD value * 100%

2.6 Cell migration and invasion assays

Chambers (8-mm pore, BD Falcon, BD Biosciences) with or without Matrigel (BD Biosciences) were used to investigate invasion and migration, respectively. Colorectal cancer cells were suspended in a serum-free medium and seeded into the chambers. These chambers were then placed in 24-well plates filled with 600 μL of the medium containing 20% FBS as an attractant. After 24 h of incubation at 37°C with 5% CO_2, the cells on the upper side were removed, and the migrated or invaded cells on the underside of the membrane were fixed and stained with 0.1% crystal violet for 30 min at 37°C. After washing twice with PBS, cells on the lower membrane were counted in three independent areas.

2.7 Apoptosis detection by flow cytometry

Apoptosis detection was performed using the FITC Annexin V Apoptosis Kit (eBioscience), according to the manufacturer's instructions. Briefly, the treated colorectal cancer cells were collected, and 1 × 10^6 cells were resuspended in 500 μL 1× binding buffer containing 5 μL FITC-labeled Annexin V and 5 μL PI solution. The cells were gently vortexed and incubated for 15 min at room temperature in the dark, followed by flow cytometry (BD, Fortessa). The proportion of apoptosis refers to the sum of Annexin V-positive cells.

2.8 RNA isolation and qPCR

Total cellular RNA was extracted using TRIzol reagent (Invitrogen), according to the manufacturer's instructions. cDNA was synthesized using total RNA as a template and Promega M-MLV reverse transcriptase. Real-time PCR was performed on an ABI 7500 Fast Real-Time PCR system (Applied Bioscience) with Power SYBR Green PCR Master Mix (Applied Biosystems), according to the manufacturer's instructions. Primers used were as follows: Mcl-1, forward primer 5′-AAAGCCTGTCTGCCAAAT-3′; reverse primer 5′-TTAGACCACCTGCCTCCT-3′; β-actin, forward primer 5′-ACACCCCAGCCAT GTACGTT-3′; reverse primer 5′-TCACCGGA GTCCATCACGAT-3′. The specificity of these primers was determined using a melting curve. The relative expression of the genes was analyzed using the 2-△△CT method, and β-actin was used as a control.

2.9 Tumor growth inhibition *in vivo*

Four-week-old female athymic BALB/c mice were subcutaneously injected with 5 × 10^6 LS411N cells. After a solid tumor formed and grew to approximately 80–100 mm^3, the tumor-bearing mice were randomized into four groups of four mice each. Control mice were intravenously administered with saline. The treatment groups were injected intravenously with S63845 (5 mg/kg body weight) alone or ABT-263 (50 mg/kg for each mouse) orally, alone or in combination once every 2 days for 12 days. All animal experiments were approved by the Animal Experimentation Ethics Committee of Zhejiang University.

2.10 Statistical analyses

All data are expressed as mean ± standard deviation (mean ± SD). Data analysis was performed using GraphPad Prism 7. All experiments were repeated thrice. Differences between groups were analyzed using the paired Student's *t*-test. $p < 0.05$ was considered to indicate statistical significance.

10.3389/fphar.2023.1072033

TABLE 1 Association between PCDH7 expression and clinical pathological features in colorectal cancer patients.

Character	Level	Low expression of PCDH7	High expression of PCDH7	P
Age	≤60	84	43	0.007
	>60	244	69	
Gender	Male	64	29	0.118
	Female	264	83	
T	Tis	1	0	0.001
	T1	7	2	
	T2	65	9	
	T3	219	82	
	T4	36	19	
N	N0	205	56	0.003
	N1	72	29	
	N2	51	27	
	N3	—	—	
M	M0	286	90	0.071
	M1	42	22	
Stage	I	65	11	0.004
	II	133	44	
	III	88	35	
	IV	42	22	

3 Results

3.1 The clinical significance of PCDH7 in colorectal cancer and its basic expression in colorectal cancer cells

We first analyzed the correlation between PP4R1 expression and the clinical pathological features in 440 patients with colorectal cancer. As shown in Table 1, significant associations were obtained between PCDH7 expression and age ($p = 0.007$), T classification ($p = 0.001$), N classification ($p = 0.003$), and stage ($p = 0.004$). To investigate the potential functions of PCDH7 in colorectal cancer, we initially used Western blotting to detect the abundance of PCDH7 in different colorectal tumor cell lines, including LS411N, DLD1, RKO, HCT116, SW620, HT29, and SW480. Our data indicated that DLD1 and RKO cells expressed the highest levels of PCDH7 protein. Moderate levels of the protein were observed in SW620 and SW480 cells, whereas relatively low levels of the protein were expressed in LS411N, HCT116, and HT29 cells (Figure 1A). To characterize the potential effects of PCDH7 on colorectal cancer, we successfully induced the expression of PCDH7 in SW480, HT29, HCT116, LS411N, and SW620 cells using an overexpression plasmid, while decreasing PCDH7 expression in DLD1 and RKO cells by transfection with a siRNA against PCDH7 (Figure 1B).

3.2 The effects of PCDH7 in colon cancer cell proliferation

Cell proliferation was detected in colorectal cancer cell lines by PCDH7 overexpression or silencing using the MTT assay. Our data revealed that the expression of PCDH7 was positively associated with the proliferation potential of CRC cells. SW480 cells overexpressing PCDH7 showed more robust proliferation than control cells transfected with the corresponding empty vector. Similar results were also observed in other cell lines, including HT29, HCT116, LS411N, and SW620 cells (Figure 2A). In contrast, PCDH7 knockdown in DLD1 and RKO cells effectively decelerated their proliferation (Figure 2B). In summary, our data implied that PCDH7 could potentially play a role in colorectal cancer progression by accelerating cancer cell proliferation.

3.3 The potential roles of PCDH7 in CRC cell metastasis

Given the widely known role of protocadherin in cell-in-cell structure to mediate cancer cell metastasis, we further determined whether PCDH7 could contribute to colorectal cancer metastasis by regulating cancer cell migration and invasion. Interestingly, our data from transwell experiments indicated that overexpression of PCDH7 in SW480, HT29, and HCT116 cells significantly weakened their migration and invasion (Figures 3A–C). To further verify the role of

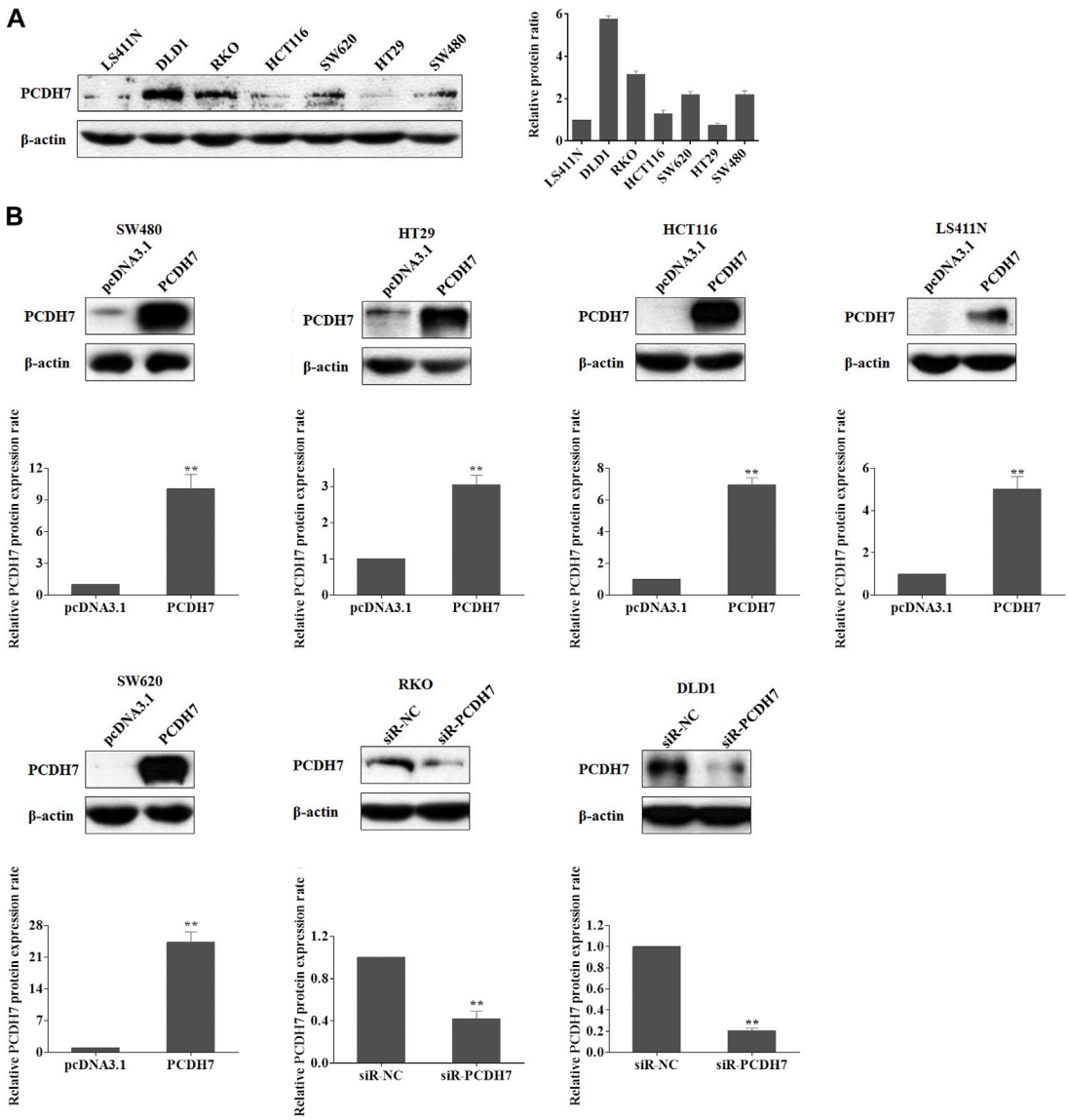

FIGURE 1
Expression of PCDH7 in colorectal cancer cell lines. **(A)** Expressions of PCDH7 protein were examined in LS411N, DLD1, RKO, HCT116, SW620, HT29, and SW480 using Western blot assay. **(B)** Overexpression of PCDH7 in SW480, HT29, HCT116, LS411N, and SW620 cells transfected with the overexpression plasmid for 24 h and the silencing of PCDH7 in DLD1 and RKO cells by siRNA transfection for 24 h were verified by Western blot assays. Data are presented as mean ± SD for three separate experiments. $^{**}p < 0.01$ *vs.* control.

PCDH7 in CRC cell migration and invasion, the transwell assay was performed in CRC cells with PCDH7 silencing. As shown in Figure 3D, downregulation of PCDH7 expression significantly promoted the migration and invasion of DLD1 cells. Thus, these results indicated that PCDH7 negatively regulates colorectal cancer cell migration and invasion rather than cell proliferation.

3.4 PCDH7 confers drug resistance of colorectal cancer cells to ABT-263 and cisplatin

Next, we investigated whether PCDH7 contributes to the development of drug resistance in CRC cells. First, we measured the sensitivity of different colorectal cancer cell lines to ABT-263 and cisplatin. ABT-263, an orally available, selective inhibitor of the anti-apoptotic BCL-2 family proteins, including Bcl-2, Bcl-XL, and Mcl-1, has been demonstrated to possess antitumor activity against various types of cancers and is in clinical trials (Lever and Fergason-Cantrell, 2019; Ohgino et al., 2020). Cisplatin, another well-known anti-cancer drug employed in treating different solid tumors, generates DNA lesions to activate the DNA damage response and induce apoptosis (Galluzzi et al., 2012). Here, we observed that both drugs effectively inhibited the viability of SW480, HT29, HCT116, LS411N, SW620, and RKO cells in a dose- and time-dependent manner (Figure 4).

To further examine the potential effect of PCDH7 on drug resistance in colorectal cancer, we performed gain- and loss-of-

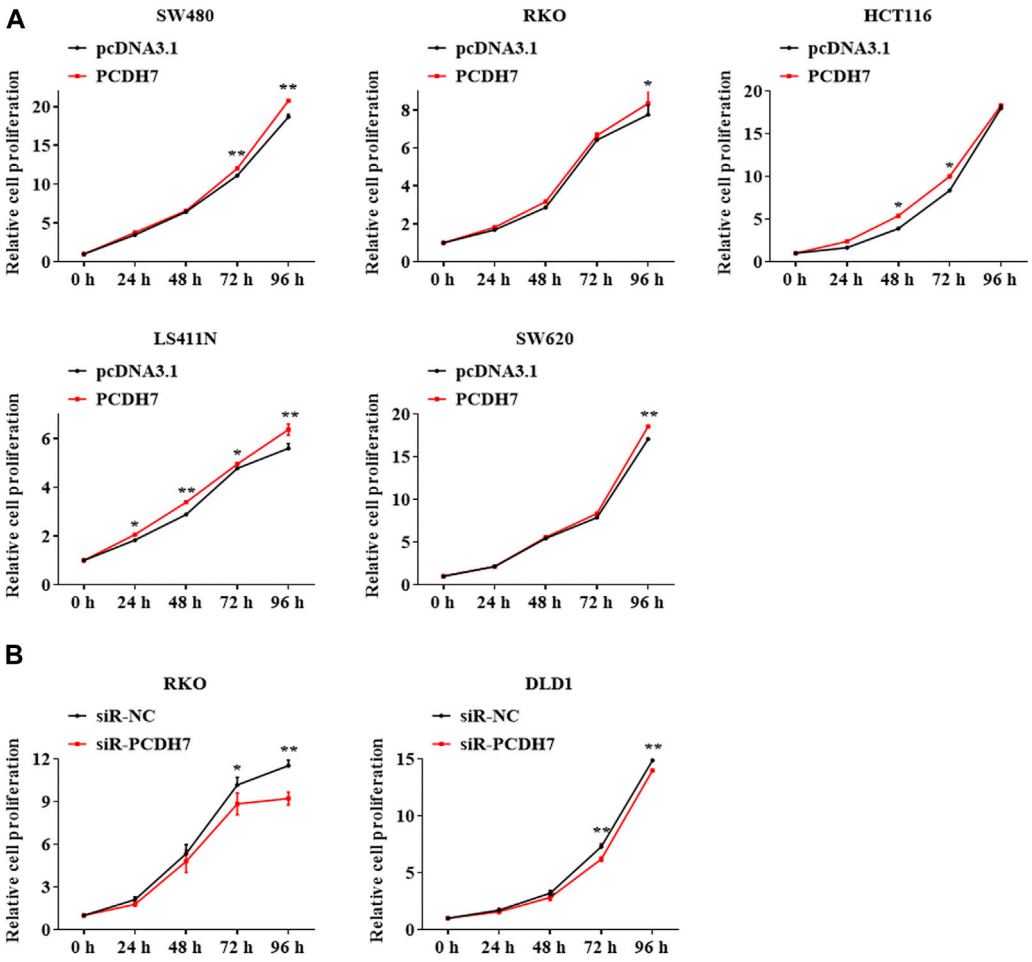

FIGURE 2
Effects of PCDH7 in colon cancer cell proliferation. **(A)** MTT assays were performed to detect the cell proliferation of SW480, HT29, HCT116, LS411N, and SW620 cells transfected with PCDH7 overexpression plasmid or empty vector pcDNA3.1 for 24 h. **(B)** Cell proliferation of RKO and DLD1 cells with PCDH7 silencing transfected with siRNA for 24 h was examined by MTT assays. Data are presented as mean ± SD for three separate experiments. $^{**}p < 0.01$ *vs.* control.

function experiments by overexpressing or knocking down PCDH7 in colorectal cancer cells. We found that the overexpression of PCDH7 in SW480, RKO, HCT116, LS411N, and SW620 cells significantly promoted their survival under either ABT-263 or cisplatin treatment (Figure 5). Conversely, the decrease in PCDH7 expression in RKO cells led to remarkably increased sensitivity to ABT-263 and cisplatin compared to that in control cells (Figure 5). Together, these results revealed that abundant PCDH7 enhances the resistance of colorectal cancer cells to chemotherapeutic drug treatment to facilitate cell viability, suggesting that PCDH7 is a potential regulatory target for colorectal cancer chemotherapy.

3.5 PCDH7 enhanced drug resistance of CRC cells to ABT-263 by inhibiting apoptosis

Given that upregulation of PCDH7 increased CRC cell survival in response to ABT-263, an effective cell apoptosis inducer, we next determined whether the function of PCDH7 resulted from its anti-apoptotic effect. We further detected the regulation of PCDH7 on ABT-263-induced cleavage of caspase 3, caspase 9, and PARP (18). As shown in Figure 6A, ABT-263 treatment effectively induced the cleavage of caspase 3, caspase 9, and PAPR in both HCT116 and RKO cells. Surprisingly, cleaved-caspase 3, cleaved-caspase 9, and cleaved PAPR levels were significantly reduced following PCDH7 overexpression in HCT116 cells treated with ABT-263 (Figure 6A, upper panel). More interestingly, the levels of cleaved-caspase 3, cleaved-caspase 9, and cleaved PAPR obviously increased with the silencing of PCDH7 in RKO cells treated with ABT-263 (Figure 6A, down panel). These results prompted us to quantify the apoptosis of CRC cells treated with ABT-263 under overexpression or silencing of PCDH7 using Annexin V-FITC/PI staining. The percentage of ABT-263-induced apoptotic HCT116 cells increased to approximately 40% from nearly 17% after ABT263 treatment, while it was reduced to approximately 30% in PCDH7-

10.3389/fphar.2023.1072033

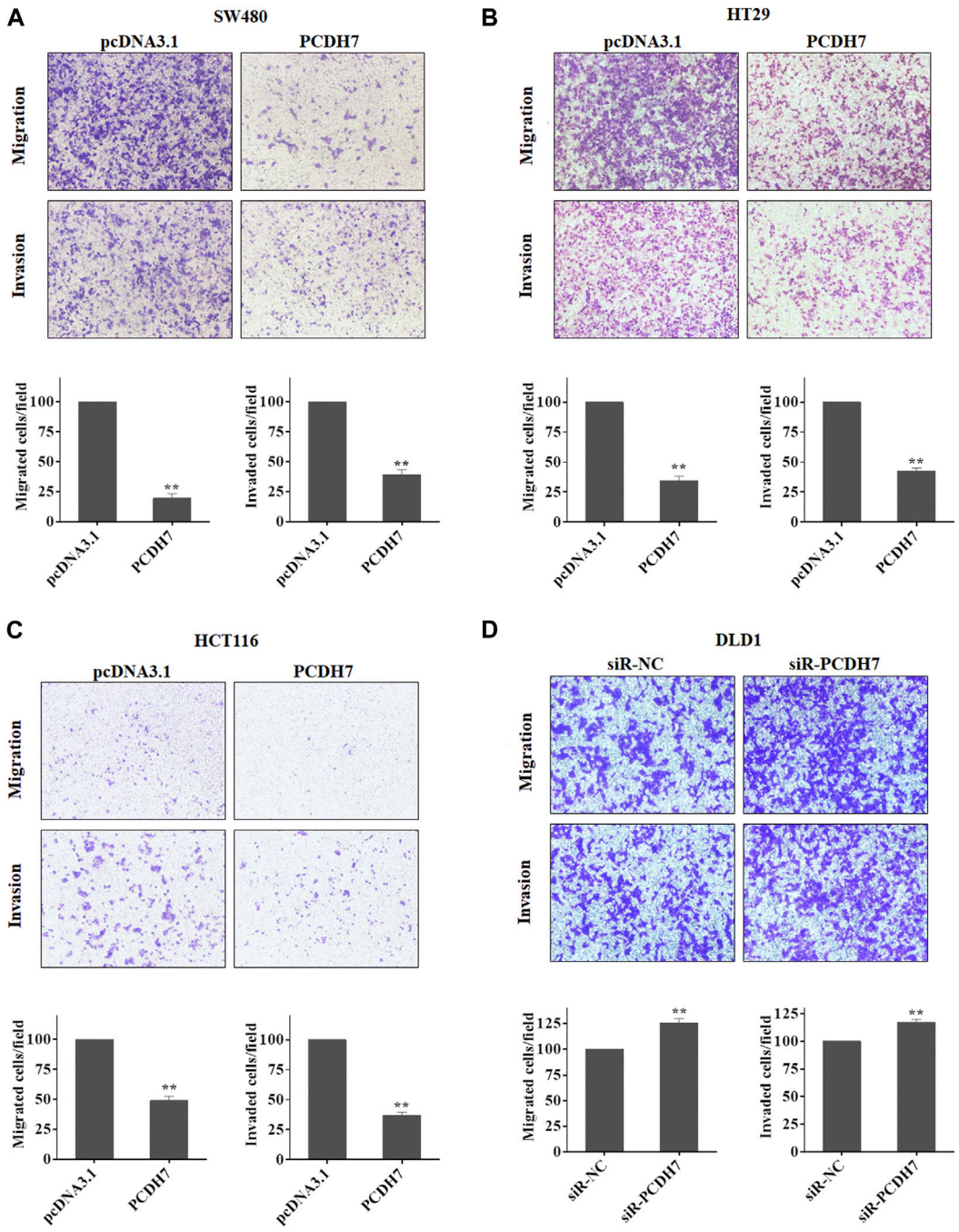

FIGURE 3
Roles of PCDH7 in CRC cell migration and invasion. **(A–C)** Transwell assays were used to determine the potentials of cell migration and invasion in SW480, HT29, and HCT116 cells with PCDH7 overexpression. **(D)** Transwell assays were performed to detect cell migration and invasion in DLD1 cells with PCDH7 knockdown. Data are presented as mean ± SD for three separate experiments. $^{**}p < 0.01$ *vs.* control.

overexpressed cells (Figure 6B, left panel). In RKO cells, the percentage of apoptotic cells increased from nearly 6% to 10% as a result of PCDH7 silencing in RKO cells under the ABT-263 treatment (Figure 6B, right panel). Hence, we proposed that higher PCDH7 levels would help colorectal cells suppress apoptosis and facilitate the survival of these cells during chemotherapeutic treatment.

3.6 The potential targets of the PCDH7 underlying molecular mechanism of its anti-apoptosis function

Subsequently, we attempted to identify the potential targets of PCDH7 in colorectal cancer cells to further elucidate the underlying mechanism of its role in the development of drug resistance in CRC.

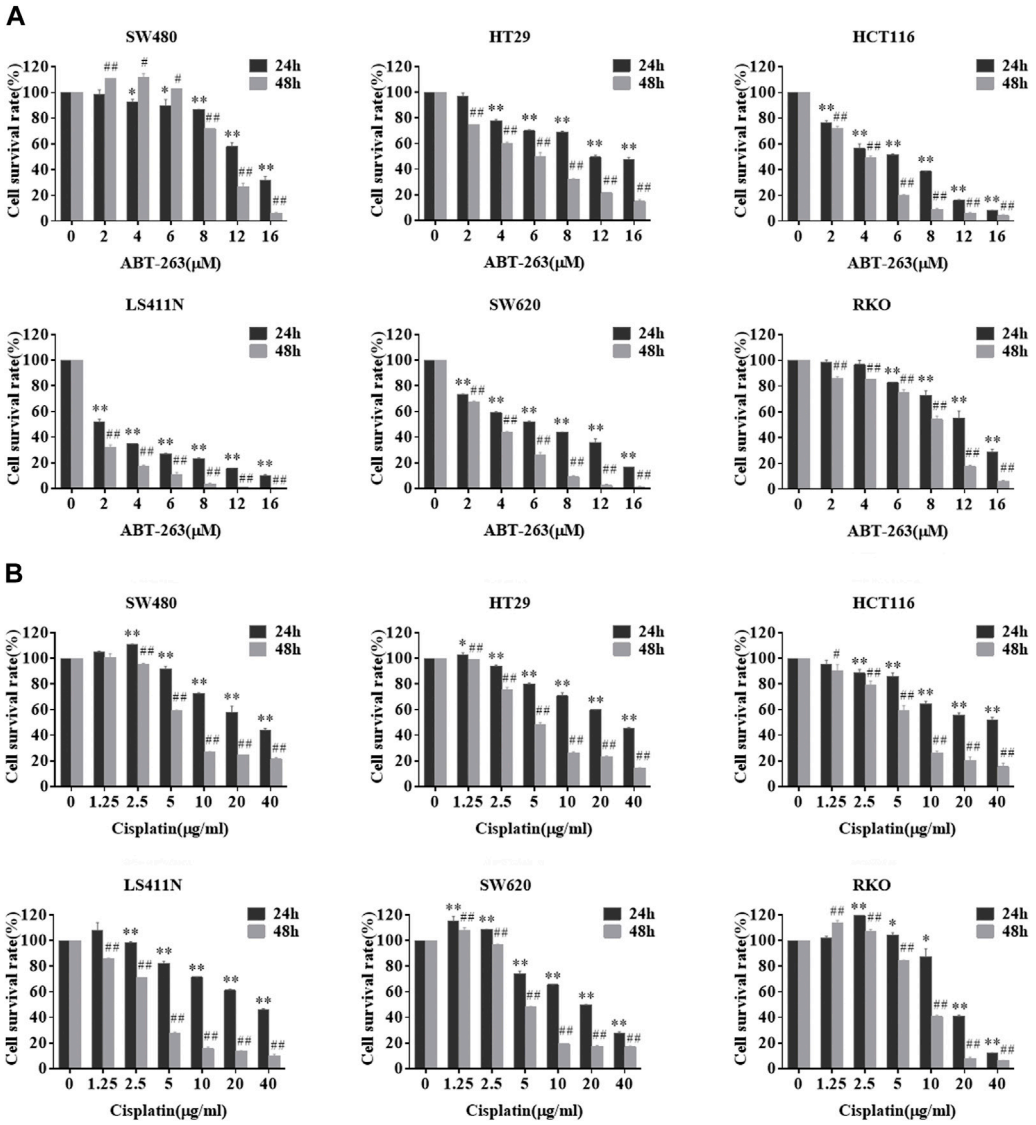

FIGURE 4
Sensitivity of different colorectal cancer cells to ABT-263 and cisplatin. After treating CRC cell lines with different concentrations of ABT-263 **(A)** or cisplatin **(B)** for 24 or 48 h, MTT assay was used to determine the cell viability to confirm the cytotoxicity of the two drugs. Data are presented as mean ± SD for three separate experiments. *, #$p < 0.05$; **, ##$p < 0.01$ *vs.* control.

Considering that ABT-263 is an inhibitor specific to anti-apoptotic BCL-2 family members, especially Mcl-1 (Timucin et al., 2019), we first determined whether Mcl-1 could be affected by PCDH7 using Western blotting. As anticipated, the protein expression of Mcl-1 was upregulated following PCDH7 overexpression in HCT116 cells and downregulated after PCDH7 knockdown in RKO cells, which may partially explain the anti-apoptotic effect exerted by PCDH7 on colorectal cancer cells (Figures 7A–C). Additionally, we further evaluated the Wnt/β-catenin signaling pathway considering the massive evidence showing a correlation with chemoresistance in colorectal cancer (Su et al., 2015; Bahrami et al., 2017). Interestingly, the downregulation of P-β-catenin and the upregulation of β-catenin and its downstream target cyclin D1 and c-Myc were observed in PCDH7-overexpressed HCT116 cells, while all of these were completely reversed in PCDH7-silenced RKO cells (Figures 7A–C). Finally, real-time PCR assays indicated that the levels of Mcl-1 mRNA were upregulated in HCT116 cells with PCDH7 overexpression, while it was inhibited in RKO cells with PCDH7 silencing (Figures 7D, E).

3.7 PCDH7 mediated the drug resistance of CRC *via* upregulating Mcl-1

To further confirm that PCDH7 affected colorectal cancer chemoresistance mainly through Mcl-1 expression, we applied an Mcl-1 inhibitor, S63845, in HCT116 cells coupled with PCDH7 overexpression. Surprisingly, Mcl-1 expression was dramatically upregulated in response to S63845 treatment compared to that in control, which may be a normal response to

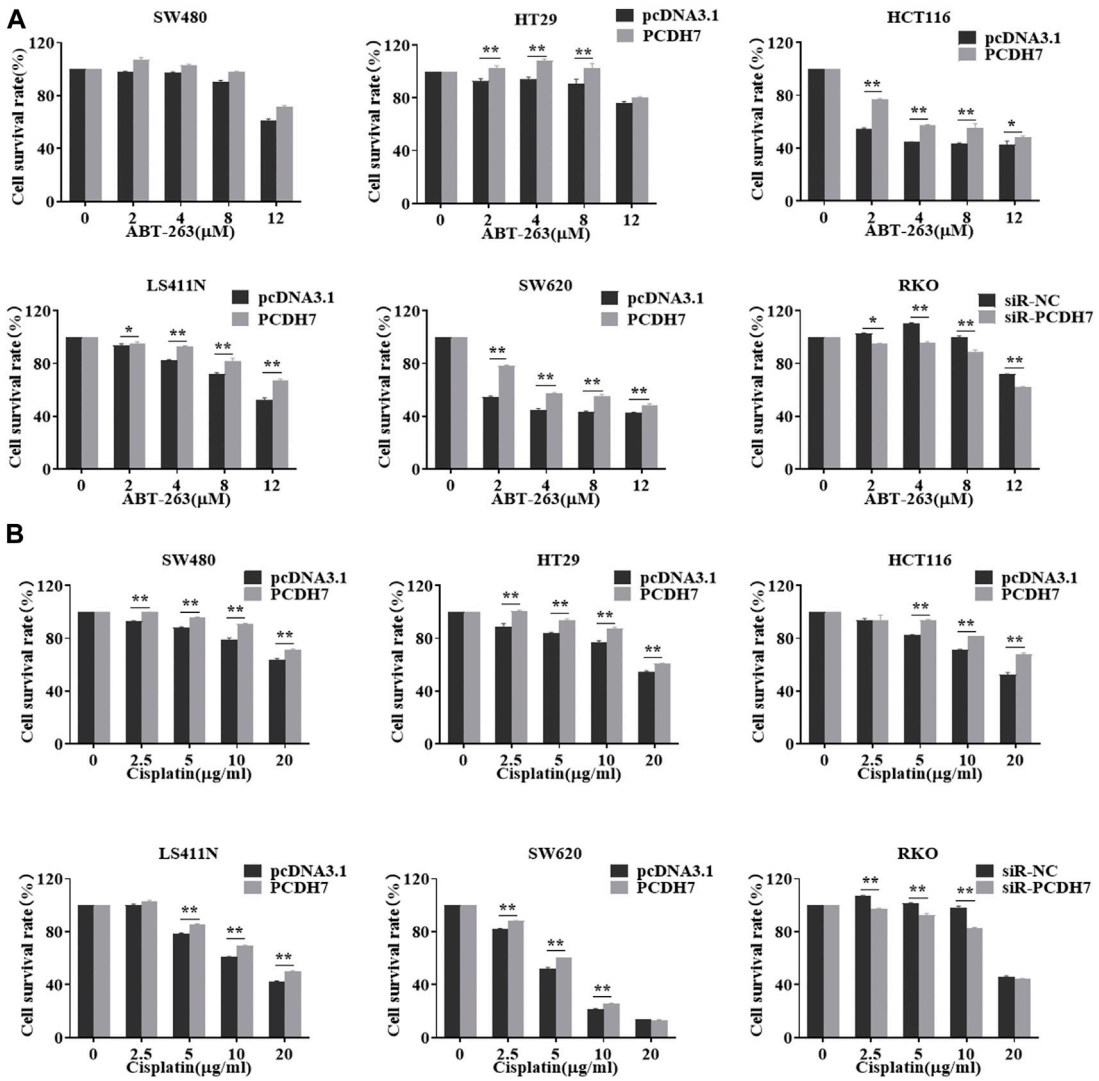

FIGURE 5
Effects of PCDH7 on the resistance of colorectal cancer cells. **(A)** MTT assays were performed to determine the cell viabilities of SW480, HT29, HCT116, LS411N, SW620, and RKO cells with the treatment of ABT-263 under PCDH7 overexpression or silencing. **(B)** MTT assays were performed to determine the cell viabilities of SW480, HT29, HCT116, LS411N, SW620, and RKO cells with cisplatin treatment under PCDH7 overexpression or silencing. Data are presented as mean ± SD for three separate experiments. *$p < 0.05$; **$p < 0.01$ *vs.* control.

stress (Figure 8A). S63845 effectively attenuated the inhibitory effect of PCDH7 on ABT-263-induced apoptosis in HCT116 cells (Figure 8B, from approximately 27%–57%). This function was further supported by the increased cleavage of PARP, caspase-3, and caspase-9 in HCT116 cells treated with S63845 in combination with PCDH7 overexpression and ABT-263 treatment (Figure 8C). Moreover, S63845 treatment alone not only suppressed the proliferation of HCT116 cells but also effectively reversed the protective role of PCDH7 on the cytotoxicity of ABT-263 (Figure 8D). Finally, we tested our hypothesis in a xenograft model in nude mice. As shown in Figure 8E, although S63845 alone only slightly inhibited tumor growth, it effectively enhanced the anti-cancerous role of ABT-263 under PCDH7 overexpression. Collectively, PCDH7 might mediate drug resistance in CRC by upregulating Mcl-1, at least partially.

4 Discussion

In the present study, we characterized the abundance of PCDH7 in CRC cells correlated with their metastasis and chemoresistance. Here, we observed that upregulation of PCDH7 in colorectal cancer cells strongly promoted the activation of the Wnt/β-catenin signaling pathway, including the upregulation of catenin protein expression, which finally resulted in the expression of c-Myc, a widely reported protein essential for cell proliferation. These results partially explain the effects of PCDH7 on colorectal cancer cells.

There have been many studies showing that PCDH7 is abnormally expressed in various cancers and has a carcinogenic or anti-tumor effect (Terry et al., 2006; Cao et al., 2017; Liu et al., 2019). However, few studies have focused on the expression and role

10.3389/fphar.2023.1072033

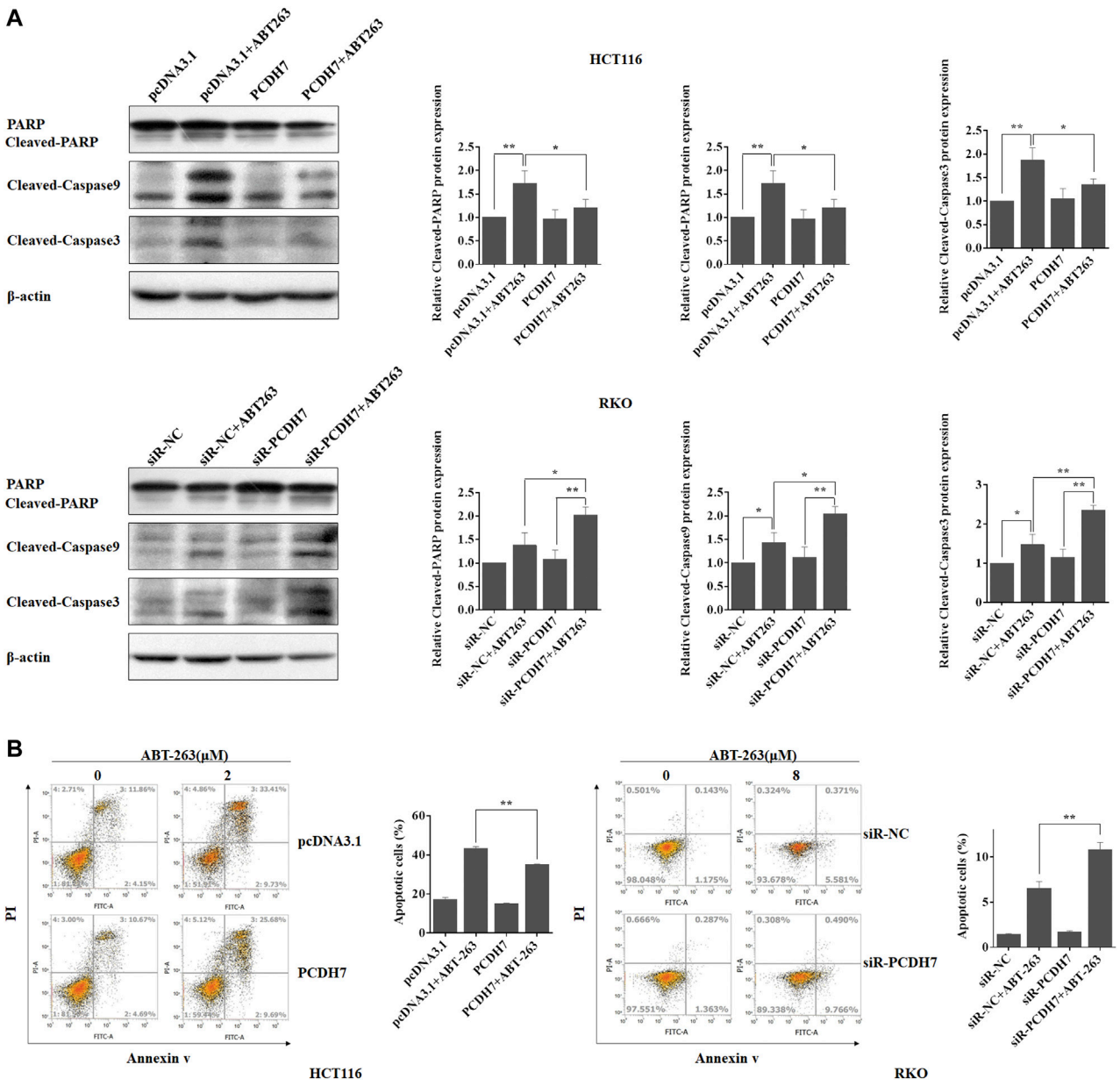

FIGURE 6
PCDH7 promoted drug resistance to CRC cells to ABT-263 by repressing apoptosis. **(A)** The cleavage of caspase 3, caspase 9, and PAPR was detected by western blot experiment in HCT116 and RKO cells treated with ABT-263 under PCDH7 overexpression or not, respectively. Representative data was shown. **(B)** HCT116 and RKO cells were treated with ABT-263 under PCDH7 overexpression or silencing, respectively. Apoptosis was examined by using flow cytometry with Annexin V-FITC/PI staining. Data are presented as mean ± SD for three separate experiments. *$p < 0.05$; **$p < 0.01$. vs. control.

of individual PCDH7s in cancer. Previous studies have found that PCDH7 expression was significantly upregulated in human non-small cell lung cancer (NSCLC) (Zhou et al., 2017). PCDH7 was significantly downregulated in non-muscle invasive bladder cancer (NMIBC), and Cox analysis revealed that PCDH7 can be used as an independent predictor of NMIBC (13). The aforementioned investigations demonstrate that PCDH7 plays a role in various cancers. Arising from the bottleneck we encountered in developing effective inhibitors specific for RAS family proteins and the high proportion of resistance in response to *BRAF* inhibitors in colorectal clinic chemotherapy, there is an urgent need to explore the intrinsic molecular mechanism to provide a strategy for the combination of chemotherapeutics or identify a novel target for developing new inhibitors. In addition to modulating cell proliferation, we showed that PCDH7 would facilitate colorectal cancer cell survival under treatment with

10.3389/fphar.2023.1072033

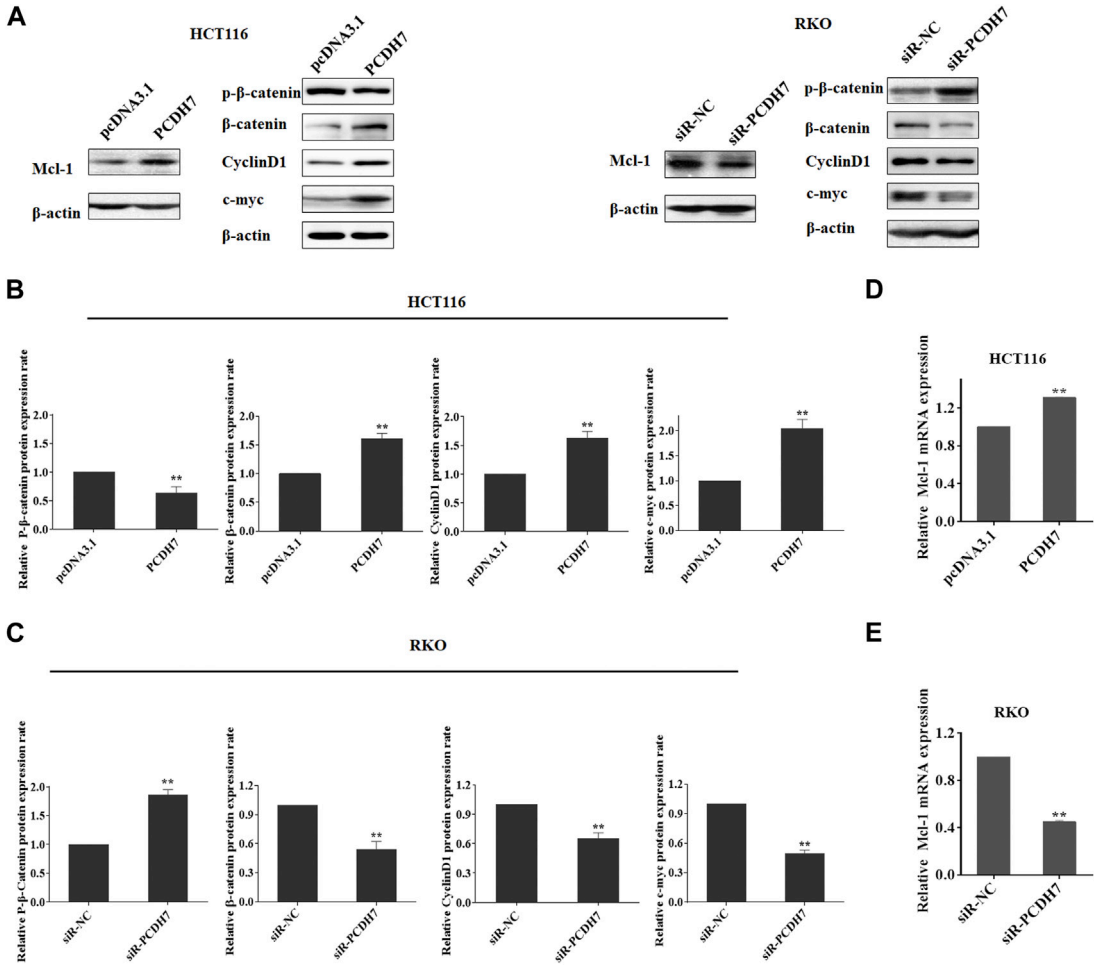

FIGURE 7
Role of PCDH7 in Mcl-1 expression and Wnt/β-catenin signaling pathway activation. **(A–C)** Western blot assays were performed to detect the protein expression of Mcl-1, p-β-catenin, β-catenin, cyclin D1, and c-Myc in HCT116 cells with PCDH7 overexpression and in RKO cells with PCDH7 knockdown, respectively. **(D, E)** Real-time qPCR experiments were performed to detect the mRNA expression of Mcl-1 in HCT116 cells with PCDH7 overexpression and in RKO cells with PCDH7 knockdown, respectively. Data are presented as mean ± SD for three separate experiments. $^{**}p < 0.01$ *vs.* control.

ABT-263 or cisplatin, which could induce apoptosis in various cancer cells by targeting anti-apoptotic proteins, which provides a scope for its development as a potential chemotherapeutic drug. Thus, PCDH7 was presumed to play an important role in chemo-treatment-induced apoptosis and was further revealed to positively modulate Mcl-1 expression, which is an anti-apoptotic protein belonging to the BCL-2 family, that results in higher cell viability in colorectal cancer with enhanced PCDH7 expression. Additionally, the combination of the Mcl-1 inhibitor S63845 with ABT-263 can eliminate chemoresistance caused by abundant PCDH7 in colorectal cancer cells. Our study provides strong evidence of the benefits of combining S63845 and ABT-263 for CRC, which is resistant to ABT-263 alone or with high levels of PCDH7.

Although numerous previous reports have illustrated the promotion of lung and breast cancer cell migration and invasion by PCDH7 (Chen et al., 2021), the increase in this protein inhibits cell migration and invasion in gastric cancer cells. However, a recent study has shown that P7 could promote lung metastasis of colorectal cancer (Liu et al., 2022), which seems contrary to our results, but we consider that this is related to different cell lines and experimental systems. This study showed that MCL-1 expression was upregulated after P7 overexpression, and the related molecules of the Wnt/β-catenin pathway were also upregulated. We speculated that P7 regulated MCL-1 through the Wnt/β-catenin pathway, thereby inhibiting apoptosis and promoting drug resistance of tumor cells. In these previous studies, the downregulation of E-cadherin expression followed by PCDH7 depletion was believed to contribute to an increased potential in the migration and invasion of gastric cancer cells (Chen et al., 2017). The contradictory effects of PCDH7 in different cancer types suggest that PCDH7 might play different roles through different molecular mechanisms. Although PCDH7 is a member of the protocadherin family, which is a subfamily of cadherins known to regulate

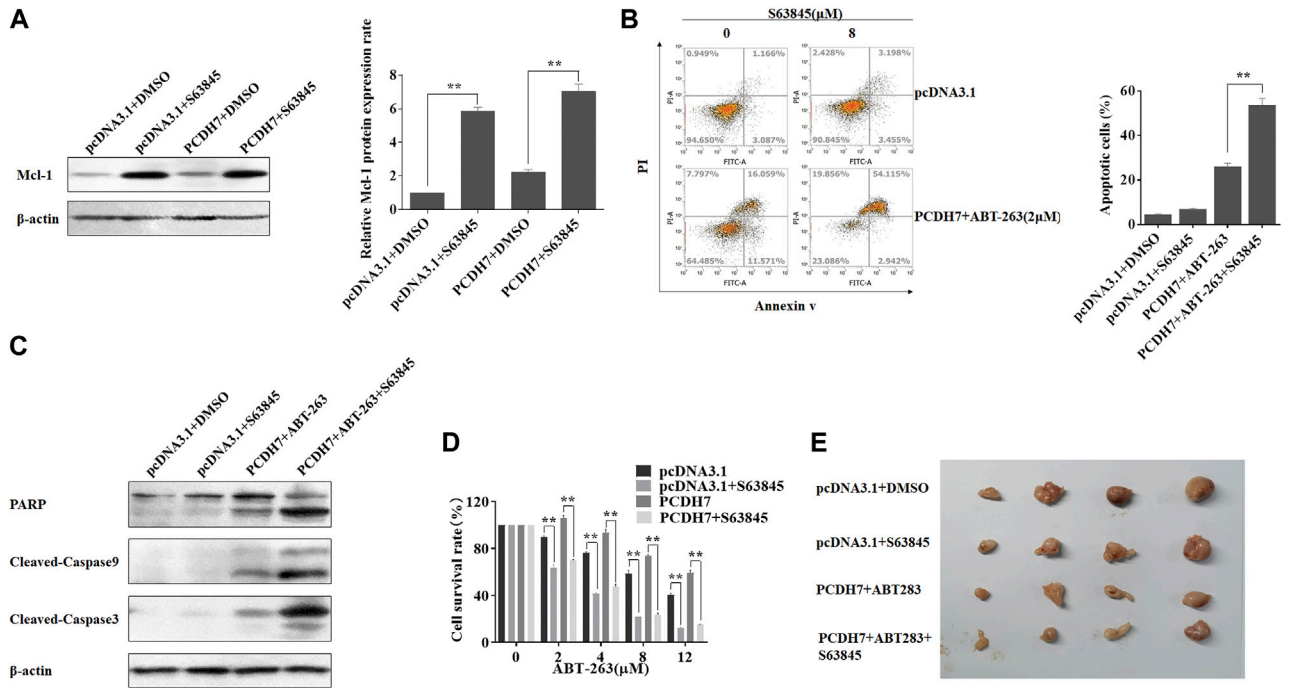

FIGURE 8
PCDH7 mediated the drug resistance of CRC *via* upregulating Mcl-1. **(A)** HCT116 cells were transfected with the PCDH7-overexpressed plasmid or treated with 8 μM S63845 for 24 h, and Mcl-1 protein expression was examined by Western blot assay. **(B)** HCT116 cells were transfected with the PCDH7 overexpressed plasmid combined with 2 μM ABT-263 with or without the treatment of 8 μM S63845 for 24 h. Cell apoptosis was determined using flow cytometry with Annexin V-FITC/PI staining. **(C)** Cleavage of PARP, caspase-3, and caspase-9 in HCT116 cells treated similarly in **(B)** was examined by Western blot assay. **(D)** HCT116 cells were transfected with the PCDH7 overexpressed plasmid with or without S63845 treatment, followed by the incubation of the indicated concentrations of ABT-263; MTT assay was performed to determine the cell viability. **(E)** HCT116 cells stably expressed PCDH7, or the control cells were used to generate xenografts in nude mice. The mice were treated as indicated, and the tumors were presented. Data are presented as mean ± SD for three separate experiments. $^{**}p < 0.01$ *vs.* control.

epithelial-to-mesenchymal transition (EMT) of tumor metastasis during cancer progression, the related study of the detailed mechanism by which PCDH7 affects colorectal cancer metastasis is too little and needs further investigation in CRC. In conclusion, colorectal cells with high PCDH7 expression showed stronger chemoresistance to apoptosis induction. Because the Mcl-1 and Wnt/β-catenin signaling pathways were molecularly identified as regulatory targets of PCDH7, we discovered a combination of the Mcl-1 inhibitor S63845 and ABT-263 as a novel chemotherapy treatment option for PCDH7-high colorectal cancer.

Data availability statement

The original contributions presented in the study are included in the article/Supplementary Material; further inquiries can be directed to the corresponding authors.

Ethics statement

All animal experiments in this study were approved by the Animal Experimentation Ethics Committee, Zhejiang University.

Author contributions

JS and JW, as the co-corresponding authors, provided the idea and designed the framework of the study. ZZ and NL conceived and designed the experiments. NL and KT performed the experiments. ZZ, NL, KT, and FL analyzed the data. JS wrote the draft. NL, KT, and FL revised the manuscript. All authors have read and approved the final manuscript.

Funding

This study was financially supported by the grants from the National Natural Science Foundation of China (Nos. 81802988, 81672364, and 81871917), the National Natural Science Foundation of Zhejiang (LY20H160039), and the Foundation of Taizhou University for the Outstanding Youth project (2017YQ001).

Conflict of interest

The authors declare that the research was conducted in the absence of any commercial or financial relationships that could be construed as a potential conflict of interest.

Publisher's note

References

Bahrami, A., Amerizadeh, F., ShahidSales, S., Khazaei, M., Ghayour-Mobarhan, M., Sadeghnia, H. R., et al. (2017). Therapeutic potential of targeting wnt/β-catenin pathway in treatment of colorectal cancer: Rational and progress. *J. Cell. Biochem.* 118 (8), 1979–1983. doi:10.1002/jcb.25903

Bray, F., Ferlay, J., Soerjomataram, I., Siegel, R. L., Torre, L. A., and Jemal, A. (2018). Global cancer statistics 2018: GLOBOCAN estimates of incidence and mortality worldwide for 36 cancers in 185 countries. *CA Cancer J. Clin.* 68 (6), 394–424. doi:10.3322/caac.21492

Cao, J., Wang, M., and Wang, T. (2017). CCAAT enhancer binding protein beta has a crucial role in regulating breast cancer cell growth via activating the TGF-beta-Smad3 signaling pathway. *Exp. Ther. Med.* 14 (2), 1554–1560. doi:10.3892/etm.2017.4659

Chen, H. F., Ma, R. R., He, J. Y., Zhang, H., Liu, X. L., Guo, X. Y., et al. (2017). Protocadherin 7 inhibits cell migration and invasion through E-cadherin in gastric cancer. *Tumor Biol.* 39 (4), 1010428317697551. doi:10.1177/1010428317697551

Chen, Y., Shen, L., Chen, B., Han, X., Yu, Y., Yuan, X., et al. (2021). The predictive prognostic values of CBFA2T3, STX3, DENR, EGLN1, FUT4, and PCDH7 in lung cancer. *Ann. Transl. Med.* 9 (10), 843. doi:10.21037/atm-21-1392

Connell, L. C., Mota, J. M., Braghiroli, M. I., and Hoff, P. M. (2017). The rising incidence of younger patients with colorectal cancer: Questions about screening, biology, and treatment. *Curr. Treat. Options Oncol.* 18 (4), 23. doi:10.1007/s11864-017-0463-3

Dekker, E., Tanis, P. J., Vleugels, J. L. A., Kasi, P. M., and Wallace, M. B. (2019). Colorectal cancer. *Lancet* 394 (10207), 1467–1480. doi:10.1016/S0140-6736(19)32319-0

Galluzzi, L., Senovilla, L., Vitale, I., Michels, J., Martins, I., Kepp, O., et al. (2012). Molecular mechanisms of cisplatin resistance. *Oncogene* 31 (15), 1869–1883. doi:10.1038/onc.2011.384

Kim, H., Takegahara, N., Walsh, M. C., Ueda, J., Fujihara, Y., Ikawa, M., et al. (2020). Protocadherin-7 contributes to maintenance of bone homeostasis through regulation of osteoclast multinucleation. *BMB Rep.* 53 (9), 472–477. doi:10.5483/BMBRep.2020.53.9.050

Kopetz, S. (2019). New therapies and insights into the changing landscape of colorectal cancer. *Nat. Rev. Gastro Hepat.* 16 (2), 79–80. doi:10.1038/s41575-018-0100-z

Lever, J. R., and Fergason-Cantrell, E. A. (2019). Allosteric modulation of sigma receptors by BH3 mimetics ABT-737, ABT-263 (Navitoclax) and ABT-199 (Venetoclax). *Pharmacol. Res.* 142, 87–100. doi:10.1016/j.phrs.2019.01.040

Li, A. M., Tian, A. X., Zhang, R. X., Ge, J., Sun, X., and Cao, X. C. (2013). Protocadherin-7 induces bone metastasis of breast cancer. *Biochem. biophysical Res. Commun.* 436 (3), 486–490. doi:10.1016/j.bbrc.2013.05.131

Lin, Y. L., Wang, Y. L., Fu, X. L., Li, W. P., Wang, Y. H., and Ma, J. G. (2016). Low expression of protocadherin7 (PCDH7) is a potential prognostic biomarker for primary non-muscle invasive bladder cancer. *Oncotarget* 7 (19), 28384–28392. doi:10.18632/oncotarget.8635

Liu, Y., Peng, K., Xie, R., Zheng, J., Guo, J., Wei, R., et al. (2019). Protocadherin gamma-A7 is down-regulated in colorectal cancer and associated with the prognosis in patients with wild-type KRAS. *Hum. Pathol.* 83, 14–21. doi:10.1016/j.humpath.2018.08.007

Liu, Z., Xu, Y., Liu, X., and Wang, B. (2022). PCDH7 knockdown potentiates colon cancer cells to chemotherapy via inducing ferroptosis and changes in autophagy through restraining MEK1/2/ERK/c-Fos axis. *Biochem. Cell. Biol.* 100 (6), 445–457. doi:10.1139/bcb-2021-0513

Moore, A. R., Rosenberg, S. C., McCormick, F., and Malek, S. (2020). RAS-Targeted therapies: Is the undruggable drugged? *Nat. Rev. Drug Discov.* 19 (8), 533–552. doi:10.1038/s41573-020-0068-6

Ohgino, K., Terai, H., Yasuda, H., Nukaga, S., Hamamoto, J., Tani, T., et al. (2020). Intracellular levels of reactive oxygen species correlate with ABT-263 sensitivity in non-small-cell lung cancer cells. *Cancer Sci.* 111 (10), 3793–3801. doi:10.1111/cas.14569

Pistritto, G., Trisciuoglio, D., Ceci, C., Garufi, A., and D'Orazi, G. (2016). Apoptosis as anticancer mechanism: Function and dysfunction of its modulators and targeted therapeutic strategies. *Aging* 8 (4), 603–619. doi:10.18632/aging.100934

Siegel, R. L., Miller, K. D., Goding Sauer, A., Fedewa, S. A., Butterly, L. F., Anderson, J. C., et al. (2020). Colorectal cancer statistics, 2020. *CA Cancer J. Clin.* 70 (3), 145–164. doi:10.3322/caac.21601

Su, L. Y., Shi, Y. X., Yan, M. R., Xi, Y., and Su, X. L. (2015). Anticancer bioactive peptides suppress human colorectal tumor cell growth and induce apoptosis via modulating the PARP-p53-Mcl-1 signaling pathway. *Acta Pharmacol. Sin.* 36 (12), 1514–1519. doi:10.1038/aps.2015.80

Terry, S., Queires, L., Gil-Diez-de-Medina, S., Chen, M. W., de la Taille, A., Allory, Y., et al. (2006). Protocadherin-PC promotes androgen-independent prostate cancer cell growth. *Prostate* 66 (10), 1100–1113. doi:10.1002/pros.20446

Timucin, A. C., Basaga, H., and Kutuk, O. (2019). Selective targeting of antiapoptotic BCL-2 proteins in cancer. *Med. Res. Rev.* 39 (1), 146–175. doi:10.1002/med.21516

Venderbosch, S., Nagtegaal, I. D., Maughan, T. S., Smith, C. G., Cheadle, J. P., Fisher, D., et al. (2014). Mismatch repair status and BRAF mutation status in metastatic colorectal cancer patients: A pooled analysis of the CAIRO, CAIRO2, COIN, and FOCUS studies. *Clin. Cancer Res.* 20 (20), 5322–5330. doi:10.1158/1078-0432.CCR-14-0332

Yoshida, K., Yoshitomo-Nakagawa, K., Seki, N., Sasaki, M., and Sugano, S. (1998). Cloning, expression analysis, and chromosomal localization of BH-protocadherin (PCDH7), a novel member of the cadherin superfamily. *Genomics* 49 (3), 458–461. doi:10.1006/geno.1998.5271

Zhou, X., Padanad, M. S., Evers, B. M., Smith, B., Novaresi, N., Suresh, S., et al. (2019). Modulation of mutant kras(g12d) -driven lung tumorigenesis *in vivo* by gain or loss of PCDH7 function. *Mol. Cancer Res.* 17 (2), 594–603. doi:10.1158/1541-7786.MCR-18-0739

Zhou, X., Updegraff, B. L., Guo, Y., Peyton, M., Girard, L., Larsen, J. E., et al. (2017). PROTOCADHERIN 7 acts through SET and PP2A to potentiate MAPK signaling by EGFR and KRAS during lung tumorigenesis. *Cancer Res.* 77 (1), 187–197. doi:10.1158/0008-5472.CAN-16-1267-T

frontiers | Frontiers in Pharmacology

TYPE Review
PUBLISHED 01 September 2023
DOI 10.3389/fphar.2023.1189799

OPEN ACCESS

EDITED BY
Sona Vodenkova,
Institute of Experimental Medicine (ASCR), Czechia

REVIEWED BY
Radka Václavíková,
National Institute of Public Health (NIPH), Czechia
Saeid Afshar,
Hamadan University of Medical Sciences, Iran

*CORRESPONDENCE
Gang Li,
Leeganng@163.com

†These authors have contributed equally to this work

RECEIVED 20 March 2023
ACCEPTED 14 August 2023
PUBLISHED 01 September 2023

CITATION
Jiang H, Zhou S and Li G (2023), Novel biomarkers used for early diagnosis and tyrosine kinase inhibitors as targeted therapies in colorectal cancer. *Front. Pharmacol.* 14:1189799. doi: 10.3389/fphar.2023.1189799

Novel biomarkers used for early diagnosis and tyrosine kinase inhibitors as targeted therapies in colorectal cancer

Huafeng Jiang†, Senjun Zhou† and Gang Li*†

Department of Anus and Colorectal Surgery, Shaoxing People's Hospital, Shaoxing, China

Colorectal cancer (CRC) is the third most common and second most lethal type of cancer worldwide, presenting major health risks as well as economic costs to both people and society. CRC survival chances are significantly higher if the cancer is diagnosed and treated early. With the development of molecular biology, numerous initiatives have been undertaken to identify novel biomarkers for the early diagnosis of CRC. Pathological disorders can be diagnosed at a lower cost with the help of biomarkers, which can be detected in stool, blood, and tissue samples. Several lines of evidence suggest that the gut microbiota could be used as a biomarker for CRC screening and treatment. CRC treatment choices include surgical resection, chemotherapy, immunotherapy, gene therapy, and combination therapies. Targeted therapies are a relatively new and promising modality of treatment that has been shown to increase patients' overall survival (OS) rates and can inhibit cancer cell development. Several small-molecule tyrosine kinase inhibitors (TKIs) are being investigated as potential treatments due to our increasing awareness of CRC's molecular causes and oncogenic signaling. These compounds may inhibit critical enzymes in controlling signaling pathways, which are crucial for CRC cells' development, differentiation, proliferation, and survival. On the other hand, only one of the approximately 42 TKIs that demonstrated anti-tumor effects in pre-clinical studies has been licensed for clinical usage in CRC. A significant knowledge gap exists when bringing these tailored medicines into the clinic. As a result, the emphasis of this review is placed on recently discovered biomarkers for early diagnosis as well as tyrosine kinase inhibitors as possible therapy options for CRC.

KEYWORDS

colorectal cancer, diagnosis, tyrosine kinase inhibitors, biomarker, therapies

1 Introduction

Colorectal cancer (CRC) is a third primary global health concern and a second leading cause of cancer-related deaths worldwide, which poses financial burdens on people and society (Morgan et al., 2023). In all clinical practice and research disciplines, CRC, including rectal and colon cancer, is treated as a single tumor type (Alzahrani et al., 2021). CRC originates from the lining of the colon or rectum and follows a specific pathological progression. In most cases, it typically begins as small growths called polyps, which can be detected during a colonoscopy. Over time, these polyps can develop into cancerous tumors, invading the surrounding tissues and potentially spreading to distant organs, frequently the liver. Over 10–15 years, this process necessitates the accumulation of

genetic mutations that can be somatic or germ-line in nature (Lotfollahzadeh et al., 2022). Some common risk factors for CRC include family, genetic, geriatric, nutritional, lifestyle, and environmental variables. Inflammatory bowel conditions, including Crohn's disease and ulcerative colitis, are additional risk factors. Moreover, issues with inactivity, obesity, smoking, and alcohol usage can be resolved (Sawicki et al., 2021).

1.1 Incidence and mortality

Certain pathological features, such as adenomatous polyps or advanced stages of carcinoma, are associated with an increased disease prevalence (Akimoto et al., 2021). The incidence and mortality of CRC differ significantly by country and region worldwide. According to the data from Global Cancer Observatory (GLOBOCAN), there were around 1.9 million new cases of CRC and 930,000 fatalities in 2020 worldwide. The incidence rates were lowest in several African countries and Southern Asia, while the highest incidence rates were reported from Europe, Australia, and New Zealand regions (Morgan et al., 2023). Similar trends were observed in CRC mortality rates, with Southern Asia having the lowest rates (2.5 per 100,000 females) and Eastern Europe having the highest rates (20.2 per 100,000 males). Additionally, there was a 10-fold difference in incidence rates between males and females in all countries. Males showed higher incidence and fatality rates than females (Wong et al., 2021). By 2040, CRC is expected to cause 3.2 million new cases and 1.6 million fatalities, mostly in high-HDI (human development index) countries (Xi and Xu., 2021). The incidence and mortality of CRC have decreased, and the US now ranks among the third-highest HDI countries. In the US, stage I colon cancer has a 5-year relative survival rate of around 92%. Stage IIA and IIB exhibit rates of 87% and 65%, respectively. Surprisingly, stage IIIA and stage IIIB have slightly greater 5-year survival rates, at 90% and 72%, respectively. While stage IV, or metastatic CRC (mCRC), has a 5-year survival rate of only 12%, stage IIIC has a survival rate of 53%. With 88% for stage I, 81% for stage IIA, 50% for stage IIB, 83% for stage IIIA, 72% for stage IIIB, 58% for stage IIIC, and 13% for stage IV, the 5-year survival rates for rectal cancer seem to be slightly lower. These stages are based on the TNM system's previous version. The unexpected increase in survival from stage II to stage III tumors can be attributed to the technique utilized to diagnose and treat different types of CRC (Rawla et al., 2019).

A higher prevalence of the disease underscores the need for effective screening programs and public awareness campaigns to promote early detection, as it significantly improves the prognosis and treatment outcomes for individuals with CRC (Stark et al., 2020). Over the past few decades, there has been remarkable progress in understanding the molecular basis of CRC, leading to the identification of novel biomarkers for early diagnosis and the development of targeted therapies, such as tyrosine kinase inhibitors (TKIs), for the treatment of CRC (Bresalier et al., 2020). Early diagnosis is critical in improving patient outcomes by enabling timely intervention and reducing mortality rates. Traditional screening methods for CRC, such as colonoscopy and fecal occult blood tests, have effectively detected early-stage tumors and precancerous lesions (Huang and Yang., 2022). However, these methods often have invasiveness, cost, and patient compliance limitations. Therefore, there is an urgent need to explore and validate novel biomarkers that can enhance the sensitivity and specificity of CRC detection while offering non-invasive and cost-effective alternatives (Shaukat and Levin., 2022).

1.2 Role of biomarkers in CRC

Biomarkers have been developed to aid in identifying patient responses to cancer diagnosis, therapy, and monitoring (Oh and Joo., 2022). Biomarkers, which include genetic alterations, epigenetic modifications, and protein expression patterns, hold immense promise as tools for CRC screening, risk assessment, and prognosis prediction. These biomarkers can be detected not only in solid tissue samples but also in blood and/or stool, allowing for non-invasive and convenient testing (Shen et al., 2022). The development of high-throughput genomic technologies has revolutionized biomarker discovery and enabled the identification of candidate markers associated with CRC initiation, progression, and response to treatment. Furthermore, integrating multiple biomarkers into diagnostic algorithms can improve the accuracy and reliability of CRC screening, facilitating the implementation of personalized medicine approaches (Islam Khan et al., 2022). Moreover, liquid biopsy approaches, which involve the analysis of circulating tumor DNA (ctDNA) and microRNAs (miRNAs), have gained significant attention as non-invasive methods for CRC screening and monitoring (Zhou et al., 2022).

1.3 Diagnosis and treatment of CRC

In addition to early diagnosis, targeted therapies have revolutionized the treatment landscape for CRC patients. Emerging evidence suggests a potential correlation between CRC and the use of TKIs. Tyrosine kinases play a crucial role in cell signaling pathways, and their dysregulation has been implicated in various types of cancers, including CRC (Thomson et al., 2022). TKIs are a class of drugs that selectively inhibit the activity of specific tyrosine kinase enzymes involved in CRC pathogenesis and progression. The aberrant activation of signaling pathways, such as the epidermal growth factor receptor (EGFR) and vascular endothelial growth factor receptor (VEGFR) pathways, has been implicated in CRC tumorigenesis and angiogenesis (Iyer et al., 2022). While TKIs have shown promising results in treating certain cancers, including gastrointestinal stromal tumors, their efficacy in CRC has been more limited. Studies have indicated that specific genetic mutations and alterations in tyrosine kinase signaling pathways may influence the response to TKIs in CRC patients (Xie et al., 2020). TKIs targeting these pathways, either as monotherapy or combined with standard chemotherapy regimens, have shown clinical efficacy in various studies (Hossain et al., 2022).

This review article will provide a comprehensive overview of the recent advancements in novel biomarkers used for early diagnosis of CRC. We will explore the potential of genetic alterations, epigenetic modifications, and other molecular markers as diagnostic tools in CRC. We will discuss the application of specific genetic markers, such as mutations in the Adenomatous polyposis coli (APC),

Kirsten rat sarcoma (KRAS), and tumor protein p53 (TP53) genes, as well as epigenetic including DNA methylation patterns and histone modifications as diagnostic and prognostic indicators. We hope to contribute to the ongoing efforts to improve CRC patient outcomes and facilitate precision medicine approaches by integrating the knowledge of these emerging biomarkers and therapies. Moreover, we will also provide an in-depth analysis of the current status and future perspectives of TKIs as targeted therapies in CRC treatment.

2 Novel biomarkers used for early diagnosis of CRC

Biomarkers are commonly used in CRC diagnostics to detect the presence of biochemical compounds that circulate in the body. These compounds may include gut microorganisms, miRNA in the blood, tumor-derived cells, tumor DNA, and proteins.

2.1 The gut microbiome as biomarkers

Inflammation, immunological modulation, dietary component metabolism, and exposure to genotoxic substances are the primary ways the gut microbiota contributes to cancer. Patients with CRC have a range of unique microbiomes that can be used as biomarkers for the diagnosis, prognosis, and treatment efficacy (Wong and Yu., 2019). There has been a lot of interest lately in the possible connection between gut bacteria and CRC.

2.1.1 Gut fungi

Gut fungi, specifically the dysbiosis or imbalance in the fungal community, have been implicated in CRC development. Recent studies have identified specific fungal biomarkers, such as *Candida tropicalis* and Debaryomyces hansenii, whose overgrowth or altered abundance in the gut may serve as potential molecular indicators of CRC, offering insights into its pathogenesis and possible diagnostic strategies. The overgrowth of gut fungi in CRC patients can be weakened immune system function and change the microenvironment of the colon, creating an environment conducive to fungal proliferation and colonization (Plaza-Díaz et al., 2021). However, there is insufficient information on the fungus microbiome in CRC. The top 3 fungi highly enriched in CRC were Phanerochaete chrysosporium, Lachancea waltii, and Aspergillus rambellii. It has been established that fungi anomalies in feces are associated with CRC (Gao et al., 2022) and in healthy individuals compared to CRC patients. It was observed that the proportion of Basidiomycota or Ascomycota was higher in CRC patients than in healthy individuals.

Moreover, two fungi, Pneumocystis and *Saccharomyces cerevisiae*, which have beneficial effects on the gut and possess anti-inflammatory properties, were found to be reduced in CRC patients. Conversely, Malasseziomycetes (fungi) were more abundant in healthy individuals than in CRC patients (Liu et al., 2022). Furthermore, the researchers noted that patients exhibited notably elevated levels of *Candida* albicans, a type of yeast. According to Stary et al. (2020), individuals who are at risk for CRC or have early asymptomatic with CRC may find it helpful to use C. albicans yeast as a diagnostic marker (Starý et al., 2020).

2.1.2 Gut bacteria

Gut bacteria, particularly the alterations in the composition and diversity of the bacterial community, have been linked to CRC development. The molecular mechanisms underlying this association involve the production of specific metabolites, such as short-chain fatty acids and secondary bile acids, as well as the activation of pro-inflammatory pathways, which can serve as potential biomarkers for the detection and monitoring of CRC (Xie et al., 2020). In a large-scale study, researchers discovered that individuals with CRC had an increased population of certain bacteria, including *Fusobacterium* nucleatum, Porphyromonas asaccharolytica, *Bacteroides fragilis*, Parvimonas micra, Prevotella intermedia, Alistipes finegoldii, and Thermanaerovibrio acidaminovorans. These seven bacteria are potential markers for diagnosing CRC (Chang et al., 2021). Adenomas were found to have unusually elevated levels of the "m3" product, particularly those originating from *Clostridium* hathewayi (Ch), *Fusobacterium* nucleatum (Fn), and Lachnoclostridium. Only these three bacteria have been identified in feces as markers for colorectal adenomas and cancers (Chan and Liang., 2022). Actinomyces odontolyticus and Atopobium parvulum were exclusively found in polypoid adenomas and/or intramucosal carcinomas (early stage), indicating the wide availability of Fn enhanced slowly from intramucosal carcinoma to early CRC (Liu et al., 2022). This discovery raises the possibility of employing these microorganisms as stool-screening indicators.

2.1.3 Gut viruses

The role of gut viruses in CRC is still being explored. Emerging evidence suggests that certain viral infections, such as high-risk human papillomavirus (HPV) and Epstein-Barr virus (EBV), may contribute to the development and progression of CRC through various molecular mechanisms, including viral integration into the host genome, dysregulation of host cell signaling pathways, and evasion of immune surveillance, providing potential avenues for viral-based biomarker identification in CRC diagnosis and treatment (Koonin et al., 2021). Most cancer-associated bacteriophages were temperate, demonstrating a connection between bacteriophage communities and CRC and the possibility that they could influence cancer progression by altering bacterial host populations (Hannigan et al., 2018). A similar study confirmed the association between viral indicators and CRC by observing a substantial rise in the variety of gut bacteriophage populations in feces from CRC patients and controls. Numerous studies have shown how closely microbes and cancer are related and how gut bacteria have opened up new possibilities for CRC detection (Handley and Devkota., 2019). However, a common microbiome biomarker has not been used to diagnose CRC because there is not yet a universally accepted standard for discovering microbiota. In order to enhance CRC diagnosis in the future, investigators must examine multiple microbiomes in patients from various ethnic groups since a microbe might not be capable of predicting CRC with adequate precision (Ding et al., 2022).

2.2 Volatile organic compounds (VOCs) as biomarkers

The ability to distinguish between diseases based on their "smell" has gained popularity as a research topic in recent years

due to the growing interest in the "smell" of diseases. A potential early CRC screening method involves the detection of VOCs, which are non-invasive biomarkers. Multiple investigations have revealed several VOCs as CRC biomarkers (Ding et al., 2022). Furthermore, changes in gut flora have a direct impact on the profile of VOC generation.

2.2.1 Fecal VOCs

Propan-2-ol, produced from ethyl 3-methyl-butanoate, hexane-2-one, and acetone, produced when ethanol and 3-methylbutaninoic react, positively correlates with the diagnosis of CRC, according to a 3-fecal volatile organic compound panel (Bond et al., 2019). One stool VOC contributing to CRC formation is hydrogen sulphide (HS). Microorganisms in the gut and internal enzymatic activities in the colon generate hydrogen sulfide. Higher levels of HS (over 2.4 mmol/kg) are hazardous, but lower levels are benign. The presence of higher-than-normal quantities of HS in both the lumen and the feces can throw off the equilibrium of the microbiota. For instance, this phenomenon affects patients with CRC (Lin et al., 2023). With the help of eNose Cyranose 320, patients with CRC could be characterized from controls with 85% sensitivity and 87% specificity (AUC 0.92). Similar results were attained with selected ion flow tube mass spectrometry (SIFT-MS), which separated CRC and advanced adenoma patients from healthy controls with 75% accuracy (72% sensitivity and 78% specificity). Recently, eNose Scent A1 was even more successful in many patients (Vernia et al., 2021).

2.2.2 Breath-exhaled VOCs

Using a pattern of 15 VOCs identified with gas-chromatography mass spectrometry (GC-MS), Altomare et al. differentiated between CRC patients and healthy controls with an accuracy of more than 80% (Altomare et al., 2015). A study isolated 4 volatile organic compounds: methyl octane, ethanol, ethyl acetate, and acetone, 4-. Acetone and ethyl acetate levels were more significant in patients with CRC (94% specificity and 85% sensitivity) and an accuracy of 91% (Zhang et al., 2021). The VOC samples from CRC patients also had considerably higher levels of 3-hydroxy-2,4,4-trimethylpentyl, trans-2-dodecen-1-ol, ethylaniline, cyclooctylmethanol, 4-ethyl-1-octyn-3-ol, 2,2-dimethyl decane, Cyclohexanone, and dodecane. But much lower levels of 2-methylpropanoate and 6-t-butyl-2,2,9,9 tetramethyl-3,5-decadien-7-yne (Amal et al., 2016).

2.2.3 Urinary VOCs

In a larger sample of 562 people, the diagnostic efficacy of urine VOCs detected by Field Asymmetric Ion Mobility Spectrometry (FAIMS) was less accurate than that of the fecal immunochemical test (FIT) (80% sensitivity and 93% specificity vs. 63% sensitivity and 63% specificity, respectively). One study found that CRC patients had significantly higher concentrations of 2-methyl-3-phenyl-2-propenal, 2,7-dimethyl-quinoline, and 1,4,5-trimethyl-naphthalene (Vernia et al., 2021).

2.3 Tissue biomarkers

2.3.1 Cadherin-17 (CDH17)

CDH17 is a glycoprotein that spans the cell membrane and requires calcium to function properly. Its primary purpose is to aid tissues in preserving their typical structure under normal conditions. The immunohistochemistry marker CDH17 helps identify primary and metastatic colorectal adenocarcinomas (Tournier et al., 2023). According to reports, 100% of metastatic and 96%–100% of primary CRC express CDH17. CDH17 and SATB2 were excellent potential biomarkers for diagnosing metastatic colorectal adenocarcinoma and pulmonary enteric malignancy (Neri et al., 2020). The expression of CDH17 in CRC tissues and plasma gradually increased as the disease progressed to more advanced stages. There is a link between liver metastasis, high CDH17 expression, and a bad prognosis for CRC patients (Tsoi et al., 2019).

2.3.2 Anti-glycoprotein 33 (GPA 33)

GPA33, a transmembrane protein overexpressed in CRC, has potential molecular mechanisms involving cell adhesion, immune evasion, and tumor growth, highlighting its significance as a biomarker and therapeutic target; however, its current clinical application as a diagnostic or prognostic tool in CRC is still under investigation and requires further validation. The tumor-associated antigen human GPA33 is expressed in approximately 95% of primary and mCRC (Markandeywar et al., 2023). It is a surface-localized, extremely persistent, and inert protein. PGA 33 has a 95.9% sensitivity and an 85.4% specificity for CRC. A33 has been the target of clinical-stage antibodies used to treat CRC (Wei et al., 2020). The new anti-A33 antibody may prevent the development of mouse CRC lung metastases, and A33-expressing murine adenocarcinoma cells may be destroyed by antibody-dependent cell-mediated cytotoxicity (ADCC) (Murer et al., 2020). The A33 had a sensitivity comparable to Caudal-type homeobox transcription factor 2 (CDX2). Still, it had a specificity that was significantly greater than that of CDX2 as an immunomarker of CRC, according to the findings of an immunohistological investigation that compared A33 with CDX2 (Davidsen, 2020).

2.3.3 Cytokeratins (CKs)

CKs are proteins found in the cytoskeleton and located in intermediate filaments. It is a member of a group of approximately 20 cytoskeletal proteins frequently used as immune-histochemical markers in diagnosing CRC in tumors that have been generated from epithelia. In most cases, neoplastic cells maintain CK expression; specialized anti-CK antibodies are frequently used in histopathology diagnoses to trace tumor origins, especially in metastases (Hrudka et al., 2021). Cytokeratins, a group of intermediate filament proteins, have potential molecular mechanisms involving epithelial cell differentiation, tumor invasion, and metastasis, making them valuable biomarkers for cancer diagnosis and prognosis; currently, cytokeratin-based assays, such as CK19 for detecting disseminated tumor cells, are utilized in clinical practice for assessing the presence of minimal residual disease and predicting treatment response in various cancer types, including CRC. Two enzymes, CK7 and CK20, are frequently involved in CRC. Different types of glandular and ductal epithelia contain CK7. Simultaneously, CK20 is abundantly expressed in mucosal cells of the gastrointestinal and urinary tracts (Hrudka et al., 2022). Tissue expression of CK15 was significantly linked with CRC subtype and stage. A higher level of CK18 expression is found in CRC tumors compared to the normal colorectal tissue

surrounding them (Sun et al., 2018). It is a single predictor of long-term survival in CRC patients when CK18 expression is upregulated in tumor tissue. The viability, migration, and invasion of CRC cells were decreased by downregulating CK18 expression (Jelski and Mroczko., 2020). All three of the detected cytokeratins 8, 18, and 19 can potentially be helpful biomarkers for the early diagnosis of CRC (Luo et al., 2020).

2.3.4 Telomerase

A telomerase ribonucleoprotein increases the number of TTAGGG repeats at the ends of chromosomes to preserve telomere length. Intrinsic RNA serves as a scaffold for reverse transcription in telomerase. The telomere controls chromosomal stability and cell life span. The telomerase enzyme is present in human cancer cells (80%–90%) and differentiated cells, such as germ-line cells (Kibriya et al., 2022). Telomere length in cancer tissue was substantially shorter than in normal mucosa. Advanced CRC (stage II–IV) cancers have longer telomeres than stage I tumors (Ye et al., 2021). According to Taheri et al. (2022), CRC tissue had reduced hTERT expression levels. Since telomerase is present in healthy and malignant intestinal epithelial cells, measuring hTERT alone may underestimate its prevalence. Numerous studies have demonstrated that telomerase has a high-level telomere-specific reverse transcriptase (hTERT), which improves Nuclear factor erythroid 2-related factor 2 (NRF2) synthesis by recruiting Y-box binding protein 1 (YBX1) to trigger the NRF2 promoter, promoting CRC proliferation and migration. These findings provide a new conceptual underpinning for CRC treatment (Gong et al., 2021).

2.3.5 Special AT-Rich sequence-binding protein 2 (SATB2)

SATB2 belongs to the group of transcription factors that bind to matrix attachment regions and control the development of the skeleton. The appendix and colon epithelium both had significant levels of SATB2 expression (Huang and Yang, 2022). SATB2, a transcription factor involved in gene regulation, has potential molecular mechanisms related to cell differentiation, cell migration, and tumor metastasis, suggesting its significance as a biomarker. However, SATB2 expression has been identified as a useful marker for CRC diagnosis and distinguishing primary colorectal tumors from metastatic tumors, and further research is needed to establish its full clinical utility and potential therapeutic implications. SABT2 has recently been identified as a biomarker for CRC, and various hereditary disorders connected to SABT2 have been reported (Mezheyeuski et al., 2020). SATB2 was positive in 83.7% of stage III/IV, 91.4% of stage II, and 92.4% of phase I colorectal adenocarcinomas, according to Dabir et al. (2018). According to multiple studies, when paired with conventional panels of CDX2, CK20, CK7, and cytokeratin 20, SATB2 is a highly specialized marker for CRC (Oh and Joo, 2020).

2.3.6 Caudal type homeobox 2 (CDX2)

Intestinal epithelial cells express the homeobox protein CDX2 in their nuclei. As a trustworthy and accurate immunomarker for CRC, CDX2 is frequently used. It is believed that CDX2 is a tumor suppressor gene because it does not manifest itself in instances of CRC. By overexpressing CDX2 using an hTERT (hypoxia-inducible human telomerase reverse transcriptase) promoter-driven plasmid, colon cancer cells were prevented from progressing malignantly (Al-Duhaidahawi., 2023). The CDX2 gene promoter region's methylation has been associated with a higher risk of CRC. The CDX2 gene promoter area was methylated in 78.5% of the CRC tissue. CDX2 downregulation was associated with high-grade, advanced cancers with liver metastases (Aasebø et al., 2020). Furthermore, disease-free and overall survival (OS) were considerably poorer in people with stage T4 CRC and low CDX2 expression (Choi et al., 2022).

2.3.7 Methylation of DNA

At every stage of carcinogenesis, from polyps to colorectal adenocarcinomas, hypermethylation drives the transcriptional silence or downregulation of suppressor genes, which renders tumor suppressor genes inactive. In CRC, numerous genes, particularly those in the promoter region, including HLTF, CDH1, SEPT, VIM, TIMP3, CDK2A, SFRP2, SFRP1, MGMT, MLH1, and APC, are methylated (Mo et al., 2023). Suppression of histone deacetylation and demethylation are used in CRC cells to increase Syndecan-2 (SDC2) expression because the SDC2 promotor region is typically hypermethylated in CRC. Methylated SDC2 for the non-invasive diagnosis of CRC has reasonable specificity (88.2%–98%) and sensitivity (77.4%–90.2%) (Siri et al., 2022). The zinc finger protein 625, LON peptidase N terminal domain and ring finger 2, WD repeat domain 17, and syndecan 2 CpG island promoters were methylation in both cancer and laterally spreading tumor non-granular (LST NG). This indicates that the LST NG phase may be the first stage of colorectal carcinogenesis (Iwaizumi et al., 2023). N-Myc downstream-regulated gene 4 (NDRG4) influences cell development and differentiation. In CRC, the NDRG4 expression is downregulated (Cao et al., 2020).

2.4 Blood biomarkers

Biomarkers can be detected using immunohistochemistry or blood-based protein quantification techniques. Blood-based markers can serve as a convenient screening tool for CRC, as blood donation or collection is a relatively simple process.

2.4.1 Circulating tumor cells (CTC)

CTCs are epithelial cancer cells in peripheral blood after they have spread from the primary tumor or metastases and entered the circulatory system. They can be utilized as biomarkers to detect CRC or as knowledge-dissemination pathways, enabling therapy decisions (Chan et al., 2023). In early-stage cancers, circulating CTCs vary from 1 to 10 cells/10 mL of blood and may be less. CTCs can be differentiated from normal blood cells by differences in size and shape. More research is needed to validate the findings. Necrosis releases circulating-free DNA (cfDNA) as significantly bigger fragments in tumor cells (Li et al., 2023). This resulted in promising findings when circulating cfDNAs were quantitatively examined using the ratio of longer to shorter DNA fragments or when the cfDNA integrity number was measured after CRC diagnosis. Although CTCs have been shown to have predictive value in CRC, their use in screening is controversial (Hendricks et al., 2021).

2.4.2 Circulating tumor DNA (ctDNA)

ctDNA (circulating tumor DNA) and cfDNA have emerged as promising biomarkers in CRC. The presence of ctDNA and cfDNA in the bloodstream allows for non-invasive detection of specific genetic alterations, such as mutations and methylation patterns, providing valuable information about tumor burden, treatment response, and disease progression, thereby enabling personalized medicine approaches in the management of CRC patients (Lyu et al., 2022). ctDNA has received extensive evaluation as a promising indicator for liquid biopsy in detecting and assessing therapeutic responses for CRC. ctDNA released from necrotic or apoptotic tumor cells. Although normal nontumor cells also shed cfDNA into the bloodstream, the cfDNA from tumor cells (i.e., ctDNA) only accounts for less than 1% of total cfDNA in the blood (Peng et al., 2021). Tests that rely on the detection of circulating tumor DNA (ctDNA), also known as liquid biopsies, are susceptible to vulnerabilities. A study conducted by Min et al. (2023) in 2023 demonstrated that quantitative analysis of ctDNA and qualitative investigation of SEPT9 methylation effectively diagnose CRC. According to a study conducted by Perdyan et al. (2020) in 2020, ctDNA demonstrated an accuracy of 87.2% and a precision of 99.2% in identifying clinically significant KRAS gene mutations in a group of 206 patients with mCRC. Several studies have reported elevated levels of cfDNA in cancer patients. According to Raunkilde et al. (2022), most cfDNA fragments of 180–200 base pairs in length originate from tumor cells that have undergone necrosis or cell death (Raunkilde et al., 2022). Tumor-specific genomic changes, including microsatellite instability, loss of heterozygosity, methylation, and mutations, are present in cfDNA.

2.4.3 Circulating MicroRNA (c-miRNA)

Small non-coding RNAs called microRNAs (miRNAs) control the expression of genes by attaching them to mRNA. C-miRNA has contributed to diagnosis. The dysregulation of miRNA activity causes a variety of diseases, including cancer. Diagnostic panels that combined single miRNAs as a CRC marker with combinations of those detected in serum or plasma miRNA indicators have been investigated recently (Abo-Elela et al., 2023). In comparison to serum, plasma has higher levels of miRNA. Hemolysis must be regulated in samples during the preanalytical stage of the experiment because it can change the amounts of circulating miRNA in samples by rupturing erythrocytes that transport miRNA. The only miRNAs that seem suitable as clinical markers are those with severe up- or downregulation (Liu et al., 2021). Nearly 2/3 of miRNAs were downregulated in CRC compared to normal mucosa. According to one study, the four-stage change from colorectal adenocarcinoma via high- and low-grade dysplasia in adenoma involved differential expression of 230 miRNAs (Sur et al., 2022).

2.4.4 Long non-coding RNA (lncRNA)

Long non-coding RNAs (lncRNAs), made up of more than 200 nucleotides and cannot be translated into proteins, are involved in several biological processes, including differentiation, immunological responses, and chromosomal dynamics. Because lncRNAs can pass across cell membranes, they can be discovered in various bodily fluids, including blood, plasma/serum, and urine (He and Wu., 2023). Numerous lncRNAs are linked to the development of CRC and carcinogenesis at all stages. The WNT/-β catenin, PI3K/Akt, EGFR, NOTCH, mTOR, and TP53 signaling pathways are only a few carcinogenic signaling cascades that their changed expression can affect (Cai et al., 2019). The extracellular phospholipid-enclosed vesicles, known as apoptotic bodies, microvesicles, and exosomes, travel with lncRNAs in the blood. Exosomes, one of the three forms of extracellular vesicles, have the largest concentrations of long micro RNAs (lmiRNAs), which aid in tumor spreading, immunomodulation, and chemoresistance (Lulli et al., 2022). The first indicators discovered to have significantly higher expression in the plasma of CRC patients compared to healthy people were HOTAIR and CCAT1. Numerous more circulating lncRNAs, including NEAT1 variants 1 and 2, MEG3, PVT-1, 91H, Nbla12061, RP11-462C24.1, and LOC285194 have been identified as possible biomarkers for the identification of CRC (Zygulska and Pierzchalski., 2022).

2.4.5 Pyruvate kinase muscle isozyme M2 (PKM2)

PKM2 is found in healthy and cancerous cells and is involved in energy metabolism. When PKM2 regulates the rate-limiting stage of glycolysis, tumor cells produce lactate rather than the normal respiratory chain for glucose metabolism (Cruz et al., 2021). There have been reports of PKM2 overexpression in colon adenomas, gastric cancer, and CRC. With its excellent sensitivity, PKM2 is adequate blood and fecal biomarker for CRC screening (Zahra et al., 2020). The study found that the fecal Tumor pyruvate kinase M2 isoform (tM2-PK) test had a 100% sensitivity and a 68% specificity in the tumor group. Specificity and sensitivity for the polyp group were 68% and 87%, respectively. The tM2-PK test is recommended as a non-invasive method to identify CRC and adenomatous polyps (Rigi et al., 2020).

2.4.6 Dickkopf-related protein 3 (DDK3) and insulin-like growth factor binding protein 2 (IGFBP2)

DDK3, a tumor suppressor gene, and IGFBP2 a growth factor regulator, have potential molecular mechanisms involving cell cycle control, growth inhibition, and modulation of the IGF signaling pathway, highlighting their potential as biomarkers. However, further studies are needed to determine their clinical utility and application in cancer diagnosis, prognosis, and targeted therapies (Zygulska and Pierzchalski, 2022). The biomarker model can identify early-stage CRC with 95% specificity, 57% sensitivity for stage I, and 76% sensitivity for stage II. As a result, this panel of biomarkers recommends being used as a non-invasive blood screening and/or diagnostic test. It is comparable to a fecal occult blood test (FOBT) and FIT in CRC detection (Zygulska and Pierzchalski., 2022).

DDK3 (DNA-damage-inducible 3) and DDK1 (Dickkopf-1) are potential biomarkers in CRC. DDK3 expression has been associated with tumor suppressive effects, and its downregulation is often observed in CRC, suggesting its potential as a diagnostic or prognostic biomarker. On the other hand, DDK, an antagonist of the Wnt signaling pathway, is frequently overexpressed in CRC, and its elevated levels may serve as a biomarker for disease progression and therapeutic response in CRC patients (Akhlaghipour et al., 2021). The human Dickkopf family includes the proteins DDK-1, DDK-2, DDK-3, and DDK-4, and the specific protein Soggy (Sgy)

related to DDK-3 is all TEMs (tumor endothelium markers). The tumor endothelium of CRC tissues displays more pronounced expression levels of the TEMs, a group of 46 genes (Safari et al., 2018). Wnt blocker genes are epigenetically inhibited in CRC, among several other factors. During cancer development, the Wnt signaling pathway is triggered. These antagonistic genes include DDK genes, which are hypermethylated in the promoter of CRC cells and epigenetically silenced (Kaur et al., 2012). According to one study, CRC that was DDK-3 positive had a considerably greater mean microvessel count (9.70 vessels) than cancer that was DDK-3 negative. Therefore, it is believed that DDK-3 is a pro-angiogenic mediator in the growth of neovascularization during the progression of CRC (Soheilifar et al., 2019).

IGFBP-2 is an extracellular protein that binds insulin growth factor 2 (IGF-2), which is involved in the development and spread of cancer through the action of heat shock protein 27. In patients with colon cancer, higher serum concentrations of IGFBP-2 are associated with neoplastic changes in the higher levels of carcinoembryonic antigen (CEA) and colon. Consequently, it has been suggested that monitoring patients with CRC includes measuring IGFBP-2 levels as a diagnostic indicator (Chen et al., 2021). Thus, by preventing cell division, IGFBP-2 overproduction during colorectal carcinogenesis slows the formation of tumors. The sensitivity may be improved by combining IGFBP-2 with additional biomarkers, such as CEA (Gligorijević et al., 2022). Zhu et al. (2019) found that IGFBP2 overexpression promoted CRC cell proliferation and migration by suppressing E-cadherin expression and enhancing cell growth. Additionally, more significant tumor sizes and lower OS rates were linked to higher plasma IGFBP-2 levels, demonstrating that IGFBP-2 may function as a prognostic and diagnostic biomarker for CRC.

2.4.7 Septin 9 (SEPT9) gene methylation

The SEPT gene family in humans consists of 13 genes (SEPT1-SEPT13). SEPT9 methylation DNA is the most well-known blood biomarker. The molecular mechanism of SEPT9 gene methylation in CRC involves the aberrant addition of methyl groups to CpG islands within the gene's promoter region. This hypermethylation leads to the silencing of the SEPT9 gene and subsequent loss of septin protein expression. The disrupted septin function contributes to defective cytokinesis, abnormal cell morphology, and increased genomic instability, promoting the development and progression of CRC (Baharudin et al., 2022). The detection rate for those with CRC stages 0-I using this method ranges from 57% to 64% (Zhao et al., 2020). According to the meta-analysis, individuals with advanced CRC cases were more likely to test positive for methylated SEPT 9 (mSEPT9) than those with early-stage CRC, and the opposite was true for people with early-stage CRC (Min et al., 2023). According to the latest meta-analysis released in 2020, the SEPT9 assay has a specificity of 92% and a sensitivity of 69% for CRC diagnoses (Hariharan and Jenkins, 2020).

2.5 Stool biomarkers

Stool samples are more suitable for the early detection of CRC than blood tests because exfoliating tumor cells appear in the large intestine or rectal lumen during colorectal carcinogenesis far earlier than the beginning of tumor cell vascular penetration.

2.5.1 Stool DNA (sDNA)

The molecular mechanism of stool DNA methylation in CRC involves detecting aberrant DNA methylation patterns in the stool samples of patients. Abnormal methylation of specific genes associated with CRC can serve as a non-invasive biomarker for the early detection and screening of the disease (Mueller and Győrffy., 2022). The human genome makes up less than 0.01% of the total DNA in stools; the other 99.99% comes from gut bacteria or food. The DNA of tumor cells expelled with feces contains abnormal genetic and epigenetic changes, which may serve as biomarkers for the detection of cancer (Gao et al., 2023). Several genes such as WIF1, VIM, TFPI2, SFRP2, RASSF2A, NDRG4, MGMT, MLH1, MINT31, MINT1, KRAS, ITGA4, IRF8, ID4, HLTF, GSTP1, GATA4, ESR1, CXCL21, CRBP1, CDH13, CDKN2A, CDH1, BMP3, ATM, and APC have all been studied for CRC diagnosis (Park et al., 2017). There is a Multitarget stool DNA (mt-sDNA) test (Cologuard, which combines hemoglobin, NDRG4, KRAS mutations, and BMP3 DNA methylation) and a plasma SEPT9 DNA methylation test (Epi proColon) that has been utilized more extensively in clinical settings. In asymptomatic people, mt-sDNA testing has a sensitivity of 90% for detecting CRC. DNA testing has a specificity range of 86.6%–98% (Ladabaum et al., 2020). A colonoscopy is a next stage in diagnosing a colorectal tumor in the event of a positive mtsDNA test. Asymptomatic participants in an intriguing study endured CT colonography and an mt-sDNA test (FDA-approved). Overall, CT colonography screening had a considerably higher detection rate for advanced neoplastic lesions (5%) than the mt-sDNA test (2.7%). There were 0.31% and 0.23% overall detection rates for CRC (Pickhardt et al., 2020).

2.5.2 Faecal immunochemical test (FIT)

The FOBT is modified into the FIT, which checks for blood that digestive proteolytic enzymes have broken down. Even though early CRC detection is crucial for reducing CRC mortality, there is limited data to support the stage-specific sensitivity of the FIT in CRC detection. The FIT detected stage I cancers with a sensitivity of 68% (95% CI, 57%–78%), stage II cancers with a sensitivity of 92% (95% CI, 87%–96%), stage III cancers with a sensitivity of 82% (95% CI, 73%–89%), and stage IV cancers with a sensitivity of 89% (95% CI, 80%–95%) (Niedermaier et al., 2020). FIT offers an extensive spectrum of susceptibility for all stages of CRC, ranging from 25% to 79% (Van Doorn et al., 2015). T3 sensitivity was 83%, and T1 sensitivity was 40% in those with greater severity of CRC (Hijos-Mallada et al., 2021).

2.5.3 FIT and stool DNA test

The diagnostic tools, such as RNA- or DNA-based testing, studied in a community-based population were found to increase the efficacy of the FIT procedure. Another study found that mt-sDNA testing was more effective than FIT at identifying advanced adenomas and sessile serrated polyps (Tanriver and Kocagoncu., 2023). However, mt-sDNA had a lower overall specificity for detecting all lesions than FIT. According to reports, a DNA-FIT test boosted detection sensitivity for CRC to 97.5% and advanced adenomas to 53.1% (Xu et al., 2022).

2.5.4 Stool miRNA

In CRC, ncRNAs are abnormally produced, and based on the genes or pathways they control downstream, they may act as oncogenes (oncomiRs) or tumor suppressors (tsmiRs). A novel

therapeutic approach and testing biomarkers have been developed due to the possible discrepancy among miRNA profiles of CRC and the normal intestinal mucosa (Fonseca et al., 2021). The study of stool miRNA has some drawbacks. First, it can be challenging to standardize procedures due to daily changes in fecal characteristics (density, volume). Second, it is essential to distinguish between the three types of feces miRNAs: fecal colonocyte miRNAs, exosomal miRNAs from fecal exosomes, and cell-free miRNAs from fecal homogenates (Ahmed et al., 2019). In the feces of CRC patients, the miR-145 and miR-143 were downregulated, while miR135, the miR17-92 cluster, miR-106a, miR-92a, miR144, and miR-21 were upregulated (Sattar et al., 2022).

2.6 Urine-based biomarkers

Urine biomarkers can be obtained non-invasively without forcing the patients to attend the clinic. Urine containing various components is considered the most effective and ideal sample for medical examination. Additionally, because the urinary tract is highly clean physiologically, substances found in urine may be less contaminated by germs than those in feces. Metabolomics has been routinely employed to identify metabolic abnormalities in CRC patients' tissue, serum, and urine materials. A recent metabolomic study discovered that CRC patients have a unique metabolic phenotype characterized by dysregulated expression of metabolites in glycolysis, the tricarboxylic acid (TCA) cycle, the urea cycle, tryptophan, arginine, proline, pyrimidine, polyamine, lactate, fatty acid, and amino acid metabolism, as well as gut microbial metabolism (Zhu et al., 2022; Qiu et al., 2023). Therefore, identifying urine biomarkers is desirable for diagnosing various cancers, including CRC (Iwasaki et al., 2019). ProstaglandinE2 and MicroRNA have demonstrated value in CRC detection. According to the available data, VOCs may be a possible biomarker for identifying CRC (Chandrapalan and Arasaradnam, 2020). Recently, researchers identified urinary metabolite biomarkers N1, N12-diacetyl spermine, hippurate, p-hydroxy hippurate, and glutamate as the best metabolites to discriminate CRC patients via low-cost point-of-care (POC) screening test (Zhou et al., 2022).

3 Targeted therapies in CRC

Early detection of colorectal tumors allows for successful management with first-line therapies such as surgery, radiation, or traditional chemotherapy. The 5-year OS rate for patients is 88%–92%, while it drops to 58%–72% for patients with stage IIIC. Even though traditional chemotherapy has a remarkable influence on cancer treatment, it is nevertheless significantly hindered by its nonspecific toxicity toward rapidly dividing cells (Mou et al., 2021). By interacting with particular genes or proteins involved in cell growth or apoptosis resistance, highly targeted medications that aim to eradicate cancer cells have been made possible thanks to the amazing advancements in molecular oncology in this field. Highly effective cancer medicines are helpful for cancer treatment since they have improved tumor selectivity and have fewer adverse effects than traditional cancer treatments (Xie et al., 2020). As a result of a better understanding of the mechanisms involved in the evolution and proliferation of cancer cells, targeted therapies and medications with action focused on these pathways/features have been developed.

An earlier meta-analysis examined chemotherapy's effectiveness and safety outcomes with bevacizumab, panitumumab, or cetuximab in mCRC. It demonstrated that bevacizumab was more effective in treating right-sided mCRC. In contrast, cetuximab was more successful in treating left-sided RAS wild-type (WT) mCRC (Cai et al., 2022). Both cetuximab and panitumumab, two different monoclonal antibodies (mAbs) that target the epidermal growth factor receptor (EGFR), are frequently used either alone or in conjunction with chemotherapy to treat people with mCRC that has the RAS wild-type. Despite being often regarded as interchangeable, the two antibodies possess distinctive molecular compositions and can function therapeutically significant in various ways (Shim, 2011). While there is less research on cetuximab or panitumumab as first-line therapies for older patients with mCRC, these drugs may still be an option for those with the wild-type KRAS mutation. Cetuximab, either alone or in combination with irinotecan, had a benign toxicity profile in elderly patients with severely pretreated mCRC, and the efficacy was comparable to that reported in younger patients, according to two retrospective studies (Bouchahda et al., 2008; Fornaro et al., 2011). Another study suggests combining bevacizumab and capecitabine is a safe and effective treatment for elderly individuals with mCRC (Sastre et al., 2012). The preliminary results that are currently available show that patients with mCRC who receive cetuximab or panitumumab treatment had higher response rates and longer PFS when KRAS mutations are absent (Kim, 2015).

4 Novel tyrosine kinase inhibitors (TKI)

Small-molecule, oral drugs that target particular tumor-causing proteins have been available to treat colorectal malignancies since the turn of the millennium. These proteins that cause tumors are known as tyrosine kinases, and over 90 are in the human genome. Based on their structure, activity, and localization, these 58 can be further separated into the two significant classes of receptor tyrosine kinases (RTKs) and non-receptor tyrosine kinases (NRTKs) (Natoli et al., 2010). RTKs and NRTKs have both been linked to the emergence of CRC. Drugs that target these proteins have several distinct benefits over conventional chemotherapy. Blocking these enzymes can help prevent cancer cell development because they may be overactive or abundant in cancer cells (Piawah and Venook., 2019).

4.1 Receptor tyrosine kinases (RTKs)

The structural characteristics of the RTK superfamily of cell membrane proteins include an extracellular ligand-binding domain, a transmembrane region, and a cytoplasmic region, including ATP-binding and catalytic kinase domains. Based on similar receptor characteristics and/or shared ligands, at least 20 subfamilies of the approximately 60 RTKs have been discovered (Schlessinger, 2014).

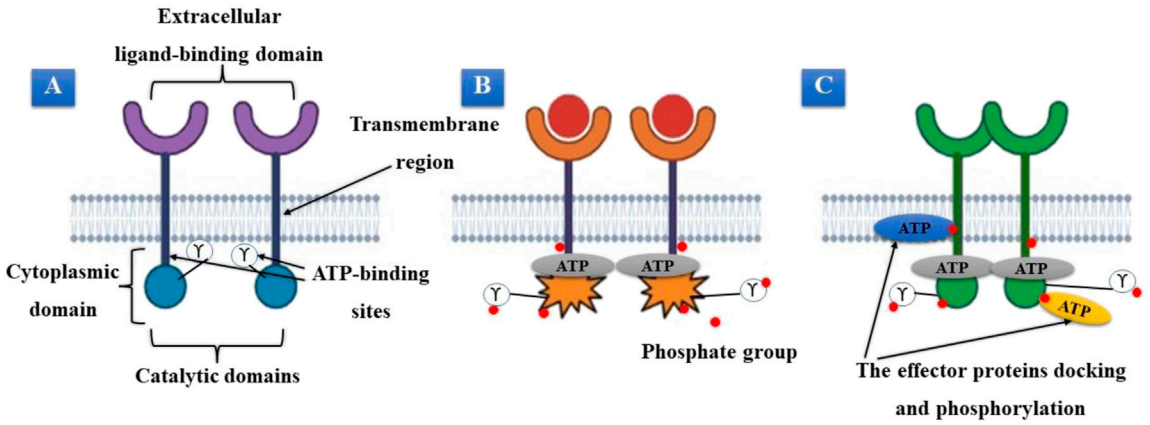

FIGURE 1
(A) Inactive tyrosine kinase receptor. **(B)** Activation of receptors, dimerization, and ATP binding. **(C)** The receptor's phosphorylated tyrosines serve as a docking site for effector proteins.

When peptide-based ligands transmit extracellular signals, these proteins are crucial for recognizing and transforming those signals. Their signals regulate cellular functions such as cell division, proliferation, and life span (Figure 1). RTKs function as monomeric transmembrane proteins when they are dormant. These proteins dimerize and create oligomeric pairs after becoming active. The receptors' enzymatic domains must be activated to produce receptor oligomers, and their intracellular region's tyrosine residues must be autophosphorylated (Figures 1A, B) (Diwanji et al., 2019). When ATP attaches to a specific receptor region, tyrosine residues on the receptor and effector proteins are phosphorylated. Many effector proteins involved in multiple signal transduction cascades associated with these receptors have been suggested to dock to the receptor's phosphorylated tyrosines (Trenker and Jura., 2020). After docking, the receptor can activate these effector proteins via various phosphorylation processes. RTK activation requires the binding of ATP. If the ability of these receptors to bind and use ATP is impaired, their function will be significantly reduced. This is crucial for targeted therapeutic interventions (Figure 1C).

RTKs are crucial for controlling numerous cellular activities in a normal state. Still, when they express themselves abnormally, they can lead to uncontrollable cell division, contributing to cancer's pathobiology (Wheeler and Yarden., 2014). Activating a particular subclass of RTKs subclass 1, or ERBB, is aberrant in epithelial cancers. Additional RTKs, including the tumor metastasis-promoting Platelet-derived growth factor (PDGF), VEGFR, and VEGFR2 receptors, appear essential for tumor growth (García-Aranda and Redondo, 2019).

4.2 Non-receptor tyrosine kinases (NRKTs)

The nucleus, the inner surface of the plasma membrane, and other cell components all include NRTKs, a sizable class of cytosolic proteins. By participating in cellular signaling cascades, these proteins play an essential role in controlling survival, migration, differentiation, cellular proliferation, and metabolism. Given the role of NRTKs in cells, it is unsurprising that the cell tightly regulates their activity (Siveen et al., 2018). When these proteins, like their receptor counterparts, fail to function correctly due to genetic mutation, resulting in overexpression, loss of autoregulatory processes, or abnormal signaling, they can lead to the pathophysiology of various cancer types. Therefore, it is unsurprising that this protein family has become a crucial therapeutic focus in the fight against cancer (Fox et al., 2019).

4.3 TKIs targeted in CRC

After the Food and Drug Administration (FDA) gave its approval for the TKI imatinib in 2001, there was a rise in people's interest in protein kinase inhibitors (Huang et al., 2020). Imatinib's anticancer activities have been confirmed by numerous *in vitro* studies against CRC, and in vivo experiments may validate these findings. Imatinib's anticancer effects in CRC were synergistic and pleiotropic (Dhiman et al., 2020). The development of small kinase inhibitors is based on the structure and sequence of the kinase catalytic core, which is defined by the presence of a smaller N-terminal subdomain (N-lobe) made up of a long α-helix and a β-sheet. A big C-terminal subdomain (C-lobe) with a primarily α-helical structure and an ATP binding site that serves as a hinge during structural adjustments (Adnan et al., 2022). A highly conserved Asp-Phe-Gly (DFG) motif, a component of the ATP-binding site that regulates magnesium binding, follows the activation loop (A-loop), which controls kinase activity (Bhullar et al., 2018).

Kinase inhibitors are divided into two major categories based on how they work: In addition to competing for the primary ATP-binding domain of the kinase catalytic core in the active form, type-I and type-II small kinase inhibitors are designed to bind to an additional allosteric pocket close to the ATP-binding site in the inactive state. Even so, type-II inhibitors are more focused than type-I inhibitors (Zhao et al., 2021). Type-I and type-II inhibitors prevent the specific protein kinase from phosphorylating a substrate molecule and deactivating downstream signaling. Kinase

inhibitors may inhibit unregulated cell growth or apoptosis inhibition because dysregulated kinases can lead to defective signaling that can cause uncontrolled cell growth and proliferation (Roskoski, 2015).

Tyrosine kinases influence cell growth, migration, differentiation, apoptosis, and death by phosphorylating certain amino acids on substrate enzymes. This alters the downstream signal transduction triggered by TKs Du and Lovly. (2018). Dysregulated signal pathways can result from mutations or other constitutive activation or inhibition processes, which can cause cancer. Therefore, blocking these early signals with TKIs can avoid abnormal behavior of mutant or dysfunctional TKs. In tandem with the development of targeted monoclonal antibodies, a greater understanding of the molecular underpinnings and oncogenic signaling of CRC growth has led to testing TKIs (Yang et al., 2022). These substances can inhibit key enzymes that regulate signaling pathways crucial for cell survival, proliferation, differentiation, and development. Several RTKs, or the pathways through which these kinases function, have prospective therapeutic targets that have been enhanced or altered in CRC. Numerous small molecule TKIs have been discovered and examined for their potential to treat CRC cancer (Jiao et al., 2018).

The US FDA has authorized more than 50 TKIs, though most of these TKIs exhibit encouraging results in CRC pre-clinical testing. In the clinic, most patients fail (Tauriello and Batlle., 2016). Various causes include the absence of complicated predictive pre-clinical models, a lack of understanding of the pharmacodynamics and pharmacokinetics of TKIs, and a lack of information on the tumor mutational background and heterogeneity, which can cause clinical failure. Despite being a primary contributing factor in CRC metastasis and a therapeutic target, the TME remains unclear, contributing to the discrepancy between pre-clinical and clinical results (Tolba, 2020).

4.4 TKIs as monotherapy

The 14 TKIs that had passed pre-clinical monotherapy testing were also investigated in a clinical trial for mCRC. Four TKIs (Lenvatinib, cediranib, cabozantinib, and apatinib) were identified as promising in non-randomized phase I/II studies, and two (fruquintinib and regorafenib) indicated therapeutic value in a randomized phase III study. 13 of them shown noticeable anti-cancer benefits in a pre-clinical setting (Han et al., 2020). Regorafenib is an oral multikinase inhibitor, that is, now approved for use in third-line mCRC therapy. It prevents tumor angiogenesis, oncogenesis, metastasis, and immunology by inhibiting tyrosine kinase receptors (Calvo-Garcia et al., 2022). Apatinib, an s-SRC, c-Kit, and VEGFR2, a relatively specific inhibitor, had a robust pro-apoptotic effect *in vitro* in animal CRC cell lines and humans. Patients with refractory CRC who did not have liver metastases responded well to apatinib alone, with a PFS of 3.9 months (Srivastava et al., 2022). A selective VEGFR1,-2,-3 inhibitors called fruquintinib has received approval in China to treat people with mCRC who have already failed at least two courses of systemic anti-neoplastic therapy. It is expected to be the 2nd TKI authorized for mCRC after receiving FDA fast-track approval for mCRC patients (Zhang et al., 2019).

Cediranib and cabozantinib, two TKIs that inhibit several kinases, produced apoptosis and antiproliferative activity in culture and slowed the growth of tumors *in vivo*. For CRC patients, it was not given any empirical investigation (Qin et al., 2019). Bosutinib is successful *in vitro* and *in vivo* in one analysis; however, its efficacy was only moderate in a following phase I clinical experiment (Isakoff et al., 2014). Numerous other TKIs also demonstrated encouraging anti-tumor pre-clinical effects, such as vandetanib (patient-derived cells), gefitinib (CRC cell lines), dasatinib (CRC cell lines and xenograft models), erlotinib (patient-derived xenografts), and linifanib (CRC cell lines, 3D micro tumor). However, none of these treatments worked effectively in the clinic as monotherapy (Table 1) (Lyer et al., 2022).

4.5 Utilization of TKIs in combination therapies

TKIs have been explored in CRC treatment combinations, and pre-clinical studies with 17 TKIs have been successful. Compared to the related pre-clinical investigations, several clinical trials employed various chemotherapy agents or antibodies with similar sites (Chen H. et al., 2022a; Chen R. et al., 2022b).

4.5.1 TKIs combination with antibodies target

Targeting the EGFR/mitogen-activated protein kinase (MAPK) pathway, TKIs are combined with antibodies. In a previous study, cabozantinib was combined with the anti-EGFR antibody cetuximab to treat CRC cell lines, and it was found that this combination helped overcome cetuximab tolerance (Strickler et al., 2021). Furthermore, when TKIs are combined with an anti-VEGF antibody, such as bevacizumab or imatinib, a greater degree of vascular normalization has been observed without activation of extracellular matrix (ECM) deposition (Schiffmann et al., 2017).

4.5.2 TKIs combination with immunotherapy

When CT-26 isografts were treated with lenvatinib, pembrolizumab, and an anti-PD-1 antibody, tumor growth *in vivo* was significantly inhibited. Regorafenib and nivolumab had a synergistic immune-modulatory effect on CRC cells in another instance (Kato et al., 2019). Anti-PD-1 antibody nivolumab was combined with regorafenib to promote anti-tumor activity (Doleschel et al., 2021). Combinations of regorafenib and ICI were the focus of subsequent research. However, the findings revealed no therapeutic value. It evaluated the potential effectiveness of the combination of pembrolizumab and lenvatinib in patients with advanced non-MSI-H mCRC (Wang et al., 2020).

4.5.3 TKIs combination with radiotherapy

Encouraging results have been reported for the pre-clinical trials of cediranib in combination with radiation in CRC. In addition, vandetanib, irinotecan, and radiation significantly diminished tumor size in human colorectal xenograft models (Meyerhardt et al., 2012). However, the combination of vandetanib with cetuximab and irinotecan did not demonstrate any improvement in effectiveness compared to earlier results in patients with mCRC who had undergone therapy (Table 2) (Wachsberger et al., 2009).

TABLE 1 The clinical results and pre-clinical efficacy of specific TKIs in monotherapy. The TKIs shown in bold have either demonstrated promising outcomes or have been effectively adapted for use in the clinic.

TKI	Target(s)	Study model	Clinical trial study	Clinical outcomes	Reference
vandetanib	VEGFR and EGFR families, TIE2, BRK, RET, and EPH receptor and Src kinase members	CRC Cell lines PDCs	open-label, randomized phase I trials	No OR observed	Kim et al. (2018)
sunitinib	RET, CSF-1R, FLT3, KIT, VEGFR1,2, 3, and PDGFRα and β	Cells with CRC Mouse Xenograft Model	A two-stage, multicentre, open-label study (Phase II)	No OR observed	Lu et al., 2021
regorafenib	Abl, PTK5, SAPK2, BRAFV600E, BRAF, RAF-1, Eph2A, Trk2A, DDR2, TIE2, FGFR2, FGFR1, PDGFRα and β, KIT, VEGFR1, 2, 3, RET	CRC PDTOs	Randomized, placebo-controlled, phase III analysis	The median OS for placebo vs. regorafenib was 6.4 vs. 5.0 months	Vlachogiannis et al. (2018)
nintedanib	FLT-3, CSF1R, VEGFR 1,2,3, FGFR 1–3, PDGFR α and β	cell lines of CRC	Randomized, double-blinded, placebo-controlled phase III experiment	Both of the study's co-primary outcomes were not met. OS has not improved. PFS has significantly but modestly improved	Cheng et al. (2021)
linifanib	VEGF, PDGF, FLT3	CRC cell lines 3D micro- Tumors	An open-label, non-randomized study (Phase II)	No tumor responses were seen, and the ORR's primary goal was not fulfilled	Chan et al. (2017)
lenvatinib	RET, KIT, FGFR, PDGFRα, VEGFR1, 2, and 3	PDX cell lines of CRC	single-centre, single-arm, phase II open-label trial	±PFS –3.6 months and ±OS—7.4 months, DCR (70.0%)	Iwasa et al. (2020)
gefitinib	IGF and PDGF-mediated signaling, EGFR exon 21 point mutation L858R, and exon 19 deletion	CRC cell lines	Phase II Randomized Trial	Median PFS is 1.9 months, with PR occurring in 1 of 110 patients (maximum 2.3 months)	Georgious et al. (2020)
fruquintinib	VEGFR1,2,3	Mouse model	a multicentre clinical trial, placebo-controlled, double-blind, Phase III randomized cohort	Fruquintinib *versus* placebo: median OS, 9.3 *vs.* 6.6 months Fruquintinib *versus* placebo: Median PFS, 3.7 vs. 1.8 months	Wang et al. (2020)
erlotinib	EGFR	PDX	Phase II study	No CR or PR	Rivera et al. (2021)
dasatinib	SRC family (FYN, YES, LCK, SRC) BCR-ABL, PDGFRβ, EPHA2, c-KIT	CRC xenograft Mice model CRC cell lines	Phase II multicentre trial	No OR observed	Scott et al. (2017)
cediranib	FGFRs, PDGFRs, VEGFR1, 2, 3	CRC cell lines Mouse model	Phase I, multicentre, open-label	DCR (81%)—26/32 patients	Melsens et al. (2017)
cabozantinib	TIE-2, FLT-3, TRKB, KIT, MER, TYRO3, ROS1, RET, AXL, VEGFR1, 2 and 3, MET	Models using Xenograft mice and CRC cell lines	Single-arm, two-stage Phase II trial	12-week PFS (34% of patients) 1 PR patient (Best response) SD with a DCR (72.7%) at week 6	Yang et al. (2022)
bosutinib	Hck, Lyn, Src, BCR-ABL	Models using Xenograft mice and CRC cell lines	Phase I, prospective clinical trial	CR—0 PR—1 ORR (6%)	Daud et al. (2012)
apatinib	s-SRC, c-Kit, VEGFR2	CRC cell lines Murine CRC cell lines	open-label, single-arm Phase II experiment	Average OS—7.9 months Average PFS—3.9 months	Cai et al. (2020)

*PDX, patient-derived xenograft; PFS, progression-free survival; OS, overall survival; PDCs, patient-derived cells; PDTOs, patient-derived tumor organoids; DCR, disease control rate; ORR, objective response rate; OR, overall response; CR, complete response; SD, stable disease; PR, partial response; mCRC, metastatic colorectal cancer; CRC, colorectal cancer.

4.5.4 TKIs combination with chemotherapy

5-fluorouracil (5-FU) treatment has enhanced survival in several cancers. The drug's most significant effect has been documented in CRC. Active metabolites of 5-FU interfere with DNA and RNA synthesis via the folate metabolic pathway (Pardini et al., 2011). Patients with mCRC treated with oxaliplatin as a single drug showed limited efficacy, with response rates (RR) ranging from 10% to 24%. In contrast, the combination of oxaliplatin with 5FU has demonstrated RRs that vary from 20% to more than 50% due to a synergistic effect with 5FU (Comella et al., 2009). A camptothecin derivative known as irinotecan hydrochloride has anticancer efficacy against several tumor types. Irinotecan's active metabolite is SN-38, which is synthesized by the enzyme carboxylesterase in the body. Survival has significantly increased since introducing irinotecan for treating CRC around the beginning of the 20th century. The overall survival time has been extended to more than 30 months due to the combination of irinotecan with 5-fluorouracil, oxaliplatin, and numerous molecularly targeted anticancer medications (Fujita et al., 2015).

The synthetic drug semaxanib, which inhibits VEGFR-1 and -2 tyrosine kinases, is a small and lipophilic molecule. For 28 patients with mCRC, semaxanib at two different dose levels

TABLE 2 Clinical results of additional TKI selected from combination therapies in pre-clinical studies.

TKI	Clinical findings	Model of the trail	Target (s)	Clinical combination	Clinical trial study	Ref
vatalanib	ORR, OS, and PFS were not enhanced	CRC cell lines	VEGFR1,2, PDGFR, c- Kit, C-Fms	vatalanib + FOLFOX4	Phase III randomized, placebo-controlled	To et al. (2015)
vandetanib	PD (34%), SD (59%), PR (7%)	Xenograft Model	Families VEGFR and EGFR, TIE2, BRK, RET, and Src kinase family members and EPH receptor	vandetanib + irinotecan + cetuximab	Trial I comprising a larger MTD population	Eng et al. (2019)
	PFS average—3.6 months					
	Average OS—10.5 months					
sunitinib	PR—8/17 patients	Mouse model and CRC cell lines	RET, CSF-1R, FLT3, KIT, β, VEGFR1,2,3, and PDGFRα	sunitinib + FOLFIRI	Phase II Multicenter, open-label	Di Desidero et al. (2019)
sorafenib	No OR detected, 1.84 months for the median PFS	CRC cell lines	PDGFR-ß, VEGFR1,2,3, RET, RET/PTC, FLT- 3, c-CRAF, KIT, mBRAF, BRAF	sorafenib + cetuximab	open-label, single-arm Phase II trial	Rizzo et al. (2021)
semaxinib	PR confirmed PR (27%) and PR unconfirmed PR (18%)	murine model using xenografts and CRC cell lines	VEGFR2, c-kit	bolus 5-FU, leucovorin, and irinotecan (IFL) + semaxinib	Phase I/II trial	Woo and Jung. (2017)
pazopanib	FOLFOX6RR (38%) pazopanib + CapeOx + RR (40%) pazopanib	PDX Mouse Model	c-Fms, Lck, ltk, interleukin-2, FGFR 1 and 3, VEGFR1,2,3and KIT	FOLFOX6 or CapeOx + pazopanib	2-part, Open-label, dose-finding Phase I	Zhu et al. (2019)
nintedanib	Primary endpoint criteria were not met	CRC Cell lines & mouse model	FLT-3, CSF1R, VEGFR 1,2,3, FGFR 1–3, PDGFR α and β	nintedanib + mFOLFOX6	Phase II randomized, placebo-controlled	Boland et al. (2018)
gefitinib	OS, PFS, and OR did not improve than the FOLFIRI arm	CRC cell lines	IGF and PDGF-mediated signaling are mediated by EGFR exon 19 deletion or exon 21 point mutation L858R	gefitinib + FOLFIRI	A multicenter randomized trial (Phase II)	Palumbo et al. (2014)
erlotinib	Patients with BRAF and KRAS mutations did not respond. In KRAS/BRAF wt tumors, the RR was 52%, while in KRAS wt tumors, it was 41%	CRC cell lines	EGFR	erlotinib + cetuximab	Phase II trial	Xu et al. (2020)
dasatinib	Patients with high srcact expression had an ORR of 75%, while those with low srcact expression had a 0% rate	CRC cell lines	PDGFRβ, EPHA2, c-KIT, BCR-ABL, SRC family (FYN, YES, LCK, SRC)	dasatinib, capecitabine, oxaliplatin, and bevacizumab	dosage escalation in Phase I and cohort	Mettu et al. (2019)
cediranib	CR (41%), ECPR (53%)	Xenograft mouse model	FGFRs, PDGFRs, VEGFR1, 2, 3	cediranib + chemoradiotherapy	Phase I, alternating cohort design	Melsons et al. (2017)
bosutinib	SD or PR > 24 weeks (13% PR or SD) (all tumor types)	cell lines for CRC mouse xenograft models	Hck, Lyn, Src, BCR-ABL	capecitabine + bosutinib	open-label, dose-escalation, multicenter Stage I trial	Wenzel et al. (2020)
apatinib	DCR (22.2%), ORR (0%)	CRC cell lines Murine CRC cell lines	s-SRC, c-Kit, VEGFR2	apatinib + anti-PD-1 antibody SHR-1210	open-label, single-arm, Phase II prospective trial	Cai et al. (2020)
	±OS—is 7.80 months					
	±PFS—is 1.83 months					

*TFTD/TAS102, trifluridine/tipiracil; CapeOx/XELOX, capecitabine, oxaliplatin; 5-FU, 5-Fluorouracil; SN-38, the active metabolite of irinotecan; FOLFOX4/6/mFOLFOX6, leucovorin calcium (folinic acid), fluorouracil, and oxaliplatin; ECPR, excellent clinical or pathological response; PR, partial response/partial remission; MTD, maximum tolerated dose.

in combination with fluorouracil and leucovorin showed a promising response of 31.6% as the first-line therapy (Rosen et al., 1999). A multicenter MABEL (Minimum anticipated biological effect level) trial studied the combination of cetuximab and CPT-11 at a dose and schedule as a pre-study in 1123 patients with mCRC exhibiting detectable EGFR. 9.2 months was the anticipated median survival, although at the expense of a tolerable toxicity profile. The efficacy and safety of C225 with CPT-11 observed in earlier studies were validated by MABEL in a larger context (Wilke et al., 2006). Gefitinib (ZD 1839) inhibits the EGFR tyrosine kinase selectively and has a 100-fold more effective potency against EGFR than other tyrosine or serine/threonine kinases. Gefitinib, unlike cetuximab, does not cause EGFR internalization or destruction in CRC cells, nor does it decrease EGF binding sites or EGFR protein levels (MacKenzie et al., 2005). Gefitinib monotherapy has shown anticancer activity in various CRC cell lines in both *in vitro* and *in vivo* investigations. Gefitinib, on the other hand, showed little activity in phase I/II clinical trials in individuals with mCRC (Rothenberg et al., 2004).

The most developed monoclonal antibody against EGFR currently under clinical development is cetuximab. A phase II trial of cetuximab with irinotecan was conducted in patients with EGFR-positive colorectal cancer who were refractory to both 5-fluorouracil (5-FU) and Irinotecan because preclinical and early clinical research indicate that cetuximab might reverse irinotecan resistance in CRC both *in vitro* and *in vivo*. The overall response rate for the 120 patients who received this regimen was 22.5% (Saltz et al., 2001). Kuo et al. reported results from a phase II research that included one cycle of FOLFOX-4, followed by further cycles of FOLFOX-4 with 500 mg/d gefitinib in 27 patients with proven progressing CRC following at least one chemotherapy regimen (generally irinotecan-based). 33% of patients experienced objective responses, whereas 48% maintained stable conditions over a prolonged period. The number of prior regimens exhibited no effect on response rates. The median event-free survival period was 5.4 months, and the total survival period was 12 months (Kuo et al., 2005).

5 Conclusion and future perspectives

CRC is a common cancer that substantially increases cancer mortality rates. Due to the complexity of colorectal carcinogenesis, the CRC survival rates of individual patients vary. It is thus beneficial to determine accurate and useful molecular biomarkers that contribute to CRC detection and management. Current studies have focused on finding precise, specialized biomarkers for CRC diagnosis and treatment success. This review article offered an overview of the latest CRC diagnostic biomarkers. Multiple signalling pathways are activated in CRC, making it impossible to address the disease with a single therapy. Combining conventional treatments with novel inhibitors that target multiple pathways is essential. Small-molecule TKIs are among the most recent additions to the vast range of cancer-treating drugs. TKI is a useful pharmacological strategy for treating a variety of malignancies, but it is not a solution. Protein tyrosine kinases appear to accelerate the growth and onset of CRC. The development of more effective biomarkers and the success of tailored medicines offer hope for the future management of CRC, but first, we need to learn more about the disease. Standardizing protocols, including extraction and quantification procedures and normalizing approaches, will be complicated in the future. Biomarker translation into the therapeutic context is also critical. Lastly, complicated laboratory equipment should be avoided for simple, inexpensive, quick solutions. We believed that developing additional novel targeted medicines could reduce the burden of CRC cancer.

Author contributions

All authors listed have made a substantial, direct, and intellectual contribution to the work and approved it for publication.

Funding

This work was supported by the Shaoxing Health Science and Technology Plan (No. 2022SY018 to SZ).

Acknowledgments

We are thankful to the Shaoxing Health Science and Technology Plan for supporting this project.

Conflict of interest

The authors declare that the research was conducted in the absence of any commercial or financial relationships that could be construed as a potential conflict of interest.

Publisher's note

References

Aasebø, K., Dragomir, A., Sundström, M., Mezheyeuski, A., Edqvist, P. H., Eide, G. E., et al. (2020). CDX2: A prognostic marker in metastatic colorectal cancer defining a better BRAF mutated and a worse KRAS mutated subgroup. *Front. Oncol.* 10, 8. doi:10.3389/fonc.2020.00008

Abo-Elela, D. A., Salem, A. M., Swellam, M., and Hegazy, M. G. (2023). Potential diagnostic role of circulating miRNAs in colorectal cancer. *Int. J. Immunopathol. Pharmacol.* 37, 03946320221144565. doi:10.1177/03946320221144565

Adnan, M., Koli, S., Mohammad, T., Siddiqui, A. J., Patel, M., Alshammari, N., et al. (2022). Searching for novel anaplastic lymphoma kinase inhibitors: structure-guided screening of natural compounds for a tyrosine kinase therapeutic target in cancers. *OMICS A J. Integr. Biol.* 26 (8), 461–470. doi:10.1089/omi.2022.0067

Ahmed, F. E., Gouda, M. M., Ahmed, N. C., and Hussein, L. (2019). Quantification of microRNAs by absolute Dpcr for the diagnostic screening of colon cancer. *J. Colon Rectal Cancer* 1 (3), 10–37. doi:10.14302/issn.2471-7061.jcrc-18-2526

Akhlaghipour, I., Bina, A. R., Abbaszadegan, M. R., and Moghbeli, M. (2021). Methylation as a critical epigenetic process during tumor progressions among Iranian population: an overview. *Genes Environ.* 43, 14. doi:10.1186/s41021-021-00187-1

Akimoto, N., Ugai, T., Zhong, R., Hamada, T., Fujiyoshi, K., Giannakis, M., et al. (2021). Rising incidence of early-onset colorectal cancer—a call to action. *Nat. Rev. Clin. Oncol.* 18 (4), 230–243. doi:10.1038/s41571-020-00445-1

Al-Duhaidahawi, M. (2023). Role of CDX2 marker in patients with colorectal cancer. *Biomed. Chem. Sci.* 2 (1), 11–15. doi:10.48112/bcs.v2i1.321

Altomare, D. F., Di Lena, M., Porcelli, F., Travaglio, E., Longobardi, F., Tutino, M., et al. (2015). Effects of curative colorectal cancer surgery on exhaled volatile organic compounds and potential implications in clinical follow-up. *Ann. Surg.* 262 (5), 862–866; discussion 866-867. doi:10.1097/SLA.0000000000001471

Alzahrani, S. M., Al Doghaither, H. A., and Al-Ghafari, A. B. (2021). General insight into cancer: an overview of colorectal cancer. *Mol. Clin. Oncol.* 15 (6), 1–8. doi:10.3892/mco.2021.2433

Amal, H., Leja, M., Funka, K., Lasina, I., Skapars, R., Sivins, A., et al. (2016). Breath testing as potential colorectal cancer screening tool. *Int. J. Cancer* 138 (1), 229–236. doi:10.1002/ijc.29701

Baharudin, R., Ishak, M., Muhamad Yusof, A., Saidin, S., Syafruddin, S. E., Wan Mohamad Nazarie, W. F., et al. (2022). Epigenome-wide DNA methylation profiling in

colorectal cancer and normal adjacent colon using Infinium human methylation 450K. *Diagnostics* 12 (1), 198. doi:10.3390/diagnostics12010198

Bhullar, K. S., Lagarón, N. O., McGowan, E. M., Parmar, I., Jha, A., Hubbard, B. P., et al. (2018). Kinase-targeted cancer therapies: progress, challenges, and future directions. *Mol. cancer* 17, 48–20. doi:10.1186/s12943-018-0804-2

Boland, P. M., Fakih, M., Lim, D., Attwood, K., Tan, W., Mastri, M., et al. (2018). A phase I/II study of nintedanib and capecitabine in refractory metastatic colorectal cancer. *J. Clin. Oncol.* 36 (15). doi:10.1200/JCO.2018.36.15_suppl.3552

Bond, A., Greenwood, R., Lewis, S., Corfe, B., Sarkar, S., O'Toole, P., et al. (2019). Volatile organic compounds emitted from faeces as a biomarker for colorectal cancer. *Alimentary Pharmacol. Ther.* 49 (8), 1005–1012. doi:10.1111/apt.15140

Bouchahda, M., Macarulla, T., Spano, J. P., Bachet, J. B., Lledo, G., Andre, T., et al. (2008). Cetuximab efficacy and safety in a retrospective cohort of elderly patients with heavily pretreated metastatic colorectal cancer. *Crit. Rev. oncology/hematology* 67 (3), 255–262. doi:10.1016/j.critrevonc.2008.02.003

Bresalier, R. S., Grady, W. M., Markowitz, S. D., Nielsen, H. J., Batra, S. K., and Lampe, P. D. (2020). Biomarkers for early detection of colorectal cancer: the early detection research network, a framework for clinical translation. *Cancer Epidemiol. Biomarkers Prev.* 29 (12), 2431–2440. doi:10.1158/1055-9965.EPI-20-0234

Cai, C., Luo, Q., Liu, Y., Peng, Y., Zhang, X., Jiang, Z., et al. (2022). The optimal first-line treatment for patients with left-sided RAS wild-type metastatic colorectal cancer: double-drug regimen or triple-drug regimen therapy. *Front. Pharmacol.* 13, 1015510. doi:10.3389/fphar.2022.1015510

Cai, J., Zuo, X., Chen, Z., Zhang, Y., Wang, J., Wang, J., et al. (2019). Long non-coding RNAs serve as potential diagnostic biomarkers for colorectal cancer. *J. Cancer* 10 (3), 611–619. doi:10.7150/jca.28780

Cai, X., Wei, B., Li, L., Chen, X., Yang, J., Li, X., et al. (2020). Therapeutic potential of apatinib against colorectal cancer by inhibiting VEGFR2-mediated angiogenesis and β-catenin signaling. *OncoTargets Ther.* 13, 11031–11044. doi:10.2147/OTT.S266549

Calvo-García, A., Pérez Abánades, M., Ruíz-García, S., Fernández Román, A. B., Letellez Fernández, J., Candel García, B., et al. (2022). Effectiveness, toxicity, and survival predictors of regorafenib in metastatic colorectal cancer: A multicenter study of routinely collected data. *Oncol. (08909091)* 36 (12), 732–738. doi:10.46883/2022.25920981

Cao, L., Hu, T., Lu, H., and Peng, D. (2020). N-MYC downstream-regulated gene 4 (NDRG4), a frequent downregulated gene through DNA hypermethylation, plays a tumor-suppressive role in esophageal adenocarcinoma. *Cancers* 12 (9), 2573. doi:10.3390/cancers12092573

Chan, E., Goff, L. W., Cardin, D. B., Ancell, K., Smith, S. J., Whisenant, J. G., et al. (2017). Phase II study of the multi-kinase inhibitor of angiogenesis, linifanib, in patients with metastatic and refractory colorectal cancer expressing mutated KRAS. *Investig. New Drugs* 35, 491–498. doi:10.1007/s10637-017-0458-8

Chan, H. T., Nagayama, S., Otaki, M., Chin, Y. M., Fukunaga, Y., Ueno, M., et al. (2023). Tumor-informed or tumor-agnostic circulating tumor DNA as a biomarker for risk recurrence in resected colorectal cancer patients. *Front. Oncol.*, 7079. doi:10.3389/fonc.2022.1055968

Chan, S. C. H., and Liang, J. Q. (2022). Advances in tests for colorectal cancer screening and diagnosis. *Expert Rev. Mol. Diagnostics* 22 (4), 449–460. doi:10.1080/14737159.2022.2065197

Chandrapalan, S., and Arasaradnam, R. P. (2020). Urine as a biological modality for colorectal cancer detection. *Expert Rev. Mol. diagnostics* 20 (5), 489–496. doi:10.1080/14737159.2020.1738928

Chang, H., Mishra, R., Cen, C., Tang, Y., Ma, C., Wasti, S., et al. (2021). Metagenomic analyses expand bacterial and functional profiling biomarkers for colorectal cancer in a hainan cohort, China. *Curr. Microbiol.* 78, 705–712. doi:10.1007/s00284-020-02299-3

Chen, H., Lu, B., and Dai, M. (2022a). Colorectal cancer screening in China: status, challenges, and prospects—China, 2022. *China CDC Wkly.* 4 (15), 322–328. doi:10.46234/ccdcw2022.077

Chen, H. M., Lin, C. C., Chen, W. S., Jiang, J. K., Yang, S. H., Chang, S. C., et al. (2021). Insulin-like growth factor 2 mRNA-binding protein 1 (IGF2BP1) is a prognostic biomarker and associated with chemotherapy responsiveness in colorectal cancer. *Int. J. Mol. Sci.* 22 (13), 6940. doi:10.3390/ijms22136940

Chen, R., Li, Q., Xu, S., Ye, C., Tian, T., Jiang, Q., et al. (2022b). Modulation of the tumour microenvironment in hepatocellular carcinoma by tyrosine kinase inhibitors: from modulation to combination therapy targeting the microenvironment. *Cancer Cell Int.* 22 (1), 73. doi:10.1186/s12935-021-02435-4

Cheng, G., Li, Y., Liu, Z., and Song, X. (2021). The microRNA-429/DUSP4 axis regulates the sensitivity of colorectal cancer cells to nintedanib. *Mol. Med. Rep.* 23 (4), 1–1. doi:10.3892/mmr.2021.11867

Choi, H. B., Pyo, J. S., Son, S., Kim, K., and Kang, G. (2022). Diagnostic and prognostic roles of CDX2 immunohistochemical expression in colorectal cancers. *Diagnostics* 12 (3), 757. doi:10.3390/diagnostics12030757

Comella, P., Casaretti, R., Sandomenico, C., Avallone, A., and Franco, L. (2009). Role of oxaliplatin in the treatment of colorectal cancer. *Ther. Clin. risk Manag.* 5, 229–238. doi:10.2147/tcrm.s3583

Cruz, A., Carvalho, C. M., Cunha, A., Crespo, A., Iglesias, Á., García-Nimo, L., et al. (2021). Faecal diagnostic biomarkers for colorectal cancer. *Cancers* 13 (21), 5568. doi:10.3390/cancers13215568

Dabir, P. D., Svanholm, H., and Christiansen, J. J. (2018). SATB2 is a supplementary immunohistochemical marker to CDX2 in the diagnosis of colorectal carcinoma metastasis in an unknown primary. *Apmis* 126 (6), 494–500. doi:10.1111/apm.12854

Daud, A. I., Krishnamurthi, S. S., Saleh, M. N., Gitlitz, B. J., Borad, M. J., Gold, P. J., et al. (2012). Phase I study of bosutinib, a src/abl tyrosine kinase inhibitor, administered to patients with advanced solid tumors. *Clin. Cancer Res.* 18 (4), 1092–1100. doi:10.1158/1078-0432.CCR-11-2378

Davidsen, J. (2020). *The role of CDX2 in colon cancer development and progression*. Denmark: Doctoral dissertation, Department of Science and Environment, Roskilde University.

Dhiman, D. K., Sanyal, S. N., and Vaish, V. (2020). Imatinib exhibit synergistic pleiotropy in the prevention of colorectal cancer by suppressing proinflammatory, cell survival and angiogenic signaling. *Cell. Signal.* 76, 109803. doi:10.1016/j.cellsig.2020.109803

Di Desidero, T., Orlandi, P., Fioravanti, A., Alì, G., Cremolini, C., Loupakis, F., et al. (2019). Chemotherapeutic and antiangiogenic drugs beyond tumor progression in colon cancer: evaluation of the effects of switched schedules and related pharmacodynamics. *Biochem. Pharmacol.* 164, 94–105. doi:10.1016/j.bcp.2019.04.001

Ding, Q., Kong, X., Zhong, W., Liu, W., and Ye, Q. (2022). Fecal biomarkers: non-invasive diagnosis of colorectal cancer. *Front. Oncol.* 12, 812663. doi:10.3389/fonc.2022.812663

Diwanji, D., Thaker, T., and Jura, N. (2019). More than the sum of the parts: toward full-length receptor tyrosine kinase structures. *IUBMB life* 71 (6), 706–720. doi:10.1002/iub.2060

Doleschel, D., Hoff, S., Koletnik, S., Rix, A., Zopf, D., Kiessling, F., et al. (2021). Regorafenib enhances anti-PD1 immunotherapy efficacy in murine colorectal cancers, and its combination prevents tumor regrowth. *J. Exp. Clin. Cancer Res.* 40 (1), 1–14. doi:10.1186/s13046-021-02043-0

Du, Z., and Lovly, C. M. (2018). Mechanisms of receptor tyrosine kinase activation in cancer. *Mol. cancer* 17, 58–13. doi:10.1186/s12943-018-0782-4

Eng, C., Kim, T. W., Bendell, J., Argilés, G., Tebbutt, N. C., Di Bartolomeo, M., et al. (2019). Atezolizumab with or without cobimetinib versus regorafenib in previously treated metastatic colorectal cancer (IMblaze370): A multicentre, open-label, phase 3, randomised, controlled trial. *lancet Oncol.* 20 (6), 849–861. doi:10.1016/S1470-2045(19)30027-0

Fonseca, A., Ramalhete, S. V., Mestre, A., das Neves, R. P., Marreiros, A., Castelo-Branco, P., et al. (2021). Identification of colorectal cancer associated biomarkers: an integrated analysis of miRNA expression. *Aging (Albany NY)* 13 (18), 21991–22029. doi:10.18632/aging.203556

Fornaro, L., Baldi, G. G., Masi, G., Allegrini, G., Loupakis, F., Vasile, E., et al. (2011). Cetuximab plus irinotecan after irinotecan failure in elderly metastatic colorectal cancer patients: clinical outcome according to KRAS and BRAF mutational status. *Crit. Rev. oncology/hematology* 78 (3), 243–251. doi:10.1016/j.critrevonc.2010.06.003

Fox, M., Crafter, C., and Owen, D. (2019). The non-receptor tyrosine kinase ACK: regulatory mechanisms, signalling pathways and opportunities for attACKing cancer. *Biochem. Soc. Trans.* 47 (6), 1715–1731. doi:10.1042/BST20190176

Fujita, K. I., Kubota, Y., Ishida, H., and Sasaki, Y. (2015). Irinotecan a key chemotherapeutic drug for metastatic colorectal cancer. *World J. gastroenterology* 21 (43), 12234–12248. doi:10.3748/wjg.v21.i43.12234

Gao, H. L., Lv, L. B., Zhao, W. F., Lu, Q. W., and Fan, J. Q. (2023). Diagnostic accuracy of the multi-target stool DNA test in detecting colorectal cancer: A hospital-based study. *World J. Gastrointest. Oncol.* 15 (1), 102–111. doi:10.4251/wjgo.v15.i1.102

Gao, R., Xia, K., Wu, M., Zhong, H., Sun, J., Zhu, Y., et al. (2022). Alterations of gut mycobiota profiles in adenoma and colorectal cancer. *Front. Cell. Infect. Microbiol.* 119, 839435. doi:10.3389/fcimb.2022.839435

García-Aranda, M., and Redondo, M. (2019). Targeting receptor kinases in colorectal cancer. *Cancers* 11 (4), 433. doi:10.3390/cancers11040433

Georgiou, A., Stewart, A., Cunningham, D., Banerji, U., and Whittaker, S. R. (2020). Inactivation of NF1 promotes resistance to EGFR inhibition in KRAS/NRAS/brafv600-wild-type colorectal cancer. *Mol. Cancer Res.* 18 (6), 835–846. doi:10.1158/1541-7786.MCR-19-1201

Gligorijević, N., Dobrijević, Z., Šunderić, M., Robajac, D., Četić, D., Penezić, A., et al. (2022). The insulin-like growth factor system and colorectal cancer. *Life* 12 (8), 1274. doi:10.3390/life12081274

Gong, C., Yang, H., Wang, S., Liu, J., Li, Z., Hu, Y., et al. (2021). hTERT promotes CRC proliferation and migration by recruiting YBX1 to increase NRF2 expression. *Front. Cell Dev. Biol.* 9, 658101. doi:10.3389/fcell.2021.658101

Han, Y., Zhu, L., Wu, W., Zhang, H., Hu, W., Dai, L., et al. (2020). Small molecular immune modulators as anti-cancer agents. *Adv. Exp. Med. Biol.* 1248, 547–618. doi:10.1007/978-981-15-3266-5_22

Handley, S. A., and Devkota, S. (2019). Going viral: A novel role for bacteriophage in colorectal cancer. *MBio* 10 (1), 02618–02626. doi:10.1128/mBio.02626-18

Hannigan, G. D., Duhaime, M. B., Ruffin IV, M. T., Koumpouras, C. C., and Schloss, P. D. (2018). Diagnostic potential and interactive dynamics of the colorectal cancer virome. *MBio* 9 (6), 02218–02248. doi:10.1128/mBio.02248-18

Hariharan, R., and Jenkins, M. (2020). Utility of the methylated SEPT9 test for the early detection of colorectal cancer: A systematic review and meta-analysis of diagnostic test accuracy. *BMJ Open Gastroenterol.* 7 (1), e000355. doi:10.1136/bmjgast-2019-000355

He, J., Wu, W., Tang, H. C., Liu, B., and Bu, L. L. (2023). Comprehensive landscape and future perspectives of long non-coding RNAs (lncRNAs) in colorectal cancer (CRC): based on bibliometric analysis. *Non-coding RNA Res.* 8 (1), 33–92. doi:10.1016/bs.ircmb.2022.11.002

Hendricks, A., Dall, K., Brandt, B., Geisen, R., Röder, C., Schafmayer, C., et al. (2021). Longitudinal analysis of circulating tumor cells in colorectal cancer patients by a cytological and molecular approach: feasibility and clinical application. *Front. Oncol.* 11, 646885. doi:10.3389/fonc.2021.646885

Hijos-Mallada, G., Lué, A., Velamazan, R., Saura, N., Abril, C., Lorenzo, M., et al. (2021). The addition of other fecal biomarkers does not improve the diagnostic accuracy of immunochemical fecal occult blood test alone in a colorrectal cancer screening cohort. *Front. Med.* 8, 665786. doi:10.3389/fmed.2021.665786

Hossain, M. S., Karuniawati, H., Jairoun, A. A., Urbi, Z., Ooi, D. J., John, A., et al. (2022). Colorectal cancer: A review of carcinogenesis, global epidemiology, current challenges, risk factors, preventive and treatment strategies. *Cancers* 14 (7), 1732. doi:10.3390/cancers14071732

Hrudka, J., Fišerová, H., Jelínková, K., Matěj, R., and Waldauf, P. (2021). Cytokeratin 7 expressions as a predictor of an unfavorable prognosis in colorectal carcinoma. *Sci. Rep.* 11 (1), 1–10.

Hrudka, J., Matěj, R., Nikov, A., Tomyak, I., Fišerová, H., Jelínková, K., et al. (2022). Loss of SATB2 expression correlates with cytokeratin 7 and PD-L1 tumor cell positivity and aggressiveness in colorectal cancer. *Sci. Rep.* 12 (1), 19152. doi:10.1038/s41598-022-22685-0

Huang, L., Jiang, S., and Shi, Y. (2020). Tyrosine kinase inhibitors for solid tumors in the past 20 years (2001–2020). *J. Hematol. Oncol.* 13, 1–23. doi:10.1186/s13045-020-00977-0

Huang, Z., and Yang, M. (2022). Molecular network of colorectal cancer and current therapeutic options. *Front. Oncol.* 12, 852927. doi:10.3389/fonc.2022.852927

Isakoff, S. J., Wang, D., Campone, M., Calles, A., Leip, E., Turnbull, K., et al. (2014). Bosutinib plus capecitabine for selected advanced solid tumours: results of a phase 1 dose-escalation study. *Br. J. Cancer* 111 (11), 2058–2066. doi:10.1038/bjc.2014.508

Islam Khan, M. Z., Tam, S. Y., and Law, H. K. W. (2022). Advances in high throughput proteomics profiling in establishing potential biomarkers for gastrointestinal cancer. *Cells* 11 (6), 973. doi:10.3390/cells11060973

Iwaizumi, M., Taniguchi, T., Kurachi, K., Osawa, S., Sugimoto, K., Baba, S., et al. (2023). Methylation of CpG island promoters at ZNF625, LONRF2, SDC2, and WDR17 in a patient with numerous non-granular type laterally spreading tumors and colorectal cancer: A case report. *Oncol. Lett.* 25 (1), 14–18. doi:10.3892/ol.2022.13600

Iwasa, S., Okita, N., Kuchiba, A., Ogawa, G., Kawasaki, M., Nakamura, K., et al. (2020). Phase II study of lenvatinib for metastatic colorectal cancer refractory to standard chemotherapy: the LEMON study (NCCH1503). *ESMO open* 5 (4), e000776. doi:10.1136/esmoopen-2020-000776

Iwasaki, H., Shimura, T., and Kataoka, H. (2019). Current status of urinary diagnostic biomarkers for colorectal cancer. *Clin. Chim. Acta* 498, 76–83. doi:10.1016/j.cca.2019.08.011

Iyer, K. K., van Erp, N. P., Tauriello, D. V., Verheul, H. M., and Poel, D. (2022). Lost in translation: revisiting the use of tyrosine kinase inhibitors in colorectal cancer. *Cancer Treat. Rev.* 110, 102466. doi:10.1016/j.ctrv.2022.102466

Jelski, W., and Mroczko, B. (2020). Biochemical markers of colorectal cancer–present and future. *Cancer Manag. Res.* 12, 4789–4797. doi:10.2147/CMAR.S253369

Jiao, Q., Bi, L., Ren, Y., Song, S., Wang, Q., and Wang, Y. S. (2018). Advances in studies of tyrosine kinase inhibitors and their acquired resistance. *Mol. cancer* 17 (1), 36–12. doi:10.1186/s12943-018-0801-5

Kato, Y. U., Tabata, K., Kimura, T., Yachie-Kinoshita, A., Ozawa, Y., Yamada, K., et al. (2019). Lenvatinib plus anti-PD-1 antibody combination treatment activates CD8+ T cells through reduction of tumor-associated macrophage and activation of the interferon pathway. *PloS one* 14 (2), e0212513. doi:10.1371/journal.pone.0212513

Kaur, P., Mani, S., Cros, M. P., Scoazec, J. Y., Chemin, I., Hainaut, P., et al. (2012). Epigenetic silencing of sFRP1 activates the canonical Wnt pathway and contributes to increased cell growth and proliferation in hepatocellular carcinoma. *Tumor Biol.* 33, 325–336. doi:10.1007/s13277-012-0331-5

Kibriya, M. G., Raza, M., Kamal, M., Haq, Z., Paul, R., Mareczko, A., et al. (2022). Relative telomere length change in colorectal carcinoma and its association with tumor characteristics, gene expression and microsatellite instability. *Cancers* 14 (9), 2250. doi:10.3390/cancers14092250

Kim, J. H. (2015). Chemotherapy for colorectal cancer in the elderly. *World J. Gastroenterology WJG* 21 (17), 5158–5166. doi:10.3748/wjg.v21.i17.5158

Kim, S. Y., Oh, S. O., Kim, K., Lee, J., Kang, S., Kim, K. M., et al. (2018). NCOA4-RET fusion in colorectal cancer: therapeutic challenge using patient-derived tumor cell lines. *J. Cancer* 9 (17), 3032–3037. doi:10.7150/jca.26256

Koonin, E. V., Dolja, V. V., and Krupovic, M. (2021). The healthy human virome: from virus–host symbiosis to disease. *Curr. Opin. virology* 47, 86–94. doi:10.1016/j.coviro.2021.02.002

Kuo, T., Cho, C. D., Halsey, J., Wakelee, H. A., Advani, R. H., Ford, J. M., et al. (2005). Phase II study of gefitinib, fluorouracil, leucovorin, and oxaliplatin therapy in previously treated patients with metastatic colorectal cancer. *J. Clin. Oncol.* 23 (24), 5613–5619. doi:10.1200/JCO.2005.08.359

Ladabaum, U., Dominitz, J. A., Kahi, C., and Schoen, R. E. (2020). Strategies for colorectal cancer screening. *Gastroenterology* 158 (2), 418–432. doi:10.1053/j.gastro.2019.06.043

Li, M., Wu, S., Zhuang, C., Shi, C., Gu, L., Wang, P., et al. (2023). Metabolomic analysis of circulating tumor cells derived liver metastasis of colorectal cancer. *Heliyon* 9 (1), e12515. doi:10.1016/j.heliyon.2022.e12515

Lin, H., Yu, Y., Zhu, L., Lai, N., Zhang, L., Guo, Y., et al. (2023). Implications of hydrogen sulfide in colorectal cancer: mechanistic insights and diagnostic and therapeutic strategies. *Redox Biol.* 59, 102601. doi:10.1016/j.redox.2023.102601

Liu, N. N., Jiao, N., Tan, J. C., Wang, Z., Wu, D., Wang, A. J., et al. (2022). Multi-kingdom microbiota analyses identify bacterial–fungal interactions and biomarkers of colorectal cancer across cohorts. *Nat. Microbiol.* 7 (2), 238–250. doi:10.1038/s41564-021-01030-7

Liu, T., Liu, D., Guan, S., and Dong, M. (2021). Diagnostic role of circulating MiR-21 in colorectal cancer: A update meta-analysis. *Ann. Med.* 53 (1), 87–102. doi:10.1080/07853890.2020.1828617

Lotfollahzadeh, S., Recio-Boiles, A., and Cagir, B. (2022). *Colon cancer*. United States: StatPearls Publishing. StatPearls [Internet].

Lulli, M., Napoli, C., Landini, I., Mini, E., and Lapucci, A. (2022). Role of non-coding RNAs in colorectal cancer: focus on long non-coding RNAs. *Int. J. Mol. Sci.* 23 (21), 13431. doi:10.3390/ijms232113431

Luo, H., Shen, K., Li, B., Li, R., Wang, Z., and Xie, Z. (2020). Clinical significance and diagnostic value of serum NSE, CEA, CA19-9, CA125, and CA242 levels in colorectal cancer. *Oncol. Lett.* 20 (1), 742–750. doi:10.3892/ol.2020.11633

MacKenzie, M. J., Hirte, H. W., Glenwood, G., Jean, M., Goel, R., Major, P. P., et al. (2005). A phase II trial of ZD1839 (Iressa™) 750 mg per day, an oral epidermal growth factor receptor-tyrosine kinase inhibitor, in patients with metastatic colorectal cancer. *Investig. new drugs* 23, 165–170. doi:10.1007/s10637-005-5862-9

Markandeywar, T. S., Narang, R. K., Singh, D., and Rai, V. K. (2023). Targeted delivery of doxorubicin as a potential chemotherapeutic agent. *Curr. Drug Deliv.* 20, 904–918. doi:10.2174/1567201819666220714101952

Melsens, E., Verberckmoes, B., Rosseel, N., Vanhove, C., Descamps, B., Pattyn, P., et al. (2017). The VEGFR inhibitor cediranib improves the efficacy of fractionated radiotherapy in a colorectal cancer xenograft model. *Eur. Surg. Res.* 58 (3-4), 95–108. doi:10.1159/000452741

Mettu, N. B., Niedzwiecki, D., Rushing, C., Nixon, A. B., Jia, J., Haley, S., et al. (2019). A phase I study of gemcitabine+ dasatinib (gd) or gemcitabine+ dasatinib+ cetuximab (GDC) in refractory solid tumors. *Cancer Chemother. Pharmacol.* 83, 1025–1035. doi:10.1007/s00280-019-03805-6

Meyerhardt, J. A., Ancukiewicz, M., Abrams, T. A., Schrag, D., Enzinger, P. C., Chan, J. A., et al. (2012). Phase I study of cetuximab, irinotecan, and vandetanib (ZD6474) as therapy for patients with previously treated metastatic colorectal cancer. *PLoS One* 7 (6), e38231. doi:10.1371/journal.pone.0038231

Mezheyeuski, A., Ponten, F., Edqvist, P. H., Sundström, M., Thunberg, U., Qvortrup, C., et al. (2020). Metastatic colorectal carcinomas with high SATB2 expression are associated with better prognosis and response to chemotherapy: A population-based scandinavian study. *Acta Oncol.* 59 (3), 284–290. doi:10.1080/0284186X.2019.1691258

Min, L., Chen, J., Yu, M., and Liu, D. (2023). Using circulating tumor DNA as a novel biomarker to screen and diagnose colorectal cancer: A meta-analysis. *J. Clin. Med.* 12 (2), 408. doi:10.3390/jcm12020408

Mo, S., Dai, W., Wang, H., Lan, X., Ma, C., Su, Z., et al. (2023). Early detection and prognosis prediction for colorectal cancer by circulating tumour DNA methylation haplotypes: A multicentre cohort study. *EClinicalMedicine* 55, 101717. doi:10.1016/j.eclinm.2022.101717

Morgan, E., Arnold, M., Gini, A., Lorenzoni, V., Cabasag, C. J., Laversanne, M., et al. (2023). Global burden of colorectal cancer in 2020 and 2040: incidence and mortality estimates from GLOBOCAN. *Gut* 72 (2), 338–344. doi:10.1136/gutjnl-2022-327736

Mou, L., Tian, X., Zhou, B., Zhan, Y., Chen, J., Lu, Y., et al. (2021). Improving outcomes of tyrosine kinase inhibitors in hepatocellular carcinoma: new data and ongoing trials. *Front. Oncol.* 11, 752725. doi:10.3389/fonc.2021.752725

Mueller, D., and Győrffy, B. (2022). DNA methylation-based diagnostic, prognostic, and predictive biomarkers in colorectal cancer. *Biochimica Biophysica Acta (BBA)-Reviews Cancer* 1877, 188722. doi:10.1016/j.bbcan.2022.188722

Murer, P., Plüss, L., and Neri, D. (2020). A novel human monoclonal antibody specific to the A33 glycoprotein recognizes colorectal cancer and inhibits metastasis. *MAbs* 12, 1714371. doi:10.1080/19420862.2020.1714371

Natoli, C., Perrucci, B., Perrotti, F., Falchi, L., and Iacobelli, S.Consorzio Interuniversitario Nazionale per Bio-Oncologia CINBO (2010). Tyrosine kinase inhibitors. *Curr. cancer drug targets* 10 (5), 462–483. doi:10.2174/156800910791517208

Neri, G., Arpa, G., Guerini, C., Grillo, F., Lenti, M. V., Giuffrida, P., et al. (2020). Small bowel adenocarcinomas featuring special AT-rich sequence-binding protein 2 (SATB2) expression and a colorectal cancer-like immunophenotype: A potential diagnostic pitfall. *Cancers* 12 (11), 3441. doi:10.3390/cancers12113441

Niedermaier, T., Tikk, K., Gies, A., Bieck, S., and Brenner, H. (2020). Sensitivity of fecal immunochemical test for colorectal cancer detection differs according to stage and location. *Clin. Gastroenterology Hepatology* 18 (13), 2920–2928. doi:10.1016/j.cgh.2020.01.025

Oh, H. H., and Joo, Y. E. (2020). Novel biomarkers for the diagnosis and prognosis of colorectal cancer. *Intestinal Res.* 18 (2), 168–183. doi:10.5217/ir.2019.00080

Palumbo, I., Piattoni, S., Valentini, V., Marini, V., Contavalli, P., Calzuola, M., et al. (2014). Gefitinib enhances the effects of combined radiotherapy and 5-fluorouracil in a colorectal cancer cell line. *Int. J. colorectal Dis.* 29, 31–41. doi:10.1007/s00384-013-1754-1

Pardini, B., Kumar, R., Naccarati, A., Novotny, J., Prasad, R. B., Forsti, A., et al. (2011). 5-Fluorouracil-based chemotherapy for colorectal cancer and MTHFR/MTRR genotypes. *Br. J. Clin. Pharmacol.* 72 (1), 162–163. doi:10.1111/j.1365-2125.2010.03892.x

Park, S. K., Baek, H. L., Yu, J., Kim, J. Y., Yang, H. J., Jung, Y. S., et al. (2017). Is methylation analysis of SFRP2, TFPI2, NDRG4, and BMP3 promoters suitable for colorectal cancer screening in the Korean population? *Intestinal Res.* 15 (4), 495–501. doi:10.5217/ir.2017.15.4.495

Peng, L., Jiang, J., Chen, H. N., Zhou, L., Huang, Z., Qin, S., et al. (2021). Redox-sensitive cyclophilin A elicits chemoresistance through realigning cellular oxidative status in colorectal cancer. *Cell Rep.* 37 (9), 110069. doi:10.1016/j.celrep.2021.110069

Perdyan, A., Spychalski, P., Kacperczyk, J., Rostkowska, O., and Kobiela, J. (2020). Circulating Tumor DNA in KRAS positive colorectal cancer patients as a prognostic factor–a systematic review and meta-analysis. *Crit. Rev. Oncology/Hematology* 154, 103065. doi:10.1016/j.critrevonc.2020.103065

Piawah, S., and Venook, A. P. (2019). Targeted therapy for colorectal cancer metastases: A review of current methods of molecularly targeted therapy and the use of tumor biomarkers in the treatment of metastatic colorectal cancer. *Cancer* 125 (23), 4139–4147. doi:10.1002/cncr.32163

Pickhardt, P. J., Graffy, P. M., Weigman, B., Deiss-Yehiely, N., Hassan, C., and Weiss, J. M. (2020). Diagnostic performance of multi-target stool DNA and CT colonography for non-invasive colorectal cancer screening. *Radiology* 297 (1), 120–129. doi:10.1148/radiol.2020201018

Plaza-Díaz, J., Solis-Urra, P., Aragón-Vela, J., Rodríguez-Rodríguez, F., Olivares-Arancibia, J., and Álvarez-Mercado, A. I. (2021). Insights into the impact of microbiota in the treatment of NAFLD/NASH and its potential as a biomarker for prognosis and diagnosis. *Biomedicines* 9 (2), 145. doi:10.3390/biomedicines9020145

Qin, S., Li, A., Yi, M., Yu, S., Zhang, M., and Wu, K. (2019). Recent advances in anti-angiogenesis receptor tyrosine kinase inhibitors in cancer therapy. *J. Hematol. Oncol.* 12, 1–11. doi:10.1186/s13045-019-0718-5

Qiu, S., Cai, Y., Yao, H., Lin, C., Xie, Y., Tang, S., et al. (2023). Small molecule metabolites: discovery of biomarkers and therapeutic targets. *Signal Transduct. Target. Ther.* 8 (1), 132. doi:10.1038/s41392-023-01399-3

Raunkilde, L., Hansen, T. F., Andersen, R. F., Havelund, B. M., Thomsen, C. B., and Jensen, L. H. (2022). NPY gene methylation in circulating tumor DNA as an early biomarker for treatment effect in metastatic colorectal cancer. *Cancers* 14 (18), 4459. doi:10.3390/cancers14184459

Rawla, P., Sunkara, T., and Barsouk, A. (2019). Epidemiology of colorectal cancer: incidence, mortality, survival, and risk factors. *Gastroenterol. Review/Przegląd Gastroenterol.* 14 (2), 89–103. doi:10.5114/pg.2018.81072

Rigi, F., Jannatabad, A., Izanloo, A., Roshanravan, R., Hashemian, H. R., and Kerachian, M. A. (2020). Expression of tumor pyruvate kinase M2 isoform in plasma and stool of patients with colorectal cancer or adenomatous polyps. *BMC Gastroenterol.* 20 (1), 241–247. doi:10.1186/s12876-020-01377-x

Rivera, M., Fichtner, I., Wulf-Goldenberg, A., Sers, C., Merk, J., Patone, G., et al. (2021). Patient-derived xenograft (PDX) models of colorectal carcinoma (CRC) as a platform for chemosensitivity and biomarker analysis in personalized medicine. *Neoplasia* 23 (1), 21–35. doi:10.1016/j.neo.2020.11.005

Rizzo, G., Bertotti, A., Leto, S. M., and Vetrano, S. (2021). Patient-derived tumor models: A more suitable tool for pre-clinical studies in colorectal cancer. *J. Exp. Clin. Cancer Res.* 40 (1), 178. doi:10.1186/s13046-021-01970-2

Rosen, L., Rosen, P., Amado, R., Chang, D., Mulay, M., Parson, M., et al. (1999). "November). A Phase I/II study of SU5416 in combination with 5-FU/leucovorin in patients with metastatic colorectal cancer," in *Clinical cancer research* (BIRMINGHAM, AL 35202 USA: AMER ASSOC CANCER RESEARCH), 3731S–3732S. PO BOX 11806.

Roskoski, R., Jr (2015). A historical overview of protein kinases and their targeted small molecule inhibitors. *Pharmacol. Res.* 100, 1–23. doi:10.1016/j.phrs.2015.07.010

Rothenberg, M. L., Lafleur, B., Washington, M. K., Levy, D. E., Morgan-Meadows, S. L., Ramanathan, R. K., et al. (2004). Changes in epidermal growth factor receptor signaling in serum and tumor biopsies obtained from patients with progressive metastatic colorectal cancer (MCRC) treated with gefitinib (ZD1839): an Eastern Cooperative Oncology Group study. *J. Clin. Oncol.* 22, 3000. doi:10.1200/jco.2004.22.90140.3000

Safari, E., Mosayebi, G., and Khorram, S. (2018). Dkk-3 as a potential biomarker for diagnosis and prognosis of colorectal cancer. *Med. J. Islamic Repub. Iran* 32, 86. doi:10.14196/mjiri.32.86

Saltz, L., Rubin, M., Hochster, H., Tchekmeydian, N. S., Waksal, H., and Needle, M. (2001). Cetuximab plus irinotecan is active in CPT-11-refractory colorectal cancer that expresses epidermal growth factor receptors. *Proc. Am. Soc. Clin. Oncol.* 20.

Sastre, J., Grávalos, C., Rivera, F., Massuti, B., Valladares-Ayerbes, M., Marcuello, E., et al. (2012). First-line cetuximab plus capecitabine in elderly patients with advanced colorectal cancer: clinical outcome and subgroup analysis according to KRAS status from a Spanish TTD group study. *Oncol.* 17 (3), 339–345. doi:10.1634/theoncologist.2011-0406

Sattar, R. S. A., Verma, R., Kumar, A., Dar, G. M., Sharma, A. K., Kumari, I., et al. (2022). Diagnostic and prognostic biomarkers in colorectal cancer and the potential role of exosomes in drug delivery. *Cell. Signal.* 99, 110413. doi:10.1016/j.cellsig.2022.110413

Sawicki, T., Ruszkowska, M., Danielewicz, A., Niedźwiedzka, E., Arłukowicz, T., and Przybyłowicz, K. E. (2021). A review of colorectal cancer in terms of epidemiology, risk factors, development, symptoms, and diagnosis. *Cancers* 13 (9), 2025. doi:10.3390/cancers13092025

Schiffmann, L. M., Brunold, M., Liwschitz, M., Goede, V., Loges, S., Wroblewski, M., et al. (2017). A combination of low-dose bevacizumab and imatinib enhances vascular normalisation without inducing extracellular matrix deposition. *Br. J. Cancer* 116 (5), 600–608. doi:10.1038/bjc.2017.13

Schlessinger, J. (2014). Receptor tyrosine kinases: legacy of the first two decades. *Cold Spring Harb. Perspect. Biol.* 6 (3), a008912. doi:10.1101/cshperspect.a008912

Scott, A. J., Song, E. K., Bagby, S., Purkey, A., McCarter, M., Gajdos, C., et al. (2017). Evaluation of the efficacy of dasatinib, a Src/Abl inhibitor, in colorectal cancer cell lines and explant mouse model. *PLoS One* 12 (11), e0187173. doi:10.1371/journal.pone.0187173

Shaukat, A., and Levin, T. R. (2022). Current and future colorectal cancer screening strategies. *Nat. Rev. Gastroenterology Hepatology* 19 (8), 521–531. doi:10.1038/s41575-022-00612-y

Shen, L., Lu, W., Huang, Y., He, J., Wang, Q., Zheng, X., et al. (2022). SNORD15B and SNORA5C: novel diagnostic and prognostic biomarkers for colorectal cancer. *BioMed Res. Int.* 2022, 8260800. doi:10.1155/2022/8260800

Shim, H. (2011). One target, different effects: A comparison of distinct therapeutic antibodies against the same targets. *Exp. Mol. Med.* 43 (10), 539–549. doi:10.3858/emm.2011.43.10.063

Siri, G., Alesaeidi, S., Dizghandi, S. E., Alani, B., Mosallaei, M., and Soosanabadi, M. (2022). Analysis of SDC2 gene promoter methylation in whole blood for non-invasive early detection of colorectal cancer. *J. Cancer Res. Ther.* 18 (Suppl. 2), S354–S358. doi:10.4103/jcrt.jcrt_1072_22

Siveen, K. S., Prabhu, K. S., Achkar, I. W., Kuttikrishnan, S., Shyam, S., Khan, A. Q., et al. (2018). Role of non-receptor tyrosine kinases in hematological malignancies and its targeting by natural products. *Mol. cancer* 17 (1), 1–21.

Soheilifar, M. H., Grusch, M., Neghab, H. K., Amini, R., Maadi, H., Saidijam, M., et al. (2019). Angioregulatory microRNAs in colorectal cancer. *Cancers* 12 (1), 71. doi:10.3390/cancers12010071

Srivastava, A., Rai, S., Bisht, D., Sachan, M., Jit, B. P., and Srivastava, S. (2022). "Targeting the altered tyrosine kinases in colorectal cancer: from inhibitors to drugs," in *Protein kinase inhibitors* (Cambridge: Academic Press), 361–391.

Stark, U. A., Frese, T., Unverzagt, S., and Bauer, A. (2020). What is the effectiveness of various invitation methods to a colonoscopy in the early detection and prevention of colorectal cancer? Protocol of a systematic review. *Syst. Rev.* 9 (1), 1–7. doi:10.1186/s13643-020-01312-x

Starý, L., Mezerová, K., Vysloužil, K., Zbořil, P., Skalický, P., Stašek, M., et al. (2020). Candida albicans culture from a rectal swab can be associated with newly diagnosed colorectal cancer. *Folia Microbiol.* 65, 989–994. doi:10.1007/s12223-020-00807-3

Strickler, J. H., Rushing, C. N., Uronis, H. E., Morse, M. A., Niedzwiecki, D., Blobe, G. C., et al. (2021). Cabozantinib and Panitumumab for RAS wild-type metastatic colorectal cancer. *Oncol.* 26 (6), 465–e917. doi:10.1002/onco.13678

Sun, S., Xiao, J., Huo, J., Geng, Z., Ma, K., Sun, X., et al. (2018). Targeting ectodysplasin promotor by CRISPR/dCas9-effector effectively induces reprogramming of human bone marrow-derived mesenchymal stem cells into sweat gland-like cells. *Stem Cell Res. Ther.* 9 (1), 1–10. doi:10.1186/s13287-017-0758-0

Sur, D., Advani, S., and Braithwaite, D. (2022). MicroRNA panels as diagnostic biomarkers for colorectal cancer: A systematic review and meta-analysis. *Front. Med.* 9, 915226. doi:10.3389/fmed.2022.915226

Taheri, M., Ghafouri-Fard, S., Najafi, S., Kallenbach, J., Keramatfar, E., Atri Roozbahani, G., et al. (2022). Hormonal regulation of telomerase activity and hTERT expression in steroid-regulated tissues and cancer. *Cancer Cell Int.* 22 (1), 1–17. doi:10.1186/s12935-022-02678-9

Tanriver, G., and Kocagoncu, E. (2023). Additive pre-diagnostic and diagnostic value of routine blood-based biomarkers in the detection of colorectal cancer in the UK Biobank cohort. *Sci. Rep.* 13 (1), 1367. doi:10.1038/s41598-023-28631-y

Tauriello, D. V., and Batlle, E. (2016). Targeting the microenvironment in advanced colorectal cancer. *Trends cancer* 2 (9), 495–504. doi:10.1016/j.trecan.2016.08.001

Thomson, R. J., Moshirfar, M., and Ronquillo, Y. (2022). "Tyrosine kinase inhibitors," in *StatPearls* (United States: StatPearls Publishing).

To, K. K., Poon, D. C., Wei, Y., Wang, F., Lin, G., and Fu, L. W. (2015). Vatalanib sensitizes ABCB1 and ABCG2-overexpressing multidrug-resistant colon cancer cells to chemotherapy under hypoxia. *Biochem. Pharmacol.* 97 (1), 27–37. doi:10.1016/j.bcp.2015.06.034

Tolba, M. F. (2020). Revolutionizing the landscape of colorectal cancer treatment: the potential role of immune checkpoint inhibitors. *Int. J. Cancer* 147 (11), 2996–3006. doi:10.1002/ijc.33056

Tournier, B., Aucagne, R., Truntzer, C., Fournier, C., Ghiringhelli, F., Chapusot, C., et al. (2023). Integrative clinical and DNA methylation analyses in a population-based cohort identifies CDH17 and LRP2 as risk recurrence factors in stage II colon cancer. *Cancers* 15 (1), 158. doi:10.3390/cancers15010158

Trenker, R., and Jura, N. (2020). Receptor tyrosine kinase activation: from the ligand perspective. *Curr. Opin. Cell Biol.* 63, 174–185. doi:10.1016/j.ceb.2020.01.016

Tsoi, H., Wong, K. F., Luk, J. M., and Staunton, D. (2019). Clinical utility of CDH17 biomarker in tumor tissues and liquid biopsies for detection and prognostic staging of colorectal cancer (CRC). *J. Glob. Oncol.* 5, 53. doi:10.1200/JGO.2019.5.suppl.53

Van Doorn, S. C., Stegeman, I., Stroobants, A. K., Mundt, M. W., De Wijkerslooth, T. R., Fockens, P., et al. (2015). Fecal immunochemical testing results and characteristics of colonic lesions. *Endoscopy* 47 (11), 1011–1017. doi:10.1055/s-0034-1392412

Vernia, F., Valvano, M., Fabiani, S., Stefanelli, G., Longo, S., Viscido, A., et al. (2021). Are volatile organic compounds accurate markers in assessing colorectal cancer and inflammatory bowel diseases? A review. *Cancers* 13 (10), 2361. doi:10.3390/cancers13102361

Vlachogiannis, G., Hedayat, S., Vatsiou, A., Jamin, Y., Fernández-Mateos, J., Khan, K., et al. (2018). Patient-derived organoids model treatment response of metastatic gastrointestinal cancers. *Science* 359 (6378), 920–926. doi:10.1126/science.aao2774

Wachsberger, P., Burd, R., Ryan, A., Daskalakis, C., and Dicker, A. P. (2009). Combination of vandetanib, radiotherapy, and irinotecan in the LoVo human colorectal cancer xenograft model. *Int. J. Radiat. Oncology* Biology* Phys.* 75 (3), 854–861. doi:10.1016/j.ijrobp.2009.06.016

Wang, C., Chevalier, D., Saluja, J., Sandhu, J., Lau, C., and Fakih, M. (2020). Regorafenib and nivolumab or pembrolizumab combination and circulating tumor DNA response assessment in refractory microsatellite stable colorectal cancer. *Oncol.* 25 (8), e1188–e1194. doi:10.1634/theoncologist.2020-0161

Wei, D., Tao, Z., Shi, Q., Wang, L., Liu, L., She, T., et al. (2020). Selective photokilling of colorectal tumors by near-infrared photoimmunotherapy with a GPA33-targeted single-chain antibody variable fragment conjugate. *Mol. Pharm.* 17 (7), 2508–2517. doi:10.1021/acs.molpharmaceut.0c00210

Wenzel, T., Büch, T., Urban, N., Weirauch, U., Schierle, K., Aigner, A., et al. (2020). Restoration of MARCKS enhances chemosensitivity in cancer. *J. Cancer Res. Clin. Oncol.* 146, 843–858. doi:10.1007/s00432-020-03149-2

Wheeler, D. L., and Yarden, Y. (2014). *Receptor tyrosine kinases: Structure, functions, and role in human disease*. Heidelberg: Springer.

Wilke, H., Glynne-Jones, R., Thaler, J. M. A. B. E. L., Adenis, A., Preusser, P., Aranda Aguilar, E., et al. (2006). MABEL—a large multinational study of cetuximab plus irinotecan in irinotecan-resistant metastatic colorectal cancer. *J. Clin. Oncol.* 24, 3549. doi:10.1200/jco.2006.24.18_suppl.3549

Wong, M. C., Huang, J., Lok, V., Wang, J., Fung, F., Ding, H., et al. (2021). Differences in incidence and mortality trends of colorectal cancer worldwide based on sex, age, and anatomic location. *Clin. Gastroenterology Hepatology* 19 (5), 955–966.e61. doi:10.1016/j.cgh.2020.02.026

Wong, S. H., and Yu, J. (2019). Gut microbiota in colorectal cancer: mechanisms of action and clinical applications. *Nat. Rev. Gastroenterology Hepatology* 16 (11), 690–704. doi:10.1038/s41575-019-0209-8

Woo, I. S., and Jung, Y. H. (2017). Metronomic chemotherapy in metastatic colorectal cancer. *Cancer Lett.* 400, 319–324. doi:10.1016/j.canlet.2017.02.034

Xi, Y., and Xu, P. (2021). Global colorectal cancer burden in 2020 and projections to 2040. *Transl. Oncol.* 14 (10), 101174. doi:10.1016/j.tranon.2021.101174

Xie, Y. H., Chen, Y. X., and Fang, J. Y. (2020). Comprehensive review of targeted therapy for colorectal cancer. *Signal Transduct. Target. Ther.* 5 (1), 22. doi:10.1038/s41392-020-0116-z

Xu, H., Chen, H., Hu, J., Xiong, Z., Li, D., Wang, S., et al. (2022). Feasibility of quantification based on novel evaluation with stool DNA and fecal immunochemical test for colorectal cancer detection. *BMC Gastroenterol.* 22 (1), 384–388. doi:10.1186/s12876-022-02470-z

Xu, H., Zhou, L., Lu, Y., Su, X., Cheng, P., Li, D., et al. (2020). Dual targeting of the epidermal growth factor receptor using combination of nimotuzumab and erlotinib in advanced non-small-cell lung cancer with leptomeningeal metastases: A report of three cases. *OncoTargets Ther.* 13, 647–656. doi:10.2147/OTT.S230399

Yang, Y., Li, S., Wang, Y., Zhao, Y., and Li, Q. (2022). Protein tyrosine kinase inhibitor resistance in malignant tumors: molecular mechanisms and future perspective. *Signal Transduct. Target. Ther.* 7 (1), 329. doi:10.1038/s41392-022-01168-8

Ye, X., Li, J., Song, C., and Chen, W. (2021). Telomere in colorectal cancer associated with distant metastases and predicted a poor prognosis. *Transl. Cancer Res.* 10 (6), 2906–2917. doi:10.21037/tcr-20-3341

Zahra, K., Dey, T., Mishra, S. P., and Pandey, U. (2020). Pyruvate kinase M2 and cancer: the role of PKM2 in promoting tumorigenesis. *Front. Oncol.* 10, 159. doi:10.3389/fonc.2020.00159

Zhang, J., Tian, Y., Luo, Z., Qian, C., Li, W., and Duan, Y. (2021). Breath volatile organic compound analysis: an emerging method for gastric cancer detection. *J. Breath Res.* 15 (4), 044002. doi:10.1088/1752-7163/ac2cde

Zhang, Y., Zou, J. Y., Wang, Z., and Wang, Y. (2019). Fruquintinib: A novel antivascular endothelial growth factor receptor tyrosine kinase inhibitor for the treatment of metastatic colorectal cancer. *Cancer Manag. Res.* 11, 7787–7803. doi:10.2147/CMAR.S215533

Zhao, G., Liu, X., Liu, Y., Li, H., Ma, Y., Li, S., et al. (2020). Aberrant DNA methylation of SEPT9 and SDC2 in stool specimens as an integrated biomarker for colorectal cancer early detection. *Front. Genet.* 11, 643. doi:10.3389/fgene.2020.00643

Zhao, Y., Bilal, M., Raza, A., Khan, M. I., Mehmood, S., Hayat, U., et al. (2021). Tyrosine kinase inhibitors and their unique therapeutic potentialities to combat cancer. *Int. J. Biol. Macromol.* 168, 22–37. doi:10.1016/j.ijbiomac.2020.12.009

Zhou, H., Zhu, L., Song, J., Wang, G., Li, P., Li, W., et al. (2022). Liquid biopsy at the frontier of detection, prognosis, and progression monitoring in colorectal cancer. *Mol. Cancer* 21 (1), 86. doi:10.1186/s12943-022-01556-2

Zhu, C., Huang, F., Li, Y., Zhu, C., Zhou, K., Xie, H., et al. (2022). Distinct urinary metabolic biomarkers of human colorectal cancer. *Dis. Markers* 2022, 1758113. doi:10.1155/2022/1758113

Zhu, H., Zhang, Y., Geng, Y., Lu, W., Yin, J., Li, Z., et al. (2019). IGFBP2 promotes the EMT of colorectal cancer cells by regulating E-cadherin expression. *Int. J. Clin. Exp. pathology* 12 (7), 2559–2565.

Zygulska, A. L., and Pierzchalski, P. (2022). Novel diagnostic biomarkers in colorectal cancer. *Int. J. Mol. Sci.* 23 (2), 852. doi:10.3390/ijms23020852

Frontiers in Oncology

Advances knowledge of carcinogenesis and tumor progression for better treatment and management

The third most-cited oncology journal, which highlights research in carcinogenesis and tumor progression, bridging the gap between basic research and applications to imrpove diagnosis, therapeutics and management strategies.

Discover the latest Research Topics

See more →

Frontiers

Avenue du Tribunal-Fédéral 34
1005 Lausanne, Switzerland
frontiersin.org

Contact us

+41 (0)21 510 17 00
frontiersin.org/about/contact